

STRUCTURAL OPTIMISATION OF SHIP HULL USING FINITE ELEMENT METHOD

JOYNAL ABEDIN

A Thesis Submitted for the Degree of Doctor of Philosophy (PhD)

School of Engineering

Newcastle University, United Kingdom

February 2025

Abstract

The design of ship structures is a multilayered process governed by numerous regulations and standards, demanding meticulous consideration of structural responses and production costs. This research presents a multi-objective structural optimisation methodology tailored for a multipurpose cargo ship. It addresses compliance with classification society regulations, cost-effectiveness, assessment of structural responses under diverse loads and conducts a comprehensive buckling analysis.

The initial phase involves transforming a 2D CAD design into a 2D model, facilitated by BV Mars 2000 software, followed by a comprehensive evaluation of the ship's scantling compliance with Bureau Veritas rules. Subsequently, the meticulous construction of a 3D cargo hold model featuring three cargo compartments sets the stage for a comprehensive analysis employing Femap-integrated NX Nastran finite element software.

This analysis scrutinises the structural response of the ship's hull under the combined influence of bending and torsional loads, including a detailed buckling analysis. The study explores the ramifications of torsion for both open-deck and closed-deck ship configurations. Furthermore, the research rigorously validates the precision of the 3D finite element model by means of exhaustive assessments involving beam theory and direct calculations.

A notable finding connected with this study is the prominence of hull girder normal stresses at midship, arising from still water and vertical wave bending moments, contributing to nearly 70% of the total stress when the ship is inclined. Horizontal wave bending moments account for approximately 10% of the stresses, whereas warping stresses contribute roughly 20% in open-deck ship designs. Additionally, the research demonstrates that torsion has minimal impact on closed-deck ship configurations.

The investigation extends to the analysis of hull girder deflection, systematically examined using numerical techniques and Euler-Bernoulli beam theory, focusing on the significance of longitudinal deflection over transverse deflection. A novel approach is presented using Minitab software's Fractional Factorial Design technique as part of the Design of Experiments (DOE) framework. The strategy aims to identify the critical parameters affecting hull girder Von Mises stress, torsional stress, as well as production costs.

Ship design optimisation is then carried out by incorporating regression equations for Von Mises stress and production costs from Minitab software into the Non-dominated Sorting Genetic Algorithm II (NSGA-II), managed using Python software. The optimally designed midship section underwent rigorous validation to ensure conformity with industry standards and classification society regulations. Essential modifications to inner bottom plates and double bottom side girders are made to meet these stringent requirements.

This optimisation process results in a substantial 10% reduction in ship weight and production costs compared to the initial design. It achieves a peak design stress of 296.2 MPa below the limit through prudent adjustments in plate thickness, web frame positioning and stiffener arrangement. This research delivers a comprehensive framework for the structural optimisation of ship hulls, potentially enhancing safety, sustainability and competitiveness within the maritime engineering industry.

Keywords: Structural optimisation, Ship hull, Scantlings, Finite element method, Structural response, Buckling analysis, Production costs, Design of Experiments (DOE), Bending and Torsional loads.

Acknowledgements

First and foremost, I sincerely thank Allah, the Almighty, for His endless mercy and blessings in granting me the strength and perseverance to complete this journey.

I extend my heartfelt gratitude to my supervisors, Dr Francis Franklin and Dr Richard Whalley, for their unwavering support, invaluable guidance, and mentorship, which have been pivotal to the success of my research.

I am deeply grateful to the faculty and staff at Newcastle University for their knowledge, resources, and the dynamic research environment that fostered my intellectual growth. I also sincerely appreciate Bureau Veritas for permitting me to use BV Mars 2000, Siemens Digital Industries Software for Femap/Nastran, and Robert McNeel & Associates for RHINO, all of which were critical to my research.

To my beloved wife, Jannat E Afrose, and our sons, Sadman Abedin and Sadab Abedin, your encouragement, patience, and prayers have been my most significant source of strength. This achievement is dedicated to you. I am equally thankful to my friends, Dr Rishad Shafik, Dr Ekhlasur Rahaman, Dr Tahir Ameen, Dr S.M. Ikhtiar Mahmud, and Sohanur Rahman, for their steadfast support and understanding throughout the various challenges and triumphs of this journey. Their love and unwavering support have been the driving force behind my perseverance.

I sincerely appreciate Ananda Shipyard and Slipways Limited for providing the studied ship drawings that are essential to my research. Finally, I thank all those who have directly or indirectly supported and inspired me along this path.

This thesis stands as a testament to the collective contributions and encouragement I have received. I am profoundly grateful for your support in reaching this milestone.

List of Publications

The research conducted and presented here has resulted in three peer-reviewed journal papers.

- Abedin, J., Franklin, F., & Mahmud, S.M.I. (2024). A Two-Stage Optimisation of Ship Hull Structure Combining Fractional Factorial Design Technique and NSGA-II Algorithm. *Journal of Marine Science and Engineering (JMSC)*, 12(3), 411. DOI: 10.3390/jmse12030411
- 2. **Abedin, J.**, Franklin, F., & Mahmud, S.M.I. (2024). Linear Longitudinal Strength Analysis of a Multipurpose Cargo Ship under Combined Bending and Torsional Load. *Journal of Marine Science and Engineering (JMSC)*, 12(1), 59. DOI: 10.3390/jmse12010059
- 3. **Abedin, J.**, Franklin, F., & Mahmud, S.M.I. (2024). Validation of the Hull Girder Deflection of a Multipurpose Cargo Ship. *ASEAN Engineering Journal (AEJ)*. eISSN: 2586-9159, Vol. 14 No. 2, June 2024, pp. 183-193, DOI: 10.11113/aej.V14.21054

Contents

Abstrac	t	••••••		iii
Acknow	ledgeme	ents		V
List of F	ublicati	ons		vi
Content	S	••••••		vii
List of F	igures .	••••••		XV
List of T	ables	•••••		xxi
Nomenc	lature	••••••		xxiii
Chapter	1	••••••		32
1.1	Overvi	ew of Shi	ip Structural Design and Optimisation	32
1.2	Key St	ructural C	Components of a Ship	33
1.3	Mecha	nical Prob	olems and Structural Challenges	35
1.4	Challe	nges Asso	ociated with Optimising Ship Structures	35
1.5	Typica	l Loading	g Conditions	37
1.6	Materi	als and In	novations in Ship Construction	39
1.7	Motiva	tion for S	Ship Structural Optimisation	40
1.8	Proble	m Statem	ent	41
1.9	Aims &	& Objecti	ves	41
	1.9.1	Aim		41
	1.9.2	Objectiv	es	42
1.10	Thesis	Organisa	tion	43
1.11	Expect	ed Result	s and Contributions	44
Chapter	2	•••••		46
2.1	Introdu	ction		46
2.2	Reviev	v of the L	iterature	47
	2.2.1	Multi-Ol	bjectives Optimisation for Ship Design Techniques	48
	2.2.2	Knowled	dge-Based Engineering in Ship Design	51
	2.2.3	Ship Hul	ll Design and Materials	51
	2.2.4	Ship Stru	ucture Optimisation Models	52
2.3	Structu	ıral Analy	vsis Techniques	55
	2.3.1	Compari	son and Evaluation of Various Optimisation Techniques	56
		2.3.1.1	Topology Optimisation Approaches	56
		2.3.1.2	Ranking Optimisation Approaches	56
		2.3.1.3	General Optimisation Approaches	57

		2.3.2	Modern Optimisation Techniques	. 58
	2.4	Key Fi	ndings	. 58
	2.5	Emerg	ing Trends and Potential Future Directions	. 60
	2.6	Resear	ch Problem	. 61
	2.7	Import	ance and Novelty of this Research	. 62
	2.8	Resear	ch Methodology	. 64
		2.8.1	Development of the Parametric Cargo Hold Model	. 64
		2.8.2	Optimisation of Scantlings	. 64
		2.8.3	Develop Finite Element Model	. 65
		2.8.4	Optimisation Plan	. 65
	2.9	Softwa	are Tools	. 66
		2.9.1	BV MARS 2000	. 66
		2.9.2	FEMAP/NX Nastran	. 67
		2.9.3	Minitab	. 67
		2.9.4	Rhino	. 67
	2.10	Conclu	asion	. 68
Ch	apter	3		. 71
	3.1	Introdu	action	. 71
	3.2	Theory	of Hull Girder Stresses	. 74
		3.2.1	Classical Beam Theory	. 74
		3.2.2	Thin-Walled Girder Theory	. 75
	3.3	Finite	Element Analysis and Associate Uncertainties	. 79
	3.4	Main I	Features of the Investigated Ship	. 83
		3.4.1	Development of Hull Shape	. 85
		3.4.2	Structural Configuration	. 86
	3.5	Princip	oles and Criteria of the Hull's Strength	. 90
		3.5.1	Overview	. 90
		3.5.2	Standard Loading Conditions	. 90
		3.5.3	Limit States	. 91
		3.5.4	Partial Safety Factors	. 92
		3.5.5	Net Scantling Approach	. 93
		3.5.6	Hull Girder Strength Check	. 98
	3.6	Design	ı Loads	. 99
		3.6.1	Overview	. 99
		3.6.2	Hull Girder Loads	. 99

			3.0.2.1	Still water Bending Moments (SWBM)	99
			3.6.2.2	Vertical Wave Bending Moment (VWBM)	100
			3.6.2.3	Horizontal Wave Bending Moment (HWBM)	100
			3.6.2.4	Wave-Induced Torsional Moment	101
		3.6.3	Load Ca	ses	102
	3.7	Analys	sed Ship S	tructural Analysis	103
		3.7.1	MARS 2		104
		3.7.2	Checking	g Criteria for Stress	108
		3.7.3	Hull Gire	der Strength Check	109
		3.7.4	Scantling	g Check of Plating	110
		3.7.5	Scantling	g Check of Secondary Stiffeners	115
	3.8	Streng	th Check	of Primary Supporting Members	125
		3.8.1	Coordina	nte System	125
		3.8.2	Modellin	ng and Mesh Characteristics	125
		3.8.3	Ship Hul	l Structural Analysis	127
			3.8.3.1	Structural Model	127
			3.8.3.2	Boundary Condition, Applications of Loads/Moments and Results	129
			3.8.3.3	Grid Convergence Study	131
			3.8.3.4	Investigated Ship's Structural Analysis – Upright Condition	133
			3.8.3.5	Structural Analysis of Ships under Combined Bending and Torsional Loads in Inclined (Oblique Sea) Conditions	138
			3.8.3.6	Impact of Still Water and Vertical Wave Bending Moment in an Inclined (Oblique Sea) Condition	140
			3.8.3.7	Impact of Horizontal Wave Bending Moment in an Inclined Load Case	142
			3.8.3.8	Impact of the Wave—Induced Torsional Moment in an Inclined (Oblique Sea) Condition	144
			3.8.3.9	Impact of Torsion between the Open—Deck and Closed—Deck Ships	146
	3.9	Buckli	ng Analys	sis	148
		3.9.1	Buckling	g of Inner Bottom Panel	150
		3.9.2	Buckling	g of Inner Shell Panel	151
	3.10	Discus	sion		151
	3.11	Conclu	ısion		153
Cha	apter	4	•••••		155
	4.1	Introdu	action		155

	4.2	Hull G	Girder Deflection	158
		4.2.1	Causes of Deflection	160
		4.2.2	Vertical and Horizontal Bending Moments	161
		4.2.3	Boundary Conditions	161
		4.2.4	Hull Girder Deflection Calculation	162
		4.2.5	Analysing the Effects of Hull Girder Deflection	164
		4.2.6	Measurement of Deflection	164
	4.3	Servic	eability	165
		4.3.1	Limiting Tolerance	165
		4.3.2	Typical Potential Problems	166
			4.3.2.1 In Shafting	166
			4.3.2.2 In Piping	166
	4.4	Safegu	nard against Excessive Deflection	167
	4.5		tical Determination of Ship's Hull Girder Deflection as a Simply rted Beam	168
	4.6		rical Determination of the Ship's Hull Girder Deflection as a Simply rted Beam	176
	4.7		rical Determination of the Ship's Hull Girder Deflection as a Complex are	
	4.8		ifference Between the Analytical and Numerical Determination of Hul Deflection	
	4.9	Discus	ssion	186
	4.10	Conclu	usion	187
Ch	apter	5		190
	5.1		uction	
	5.2	Develo	opment of the Models	194
		5.2.1	Overview	194
		5.2.2	Significance of the Parameters	195
		5.2.3	Boundary Values	197
		5.2.4	Design Matrix Construction	197
		5.2.5	Parameter Modification and New Model Generation	198
	5.3	Integra	ated Structural and Stress Analysis Methods	198
		5.3.1	Von Mises Stress Analysis	199
		5.3.2	Warping Stress Analysis	200
	5.4	Evalua	ating the Production Costs	
	5.5	Design	n of Experiments (DOE)	201

	5.5.1	Factorial	l Designs	202
	5.5.2	Plackett/	/Burman Design	203
	5.5.3	Fraction	Factorial Designs	206
		5.5.3.1	Identification of Influential Factors and Interactions Affecting Ship Hull Girder Stress	206
			5.5.3.1.1 Pareto Chart	208
			5.5.3.1.2 Residual Plots	209
		5.5.3.2	Identification of Influential Factors and Interactions Affecting Warping Stress	211
			5.5.3.2.1 Pareto Chart	213
			5.5.3.2.2 Residual Plots	214
		5.5.3.3	Identification of Influential Factors and Interactions Affecting Production Costs	215
			5.5.3.3.1 Pareto Chart	217
			5.5.3.3.2 Residual Plots	218
5.6	Discus	ssion		219
5.7	Concl	usion		220
Chapter	r 6	•••••		224
6.1	Introd	uction		224
	6.1.1	Objectiv	res of Ship Structural Optimisation	224
	6.1.2	Explorin	g the Benefits	225
	6.1.3	Optimisa	ation Types and Challenges	225
6.2	Optim	isation St	rategy	227
6.3	Mathe	matical F	ramework for Ship Structural Optimisation	228
	6.3.1	Objectiv	re Functions	228
		6.3.1.1	Weight Function	229
		6.3.1.2	Cost Function	229
			6.3.1.2.1 Work Preparation Costs	231
			6.3.1.2.2 Cutting Costs	232
			6.3.1.2.3 Transport Costs	234
	6.3.2	Design V	Variables	236
	6.3.3	Design (Constraints	236
	6.3.4	Single C	Criterion Problem	237
	6.3.5	Multi-Cı	riterion Problem	238
	6.3.6	Global C	Criterion Optima	238
	6.3.7	Pareto O	Optimal Solution	239

	6.4	Optimi	sation Algorithm	240
		6.4.1	The Purely Deterministic Approaches	241
		6.4.2	The Heuristic Approaches	241
	6.5	Data C	ollection and Implementation	242
	6.6	Assum	ptions and Constraints Used for the Optimisation Model	243
		6.6.1	Assumptions	243
		6.6.2	Constraints	244
		6.6.3	Detailed Steps for Implementing the Python Code	245
	6.7	Case S	tudy 1	248
	6.8	Case S	tudy 2	251
	6.9	Optimi	sed Results and Pareto Front	253
	6.10	Valida	tion	264
		6.10.1	The Imperative for Validating Optimised Midship	265
		6.10.2	Progressive Collapse Analysis of Ship Hull Girder	266
		6.10.3	Validation of the Optimised Midship Section	268
			6.10.3.1 Yielding Assessment	274
			6.10.3.2 Buckling Assessment	280
			6.10.3.3 Ultimate Strength Assessment	281
	6.11	Robust	ness of the Optimisation Results	283
	6.12	Discus	sionsion	285
	6.13	Conclu	sion	288
Cha	apter	7		290
	7.1	Introdu	action	290
	7.2	Resear	ch Objectives and Achievements	291
		7.2.1	Assessment of Longitudinal Strength, Deflection and Buckling	
			Analysis	
		7.2.2	Torsional Stress Analysis	
		7.2.3	Identification of Significant Factors Affecting Ship Design	
		7.2.4	Optimisation Strategy	
	7.3	Valida	tion and Results	
		7.3.1	Yielding Evaluation	293
		7.3.2	Buckling Assessment	
		7.3.3	Local Sea and Cargo Loads Applied	
		7.3.4	Analysis of Torsional Moments	
		7.3.5	Assessment of Hull Girder Ultimate Strength	294

7	7.4	Optimised Midship Section for Structural Compliance and Cost Efficiency	295
7	7.5	Summary of Findings	295
7	7.6	Implications	295
		7.6.1 Practical Applications	296
		7.6.2 Milestone for the Maritime Industry	296
7	7.7	Conclusion	296
7	7.8	Comparative Analysis of Current and AI-Based Optimisation Methods	297
7	7.9	Limitations of the Research	298
7	7.10	Direction of Future Research	299
Refer	renc	es	302
Appe	ndi	x A	312
Appe	ndi	x B	317
Appe	ndi	x C	319



List of Figures

Figure 1-1: Section of a ship structure illustrating the principal structural components .	34
Figure 1-2: The effect of Hogging and Sagging on a ship's hull.	36
Figure 1-3: Heading angle of the ship against the wave	39
Figure 2-1: Procedure for optimising ship structure	66
Figure 3-1: A ship travelling through oblique waves.	69
Figure 3-2: Distribution of longitudinal stress in the cross-section under vertical bending, horizontal bending and torsion.	74
Figure 3-3: Beam subjected to torsion.	75
Figure 3-4: General arrangement plan of the analysed ship	84
Figure 3-5: Perspective view of a general multi-purpose cargo ship [122]	85
Figure 3-6: Perspective view of the typical hull form of the analysed ship in RHINO	86
Figure 3-7: Midship section of the analysed ship	87
Figure 3-8: Comparison of the analysed ship's bending moments along the ship's length (L)	100
Figure 3-9: Wave-induced torsional moment of the analysed ship along the ship's length (L) (wave at 60°).	101
Figure 3-10: Wave-induced torsional moment of the analysed ship along the ship's length (L) (wave at 120°)	101
Figure 3-11: MARS Inland main interface.	105
Figure 3-12: Basic ship's input data.	106
Figure 3-13: Midship section in MARS 2000.	107
Figure 3-14: Calculations and rule check in MARS 2000.	108
Figure 3-15: Inner bottom plate 2 (Hogging condition).	113
Figure 3-16: Double bottom longitudinal girder 3786 OCL (Hogging condition)	113
Figure 3-17: Double bottom longitudinal girder 6325 OCL (Hogging condition)	114
Figure 3-18: Inner bottom plate 2 (Sagging condition)	115
Figure 3-19: Bottom Stiffener (Hogging condition).	117
Figure 3-20: Inner Bottom Stiffener (Hogging condition).	117
Figure 3-21: Side Shell stiffener (Hogging condition)	118
Figure 3-22: Inner side shell stiffener (Hogging condition)	118
Figure 3-23: Main deck stiffener (Hogging condition).	119
Figure 3-24: Hatch coaming stiffener (Hogging condition)	119
Figure 3-25: Bottom stiffener (Sagging condition).	121
Figure 3-26: Inner Bottom stiffener (Sagging condition)	122

Figure 3-27:	Side shell stiffener (Sagging condition)	122
Figure 3-28:	Inner side shell stiffener (Sagging condition).	123
Figure 3-29:	Main deck stiffener (Sagging condition).	123
Figure 3-30:	Hatch coaming stiffener (Sagging condition).	124
Figure 3-31:	Coordinate system for modelling [36].	125
Figure 3-32:	Harmonised first edge (left) and normal vectors (right) [36]	126
Figure 3-33:	Mesh shapes [36].	126
Figure 3-34:	A typical mesh arrangement of the transverse web in FEMAP	128
Figure 3-35:	Generated FE model of the analysed ship in FEMAP.	128
Figure 3-36:	Cantilever beam applied with constant bending moment [129]	130
Figure 3-37:	Rigid Element in FEMAP.	131
Figure 3-38:	Convergence curve illustrating optimal mesh density for simulation accuracy.	132
Figure 3-39:	Comparison of normal longitudinal bending stress between beam theory and FE model (Hogging-Upright load case).	134
Figure 3-40:	Hull girder normal stress at midship (Hogging—upright condition)	135
Figure 3-41:	Comparison of normal longitudinal bending stress between beam theory and FE model (Sagging-Upright load case).	136
Figure 3-42:	Hull girder normal stress at midship (Sagging—upright condition)	137
Figure 3-43:	Hull girder normal stress at midship due to combined bending and torsional loads (Sagging—inclined conditions) along the depth (height) of the ship.	139
Figure 3-44:	Hull girder normal stress at midship due to combined bending and torsional load (Sagging—Inclined condition).	
Figure 3-45:	Comparison of hull girder stress between beam theory and direct calculation at midship due to still water and vertical wave bending moment (Sagging—inclined condition) along the depth (height) of the ship.	141
Figure 3-46:	Hull girder normal stress at midship due to still water and vertical wave bending moment (Sagging—inclined condition).	141
Figure 3-47:	Comparison of normal longitudinal bending stress due to horizontal wave bending moment between beam theory and FE model.	143
Figure 3-48:	Maximum hull girder normal stress due to horizontal wave bending moment (Beam Sea condition).	143
Figure 3-49:	Comparison of hull girder warping normal stress due to wave-induced torsional moment between thin wall girder theory and direct calculation (Sagging—inclined condition) along the depth (height) of the ship	145
Figure 3-50:	The hull girder warping normal stress due to torsion (open—deck ship)	145
Figure 3-51:	Comparison of hull girder warping normal stress between open—and closed—deck ships along the depth (height) of the ship	147

Figure 3-52: The hull girder warping normal stress due to torsion (closed—deck ship)	148
Figure 3-53: Buckling of plate panel in BV Mars, 2000.	149
Figure 3-54: Inner Bottom Plate Panel Buckling under Hydrostatic and Inertia Loads in Femap.	150
Figure 3-55: Inner Shell Plate Panel Buckling under Hydrostatic and Inertia Loads in Femap.	151
Figure 4-1: Deflection of both ends of the supported beam [149].	160
Figure 4-2: Distribution of the moment of inertia (Y axis) along the ship's length	171
Figure 4-3: Distribution of the moment of inertia (Z axis) along the ship's length	172
Figure 4-4: M _B /I curve along the ship's length (Hogging-Head Sea).	172
Figure 4-5: M _B /I curve along the ship's length (Sagging-Head Sea)	173
Figure 4-6: M _B /I curve along the ship's length (Beam Sea).	173
Figure 4-7: Longitudinal hull girder deflection (mm) along the ship's length (Hogging-Head Sea).	174
Figure 4-8: Longitudinal hull girder deflection (mm) along the ship's length (Sagging-Head Sea).	175
Figure 4-9: Transverse hull girder deflection (mm) along the ship's length (Beam Sea)	175
Figure 4-10: Longitudinal hull girder deflection (mm) along the ship's length (Hogging Head Sea).	176
Figure 4-11: Longitudinal hull girder deflection (mm) along the ship's length (Sagging Head Sea)	177
Figure 4-12: Transverse hull girder deflection (mm) along the ship's length (Beam Sea).	177
Figure 4-13: Comparison of Analytical vs. Numerical deflection (Hogging Head Sea)	179
Figure 4-14: Comparison of Analytical vs. Numerical deflection (Sagging Head Sea)	180
Figure 4-15: Comparison of Analytical vs. Numerical deflection (Beam Sea)	181
Figure 4-16: Comparison of different Numerical deflection for Head Sea Hogging, Sagging and Beam Sea conditions.	182
Figure 4-17: Longitudinal hull girder deflection (mm) along the ship's length (Hogging Head Sea).	183
Figure 4-18: Longitudinal hull girder deflection (mm) along the ship's length (Sagging Head Sea).	184
Figure 4-19: Transverse hull girder deflection (mm) along the ship's length (Beam Sea).	184
Figure 5-1: Plackett and Burman's Screening Scheme for Investigating Twelve (12) Factors	204
Figure 5-2: Plackett-Burman Screening Plan for Identifying Main Effects of Stress on Ship Hull.	205
Figure 6-1: Flow chart for the NSGA-II	227

Figure 6-2: Feasible Solution Space [198]	240
Figure 6-3: Pareto Optimal Curve [198].	240
Figure 6-4: Panel definition of midship section.	249
Figure 6-5: Distribution of production costs for the analysed ship.	251
Figure 6-6: Number of Iterations vs. Best Individual Stress Value.	253
Figure 6-7: Number of Iterations vs. Best Individual Production Cost Value	254
Figure 6-8: Pareto Optimal curve: Costs vs. Stress.	255
Figure 6-9: Midship section of the investigated ship after optimisation.	257
Figure 6-10: Before optimisation, hull girder Von Mises stress at midship (Sagging—upright condition)	258
Figure 6-11: After optimisation, hull girder Von Mises stress at midship (Sagging—upright condition)	258
Figure 6-12: Keel plate Von Mises stress.	259
Figure 6-13: Bottom plate Von Mises stress	259
Figure 6-14: Side shell plate Von Mises stress.	260
Figure 6-15: Inner side shell plate Von Mises stress.	260
Figure 6-16: Inner bottom plate Von Mises stress.	261
Figure 6-17: Shear strake plate Von Mises stress.	261
Figure 6-18: Main Deck plate Von Mises stress.	262
Figure 6-19: DB longitudinal girder, CL (Centre Line) Von Mises stress	262
Figure 6-20: Hatch coaming plate Von Mises stress.	263
Figure 6-21: Hatch coaming top plate Von Mises stress.	264
Figure 6-22: Curvature due to hull girder bending [217].	267
Figure 6-23: Local Sea loads acting on the hull (Head Sea)	270
Figure 6-24: Local Sea loads acting on the hull (Beam Sea)	270
Figure 6-25: Local Sea loads acting on the hull (Oblique Sea).	271
Figure 6-26: Cargo loads acting on the inner bottom and inner side shell.	271
Figure 6-27: Torsional load acting on hull girder.	272
Figure 6-28: Yielding criteria of the optimised midship.	273
Figure 6-29: Buckling criteria of the optimised midship.	273
Figure 6-30: Validation of hull girder bending strength for plating (Head Sea)	275
Figure 6-31: Validation of hull girder bending strength for plating (Oblique Sea)	275
Figure 6-32: Validation of hull girder strength for ordinary stiffener (Head Sea)	276
Figure 6-33: Validation of hull girder strength for ordinary stiffener (Oblique Sea)	277
Figure 6-34: Validation of hull girder shear strength for plating (Head Sea)	278
Figure 6-35: Validation of hull girder shear strength for plating (Oblique Sea)	278

Figure 6-36: Primary vertical hull girder shear stress distribution	279
Figure 6-37: Validation of buckling of plate panel.	280
Figure 6-38: Validation of buckling of ordinary stiffener.	281
Figure 6-39: Hull girder's ultimate strength.	282

List of Tables

Table 3–1: Main Particulars of the Investigated Ship.	83
Table 3–2: Stiffener Spacing.	88
Table 3–3: Gross Scantlings and Materials Grade.	89
Table 3–4: Serviceability limit states.	92
Table 3–5: Plating partial safety factors.	93
Table 3–6: Ordinary stiffeners-partial safety factors.	93
Table 3–7: Corrosion additions according to BV Rules.	92
Table 3–8: Coefficients and β for bulb profiles	93
Table 3–9: The net thickness of plate elements.	96
Table 3–10: Material factor.	96
Table 3–11: Wave hull girder loads in each load case.	100
Table 3–12: Rule-based load cases and loading conditions.	101
Table 3–13: Section modulus comparison.	109
Table 3–14: Gross/Net Moduli.	108
Table 3–15: Hull girder bending stress.	110
Table 3–16: Scantling check of plating (Hogging condition).	111
Table 3–17: Scantling check of plating (Sagging condition).	112
Table 3–18: The net thickness of the stiffener web (Hogging condition).	116
Table 3–19: Shear area/Section modulus (actual v/s required); Net values (Hogging condition).	116
Table 3–20: The net thickness of the stiffener web (Sagging condition).	120
Table 3–21: Shear area/Section modulus (actual v/s required); Net values (Sagging condition).	121
Table 3–22: Material properties of steel [127].	
Table 3–23: Boundary conditions (Cantilever).	
Table 3–24: Comparative analysis of Von Mises stresses across multiple ship models using varied mesh refinement levels	
Table 3–25: Still water and vertical wave bending moments.	
Table 3–26: Comparison of normal stress between beam theory and FE model (Hogging- Upright load case).	
Table 3–27: Comparison of normal stress between beam theory and FE model (Sagging- Upright load case).	
Table 3–28: Normal stress in FE model (Sagging- Inclined load case).	

Table 3–29: Comparison of normal stress due to still water and vertical wave bending moment between beam theory and FE model (Sagging—Inclined load	
case)	140
Table 3–30: Comparison of normal stress due to horizontal wave bending moment between beam theory and FE model (Sagging—Inclined load case)	142
Table 3–31: Comparison of warping normal stress due to wave-induced torsional moment between thin wall girder theory and FE model (Inclined load case)	144
Table 3–32: Comparison of Warping Normal Stress for Open-Deck and Closed-Deck Ships, Calculated Directly Due to Wave-Induced Torsional Moments (Inclined Load Case).	147
Table 3–33: Boundary conditions (Cantilever).	150
Table 4–1: Boundary conditions (For Head Sea)	162
Table 4–2: Boundary conditions (For Beam Sea).	162
Table 4–3: Hull Girder Deflection Analysis Results (Analytical Calculation, Hogging Condition)	169
Table 4–4: Hull Girder Deflection Analysis Results (Analytical Calculation, Sagging Condition)	170
Table 4–5: Hull Girder Deflection Analysis Results (Analytical Calculation, Beam Sea Condition)	
Table 4–6: Analytical and Numerical deflections data for Head Sea Hogging condition.	179
Table 4–7: Analytical and Numerical deflections data for Head Sea Sagging condition.	180
Table 4–8: Analytical and Numerical deflections data for Beam Sea condition	181
Table 4–9: Numerical comparison of hull girder deflections in various sea conditions	182
Table 4–10: Difference between the analytical and numerical determination of hull girder deflection.	186
Table 5–1: Variables Ranges.	195
Table 5–2: Model Summary (Hull Girder Stress).	207
Table 5–3: Model Summary (Warping Stress).	212
Table 5–4: Model Summary (Production Costs).	216
Table 6–1: Comparison of Original and Optimised Parameters for Cargo Hold Design.	256
Table 6–2: Von Mises stress before and after optimisation	264

Nomenclature

Symbols

M	Bending moment	kN.m
I	Moment of inertia	$kg.m^2$
F_n	Longitudinal force	N
M_{v}	Vertical bending moment	kN.m
M_h	Horizontal bending moment	kN.m
A	Cross-sectional area	mm^2
Δ_z, Δ_y	Distances between the detail and the neutral axes	mm
$\sigma_{\scriptscriptstyle \mathcal{W}}$	Warping stress	MPa
$I_{\mathcal{V}}$	Vertical moment of inertia	$kg.m^2$
I_h	Horizontal moment of inertia	$kg.m^2$
T	Torsional moment	kN.m
T_t	St. Venant torsional moment	kN.m
T_{w}	Warping torsional moment	kN.m
E, G	Young's modulus and Shear modulus	GPa
I_t	Torsional constant	
I_{w}	Sectorial moment of inertia	$kg.m^2$
ψ	Twist angle	0
\overline{u}	Relative sectional warping	radians/m
u	Warping function	Nm
$B_{\scriptscriptstyle W}$	Warping bimoment	Nm
δ_i	Flexibility influence coefficient	
F_j	Load	kN
C	Flexibility matrix	N/m
f	Nodal force vector	N
d	Nodal displacement vector	m
k	Stiffness matrix coefficient	_
Yw1	Partial safety factor covering the uncertainties regarding	
	wave hull girder loads	
γ_{w2}	Partial safety factor covering the uncertainties regarding	

wave local loads Partial safety factor covering the uncertainties regarding γ_R resistance Partial safety factor covering the uncertainties regarding γ_M the material Total corrosion addition t_c mm

 m^3 W_G Stiffener gross section modulus Coefficients for bulb profiles σ, β

Hull girder stress caused by vertical bending moment **MPa** σ_1 Material's yield stress MPa R_{EH}

K Material factor

 M_{WV} Vertical wave bending moment kN.m M_{WH} Horizontal wave bending moment kN.m

Master allowable stress **MPa** σ_{Master}

 R_{ν} , R_{e} Yield stress MPa MPa Von Mises stress

 σ_{VM} Hull girder bending stress in Sagging condition MPa σ_{S}

Hull girder bending stress in Hogging condition **MPa** σ_H

Elastic modulus GPa \boldsymbol{E}

 kg/m^3 Density ρ Poisson's ratio ν

Length of the ship Lm

Depth of the ship D m

Number of erection butts on the upper deck n

Deflection of hull girder at midship δ mm

W Load applied on hull girder kN

l Half-length of the ship m y

Distance between the neutral axis and the upper deck or m

bottom

Distance between midship and loaded point m \boldsymbol{x}

Distance from the neutral axis to the extreme member \boldsymbol{C} m

w(x)General hull deflection at section x mm

Specific ship hull deflection at amidship mm W_m

The Von Mises stress of the structure MPa σ_e

$\sigma_{\scriptscriptstyle O}$	Permissible stress	MPa
a	The first constant of integration of the MB/I curve	
b	The second constant of integration of the MB/I curve	
S1	Partial safety factor	
σ_y	The minimum yield point	MPa
N	The number of experiments	
L	The number of levels	
F	The number of factors	
Y	The predicted response	m
eta_0	The model intercept	
eta_i	The linear coefficient	
X_i	The level of an independent variable	
f(x)	The objective function	(t or €)
r	Number of structural regions	
w_j	Relative weight coefficient	
SW_j	The weight of the j-th structural region	t
PC	The production costs	€
MC	Materials costs	€
LC	Labour costs	€
HC	Hourly costs	€
OC	Overhead costs	€
C_{PRE}	Work preparation costs	€
n_p	Number of works prepares	M
S_p	Work preparer wages	€/Mh
h_p	Work preparation time	h
K_e	Electricity consumption	kW/h
P_e	Electricity prices	€/kW
C_d	Depreciation costs	€/h
P_b	Block weight	t
γ_b	Block complexity-coefficient	
CER_p	Work preparation costs estimation relationship	$M_{\text{h}}\!/t$
MDO_p	Work preparation labour costs	€/ M_h
CEQ_p	Work preparation equipment costs	€/t
C_{PLA}	Plasma cutting costs	€

n_{tc}	Number of cutting technicians	M
S_{tc}	Cutting technician wages	€/ M_h
h_c	Cutting time	h
v_c	Cutting speed	m/h
d_c	Cutting length	m
K_{Ar}	Plasma gas consumption	kg/h , m^3/h
P_{Ar}	Plasma gas prices	€/kg, €/m ³
K_O	Oxygen consumption	kg/h , m^3/h
P_O	Oxygen prices	€/kg, €/m ³
K_A	Acetylene consumption	kg/h , m^3/h
P_A	Acetylene prices	ϵ /kg, ϵ /m ³
C_{MOXI}	Manual Oxy gas cutting costs	€
C_c	Steel weight produced costs	€
CER_c	Cutting costs estimate relationship	M_h/t
MDO_c	Cutting labour costs	€/M _h
CC_c	Cutting consumable costs	€/t
CEQ_c	Cutting equipment costs	€/t
C_{PON}	Transport vehicles costs	€
n_{ot}	Number of transport workers	M
S_{ot}	Transport workers' wages	\in / M_h
h_t	Transportation time	h
C_{VEI}	Vehicles fuel costs	€
K_C	Fuel consumption	l/h
P_C	Fuel price	€/1
CER_t	Transport costs estimate relationship	M_h/t
MDO_t	Transport labour costs	€/M _h
CEQ_t	Transport equipment costs	€/t
C_{CAL}	Forming costs	€
n_{oe}	Number of forming workers	M
S_{oe}	Forming workers' wages	€/h
h_e	Forming time	h
CER_e	Forming costs estimation ratio	M_h/t
MDO_e	Labour costs for forming	€/M _h
CC_e	Consumable costs for forming	€/t

CEQ_e	Equipment costs for forming	€/t
C_{MON}	Assembly costs	€
n_m	Quantity of marine assemblers	M
S_m	Marine assembler wages	€/Mh
h_m	Assembly time	h
h_s	Welding time	h
K_{ele}	Consumption of coated electrodes	kg/m
d_{sol}	Length of welding	m
P_{ele}	Costs of coated electrodes	€/kg
CER_m	Assembly costs estimation ratio	$M_h \! / t$
MDO_m	Labour costs for assembly	€/ M_h
CC_s	Costs of welding consumables	€/t
CEQ_m	Equipment costs for assembly	€/t
C_{SAW}	Submerged arc welding costs	€
n_s	Number of welders	M
S_s	Welders' wages	€/ M_h
K_{fio}	Coded wires consumption	kg/m
K_{flu}	Protection flux consumption	kg/m
P_{fio}	Cored wires prices	€/kg
P_{flu}	Protection flux prices	€/kg
C_{FCAW}	Flux core arc welding costs	€
K_{pro}	Protection gas consumption	kg/h , m^3/h
P_{pro}	Protection gas prices	€/kg, €/m³
CER_s	Welding cost estimation ratio	$M_{h}\!/t$
MDO_s	Labour costs for welding	€/ M_h
CEQ_s	Equipment costs for welding	€/t
C_{EXTRAS}	Extra costs for ship construction	€
C_{TOTAL}	Total costs for constructing a ship's steel hull	€
ps	Still water pressure	bar
p_W	Wave-induced pressure	bar
S	The shorter side of the plating	mm
l	The longer side of the plating	mm
C_a	The aspect ratio of the plate panel	
C_r	Coefficient of curvature	

R_{y}	Minimum yield stress	MPa
$\gamma_R, \gamma_m, \gamma_{S2}, \gamma_{W2}$	Utilisation factors	_
A_{Sh}	The minimum net share sectional area	m^2
W	The net section modulus	m^3
β_s, β_b	Coefficients of structural members	
σ_{comb}	The combined critical stress	MPa
F	Compressive force	MPa
R_{eH}	Upper yield strength	MPa
σ_C	Critical buckling stress	MPa
σ_E	Euler buckling stress	MPa
σ_b	Axial stress	MPa

Acronyms

SMAW Shielded metal arc welding

GMAW Gas metal arc welding

GTAW Gas tungsten arc welding

CAD Computer-aided design

CAM Computer-aided manufacturing

FEA Finite element analysis

VCG Vertical centre of gravity

PSA Pareto simulated annealing

PSO Particle swarm optimisation

RO-PAX Roll-On/Passenger

BPNN Backpropagation neural network

TOPSIS Technique for order of preference by similarity to ideal solution

SSA Sparrow search algorithm

KBE Knowledge-based engineering

NURBS Non-uniform rational B-splines

CO Collaborative optimisation

SHDMF Ship hull design magnification factors

MADM Multi-attribute decision-making

OSV Offshore supply vessel

ABC Artificial bee colony

GA Genetic algorithm

BEM Boundary element method

CFD Computational fluid dynamics

NSGA-II Non-dominated sorting genetic algorithm II

DOE Design of experiments

CSR Common structural rules

BV Bureau Veritas

2D Two dimensional

3D Three dimensional

FEM Finite element model

FEMAP Finite element modelling and post-processing

IACS International Association of Classification Societies

MARS Marine and Offshore software

NR Naval Rules

1R One Run
2R Two Runs

GA General Arrangement

HP Holland Profile

FB Flat Bar

SWBM Still Water Bending Moments

VWBM Vertical Wave Bending Moment

HWBM Horizontal Wave Bending Moment

GUI Graphical User Interface

BSD Basic Ship Data

DB long girder CL Double bottom longitudinal girder centre line

OCL Offset centre line

EPP Element property point

MDO Multi-disciplinary design optimisation

RSM Response Surface Methodology

FPSO Floating Production Storage and Offloading

PBD Plackett/Burman Design

GHG Greenhouse gas

VCG Vertical Centre of Gravity

SQP Sequential quadratic programming

DEAP Distributed Evolutionary Algorithms in Python

CXPB Crossover probability

MUTPB Mutation probability

NGEN Number of generations

POPSIZE Population size



Chapter 1

Introduction

1.1 Overview of Ship Structural Design and Optimisation

The structural integrity of a ship is at the core of shipping, permitting global trade, transport and sustainability [1]. A well-designed structure will guarantee and deliver operational safety, efficiency and reliability in different conditions while responding to the economic and environmental challenges arising in contemporary shipbuilding [2]. Contemporary developments in structural optimisation expect to standardise these goals to attain cost savings, boost fuel efficiency and conform with international regulations [3].

Improvements in numerical methods, essentially the finite element method, have transformed ship structural optimisation by permitting analyses of even exceptionally complicated designs. FEM is a tool that is applied to analyse the stress, deformation and distribution of loads throughout the members of a structure [4].

Optimisation in the development of ships begins in the early stages with fundamental decisions pertaining to size, layout and design [5]. It has a direct impact on the ecology, production costs and performance of the ship [6]. Key factors to consider consist of the following:

- Customer Requirements: The design should be in accordance with customer expectations concerning certain preset features, for example speed, capacity and navigational range [5].
- **Design Constraints:** Strength, stability and manufacturability must be considered in conjunction with the budget and project timetable [5].

The principal challenges connected with optimisation techniques in ship design include:

- **Reducing Weight:** Less use of steel without compromising the strength and security of the ship [6].
- **Improving Efficiency:** Fuel-efficient to minimise greenhouse gas emissions [7].

• Guaranteeing Robustness: Capable of dealing with complicated loading conditions [8].

The optimisation of a hull's structural design is a crucial way to improve environmental sustainability, safety, efficiency and stability [9]. A satisfactory hull design and optimisation reduces the chances of an accident or capsizing, as well as increased fuel efficiency [10].

The latest developments in ship structural optimisation range from energy system optimisation, light structure design and the robust analysis of structures, even to specific attempts to decrease the weight and production cost of steel while simultaneously reducing the emission of greenhouse gas (GHGs). Ordinarily, marine construction considers lightness, security and cost-efficiency at each stage of the life cycle [6].

Structural optimisation helps the shipping industry to respond to contemporary challenges regarding efficiency, safety and sustainability. This thesis applies a two-stage hybrid optimisation technique combining fractional factorial design and the Non-Sorting Genetic Algorithm-II (NSGA-II), together with the finite element method. This approach optimises ship hull structures by addressing key issues, for example weight reduction, production cost savings and regulatory compliance.

1.2 Key Structural Components of a Ship

The primary components of a ship's structure comprise the hull, bulkheads, girders, frames and decks [11]. A schematic representation of these components is presented in Figure 1.1.

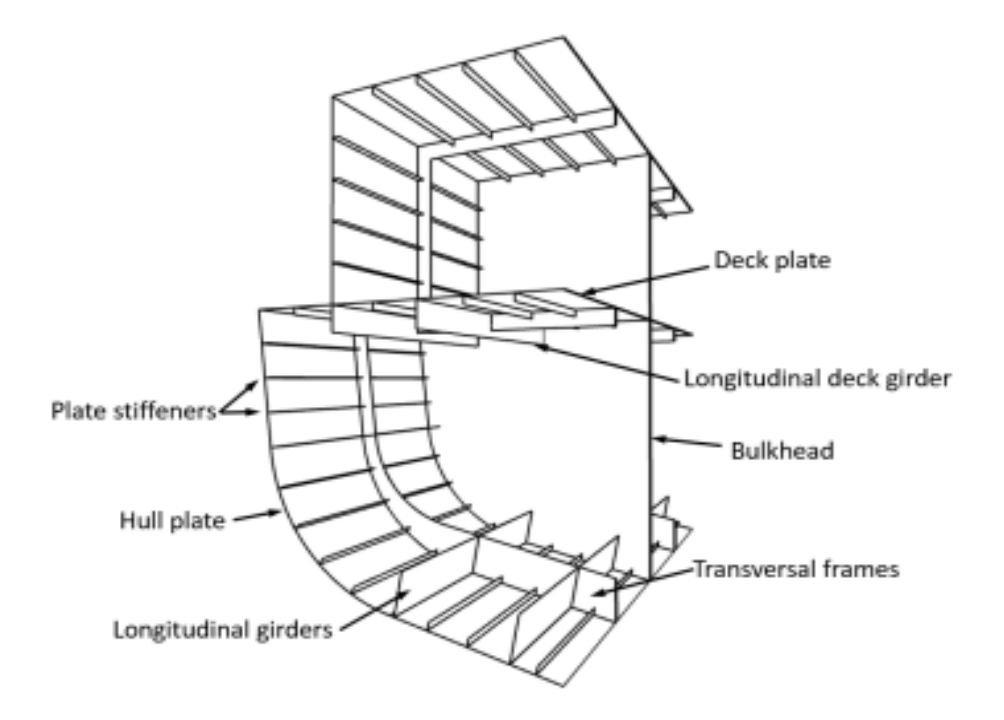


Figure 1-1: Section of a ship structure illustrating the principal structural components [11].

Figure 1-1 shows the main structural components of a ship's hull, which act as the foundation for its design and strength. These components must work together to endure operational stresses. The key components typically shown in these diagrams include:

- **Hull**: The hull is the outer skin of the ship, providing buoyancy. It withstands all hydrostatic and hydrodynamic pressures exerted on the hull [3].
- **Bulkheads**: Bulkheads are vertical partitions that increase the ship's structural strength and sub-divide its interior for additional safety [3].
- **Girders and Frames**: Girders and frames stiffen the hull to oppose bending and shearing forces, whilst distributing the load effectively [2].
- **Decks**: Decks are flat surfaces that support cargo and equipment while also promoting the overall strength of the structure [2].
- **Stiffeners**: These are secondary structural components strengthening plates and panels [12].

These components must synergise to withstand complex loading conditions over the ship's operational life.

1.3 Mechanical Problems and Structural Challenges

The mechanical challenges in relation to ship design are the basics of naval architecture. It is paramount to achieve a balance between strength, stability, weight and cost for safety and efficiency in operations [13]. The primary challenges entail:

- **Structural Strength:** Ships can withstand the forces generated by waves, cargo and environmental loads. Hulls are designed to resist hydrostatic and hydrodynamic pressures without experiencing fatigue or failure [2].
- **Stability:** This is the ability of a ship to avoid capsizing. The centre of gravity, buoyancy and overall design of a ship significantly influence its stability and performance [14].
- **Weight Management:** Using advanced materials and innovative design techniques, weight can be reduced to boost fuel efficiency while maintaining the structural integrity of a ship [15].

These challenges are fundamental to developing ships that satisfy modern safety, performance and economic requirements.

1.4 Challenges Associated with Optimising Ship Structures

There are four key considerations within design optimisation:

- 1. **Cost:** The purpose of the optimisation is to minimise the cost, which can, in some cases, be simply the financial cost of manufacture, but can, in some cases, consist of multiple distinct objectives. In this case, ship structure optimisation seeks to minimise financial cost and structural weight, while maximising the safety of the overall design. In general, reducing structural weight also reduces manufacturing costs, but the effect of material selection on cost needs to be factored in. Improving design safety also tends to increase structural weight and overall cost, and so the three objectives can be competitive [16].
- 2. Constraints: Design constraints take many forms and are defined to ensure the final product is within spec and safe to operate. Stresses must not exceed the safe limits for the chosen materials; structural deflection under normal operating conditions must also be within limit, and there should be no risk of buckling; additional constraints come

from international standards for ship design; and the customer will inevitably impose further constraints depending on expected cargos and operation [6].

- 3. **Variables:** The ship structure is highly complex, with many components (girders, frames, stiffeners, etc.). Associated with each of these are material selection, steel thickness, and, in some cases, even the number of such components within the design. An important first step of optimisation is determining which of these many variables is the most critical in order to reduce the scale of the problem [17].
- 4. **Computation:** Ship structure optimisation not only requires a complex model to create with many design variables and many design constraints, but the essential task of evaluating each design to determine the stresses and deflections for the required load cases is time-consuming. The brute-force approach of evaluating tens of thousands of potential ship designs is not a realistic option [10].

Optimising ship structures entails creating designs that capitalise on strength, stability and safety while minimising weight and cost, and faces a number of challenges:

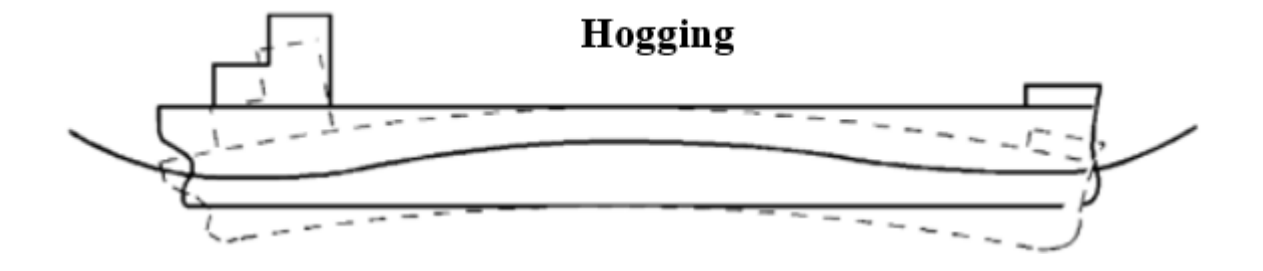
- 5. **Conflicting requirements:** The optimisation of ship design comprises balancing competing requirements arising from constraints pertaining to design and objectives [18]. For instance, balancing performance, costs, and safety in a ship's design can be incredibly demanding [19].
- 6. **Stricter rules and regulations:** The optimisation of ship structures is complicated when considering the laws and regulations pertaining to safety, along with other relevant factors. The design process must guarantee that vessels comply with seaworthiness requirements and can endure severe weather conditions [20].
- 7. **Multi-objective optimisation:** Optimising ship structures necessitates balancing weight reduction, savings in production costs and maintaining strength and stability. Nonetheless, this undertaking can create substantial challenges [21].
- 8. **Computational challenges**: When designing ship structures, it is imperative to employ fast and efficient finite element methods, with the aim of analysing large and complex thin-walled steel structures, for instance ship hulls. Conversely, this presents a considerable computational challenge [22].

- 9. **Several design variables**: The structural design of a ship comprises numerous design factors, incorporating the size and shape of the hull and the placement of structural components. Optimising these factors can be complex, as well as time-consuming [10].
- 10. **Design constraints**: Constraints relating to equality and inequality are exploited to guarantee that the optimised design meets the specifications. Nevertheless, working within these constraints adds complexity to the optimisation process [23].
- 11. **Objective functions**: Identifying the objective functions for ship structural optimisation can be challenging, predominantly when seeking to achieve conflicting goals, for example minimising production costs and reducing steel weight [24].
- 12. **Managing complicated geometries**: Optimising ship hulls can present challenges on account of their complex geometry [22].
- 13. **Practical application:** Employing the results in practice is frequently demanding owing to the issues connected with manufacturing ship hulls with the appropriate shape. For instance, problems can occur when the hull is too thin to accommodate propulsion systems and when a ship has inadequate capacity [10].

Optimising the structure of a ship is an elaborate task that consists of balancing various objectives, such as weight, cost, safety and the environmental impact. Engineers and designers must not only overcome computational challenges but also take into account the distinct requirements of modern ships, for example their potential for autonomous operation [25].

1.5 Typical Loading Conditions

When navigating rough seas, a ship experiences wave-induced forces that induce "Hogging" and "Sagging" motions, as shown in Figure 1.2.



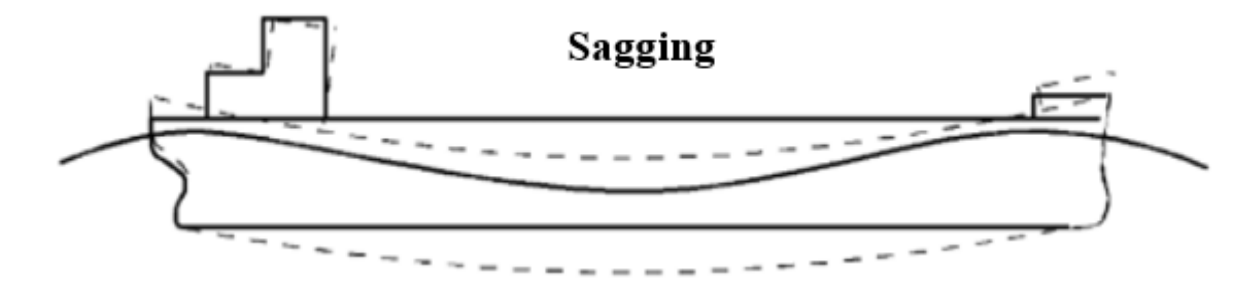


Figure 1-2: The effect of Hogging and Sagging on a ship's hull [3].

Figure 1-2 shows the impact of Hogging and Sagging on a ship's hull, exhibiting the basic principles of load distribution attributable to wave-induced motions.

- **Hogging:** Hogging appears when the middle of the ship is raised on the crest of a wave, while the bow and stern remain unsupported in a trough. The motion produces tensile stresses along the deck and compressive stresses along the bottom of the hull [26].
- **Sagging:** Conversely, when the bow and stern are supported by the crest of a wave and the midsection is unsupported in the trough of a wave, sagging arises. Sagging produces compressive stresses on the deck and tensile stresses on the bottom [26].

Furthermore, the interaction of the ship with waves depends on its heading in relation to the direction of the waves, as shown in Figure 1-3.

- **Head Sea** (**Longitudinal Sea**): During a Head Sea condition, the waves meet the ship head-on at an angle of 180 degrees relative to the heading of the ship. This can significantly impact the stability and operational efficiency of the ship with waves that result in steep pitching [27].
- **Beam Sea (Transverse Sea):** Beam Sea refers to waves that come against the vessel from the side, i.e., at a 90° angle to its course. This direction of the wave is usually associated with the heavy rolling of the ship [27].
- Oblique Sea: Oblique Sea is a wave condition whereby waves approach a ship at an angle that is neither head-on nor directly from the side. The waves come at an intermediate angle relative to the ship's heading, which can vary but is neither 0, 90, or 180 degrees. It involves, therefore, a combination of head and beam sea conditions with a complex loading response of the hull. Wave forces interacting with ship motions may induce torsional moments and considerable structural stress, increasing the possibility of failures, especially in open ships [28].

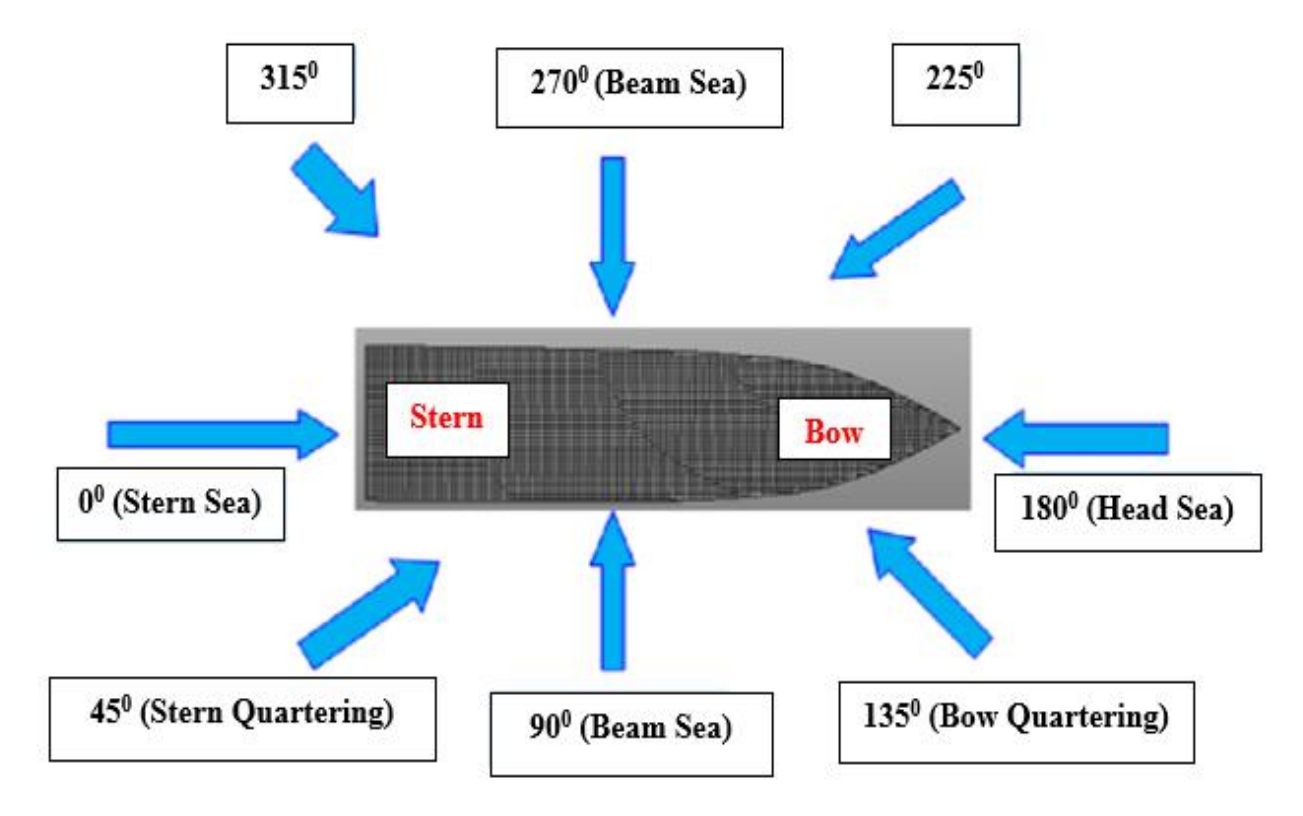


Figure 1-3: Heading angle of the ship against the wave [29].

Knowing various loading conditions in designing safe and structurally sound ships under different operational situations is essential.

1.6 Materials and Innovations in Ship Construction

Advanced materials and designs are playing a crucial role in tackling the challenges encountered in shipbuilding, generating improvements in performance, sustainability and adaptability [30]. The following are some of the innovative materials that are extensively applied in shipbuilding:

• Steel: Steel remains the most commonly used material in shipbuilding on account of its extraordinary strength, durability and cost-effectiveness. High-strength steels certified by different classification societies, such as Bureau Veritas (BV) and The American Bureau of Shipping (ABS), combine the toughness and resilience that are necessary to deal with harsh marine conditions. Steel was chosen for the studied ship owing to its reasonable price, excellent performance in adverse conditions and the ability to meet the structural requirements [31].

- **Aluminium Alloys:** Aluminium alloys are light and extremely resistant to corrosion. Therefore, they are suitable for superstructures and high-speed vessels [32].
- **Titanium Alloys:** Titanium alloys are favoured for their high strength-to-weight ratio and excellent corrosion resistance. Though expensive, they are often used in specialised marine applications and are ideal for critical components [33].
- **Ferrocement:** This cement and steel composite is made from mortar reinforced with steel wire mesh. For bigger hulls, it provides durability and is reasonably priced [34].
- **Fibre-reinforced and Composite Materials:** Glass Fibre-Reinforced Polymers (GFRP) and Carbon Fibre-Reinforced Polymers (CFRP) are generally acknowledged for their high strength-to-weight ratios, corrosion resistance and durability. GFRPs are extensively employed in smaller vessels, while CFRPs are preferred for high-performance ships, for example racing yachts [35].

Steel and composite materials have a vital role to play in modern shipbuilding. Steel, notably the high-strength type, certified by classification societies, offers durability and economy, which is imperative in harsh marine environments [36]. Composites include Glass Fibre-Reinforced Polymer (GFRP) and Carbon Fibre-Reinforced Polymer (CFRP), which have a high strength-to-weight ratio and resistance to corrosion, making them suitable for lightweight and high-performance applications [37]. This research focuses on steel materials in order to attain optimal structural performance and sustainability.

1.7 Motivation for Ship Structural Optimisation

Specifically, the emphasis on sustainability and efficiency within shipping underlines the urgent need for optimisation in the field of ship hull structure.

- **Economic Considerations:** With increased fuel and material costs, designs must consider approaches to reduce weight and consequently production costs. Structural optimisation generates substantial savings in material use and production costs [3].
- **Environmental Objectives:** To increase the sustainability of maritime transport, weight-optimised ships will have a significant role to play in further reducing emissions. The development of an energy-efficient hull design is fundamental as regards the decarbonisation of the naval industry [38].

• **Regulatory Requirements:** Stringent international regulations also support innovation, leading to improvements in safety and increasing operational performance. Classification societies produce guidelines to guarantee that ship structures conform to safety and environmental standards [2].

Optimisation of the ship hull is essential in response to the economic, ecological and regulatory challenges, as it gives rise to a more sustainable and efficient shipping industry.

1.8 Problem Statement

The design and optimisation of ship structures maintain a delicate balance in guaranteeing that weight, cost and environmental impact are met, in conjunction with structural strength, operational safety and performance. In most conventional approaches, fuel efficiency and management have not been given precedence, culminating in increased operational costs and extensive environmental consequences.

This research exploits property optimisation so as to achieve significant weight reductions in essential components, for instance the hull, while rigorously maintaining safety and performance. The study will establish a new concept in ship design that will meet these challenges and further augment operational efficiency and environmental sustainability.

The study reveals contemporary optimisation techniques and sophisticated structural design methods to deal with the significant challenges identified in shipbuilding. Specifically, it evaluates the property optimisation methods employed in steel mid-ship structures, with the intention of minimising over-scantlings (the structural dimensions of plating and stiffeners) and attaining an optimum strength-to-weight ratio. The results will present novel approaches naval architects and designers can exploit to develop 'green' and cost-effective vessels that will considerably improve efficiency, performance and sustainability in hull construction.

1.9 Aims & Objectives

1.9.1 Aim

To develop and implement advanced optimisation techniques concerning ship structural design, in order to increase safety, performance, cost-effectiveness and environmental sustainability.

1.9.2 Objectives

1. Develop and Analyse a Three Cargo Hold Model for the studied Ship

- To evaluate maximum stresses and deflections under various operational conditions to guarantee structural integrity.
- To assess longitudinal strength under oblique and head sea conditions, while considering the torsional effects in both open-deck and closed-deck configurations and conduct a comparative analysis.

2. Identify Key Influencing Factors

- To investigate the variables influencing stress distribution, torsional behaviour and production costs.
- To develop regression models to quantify relationships among these variables. To develop regression models to determine the relationships between these variables.

3. Incorporate Critical Design Considerations

- To guarantee stress levels remain below critical thresholds to prevent corrosion and maintain long-term integrity.
- To optimise lightship weight in order to increase economic performance by maximising carrying capacity.
- To minimise structural maintenance costs by means of effective design strategies.
- To consider environmental and operational challenges, including collision management and emissions reduction.

4. Design an Optimisation Framework

- To formulate a strategy to reduce structural weight and production costs while adhering to safety and regulatory constraints.
- To achieve a balance between structural integrity, economic viability, and environmental sustainability.

1.10 Thesis Organisation

This thesis is structured into seven chapters, each exploring a vital aspect of ship structural optimisation and its application in contemporary ship design.

Chapter 1: Introduces the significance, challenges, motivations, and objectives of ship structural optimisation in contemporary design and construction.

Chapter 2: This chapter provides the foundational context for the research by reviewing past studies and methodologies, highlighting gaps that this thesis aims to address.

Chapter 3: Examines the longitudinal strength of ship hulls under varying sea conditions, with a focus on structural behaviour. It introduces calculation models and techniques for assessing longitudinal strength and compares analytical and numerical results.

Chapter 4: Examines hull girder deflection under different loads and conditions, detailing methods and tools used for analysis. The findings offer insights into structural performance and integrity for future design considerations.

Chapter 5: Conducts a fractional factorial design study to identify key parameters influencing Von Mises stress, torsional stress, and production costs. This chapter highlights the experimental setup and identifies factors critical for structurally sound and cost-efficient ship designs.

Chapter 6: Explores the optimisation and validation process for ship hull structures, addressing design variables, constraints, and objectives. Comparative analyses evaluate performance, durability, and the practical applicability of optimised designs.

Chapter 7: Summarises key findings, contributions, and the broader implications of this research on ship design and optimisation. Recommendations for future studies and applications are also provided.

This thesis offers a comprehensive framework for optimising ship hull structures, addressing both theoretical and practical challenges in ship design.

1.11 Expected Results and Contributions

By employing advanced optimisation techniques, this work deals with the drawbacks associated with traditional design methods, giving rise to innovative solutions that increase safety, operational efficiency and sustainability whilst reducing costs. The expected contributions comprise:

- Enhanced Safety: Guaranteeing heightened structural integrity reduces the risk of failure and maximises operational reliability under various adverse conditions.
- Improved Operational Efficiency: Improved structural designs will reduce the operational costs and increase economic viability.
- **Promoted Environmental Sustainability:** Global sustainability goals are effectively promoted, given that improving material use significantly reduces emissions.
- Boosted Economic Competitiveness: Reduced production costs will ensure that shipbuilding is more available and, consequently, more innovative, establishing global competitiveness in the sector.

The Fractional Factorial Design technique, NSGA-II algorithm and Finite Element Method (FEM) can aid in resolving problems in contemporary ship design.

Chapter 2

Literature Review

2.1 Introduction

The study of ship hull structural optimisation involves designing and improving the structure of ships to enhance their performance, safety and efficiency. This field is crucial in naval architecture and engineering because a ship's structural design significantly impacts its stability, strength and ability to withstand environmental loads such as waves and wind. Ship structural optimisation is also of relevance to the broader maritime industry by reducing the weight of ships and their greenhouse gas emissions, thus mitigating their environmental impact [6].

The core principle of structural optimisation is to maximise or minimise an objective function that quantifies a design's fitness subject to specific constraints. Optimisation techniques incorporate various approaches, including sizing, topology, material selection and shape optimisation. Structural optimisation has gained increasing importance in engineering over recent decades and is indispensable in design. Traditional formula-based design methods may not always yield the optimal solution. Constructing an optimisation methodology that accurately represents the real problem when dealing with a particular structure or structural elements is crucial for optimal designs that are effective and trustworthy [39].

Identifying solutions that meet design constraints, enhance performance and reduce production costs can be achieved by employing optimisation techniques in ship construction to permit ship designers and engineers to make more judicious decisions, resulting in a more efficient ship structure [40].

Ship structural optimisation traces its origins to the embryonic stages of ship design and construction. In recent decades, the field has witnessed the development of numerous innovative and specialised hull configurations, structural enhancements, propulsion systems, dimensional variations, and other key parameters. Integrating advanced design technologies has empowered shipbuilders to rapidly iterate via multiple design iterations, revealing the effects of even minor design modifications on ship performance. These advancements in shipbuilding technology have ushered in an era of heightened precision and efficiency in ship design and optimisation. This development has empowered shipbuilders to capitalise on the benefits of

these developments [41]. Over the past few decades, structural optimisation has been effectively applied to optimise structures and mechanical systems [42]. In most cases, the constraints utilised for ship structural optimisation can be traced back to classification societies or direct calculations. Therefore, technical improvements and the need to enhance ship performance while complying with classification society standards have produced ship structural optimisation's historical foundation and advancements [6].

Ship structural optimisation techniques have significantly progressed, achieving numerous notable milestones and breakthroughs. During the initial phases, ship structural design and optimisation were primarily influenced by empirical rules and experience. Engineers apply established classification regulations and guidelines to design ships. The advent of computational methods and tools like finite element analysis (FEA) permitted more accurate modelling and analysis of ship structures [43].

Over time, engineers expanded their approach to ship structural optimisation by considering multiple objectives, including weight reduction, cost-effectiveness and safety. Through multi-objective optimisation techniques, they can realise trade-offs between conflicting goals and achieve more balanced designs [44]. The integration of topology and shape optimisation techniques has generated significant advancements in optimising ship structures to enhance structural performance and reduce weight by improving the layout and shape of various ship components [45].

Optimising the crashworthiness of ship structures has become a crucial aspect of their design. Various approaches have been developed to improve their ability to withstand collision and impact forces, ensuring the safety of both the ship and its occupants [46]. Ship structural optimisation has evolved toward a more rational-based approach, employing sophisticated procedures and techniques based on engineering analysis and scientific principles. This approach considers various aspects, including hydrodynamics, structural mechanics, as well as material properties [47].

2.2 Review of the Literature

The shipbuilding industry has made substantial progress in optimising ship structures by way of significant developments and innovations. This progress has improved ship design performance, safety and cost-effectiveness. This sector's evolution is constantly driven by ongoing research and technical improvements.

2.2.1 Multi-Objectives Optimisation for Ship Design Techniques

Rahman (1996) introduced a model to optimise tee-stiffened, flat-bar stiffened and corrugated panels commonly used in ship structures. The model was tested against various design factors, for instance loads, span variation, price ratio index (labour rate to material price ratio), and design requirements (minimal cost, minimum weight, and equal priority). The model proved their effectiveness in real-world applications, providing a beneficial guide to improve ship structures while balancing competing design requirements. Similarly, research into Pareto-optimal designs has demonstrated the designer's ability to prioritise specific criteria [48].

Rigo and Liege (2003) developed an integrated software component called LBR5, which optimises ship cost and weight. This program enables users to analyse large-scale structures, including up to 100 panels, 900 design variables and 5000 constraints, and manage multiple loading scenarios. By utilising the optimisation techniques provided by LBR5, hull tank building costs can be reduced by 8.5%. Conversely, it should be noted that the optimal overall cost results in a 3.4% increase in weight [49].

Klanac and Jelovica (2007) created a genetic algorithm to optimise the midship section of an 88 m-long aluminium fast ferry while ensuring compliance with relevant structural, technical and classification regulations. The study demonstrated a significant 10% weight reduction and a 6.5% reduction in the vertical centre of gravity (VCG), leading to a clear Pareto front, illustrating the practicality of optimisation for high-speed vessels [50].

Sekulski (2009) applied the evolutionary algorithm to optimise the hull constructions of high-speed catamarans. The study achieved a more efficient and lightweight design by adjusting the plate thickness, section size and spacing characteristics, while meeting design requirements [10].

Yu et al. (2010) introduced a ship structural optimisation technique to cut material and labour costs without compromising safety standards. This approach achieved an optimised structure that weighs 991.8 tonnes, which is lighter than the initial 1099.7 tonnes [51].

Caprace et al. (2010) devised a technique to optimise the dimensions of ship sections, considering various factors, such as production cost, minimum weight and maximum moment of inertia, using the LBR-5 software. The researchers observed that increasing the weight of a ship by 10% to 15% resulted in only a 3% reduction in price, while a weight increase of 15%

to 18% brought about a 12% rise in manufacturing costs, highlighting the trade-offs in structural design [52].

Ma et al. (2013, 2014) established a robust multi-objective optimisation technique employing the Pareto Simulated Annealing (PSA) algorithm to improve tanker design by reducing weight and cost while minimising buckling and stress levels. As a consequence, its weight was reduced to 59,370 kilograms, resulting in a significant 2.5% weight reduction. Additionally, optimising the hull girder cross-section scantlings for a 200,000-tonne oil tanker reduced the weight by 2.1%, from 270.4 tonnes to 264.6 tonnes, while enhancing its ultimate strength and safety [53, 54].

Sekulski (2014) proposed an innovative evolutionary approach to ship design that optimises the structural components of large spatial sections of ships. By incorporating multi-objective functions, this approach contributes to more cost-effective and efficient ship hull designs, making it an impressive tool as regards optimising ship structures [55].

Yu et al. (2015) presented a new method to improve the inner shell of ships, employing a parametric technique that involved a genetic algorithm to optimise the design and increase the volume of cargo oil tanker/cargo hold. The results established that this approach successfully improved the inner shell structure of ships, culminating in greater efficiency and safety [56].

Akpan et al. (2015) proposed a method for designing ship structures to reduce weight while satisfying moment and buckling constraints. This technique was applied to two ships with varying complexities, achieving a total weight reduction of 5.6% in ship structures by combining minor modification [57].

Bayatfar et al. (2019) established a novel approach to optimise the structure of a three-dimensional midship section of a RoPax ship using a unified design platform that combined well-known tools, such as AVEVA Marine®, ANSYS® and MODEFRONTIER®. This approach improved the efficacy of ship design and demonstrated reliability, generating optimal designs within a reasonable time frame during the contract design phase [58].

Nwaoha and Adumene (2019) examined a ship safety assessment and optimisation approach. The study proposed an integrated strategy that combines artificial intelligence and multi-criteria decision-making techniques to optimise ship structural safety. The researchers considered various factors and applied fuzzy set theory to achieve their primary objective. The findings intimate that the proposed method can effectively evaluate and improve the structural safety of

passenger ships. The TOPSIS model was also adopted to reveal each factor's importance logically. This research provides useful insights into ship design and presents practical advice with respect to enhancing the safety and effectiveness of ship structures [59].

Andric (2019) presented a ground-breaking methodology for decision support in ship structural design. It combines the topological (number of decks), structural (material and cross-section dimensions) and layout (compartmentation) aspects of the ship's structure. The study uses the design of a Roll-On/Passenger (RO-PAX) ship structure by proposing a systematic and effective method for the multi-objective and multi-level design optimisation problem, opening the way for more enhanced and sustainable ship structures [40].

Palaversa et al. (2020) extensively examined techniques for ship structural design and optimisation. The research covered a range of areas, including advanced materials, structural optimisation methods, design analysis techniques, in conjunction with the emerging trends and challenges in the field. The study emphasised the importance of environmental factors, such as wave forces and corrosion in the design of sustainable ship structures [47].

Louvros et al. (2022) employed a multi-objective optimisation strategy to design the internal layout of innovative ships in the early stages. It emphasises the importance of considering different goals and trade-offs to create practical and efficient ship designs. The procedure seeks to determine the most appropriate solutions for various design objectives by relocating ship components [60].

Qiu et al. (2023) developed a surrogate model to optimise ship collision scenarios, integrating orthogonal testing with backpropagation neural networks (BPNN) and advanced algorithms. This approach significantly improved crashworthiness while adhering to lightweight design constraints [33].

Qiu et al. (2023) proposed a novel approach to create an effective surrogate model to optimise collision scenarios by considering various working circumstances that combine orthogonal testing with a backpropagation neural network (BPNN) and advanced genetic algorithms. The study established the efficacy of the proposed strategy in improving the ship structure's crashworthiness and provides constructive guidance for engineering design in this domain [46].

2.2.2 Knowledge-Based Engineering in Ship Design

Cui and Wang (2013) developed two ship structural design approaches employing knowledge-based engineering (KBE) to evaluate the yielding and buckling strength. Their method achieves three-dimensional rapid optimal design by utilising parametric technology, cutting costs and boosting outcomes in deterministic design processes [61].

Guan and Yang (2016) proposed a method to enhance the accuracy and efficiency of ship structural design and optimisation. Their approach integrates parametric technology and knowledge-based engineering to establish a knowledge base for ship structure design, allowing rapid three-dimensional optimisation. According to their research, this technique can significantly improve the ship's strength, resulting in lighter and less expensive vessels, demonstrating that knowledge-based engineering can enhance the quality and efficiency of ship structures [62].

Further refining their approach, Guan and Yang (2018) presented a method for designing and optimising ships by integrating parametric technology with knowledge-based engineering. It derives the scantlings of ship structural components based on the knowledge base and Non-Uniform Rational B-Splines (NURBS) interpolation, using positional parameters to drive the positions of ship structure components. The technique generates stable, efficient and precise three-dimensional design of ship structures [63].

2.2.3 Ship Hull Design and Materials

Huang and Wang (2009) established a collaborative optimisation (CO) mathematical model to design ship hulls that incorporate a unique objective function which considers static and dynamic analyses. Accordingly, the design of the ship's hull met the requirements and reduced the total weight from 39,712.96 to 35,769.18 kg, with a peak design stress of 142.99 MPa below the limit [64].

Papanikolaou et al. (2010) developed a procedure to construct energy-efficient Aframax tankers, achieving an 8% increase in cargo capacity, a 2% reduction in the weight of the steel cargo block, together with a 10% improvement in the accidental petroleum outflow parameter while complying with legal requirements. This design is better than previous references and is practical and environmentally sustainable [65].

Kim and Paik (2017) developed an automated system for optimising the design of hull structural scantlings in merchant cargo ships using plate-shell finite element modelling. The paper compares the new technique with the existing design approach and proves that it effectively reduces weight and increases safety [44].

Saravanan and Kumar (2021) conducted a comprehensive analysis of the impact of marine conditions on marine composites. They stressed the importance of using eco-friendly composite materials derived from renewable and biodegradable sources in maritime engineering. Their analysis implies that incorporating advanced composite materials in navy ships could enhance their performance while reducing maintenance costs [66].

Pereira and Garbatov (2022) proposed a risk-based ship design integrating safety, efficiency, and cost considerations. Their approach optimised cargo capacity and reduced risks using SHDMF and MADM techniques throughout a ship's lifecycle [56].

Pereira and Garbatov (2022) developed an innovative risk-based ship hull structural design procedure that integrates capital and operational expenditure, cargo capacity and energy efficiency. The chosen design approach minimises costs and improves efficiency while increasing cargo capacity and reducing risks, exploiting ship hull design magnification factors (SHDMF) and multi-attribute decision-making (MADM) techniques to ascertain the best design solutions for all scenarios throughout the ship's service life [67].

2.2.4 Ship Structure Optimisation Models

Hamada et al. (2009) introduced a novel technique to optimise the midship section of a bulk carrier using various stages and regression analyses to determine the best design, which differed from the traditional method. Their final design weighed 4,138 tonnes, only 2 tonnes lighter than the conventional approach [68].

Motta et al. (2011) developed the LBR-5 software to improve a non-cylindrical ship to construct mega yachts. Their study revealed that while the initial optimisation assessment increased costs and weight, the subsequent optimisation analysis eventually reduced them by 20% and 8%, respectively, compared to the original scantlings [23].

Rigo and Caprace (2011) conducted a study on the relationship between "Design" and "Optimisation" in the context of ship structures. Their research revealed that optimising the structural design of a ship can lead to cost savings, decreased steel usage and enhanced

performance. This optimisation process can be applied to various ship components, including its side shells [6].

Bayatfar et al. (2013) proposed a pioneering approach to enhance ship structures during the initial design phase. This method helps improve the design of ships and offshore structures by evaluating the objective function and constraints. The method is expected to improve the structural design of ships and boost their performance throughout their operational life [4].

Zanic et al. (2013) demonstrated a promising approach to structural design for RoPax ships. Their strategy yielded a weight reduction of 6.97% compared to the original model. The research results encompass a broad range of information on the ship and offshore construction design, including the implementation of design support systems, structural optimisation techniques, surrogate modelling and sensitivity analysis [69].

Elhewy et al. (2016) conducted a study using a blind search technique on an offshore supply ship (OSV). This study reduced the weight of ships by 42% or 121.9 tonnes while maintaining their structural integrity. This weight reduction offers various financial benefits, including lower fuel consumption, reduced initial costs, improved manoeuvrability and increased lightship service speed in ports and canals [70].

Brown et al. (2016) optimised a large and complex structure using a hierarchical multi-level collaborative optimisation approach, considering weight, safety and vertical centre of gravity. The case studies demonstrate that the approach can quickly identify an optimal design, even if the initial design was suboptimal, making it a valuable and attractive tool for maximising the structure of naval vessels [71].

Li et al. (2018) presented an optimisation approach for a 32.98 m fibre-reinforced plastic (FRP) fishing boat ship structure using the artificial bee colony (ABC) algorithm. The results demonstrate that the program implemented can achieve a structural weight reduction of approximately 8.31%. Consequently, this study contributes to developing environmentally friendly and energy-efficient ships [72].

Raikunen et al. (2019) presented a method to enhance the design of passenger ships during the early concept phase. The Particle Swarm Optimisation (PSO) algorithm was employed to decrease the weight of the steel structure in the optimisation process. The study found that relaxing the stress significantly impacted the ship's overall mass [73].

Putra et al. (2019) proposed a hybrid genetic algorithm (G.A.) to address the optimisation challenge of stiffened plate layouts. Factors such as stiffener spacing, plate thickness, and the type and quantity of stiffeners were considered throughout the optimisation process. The optimisation outcomes promoted the efficacy of the suggested hybrid G.A. in identifying the most favourable solutions for each design variable [74].

Numerous ideas, models and methods have enhanced ship construction, for example:

- 1. **Models for Yield, Buckling and Fatigue**: In ship construction models, it is common to factor in yield strength, buckling resistance, in addition to fatigue life. These simulations help ensure the structural plan withstands the expected loads and operational conditions [51].
- 2. **Rational Design Methods:** Using rational methodologies, ship structures can be approached systematically and logically. To improve efficiency and attain the best structural layout, it is vital to create algorithms and optimisation techniques for automation [75].
- 3. **Optimisation of Material Selection:** Material cost minimisation techniques determine the choice of materials for ship structures. These techniques aim to develop cost-effective designs that fulfil the required structural performance while optimising the type of materials and plate thickness [76].
- 4. **Analysis at Multiple Levels:** Multi-level analysis entails dissecting the ship's structure into various levels or sections. Utilising multi-level analysis allows for a more comprehensive evaluation and optimisation of each component while considering its connection and dependencies [75].
- 5. **Super-Element Modelling:** Super-element modelling is a method that breaks down complicated structures into a collection of smaller, interconnected elements, making it easier to evaluate them. This method makes it possible to analyse and improve ship structures effectively [75].
- 6. **Pareto Optimisation:** The process aims to identify solutions that optimally balance competing design objectives. It permits designers to investigate several options and make sensible choices based on various parameters [40].

These are just a few examples of the various ideas, models and approaches utilised in previous research relevant to optimising ship structures. The optimisation of ship structures is an

evolving field, with researchers continually developing new strategies and methods to boost design and functionality.

2.3 Structural Analysis Techniques

The structural analysis of a ship is a sizable part of the design process and several different approaches may be taken to measure a ship's structural integrity. The following are some of the methods that are most commonly employed:

- 1. **Finite Element Analysis (FEA)**: Discretisation of a structure's geometry occurs when it is divided into a mesh composed of finite components, with each element possessing a specific level of accuracy. One of the key responsibilities in the finite element analysis of a structure requires the generation and specification of all the necessary data for the computational processes [77].
- 2. **Boundary Element Method (BEM)**: The boundary element method (BEM) is a numerical technique used to solve engineering and physical problems defined in the context of boundary integral equations. The divergence theorem and basic solutions are used to convert the main differential equations of the BEM to boundary integral equations. The BEM methodology divides the structure into the boundary and the interior [78].
- 3. **Matrix Stiffness Method**: The stiffness method, also known as the displacement method, is a fundamental technique used in the matrix analysis of structures. The mathematical methodology used in structural analysis involves dividing a given structure into smaller parts, which are then scrutinised individually. The stiffness method is considered a suitable approach for computer programming and is generally used in structural engineering [79].
- 4. **Grillage Analysis:** The grillage method is a standard technique that is extensively used to analyse the structure of ships [80]. This process involves calculating the stress and deflection in the grillage beams, which is subsequently used to determine the overall strength and stiffness of the ship's structure [81].

These are a few typical approaches applied to examine ship structures. Depending on the specific needs of the design project, more complex computational methods, such as computational fluid dynamics (CFD) and multi-body dynamics analysis, may also be employed.

2.3.1 Comparison and Evaluation of Various Optimisation Techniques

Many industries use optimisation techniques to solve complex problems and improve efficiency. Optimisation strategies entail analysing their strengths and weaknesses and evaluating the latest advancements in ship structural optimisation:

2.3.1.1 Topology Optimisation Approaches

The objective of topology optimisation techniques is to ascertain the most effective placement and distribution of materials within a designated design area with the aim of achieving the user's desired performance standards [82].

Advantages of Implementing Topological Optimisation Methods:

- Capability to generate creative and effective ideas by way of exploring the entire design space.
- Ability to adapt to different design constraints and objectives.
- Potential to reduce weight and material requirements while maintaining structural integrity.

Drawbacks of Topological Optimisation Methods:

- High computational cost and complexity, especially for larger problems.
- Challenges associated with handling discrete variables and production limitations.
- Sensitivity to numerical parameters and initial design conditions.

Recent developments in density-based and level-set approaches have yielded prominent advancements in topology optimisation. Challenges such as dealing with complex constraints, scalability and incorporating manufacturing considerations into optimisation still need to be addressed [83].

2.3.1.2 Ranking Optimisation Approaches

The primary objective of ranking optimisation methodologies is to adapt recommendations according to the feedback provided by the user's preferences [84].

Advantages of Ranking Optimisation Strategies:

- Personalisation recommendations tailored to user preferences.
- Gradual adaption of recommendations in response to modifying user feedback.
- Potential to increase user engagement and satisfaction.

Drawbacks of Ranking Optimisation Strategies:

- Dependence on precise and up-to-date user feedback for efficient adaption.
- Challenges associated with cold-start problems and data sparsity.
- Potential to create filter bubbles and reinforce pre-existing biases.

Emerging techniques for improving recommendation systems by means of ranking optimisation exhibit promise. Conversely, further research is required to address data quality, privacy and fairness in recommendations [84].

2.3.1.3 General Optimisation Approaches

Numerous techniques exist as regards tackling non-linear, constrained optimisation problems within the scope of general optimisation methods [85].

Advantages of General Optimisation Techniques:

- Flexibility to handle a wide range of objective functions and constraints.
- Accessibility to a multitude of algorithms and solvers.
- Potential to locate globally optimal solutions.

Drawbacks of General Optimisation Techniques:

- Sensitivity to parameter adjustment and problem design.
- Computational complexity, particularly for large-scale problems.
- Challenges in connection with non-convex problems and discrete variables.

In recent years, there have been significant developments in general optimisation techniques, focusing on algorithm development and effectiveness. Nevertheless, challenges persist

concerning high-dimensional problems, uncertainty and convergence issues in complex optimisation landscapes [85].

2.3.2 Modern Optimisation Techniques

In engineering, non-traditional optimisation methods have gained popularity on account of their ability to address complex problems effectively. These methods encompass genetic algorithms, simulated annealing, particle swarm optimisation, ant colony optimisation, neural network-based optimisation, besides fuzzy optimisation. Computerised search and optimisation algorithms, known as genetic algorithms, were introduced by John Holland in 1975 and are rooted in the principles of natural selection and genetics. Simulated annealing, developed by Kirkpatrick, Gelatt and Vecchi, draws inspiration from the cooling process of molten metals.

By reason of their parallel processing power, neural network methods rely on the enormous computational capacity of the nervous system to address cognitive issues in the context of massive volumes of sensory data. The technique was initially applied to optimisation in 1985 by Hopfield and Tank. Fuzzy optimisation methods were developed to handle optimisation issues, including design data, an objective function, besides loosely articulated linguistic constraints. In 1986, Rao was the first to mention fuzzy approaches for single- and multi-objective engineering design [86].

2.4 Key Findings

Ship structural optimisation aims to modify ship structures efficiently and safely within a specified time frame. The following are the primary outcomes achieved via the optimisation of ship structures:

1. Optimising ship scantlings within the Multi-structures Module cuts fuel consumption and greenhouse gas emissions by minimising steel weight while keeping production costs within an acceptable range. The primary focus lies in achieving cost and weight reduction through adjustments to the initial scantlings [6, 23] and determining optimal positions for structural components [87]. These findings are in accordance with the outcomes of this study, demonstrating a remarkable 10% reduction in ship weight and production costs achieved through modifications to initial scantlings (plate thickness) and the optimisation of structural component positioning (web frame and stiffener

- spacing). These results have substantial implications, enhancing safety and sustainability while simultaneously reducing fuel consumption and greenhouse gas emissions, thereby increasing competitiveness within the maritime engineering sector. These objectives are consistent with the goals of prior research, further emphasising that the insights from previous studies into scantling optimisation directly support and endorse the conclusions drawn from the findings obtained by the current study.
- 2. By integrating knowledge-based engineering and parametric technology, it is possible to achieve rapid and optimal three-dimensional ship structural design [63].
- 3. A hybrid genetic algorithm can be applied to optimise the design of the stiffening plate for the majority of the ship [74].
- 4. The selection of an evolutionary algorithm for the multi-objective optimisation of ship structural elements in large geographical sections is based on the aggregated objective function, domination properties and distance to the asymptotic solution [55].
- 5. Optimisation allows ship owners and operators to save significant costs [70].
- 6. Discrete fuzzy set theory can improve artificial intelligence and multi-criteria decision-making in safety evaluation and ship structure optimisation [59].
- 7. A probabilistic approach is preferable to a deterministic approach for designing and optimising adaptive maritime structures that depend on fluid-structure interaction for improved performance [88].
- 8. A three-panel design model that consists of corrugated, flat-bar stiffened and tee-stiffened panels can be advantageous for ship structures [48].
- 9. Ships can be designed and planned using multi-objective optimisation techniques, which may include genetic algorithms to determine the best general arrangements and layout [60].
- 10. Using parametric methods can improve the structural efficiency of ship inner shells [56].
- 11. The positions and shapes of the hatch cover's structural components are determined based on an enlarged ground structure [89].

- 12. Artificial neural networks can enhance the accuracy of ship construction predictions, leading to better designs [90].
- 13. Advanced materials such as composites can significantly enhance the structural performance of a ship [66].
- 14. Additive manufacturing can enhance ship structural design and production by enabling the creation of intricate geometries and reducing lead times [91].
- 15. Bulkhead placement in ship concept designs can be maximised using floodable lengths for various loading scenarios [92].

2.5 Emerging Trends and Potential Future Directions

Developing novel methods, tools and applications is a current trend and future direction for ship structural optimisation. There are several advancements and potential paths for this industry that are of note:

- 1. **Improving the efficiency of a ship's energy systems**: Ship energy systems are being optimised to achieve improved efficiency and lower pollution. The synthesis, design and operation of integrated energy systems must be maximised to realise this [21].
- 2. **Enhancement of marine structures:** To enhance the functionality, robustness and safety of marine structures, it is necessary to conduct further research into their design and construction [93].
- 3. **Reducing steel weight**: One area of research concerns optimising ship constructions to minimise steel weight without compromising structural integrity. This research can lower production costs and cut greenhouse gas emissions [6].
- 4. **Voyage optimisation**: Developing voyage optimisation techniques can lower the risk of fracture propagation in ship structures at sea. Structural breakdowns can be minimised by optimising the ship's route, speed and other factors [94].
- 5. Multifidelity approach: Researchers are exploring using a multifidelity technique to optimise a ship's structure. This technique involves the integration of multiple simulations and models to enhance the accuracy and efficiency of the optimisation process [95].

- 6. **Integration of artificial intelligence**: Ship structural designs can benefit from integrating artificial intelligence (AI) techniques, such as machine learning and genetic algorithms, to improve performance [21].
- 7. **Lifecycle optimisation**: When improving a ship's structure, it is essential to consider the entire lifecycle of the ship. This includes aspects such as maintenance, repairs and considering its end-of-life [96].

The latest trends and upcoming research areas in ship structural optimisation focus on enhancing the ship's efficiency, safety and sustainability. This study is in keeping with points 3 and 5, aiming to achieve a notable reduction of 10% in both weight and production costs through a multi-objective optimisation approach and the integration of 128 distinct model simulations to enhance the accuracy and efficiency of the optimisation process. Importantly, these reductions have been achieved without compromising the ship's structural integrity. Furthermore, environmental concerns are being targeted by concurrently reducing fuel consumption and greenhouse gas emissions. This comprehensive approach underlines the commitment to making significant advancements and highlights the scope and extent of the research endeavours.

2.6 Research Problem

The aim of this study is to address a significant research gap pertaining to ship structural optimisation, primarily regarding open-deck ships, such as cargo and container ships. In contrast to closed-deck ships, for which there is an extensive amount of literature on weight and production cost optimisation, open-deck ships have received comparatively less consideration. Owing to the more significant environmental loads, open-deck ships require additional reinforcement considering weight reduction while maintaining hull strength and structural efficiency. Notwithstanding that numerous studies have investigated the balance between weight reduction, structural integrity and production cost, a more integrated and economical optimisation framework specifically developed for open-deck ships is necessary. The current study develops a more integrated and effective optimisation strategy by expanding upon existing approaches.

This study focused on twelve (12) significant parameters that have a considerable influence on structural scantlings, with the purpose of simplifying the optimisation process. In comparison, other studies frequently consider a larger numbers of factors. Accordingly, the solutions are

more effective and practical as regards the problems that occur during ship structural optimisation.

The work significantly advances recent theoretical developments and practical applications in the field of ship structural design by considering both performance and financial factors. It develops a valuable approach to ship structural optimisation, essentially open-deck ships, by providing a more appropriate and workable solution to the structural problems, permitting safer and more efficient operation under real-world conditions. This work further guarantees compliance with industry standards and class society regulations. It is important to note that in many optimisation studies, the optimum solution may not always meet the highest safety and quality standards established by the maritime engineering industry.

2.7 Importance and Novelty of this Research

The research proposes several crucial innovations that significantly boost the field of ship design optimisation and benefit naval architecture and marine engineering:

- 1. **Two-stage Hybrid Optimisation Method:** The research presents a two-stage hybrid optimisation method that combines DOE with the NSGA-II algorithm employed in Python. This brings about a significant reduction in ship weight and production costs from the traditional approach when structural modifications up to 10% are targeted. These tangible results indicate the practical benefits and suggest that a substantial impact can be achieved if these findings are employed in shipbuilding.
- 2. Comprehensive Cost Allocation Breakdown: The current research provides practical information on cost allocation that is of value to decision-makers in regard to fabricating steel hulls. It will be beneficial in relation to resource allocation and improving procedures that deliver a more sustainable approach. The cost of the current model exceeds others in its understanding of this aspect of the industry, allowing it to be commonly accepted.
- 3. **Identification of Key Parameters:** By identifying the essential ship parameters that affect stresses and production costs, the study simplified and streamlined the design process. By identifying important areas for weight reduction and cost minimisation, creating a design matrix, as well as generating two regression equations for stress and

production costs, this study provides a solid foundation for further developments in ship design.

- 4. Hull Girder Stress Analysis: A thorough analysis of hull girder stress components provides crucial data related to the ship design process by quantifying the influence of various load types on the ship. This approach provides a more wide-ranging understanding of structural behaviour in comparison to traditional design load cases, providing designers with essential information for safety assessments and early design phases, specifically when determining structural scantlings under various sea conditions. By offering a more integrated understanding of structural performance across a wider range of operational scenarios, this analysis extends current practice.
- 5. **Torsion Impact and Structural Simplification:** This underlines that a closed-deck ship has minimal impact on torsion in comparison with an open-deck ships, permitting a more effective structural design.
- 6. **Longitudinal vs. Transverse Deflection:** The research underlines the importance of longitudinal deflection as opposed to transverse deflection and is fundamental in terms of optimising structural design. This approach can result in more effective and focused design methods in the shipbuilding industry, enabling future designs to be updated.
- 7. **Comprehensive Validation:** The optimised midship section is systematically tested to confirm that both the industry standards and relevant classification society regulations are followed and communicated. Furthermore, the testing boosts the practicality and reliability of the optimisation framework proposed for genuine ship design projects.

The innovations discussed are pertinent to shipbuilding aiding the pursuit of more economical and efficient ship designs without compromising on safety or sustainability. This research, together with industry-focused understanding, combines advanced computational techniques that will significantly improve ship design procedures. It has the potential to impact the future of naval architecture worldwide and transform industry standards in marine engineering.

2.8 Research Methodology

This research aims to develop a parametric cargo hold model for a multipurpose cargo ship, considering various characteristics related to the primary and significant dimensions of the hull. The proposed methodology comprises several key steps:

2.8.1 Development of the Parametric Cargo Hold Model

- **Data Collection**: Gather relevant data and specifications on the multi-purpose cargo ship, including its primary dimensions, structural requirements and intended use.
- **Parametric Modelling**: Using FEMAP software to represent the cargo hold and create a parametric model. This model will act as the foundation for subsequent analyses.
- Incorporation of Structural Rules: Utilise the Common Structural Rules (CSR) to make certain that the parametric model adheres to classification society, industry, and safety regulations.
- **Integration of Components**: Incorporate primary and secondary components of the ship, such as plate distribution, stiffener arrangement and load specifications, into the parametric model.

2.8.2 Optimisation of Scantlings

- **Preservation of General Configuration**: Maintain the general configuration of the ship throughout the optimisation process to assure operational safety and efficiency.
- Material and Structural Modifications: Modify aspects of the ship's structure, including outer and inner hull/shell plates, deck plates, main frames, web frames, girders, stringers, deck beams, etc., to lessen the hull's weight while assuring structural integrity.
- **Software and Techniques**: Integrate specialised software programs and Finite Element Analysis (FEA) techniques to comprehensively analyse the ship's structural strength under varying sea conditions.
- **Innovative Workflow**: Establish a systematic and creative workflow to guide the project through the following stages.

2.8.3 Develop Finite Element Model

- Creation of 2D Model: Generate a 2D model using the BV Mars 2000 program based on the 2D CAD model, guaranteeing compliance with Bureau Veritas CSR standards.
- **3D Finite Element Model (FEM)**: Develop a 3D FEM model representing the ship's hull and structure. Emphasise the importance of high-quality mesh generation using FEMAP/NASTRAN software. Simulate the ship's movement in calm water at 12 knots (6.17 m/s).
- **Boundary and Loading Conditions**: Define and apply boundary and loading conditions as the analysis requires.
- Static Structural Analysis: Perform a static structural analysis to evaluate the ship's strength under varying sea conditions, including head sea and oblique sea conditions, assessing structural integrity and performance.

2.8.4 Optimisation Plan

- **Fractional Factorial Design**: The initial fractional factorial design includes twelve variables, resulting in 128 distinct analyses.
- Outcome Analysis: Study key outcomes, such as Von Mises stress, torsional stress, production costs, and others, using Minitab to identify the factors that exert the most influence on these outcomes.
- Advanced Optimisation: Utilise a non-dominated sorting genetic algorithm, NSGA-II, implemented in Python to optimise both the weight and production costs based on the findings from the initial study.

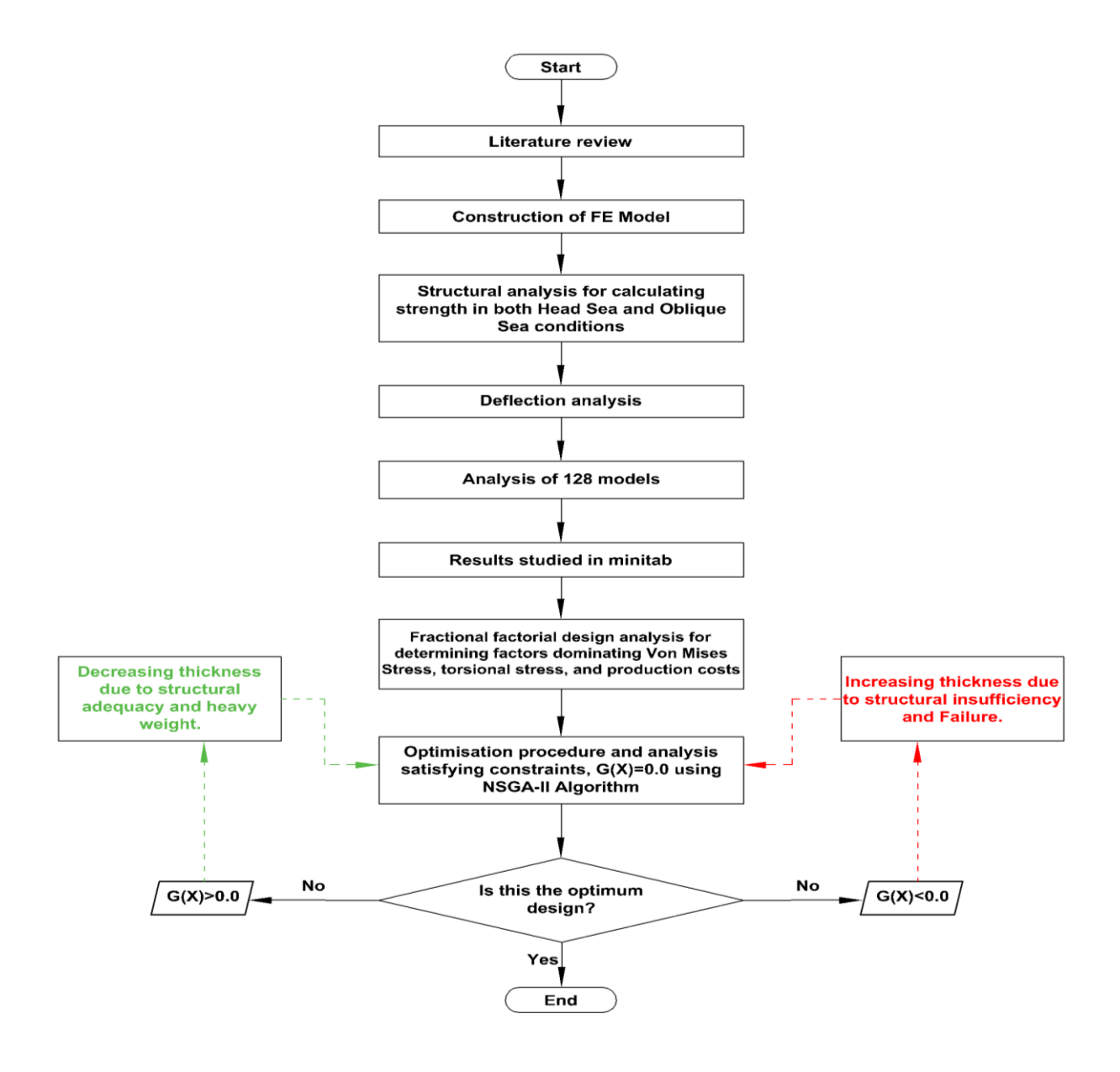


Figure 2-1: Procedure for optimising ship structure.

2.9 Software Tools

2.9.1 BV MARS 2000

The MARS 2000 software, developed by Bureau Veritas, represents an advanced 2D tool to assess ship structural integrity, including plate scantlings and ordinary stiffeners within transverse cross-sections and transverse bulkheads along the vessel's length. MARS 2000 offers a comprehensive suite of invaluable features, including intuitive modelling capabilities, robust consistency and error-checking mechanisms, rapid calculations, in conjunction with a user-friendly interface. Moreover, this versatile software transcends the confines of specific ship

types, extending its applicability to a diverse range of vessels, encompassing steel ships, offshore units, floating gas units, drilling units, polar-class and icebreaker ships, as well as those adhering to the IACS standard structural rules for bulk carriers and oil tankers. The software is meticulously organised around seven distinct modules, each performing a unique function within the structural assessment process. These modules encompass Shell/Basic Ship Data, Definition of a Section, Calculation of a Section, and others of similar importance.

2.9.2 FEMAP/NX Nastran

Femap stands out as a crucial software tool for finite element analysis (FEA). It plays a vital role in simulating and comprehending structural and system behaviour, integrated with solvers like Nastran. Nastran, a highly respected FEA solver, employs intricate mathematical computations to model physical phenomena accurately. Femap simplifies the FEA workflow by automating input file preparation and streamlining result interpretation. Its CAD-independent nature lends versatility, making it a preferred choice for various engineering applications across multiple industries. Femap also offers a free student version within the academic realm, enhancing accessibility and supporting research efforts in finite element analysis.

2.9.3 Minitab

Minitab is a comprehensive statistical software package that provides a wide range of data analysis tools, rendering it an invaluable resource for research. Its robust statistical analysis capabilities enable in-depth data exploration, including descriptive statistics, correlation analysis and regression analysis. With its user-friendly interface, Minitab ensures accessibility for both novice and experienced users. It is renowned for its role in quality improvement, process capability assessment and handling large datasets. Minitab is an ideal tool for researchers seeking to analyse data, identify patterns and make well-informed decisions.

2.9.4 Rhino

Rhino, also known as Rhinoceros 3D, is a powerful 3D computer graphics and CAD software developed by Robert McNeel & Associates. It offers many features, including modelling, rendering, animation and support for the Non-Uniform Rational B-Splines (NURBS)

mathematical model. Particular critical improvements in Rhino 6 include a faster display pipeline, better control of annotation styles and support for real-time ray-traced viewport mode. The software has found applications in various industries, such as architecture, engineering, in addition to product design and jewellery design, and it has received positive reviews for its versatility and functionality.

2.10 Conclusion

In conclusion, this literature review emphasises the importance of ship hull structural optimisation in maritime engineering. The study draws attention to the benefits of optimising ship scantlings by reviewing relevant literature and providing a comprehensive overview of the various methods and techniques employed in the field. These approaches include hull form optimisation during the conceptual design stage, parametric design, and multi-objective optimisation technology for hull structural scantlings, surrogate models, besides evolutionary algorithms for multi-objective optimisation of structural elements.

The research findings, derived from an extensive review of the literature, accentuate the transformative potential of structural optimisation in addressing critical factors, for example reducing fuel consumption, mitigating greenhouse gas emissions, and minimising weight and production costs. These concrete results attest to structural optimisation's direct and practical benefits, enhancing competitiveness and reducing the industry's environmental footprint. As the maritime industry grapples with efficiency and ecological responsibility challenges, structural optimisation has emerged as a practical solution, proposing a route towards a more environmentally friendly and cost-effective future.

Furthermore, the review has clarified the remarkable optimisation capabilities of hybrid genetic algorithms. Their application in shaping three-dimensional ship structural designs, especially in focusing on complex topology and scantling optimisation problems, has demonstrated exceptional efficiency and effectiveness. This understanding goes beyond theoretical innovation, equipping the industry with powerful tools to confront and conquer intricate structural challenges, ultimately enhancing safety and performance.

To conclude, this comprehensive research has reaffirmed the vital role of ship hull structural optimisation and illuminated its far-reaching implications. Simultaneously reducing costs, increasing safety and promoting sustainability, the optimisation of ship scantlings stands as a cornerstone in advancing maritime engineering. As revealed in this review, the promising role

of hybrid genetic algorithms adds a new dimension to the field's capabilities, further solidifying its position as a driving force in addressing complex structural challenges. As this journey towards a more efficient, eco-conscious maritime industry unfolds, ship structural optimisation has materialised as an indomitable force poised to shape the future of marine engineering.

Chapter 3

Longitudinal Strength Calculation of the Analysed Ship

3.1 Introduction

The strength and integrity of a ship's structural system predominantly depend on its hull girders. To determine the strength of a hull girder, it is important to evaluate the most extreme loads that can be imposed on it. Three categories are typically considered when determining a ship's strength: longitudinal, transverse and local. The longitudinal strength of all of its components profoundly impacts the ship's stability [97]. Ships with open decks have wider hatches, which can pose a more complex challenge for maintaining hull strength. The size of these deck openings impacts the hull's stresses in both longitudinal and transverse bending, while broad deck openings in rough seas can also reduce hull stiffness under torsion loads [98]. Axial (warping) and shear stresses develop in thin-walled beams subjected to torsion, and torsional loading causes warping stresses near hatch corners. Torsional loading occurs when the ship is in the oblique wave but with a reduced vertical wave bending moment [99].

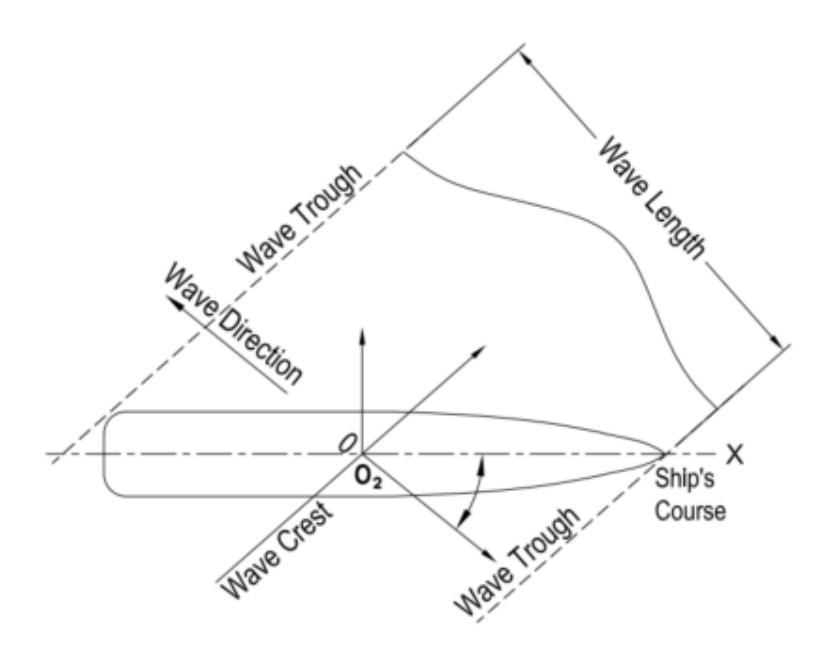


Figure 3-1: A ship travelling through oblique waves [3].

In previous research pertaining to the strength analysis of ship hull constructions under combined bending and torsion, Elbatouti et al. (1974) investigated the SS-7 container ship's structure using finite element methods to analyse the effects of vertical, lateral and torsional moments on the ship's structure. Their findings indicated that due to the non-prismatic properties of the structure and deck holes, there could be local deformation that would result in a significant increase in the total stress level in the inner bulkhead plate [100]. Ostapenko and Vaucher (1986) showed that when a ship travels in oblique seas with heavy waves, torsion may lessen the longitudinal strength of the hull. Their study is critical as regards ship hull design and safety since it clarifies how to ensure structural strength and how ships behave under various loading conditions [101]. Vernon and Nadeau (1987) compared the St. Venant and warping-based thin-walled beam theories. The results their study obtained concluded that warping-based theory provides a better model of the behaviours of prismatic thin-walled sections because longitudinal deformation is considered [102]. Valsgard et al. (1995) explored how significant torsion causes large diagonal shear deformations of the hatch openings and stress concentrations and fatigue risk at the hatch corners from a structural perspective [103]. Through theoretical and numerical investigations, Paik et al. (2001) examined the ultimate strength of the hull of a 4300 TEU container ship under combined vertical bending and torsion. They established that torsion is not a sensitive factor for the ultimate strength of a ship hull. However, the relatively large torsional moment can significantly impact ship hulls with low torsional rigidity [104]. Iijima et al. (2004) outlined a simplified method to determine the torsional strength of a container ship structure. The approach involves dividing the hull girder into sections and applying beam theory to calculate the torsional strength of each section. The researchers then combined the results to determine the overall torsional strength of the hull girder. This evaluation is crucial in relation to the structural design process for container ship hull girders [105]. Senjanović et al. (2008) used a 3D finite element model torsional analysis of large container ships with and without transverse bulkheads. The research concluded that adding transverse bulkheads does not significantly affect the stiffness of vertical and horizontal bending; therefore, it can be disregarded. However, the study highlighted the importance of hydroelastic strength analysis in designing these types of ships [106]. Chirică et al. (2009) explored various numerical and experimental techniques for analysing the torsional behaviour of composite ship hulls. Based on thin wall beam theory, their proposed method can serve as a quick calculation tool for ship hull torsion analysis [107]. Parunov et al. (2010) utilised FE analysis to investigate the structural behaviour of a general cargo ship of 2240 DWT and presented the need for those areas prone to stress concentration, such as hatch corners at the

ends of the large cargo hold and hatch coaming in the cargo hold, to have fine mesh modelling. They ascertained that structural analysis improves general cargo ship's safety by reinforcing crucial regions [108]. Senjanović et al.(2011) analysed torsion, warping and distortion in large container ships. They established that distortion is caused by variable shear flow distributions of open and closed segments joined at engine room bulkheads and that distortion may be decreased by increasing bulkhead thickness [109]. Novikov et al. (2015) evaluated normal stresses in the main deck with bending and torsion loads, noting their correlation. According to this investigation, hull stresses occurred during simultaneous bending and torque moments, and wider main deck openings increased hull torsion stresses [98]. Rörup et al. (2016) utilised more complex loads and improved methods for various FE analysis types, such as global models, partial ship modelling and fine mesh models, to improve the design process and class approval while emphasising the need for effective design tools. In addition, the regulations effectively support the use of finite element analysis. The most typical FE application for class approval is cargo hold analysis [110]. Tang et al. (2019) used three real-time structural strength assessment methods to identify hull longitudinal strength, yielding local strength and fatigue strength. The system evaluates short and long-term structural strength. Comparing and analysing assessment data in different wave azimuths revealed certain problematic areas and causes of structural damage. Finally, specific trimaran optimisation depends on the measured data and results of the assessment [111]. Jurišić and Parunov (2021) assessed the strength of two general cargo ships and discovered sufficient stress levels and safety parameters in all load conditions. The stress distributions for specified load circumstances met the Croatian Registry of Shipping rules, intimating an acceptable and redundant ship structure. Results indicated that ships can be used under expected loading circumstances [112].

This study confirmed stress values by comparing the results obtained from the Euler–Bernoulli beam theory and direct calculations. Furthermore, the validity of torsional stress was established by comparing the thin wall girder theory with the results of the direct calculation. The direct calculation is based on finite element model analysis, while beam theory relies on the following three assumptions [113]:

- 1. The cross-section is infinitely stiff in its own plane.
- 2. The cross-section remains plain after deformation.
- 3. The cross-section stays parallel to the bent axis of the beam.

3.2 Theory of Hull Girder Stresses

Three methods, which are briefly outlined below are employed in this study to determine the stresses caused by external forces in a ship's hull girder: beam theory, thin wall girder theory and FE analysis. The deformation of the ship girder is classified into four main parts: axial compression, vertical bending, horizontal bending and torsion (twisting).

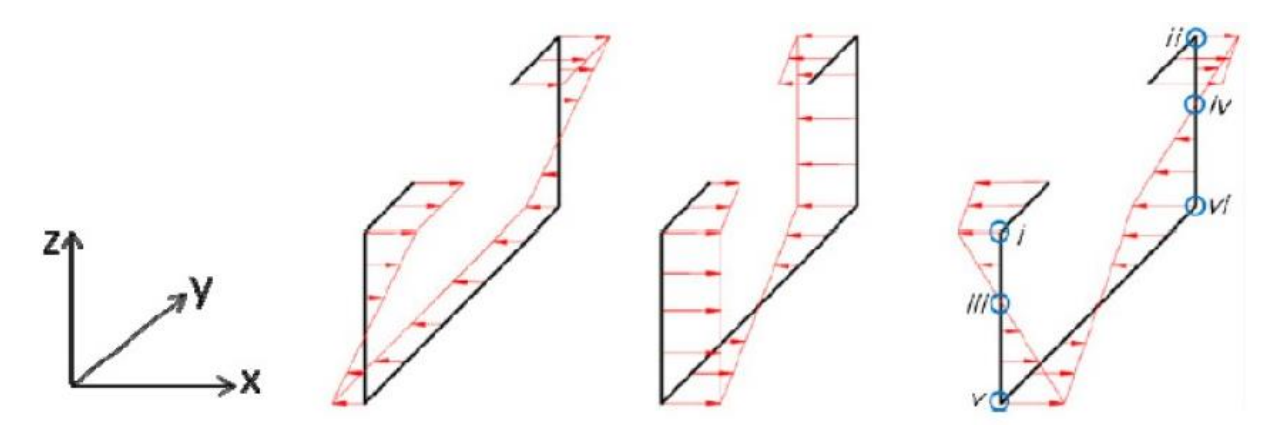


Figure 3-2: Distribution of longitudinal stress in the cross-section under vertical bending, horizontal bending and torsion [114].

Figure 3.2 shows the longitudinal stress distribution in the cross-section of the latest deformation modes. The longitudinal stresses on the hull are distributed equally across all longitudinally continuous fibres under axial compression or tension. When the hull is subjected to vertical bending because of Hogging, the upper section will experience tension while the lower portion will be compressed. The stress distribution during horizontal bending is identical. The longitudinal displacement or warping of the cross-section during torsion is prevented by bulkheads, resulting in longitudinal strains. The absolute maximum values of vertical and horizontal bending stresses, as well as warping stresses, are anticipated in the outer deck section [114].

3.2.1 Classical Beam Theory

The classical beam theory is the most straightforward method of estimating hull girder strength; that is also relatively straightforward to apply. Nonetheless, it regards the entire ship as a single beam with equivalent bending stiffness and area, making it impossible to consider the local structural component failures.

$$\sigma = \frac{Mz}{I} \tag{3-1}$$

M represents the applied bending moment, while *I* denotes the moment of inertia for one ship section. The vertical distance from the calculation position to the neutral axis is represented by *z*. Consequently, the deck or ship's bottom will experience the greatest stress [115].

Statics can be exploited to quickly determine the forces and moments required to maintain any two elements of the ship together, given all of the forces acting on the ship's hull. This enables defining the bending moments, shear forces and axial forces across any ship cross-section [114].

The engineering beam theory permits the calculation of stresses in any part of a beam's cross-section. The stress in any position of any cross-section can be determined using the following formulas, provided that the conditions of small displacements, unchanged sectional geometry, an initial straight and prismatic beam, and linear elasticity are met [114]:

$$\sigma_l = \frac{F_n}{A} + \frac{M_v}{I_v} \Delta_z + \frac{M_h}{I_h} \Delta_y + \sigma_w \tag{3-2}$$

where the longitudinal force, as well as the vertical and horizontal bending moments are represented by F_n , M_v and M_h . The cross-sectional area and moments of inertia are defined by the properties A, I_v and I_h , whereas Δ_z and Δ_y are the distances between the detail and the neutral axes, whilst σ_w is the stress caused by warping.

Hence, considering the ship as a prismatic beam with the cross-sectional geometry of the section of interest, using Eq. 3–2, the longitudinal stress in any detail within this section can be approximated [114].

3.2.2 Thin-Walled Girder Theory

A ship will experience a torsional moment if it enters a wave train obliquely. Torsion is a deformation that occurs when torque is applied in the opposite direction to one end of an object. Shear stresses arise entirely from torsion within the material. When the line of action does not intersect the shear centre of the beam, tension loading develops. Shear force without torsion can occur at the shear centre—an imaginary point in the cross-section. For sections with a single axis of symmetry, the shear centre lies along the axis; for those with two axes of symmetry, it coincides with the centroid. Torsion-related problems arise when an eccentric (off-centre)

transverse force is applied, causing the force to bypass the shear centre, leading to twisting moments calculated as the product of the load and its perpendicular distance from the shear centre [116].

The torsional moment T is divided into two components, specifically the St. Venant torsional moment T_t and warping torsional moment T_w .

$$T = T_t + T_w \tag{3-3}$$

Pure torsion or St. Venant torsion is commonly witnessed when the cross-sectional shape remains planar while undergoing torsional deformation. This deformation induces an out-of-plane effect termed warping, leading to lateral displacement of the cross-section. Upon the application of a torsional moment to a structural member, three distinct stresses manifest within the cross-sectional geometry:

- Pure torsional stresses.
- Shear stresses arising from warping.
- Normal stresses arising from warping.

The pure torsional shear stresses represent in-plane shear stresses oriented parallel to the edges of the cross-section. These stresses exhibit a linear variation along the thickness of the cross-section. Torsion frequently coexists with bending moments and shearing forces, demanding a comprehensive understanding of their interplay and combined effects.

Warping torsion is inherently linked to the bending deformation within the planes of each plate, whereas St. Venant's torsion arises owing to the manifestation of pure shear deformations within the planes of the plates constituting the thin-wall member. The torsional behaviour of a thin-walled box section is contingent upon the material's shear modulus and torsional constant, which are intricately associated with the geometric characteristics of the cross-sectional profile [116].

Employing a streamlined structural analysis methodology during the initial design phase is vital, as it provides a comprehensive approach for evaluating the shear and flexural warping stresses and the torsional deformations induced by torsional loading in open ships. This approach is contingent upon the sectorial attributes fundamental to the ship's cross-sectional geometry, which are acquired through an idealised ship section configuration subject to simplification [99].

Thin wall girder theory is based on the following assumptions [117]:

- 1. In its plane, the cross-section's shape and all of its geometrical dimensions are unchanged.
- 2. The transverse stresses are constant over the beam's cross-section.
- 3. At any point along the beam wall, the wall thickness to the curvature radius ratio is very close to unity.

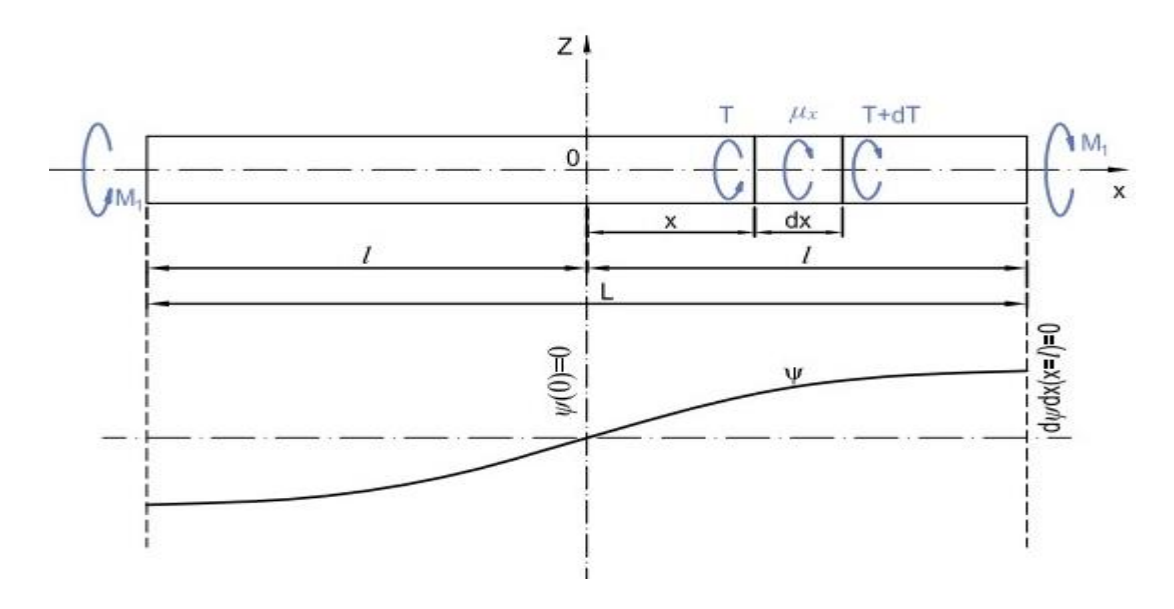


Figure 3-3: Beam subjected to torsion [118].

Figure 3–3 shows a prismatic girder subjected to torsional forces. This diagram explains the complex relationship between torsion, warping and deformation in large container ships. It effectively highlights the connection between sectional torque and external torsional loads along the structural length.

Sectional torque, T and the distributed external torsional load, μ_x are in equilibrium and produce [118]

$$dT = -\mu_x dx \tag{3-4}$$

According to the theory of thin-walled girders, the sectional torque consists of a pure torsional component (T_t) plus a warping contribution (T_w) [118].

$$T = T_t + T_w = GI_t \frac{d\psi}{dx} - EI_w \frac{d^3\psi}{dx^3}$$
 (3-5)

where,

E, *G* − Young's modulus and shear modulus

 I_t – Torsional constant

 I_w – Sectorial moment of inertia

 ψ – Twist angle

Substitution of Eq. 3–4 into Eq. 3–5 results in the ordinary differential equation of the fourth–order

$$EI_{w}\frac{d^{4}\psi}{dx^{4}} - GI_{t}\frac{d^{2}\psi}{dx^{2}} = \mu_{x}$$
 (3-6)

Its solution reads

$$\psi = A_0 + A_1 x + A_2 ch\beta x + A_3 sh\beta x + \psi_p \tag{3-7}$$

where,

$$\beta = \sqrt{\frac{GI_t}{EI_w}} \tag{3-8}$$

and A_i is integration constants, while ψ_p represents a particular solution which depends on μ_x .

Let us consider the girder's twisting phenomenon described in Figure 3–3. The girder is subjected to torsional torque M_t at its end when μ_x is zero. It is important to state that the extremities of the girders are constrained against warping. Given the antisymmetric nature of the twist angle in this scenario, i.e., $A_0 = A_2 = 0$, fulfilling boundary conditions leads to the computation of the ultimate constants A_1 and A_3 [118].

$$x = l: T = M_t, u = \frac{d\psi}{dx}\bar{u} = 0 (3-9)$$

The relative sectional warping generated by the unit beam deformation is denoted by the symbol \bar{u} and the warping function (axial displacement) by the symbol u. The final expression used to describe the twist angle is:

$$\psi = \frac{M_t l}{GI_t} \left[\frac{x}{l} - \frac{sh\beta x}{\beta l. ch\beta l} \right]$$
 (3-10)

Now, it is possible to determine sectional forces, i.e., pure torsional and warping torques

$$T_t = M_t \left(1 - \frac{ch\beta x}{ch\beta l} \right), \quad T_w = M_t \frac{ch\beta x}{ch\beta l}$$
 (3-11)

and warping (sectorial) bimoment

$$B_w = EI_w \frac{d^2\psi}{dx^2} = -M_t \frac{sh\beta x}{\beta ch\beta l}$$
 (3-12)

Furthermore, the warping function (8) takes the form of

$$u = \frac{M_t}{GI_t} \left(1 - \frac{ch\beta x}{ch\beta l} \right) \bar{u} \tag{3-13}$$

3.3 Finite Element Analysis and Associate Uncertainties

Alternatively, the hull girder stresses may be ascertained using the ship's global finite element (FE) model. The finite element method is a potent and extensively utilised tool in contemporary structural analysis paradigms. Applying the finite element technique (FEM) for structural analysis enables the precise computation of stress distributions within the hull structure [119].

The finite element method (FEM) serves as a computational framework for solving differential equations by breaking down continuous systems into discrete elements. This approach involves dividing a structure into smaller components, or elements, that are interconnected at specific nodes. These elements are selected from a set of predefined types provided by specialised software. Each element exhibits a distinct topology characterised by a sequential arrangement of points or nodes alongside an array of pertinent structural and material attributes encompassing parameters such as density and Young's modulus. Structural components like beams and plates are designed to handle loads during bending, relying on principles from beam and plate theories, such as the concept that "plane sections remain plane." In FEM, the governing equation asserts that the total displacement at any point within the structure results from the sum of displacements caused by individual loads applied incrementally. Moreover,

displacements are proportional to the magnitudes of the applied loads, ensuring precision in structural analysis [120].

Quantity is the displacement resulting from a nodal force without any other external loads. This concept can be expressed quantitatively by means of the following formulation [120]:

$$\delta_{1} = \delta_{11} + \delta_{12} + \delta_{13} \dots + \delta_{1n}$$

$$\delta_{2} = \delta_{21} + \delta_{22} + \delta_{23} \dots + \delta_{2n}$$

$$\vdots$$

$$\delta_{n} = \delta_{n1} + \delta_{n2} + \delta_{n3} \dots + \delta_{nn}$$
(3-14)

This statement implies that a constant proportionality determines how much the load f_j impacts the displacement. This constant is known as the flexibility influence coefficient (C) and can be expressed through the following equation [120]:

$$\delta_{ij} = C_{ij} f_j \tag{3-15}$$

It is possible to create a system of linear equations that links nodal displacement (δ) to nodal forces (f) by substituting Eq. 3–15 with Eq. 3–14. However, the difficulty associated with computing these values should be disregarded. The values in the equation are [120]:

$$\delta_{1} = C_{11}f_{1} + C_{12}f_{2} + \dots + C_{1n}f_{n}$$

$$\delta_{2} = C_{21}f_{1} + C_{22}f_{2} + \dots + C_{2n}f_{n}$$

$$. \qquad (3-16)$$

$$\delta_{n} = C_{n1}f_{1} + C_{n2}f_{2} + \dots + C_{nn}f_{n}$$

They may be expressed more concisely in matrix form as:

$$d = Cf (3-17)$$

where

$$d = \begin{bmatrix} \delta_1 \\ \delta_2 \\ \vdots \\ \delta_n \end{bmatrix}, C = \begin{bmatrix} C_{11}C_{12} \dots C_{1n} & C_{1n} \\ C_{21}C_{22} \dots C_{2n} & C_{2n} \\ \vdots & \vdots & \vdots \\ C_{n1} \dots C_{nn} & C_{nn} \end{bmatrix}, f = \begin{bmatrix} f_1 \\ f_2 \\ \vdots \\ f_n \end{bmatrix}$$
(3-18)

The flexibility matrix C has n rows and n columns. Matrix f stands for nodal force vector, while matrix d represents nodal displacement vector.

To better understand the structure of comparable finite element equations, one can consider the equations that result from inverting Eq. 3–17. By multiplying both sides of Eq. 3–17 with the inverse of C, we can obtain the following [120]:

$$C^{-1}d = f \tag{3-19}$$

The matrix C^{-1} is the "stiffness matrix" of the system. It is typically denoted by the symbol K and the above equation is written [120].

$$Kd = f (3-20)$$

The stiffness matrix coefficients represented as *K* within the context of finite element formulation, are obtained via a direct derivation from the structural properties, avoiding the need for dependence upon a reference flexibility coefficient. The determination of nodal displacements for the structure is achieved by solving Eq. 3–20, which then allows for the determination of strain distribution in individual components. As the primary unknowns are displacements, the finite element model is a displacement-based analytical method [120].

Consequently, an initial solid structural representation is formulated and scrutinised in constructing a model using FEMAP. This solid structure representation is therefore transitioned into a finite element model using mesh generation techniques. This procedural alteration ensures that our model is delineated explicitly through nodes. Moreover, these nodes, aligned with the specified coordinate system, are converted into the stiffness matrix, while applied loads are translated into a load vector. The stiffness matrix and load vector form the governing equation, which is solved using computational linear algebra techniques to ensure precise structural analysis [120].

To develop a finite element model, an initial solid structure is generated and transformed into a mesh representation using FEMAP. This process defines the model explicitly through nodes. It is essential to verify the analysis during structural analysis. Although the finite element method (FEM) is dependable, it is necessary to recognise that inaccurate models or imprecise data can generate many potential sources of inaccuracies. To address these concerns, various validation techniques must be carefully executed to confirm the accuracy of the study's findings [121].

Therefore, it is vital to have a meticulous verification process at critical stages, including the following [121]:

- Basic input
- Assumptions and simplifications made in modelling/analysis
- Models
- Loads and load transfer
- Analysis
- Results
- Strength calculations

To verify the performance of a mechanical system necessitates a thorough analysis of its behaviour, comparing the amount of stress and deformation against expected levels. This is a vital step in the verification process, with all verification stages bearing equal significance in substantiating the findings. In validating structural integrity, it is essential to acknowledge that most structural models necessitate incorporating assumptions and simplifications during the verification procedure. These assumptions and simplifications must be systematically enumerated, aiding a comprehensive assessment of their influence on the outcomes. Mitigating inherent stresses demands that the overarching structural model's boundary conditions accurately reflect uncomplicated support mechanisms [121].

Moreover, Fixation points should be carefully positioned away from areas of high-pressure concentration, commonly located along the midline near the fore and aft ends of the vessel. One of the primary sources of error in load validation is the inaccurate transfer of loads from hydrodynamic analysis to the structural model, highlighting the importance of precise load

allocation. Assessing the structural response and the efficiency of the load transfer process are essential measures for ensuring the accuracy of load transfer mechanisms [121].

3.4 Main Features of the Investigated Ship

This study focuses on a multipurpose cargo ship that is currently in operation. The analysed ship has a bulbous bow, a transom and a single-screw diesel engine. Moreover, it was built as a double-skinned box with only one cargo hold. This ship can transport cargo, including oversized freight, regular cargo, containers and bulk grain. The studied ship complies with the Bureau Veritas (BV) NR 467 rules for the Classification of Steel Ships to guarantee its structural strength [36].

Table 3–1 provides an exhaustive description of crucial ship attributes, encompassing principal dimensions, material specifications, propulsion system details, navigational range, as well as loading sequences. It functions as a comprehensive resource for understanding the ship's core characteristics. It covers the ship's physical design, structural durability, manoeuvrability, operational capabilities, and cargo handling. As such, Table 3–1 is a key reference for comprehending the complexities connected with maritime engineering.

Table 3–1: Main Particulars of the Investigated Ship.

Sr. No.	Particulars	Dimension
1	Length overall	104.135 m
2	Length between perpendicular	98.535 m
3	Breadth mould	15.25 m
4	Depth	7.45 m
5	Design Draught	4.9 m
6	Scantling Draught	5.6 m
7	Range of navigation	Unrestricted
8	Loading sequence	2R (2 Runs)
9	Propulsion	Self-propelled
10	Material used	Steel - Grade A ($R_{eh} = 235$ MPa) - For Hull structure Grade AH-36 ($R_{eh} = 355$ MPa) - For Topside structure

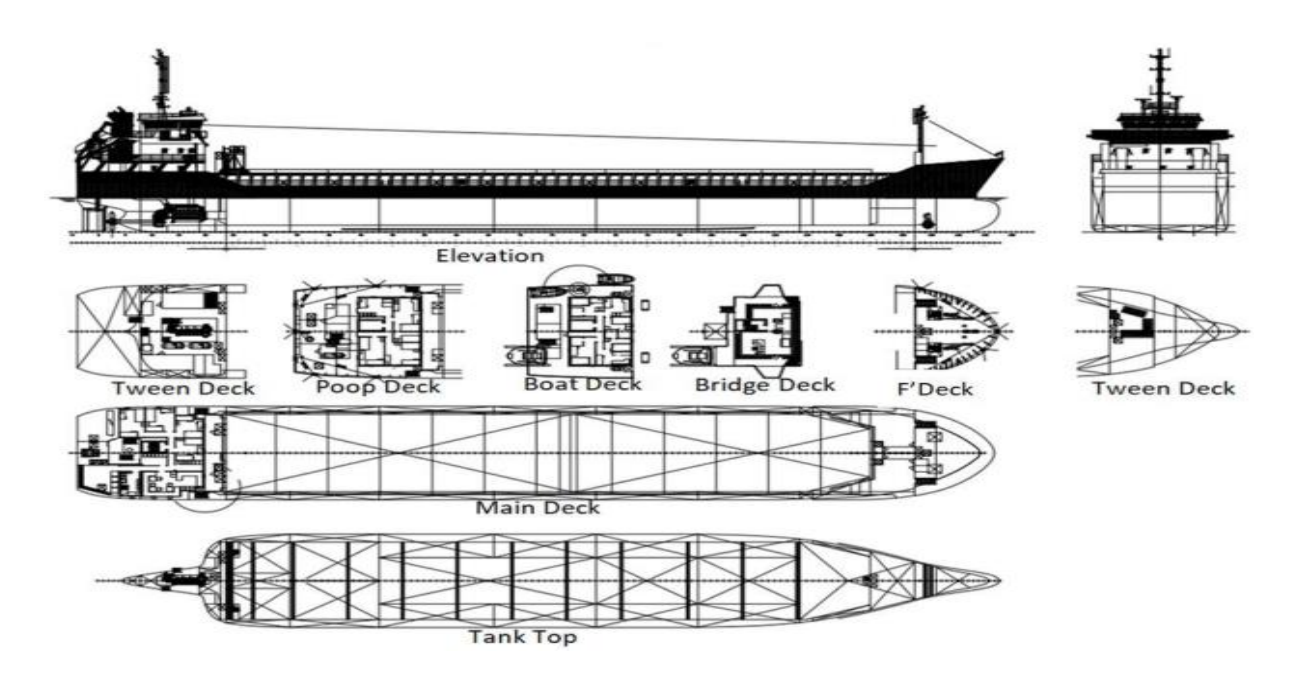


Figure 3-4: General arrangement plan of the analysed ship.

The ship's general arrangement (GA), shown in Figure 3–4, provides a comprehensive depiction of its layout, encompassing various decks, such as the forecastle deck, forward and aft tween decks, poop deck, boat deck, bridge deck, main deck and tank top. This detailed plan offers a more complete understanding of the ship's spatial organisation, including key features, such as hatches, cargo holds, fuel oil tanks, engine rooms, in conjunction with other critical areas. This information is essential in ship design, construction and operation, facilitating a thorough understanding of the ship's configuration and significant locations.



Figure 3-5: Perspective view of a general multi-purpose cargo ship [122].

Figure 3–5 shows a visually appealing representation of a multipurpose cargo ship that can handle various cargo types, such as containers and bulk commodities. The ship's design is skilfully crafted to highlight its impressive capacity to meet diverse cargo demands, demonstrating its adaptability and exceptional hull engineering. This ship is a symbol of innovation in the maritime industry, promising greater efficiency and versatility in global cargo transportation and potentially setting new standards for the future of cargo shipping.

3.4.1 Development of Hull Shape

The design of the hull shape utilises parametric production to explore various potential hull shapes made possible by the RHINO program. To develop hull designs that are both practical and effective, a meticulous definition of ideal design parameters and relevant ranges of variation is essential.

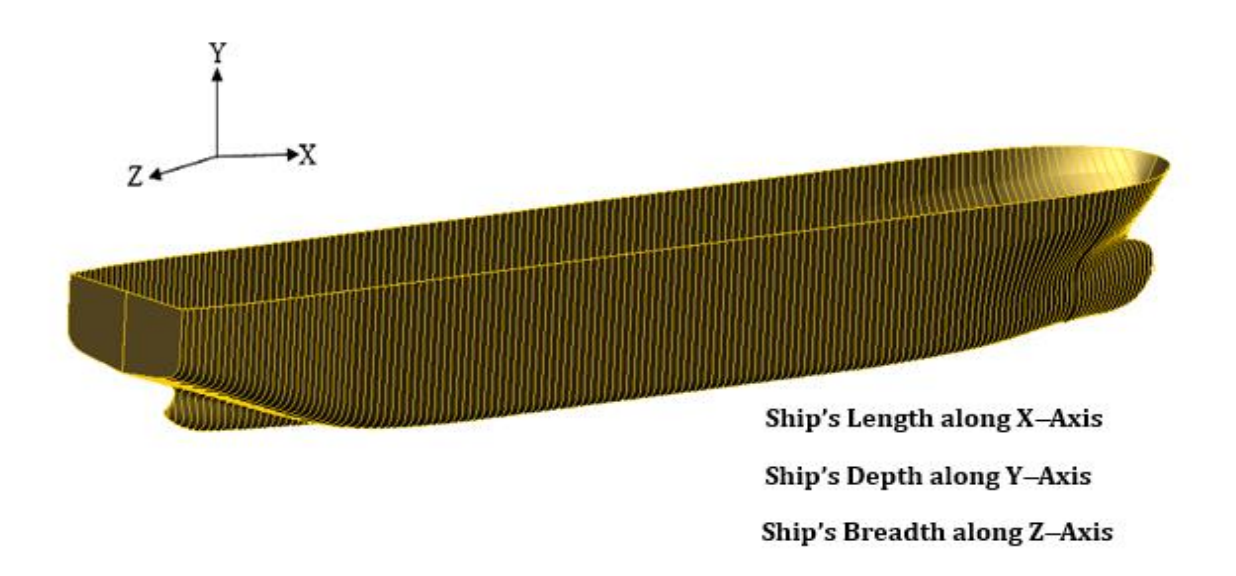


Figure 3-6: Perspective view of the typical hull form of the analysed ship in RHINO.

Figure 3–6 shows the design approach, exhibiting a detailed 3D representation of the shape of the ship's hull. This hull is created using Rhino's NURBS (Non-Uniform Rational B-Spline) modelling based on the ship's lines plan. This visualisation emphasises the critical significance of the hull shape in ship design, as it plays a pivotal role in determining stability, speed and fuel efficiency. It is paramount in maritime engineering and design, directly influencing overall performance and efficiency.

3.4.2 Structural Configuration

For the construction of this ship, a longitudinal framing system was applied. The cargo compartment of the multipurpose cargo ship features twin hull sides that consist of deep tanks.

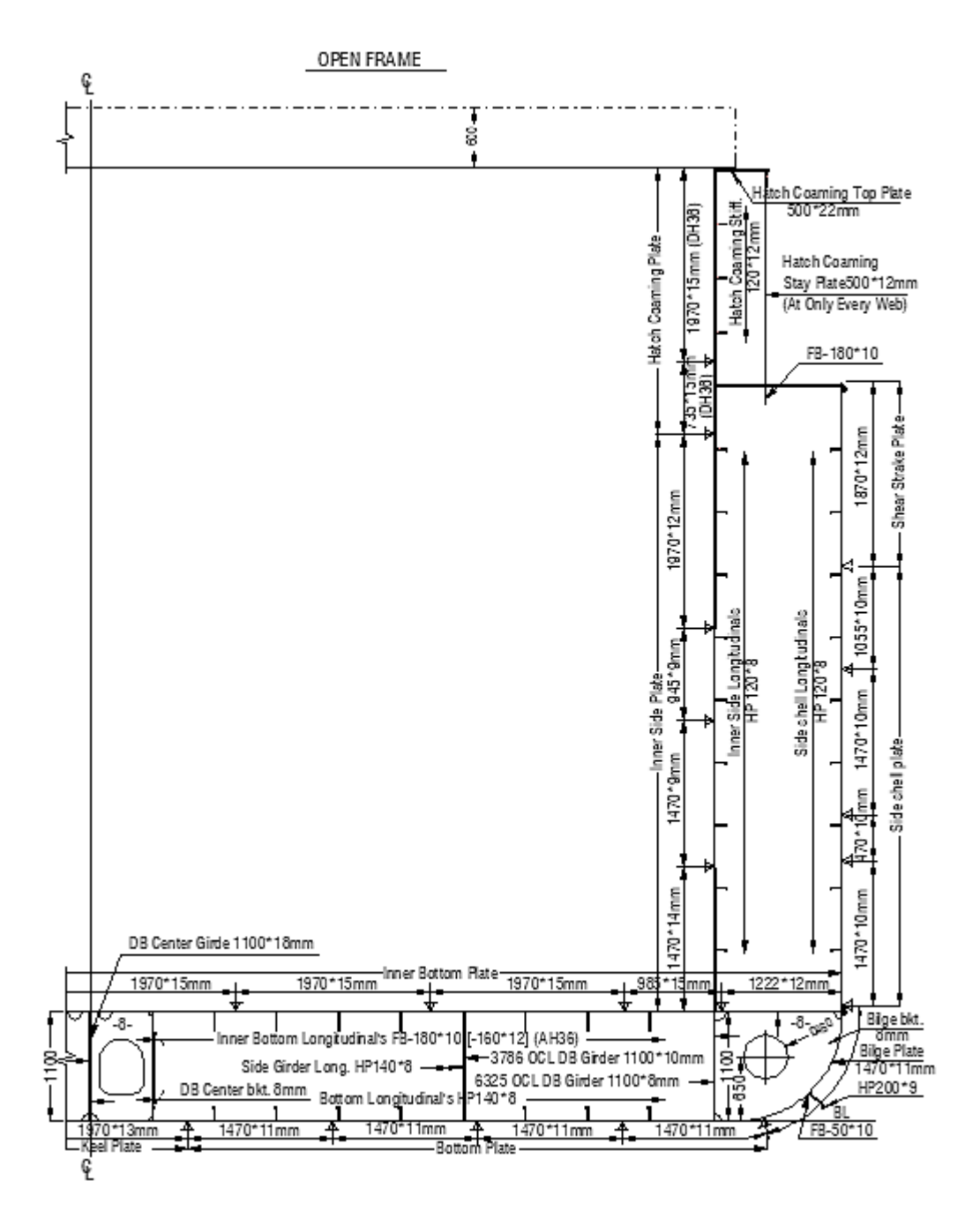


Figure 3-7: Midship section of the analysed ship.

Figure 3–7 presents the analysed ship's midship section, which shows the ship's double bottom, side shell and transverse section. The stiffening at the bottom of the structure is made up of vertical plates, also known as floors, which strengthen the bottom. Side stringers and beams of angles or channels reinforce the sides and decks. The transverse material provides transverse strength and prevents longitudinal buckling. The span-to-thickness ratio is crucial for resisting compressive stresses and preventing local deformation caused by water pressure.

Table 3–2 provides the Web frame, Ordinary frame and stiffener spacing measurements, which are crucial in maritime engineering. These values directly impact the ship's ability to resist external forces, ensuring appropriate load distribution and structural strength. The spacing of the stiffeners and frames significantly influences the overall structural integrity of the ship's hull, affecting its ability to withstand bending, shear and torsional loads. Additionally, optimising stiffener layout, is a key aspect of structural design, aiming to achieve the most efficient and safe configuration for the ship's hull.

Table 3–2: Stiffener Spacing.

Sr. No.	Structural Members	Spacing (mm)
1	Inner side longitudinals (HP)	631
2	Side shell longitudinals (FB)	631
3	Inner bottom longitudinals (HP)	631
4	Bottom longitudinals (HP)	631
5	Spacing of web frames	1430
6	Spacing of ordinary frames	715

Table 3–3 provides a detailed view of the gross scantlings and materials grade of the main structural components of the ship, which are crucial for understanding its structural strength and ability to cope with the various challenges it might encounter during its journey at sea. The gross scantlings, including the dimensions and material grades of the main structural elements, for example the hull, decks and bulkheads, are fundamental to safeguarding the ship's overall integrity and safety. These measurements directly influence the vessel's capability to resist the complex and dynamic forces experienced at sea, encompassing aspects such as wave impact, cargo load, along with harsh environmental conditions.

 Table 3–3: Gross Scantlings and Materials Grade.

Sr. No.	Parts Name	Material Grade	Gross Thickness (mm)
1	Keel plate	A	13
2	Bottom and bilge plate	A	11
3	Side shell plate	A	10
4	Shear strake plate	AH36	12
5	Inner bottom plate 1	A	15
6	Inner side shell plate 1	A	14
7	Inner side shell plate 2	A	9
8	Inner side shell plate 3	A	12
9	Bulkhead plate stiffener	A	12
10	Bulkhead plate	A	12
11	Hatch coaming stay plate	AH36	10
12	Hatch coaming stiffener	DH36	12
13	Hatch coaming top plate	DH36	22
14	Hatch coaming plate	DH36	15
15	Main deck plate	AH36	15
16	Inner bottom plate 2	A	12
17	DB long girder CL	A	18
18	DB long girder 3786-OCL	A	12
19	DB long girder 6325-OCL	A	9
20	Bottom longitudinal	A	8
21	Inner bottom longitudinal	AH36	10
22	Side shell longitudinal	A	8
23	Inner side shell longitudinal	A	8
24	Main deck longitudinal	AH36	10
25	Flat bar-side shell	A	8
26	Web frame plate_side shell 1	AH36	8
27	Web frame plate_side shell 2	AH36	11
28	Web frame plate_bottom 1	A	9
29	Web frame plate _ bottom 2	A	11
30	Flat bar-bottom	A	10
31	Ordinary frame bracket	A	9

3.5 **Principles and Criteria of the Hull's Strength**

3.5.1 **Overview**

In this section, the principles and criteria of Hull's strength are described. The scantlings

(Plating and longitudinal stiffener) of the studied ship are checked using BV rules for the

Classification of Inland Navigation Vessels, NR 467. The strength check of the primary

supporting members (like Longitudinal Girders), transversals and other critical areas were

completed utilising direct calculation techniques and FEMAP/NX NASTRAN software.

3.5.2 Standard Loading Conditions

The distribution of weights carried in the vessel spaces arranged for storage is the loading

condition. The loading requirements for self-propelled container vessels can be separated into

the following categories: BV rules NR 467, Part B, Chapter 3 and Section 1 [36].

1. Lightship

The light standard loading conditions are:

Supplies: 100%

Ballast: 50%

Fully Loaded Vessel

The vessel is homogeneously loaded with 10% of supplies at its maximum draught, without

ballast.

Transitory Conditions 3.

The following number of supplies is assumed to be carried by the ship without ballast:

In Hogging condition: 100% of supplies

In Sagging condition: 10% of supplies

4. Loading/unloading in two runs (2R)

Loading and unloading are accomplished in two parallel runs of almost equal mass, beginning

at one end of the cargo compartment and advancing to the other.

90

5. Loading/unloading in one run (1R)

Loading and unloading are performed uniformly in one run, starting from one end of the cargo space and progressing towards the opposite end.

6. Loading/unloading for liquid Cargoes

Unless otherwise noted, loading and unloading for liquid cargoes is expected to be conducted in two runs.

3.5.3 Limit States

Structural designers aim to prevent structural breakdowns. To accomplish this goal, the designer must be aware of possible limit states, failure modes and strategies to forecast their occurrence.

Any situation in which a structure or a structural element becomes unsuited to fulfil its structural function because of effects generated by a load or a combination of loads is referred to as a limit state.

There are four different types of limit states in steel structural design:

- 1. Service or serviceability limit state.
- 2. Ultimate limit state.
- 3. Fatigue limit state.
- 4. Accidental limit state.

Table 3–4 provides a comprehensive overview of the serviceability limit states related to the hull structure, encompassing components, such as the hull girder, primary supporting members, plating and ordinary stiffeners. These limit states are crucial in assessing the ship's structural performance and safety across diverse operational scenarios. The yielding limit state addresses the maximum stress levels materials can sustain without experiencing permanent deformation. In contrast, the plate strength under lateral loads and buckling limit states are essential with the aim of evaluating the hull's capacity to resist lateral loads and its stability against buckling, respectively.

Table 3–4: Serviceability limit states.

Sr. No.	Particular	Yielding	Plate strength under lateral loads	Buckling
1	Hull girder	X		
2	Primary supporting members	X		X
3	Plating		X	X
4	Stiffener	X		X

The service limit state was considered in this research. A service limit state occurs when a structure can no longer perform its designed function, such as severe deck deflection, elastic buckling in a plate or local cracking caused by fatigue. They are usually related to aesthetic, functional or maintenance issues, but they do not result in collapse [36].

3.5.4 Partial Safety Factors

To account for uncertainty, partial safety factors were considered based on rule formulations [36].

The partial safety factors presented in Tables 3–5 (Plating partial safety factors) and 3–6 (Ordinary stiffeners-partial safety factors) are essential for ensuring that the structural components of vessels are designed with adequate safety margins to withstand the complex and dynamic forces experienced during their operational life at sea, by way of the IACS common structural rules. These factors, which include γ_{W1} , γ_{W2} , γ_R and γ_M , are meticulously calculated to account for uncertainties related to wave hull girder loads, wave local loads, resistance and material properties.

 γ_{W1} : Partial safety factor covering the uncertainties regarding wave hull girder loads.

 γ_{W2} : Partial safety factor covering the uncertainties regarding wave local loads.

 γ_R : Partial safety factor covering the uncertainties regarding resistance.

 $\gamma_{\rm M}$: Partial safety factor covering the uncertainties regarding the material.

Table 3–5: Plating partial safety factors.

Limit State	Condition	γw1	γw2	γR	γм
Strength check of plating	General	1.15	1.20	1.20	1.02
subjected to lateral pressure	Flooding (1)	NA	NA	1.05	1.02
pressure	Testing	NA	NA	1.05	1.02
Buckling check		1.15	NA	1.10	1.02

This applies only to plating to be checked in flooding conditions.

For plating of the collision bulkhead, $\gamma_R = 1.25$.

Note 1: NA = not applicable.

Table 3–6: Ordinary stiffeners-partial safety factors.

Limit State	Condition	γw1	γw2	γR	γм
Yielding check	General	1.15	1.20	1.02	1.02
	Flooding (1)	NA	NA	1.02	1.02
	Testing	NA	NA	1.02	1.02
Buckling check		1.15	NA	1.10	1.02

This applies only to ordinary stiffeners to be checked in flooding conditions.

For ordinary stiffeners of the collision bulkhead, $\gamma_R = 1.25$.

Note 1: NA = not applicable.

3.5.5 Net Scantling Approach

The hull structure's scantlings required to support the active loads without any implicit corrosion margin are termed "net scantlings." The corrosion additives are outlined in the rules and applied to the net scantlings to produce the scantlings used to construct the vessel.

The "net scantling concept" allows the strength criteria for various limit states to be explicitly described in terms of net thickness without any implicit corrosion safety margins. Corrosion additives can be specified in the Rules based on the severity of the environment to which each structural element is exposed. This formulation allows a more rational calculation of class renewal thicknesses and a more rational reassessment of vessels in service [36].

Table 3–7, vital for structural analysis, provides a detailed breakdown of corrosion additions for both sides of a structural member, denoted as t_{c1} and t_{c2} . This data compilation is essential to comprehend the effects of corrosion on the durability and integrity of structural components,

enabling a precise evaluation of potential weaknesses and vulnerabilities. It accentuates the significance of accounting for varying corrosion rates on each element. The corrosion addition values are determined independently of the net scantling requirements, offering a comprehensive foundation as regards assessing the impact of corrosion on the ship's structural strength.

Table 3–7: Corrosion additions according to BV Rules [36].

Compartment Typ	e	Corrosion addition		
Ballast tank		1.00		
Cargo tank and	Plating of horizontal surfaces	0.75		
fuel oil tank	Plating of non-horizontal surfaces	0.50		
	Ordinary stiffeners	0.75		
	Primary supporting members			
Dry bulk Cargo	General	1.00		
hold	Inner bottom plating	1.75		
	Side plating for single-hull vessel			
	Inner side plating for double-hull vessel			
	Transverse bulkhead plating			
	Frames	1.00		
	Ordinary stiffeners			
	Primary supporting members			
Hopper well of dred	ging vessels	2.00		
Accommodation spa	ace	0.00		
Compartments and areas other than those mentioned above 0.50				
*Corrosion additions	s are applicable to all the members of the considered ite	m.		

The total corrosion addition t_c , in mm, for both sides of a structural member, is equal to:

For plating with a gross thickness of more than 10 mm, use the following formula:

$$t_c = t_{c1} + t_{c2} (3-21)$$

For plating with a gross thickness of less than or equal to 10 mm, use the following formula:

 $-t_c = 20\%$ of the gross thickness of the plating, or $t_c = t_{c1} + t_{c2}$, whichever is smaller.

The total corrosion addition t_c for an internal member within a compartment is calculated as follows:

For plating or stiffener plating with a gross thickness of more than 10 mm, use the following formula:

$$t_c = 2t_{c1} (3-22)$$

For plating or stiffener plating with a gross thickness of less than or equal to 10 mm, apply the following formula:

 $-t_c = 20\%$ of the gross thickness of the plating considered, or $t_c = 2t_{c1}$, whichever is smaller.

Where t_{c1} is the value of the corrosion addition specified in Table 3–7 for one side of the compartment's exposure and t_{c2} is the value of corrosion addition for the other side.

The net transverse section's net strength characteristics must be computed. The net section modulus of bulb profiles can also be calculated using the following formula:

$$w = w_G \left(1 - \alpha t_c \right) - \beta t_c \tag{3-23}$$

where

 w_G : stiffener gross section in cm³.

Table 3–8 defines the coefficients α and β for bulb profiles based on the range of the stiffener cross-section (cm³). In ship structures, bulb profiles function as asymmetrical plate stiffeners for ship hull construction and various other structural applications. The dimensions and properties of these stiffeners significantly impact the ship's structural performance under uniform pressure loads and buckling requirements.

Table 3–8: Coefficients α and β for bulb profiles [36].

Range of w_G	α	β
$w_G \le 200 \text{ cm}^3$	0.070	0.4
$w_G > 200 \text{ cm}^3$	0.035	7.4

The calculation of the net thickness of plate elements according to BV rules NR 467, Part B Chapter 2 Sec. 5 is shown in Table 3–9 [36]. This complex calculation subtracted the corrosion addition from the plating thickness. The resulting net thickness is an essential engineering parameter that helps maintain steel ships' structural integrity and safety, particularly during continuous service and the effects of corrosion.

Table 3–9: The net thickness of plate elements.

Sr. No.	Parts Name	Material Grade	Gross thickness (mm)	Compartment type	sides	or both s of a ctural aber				Net thickness (mm)
					t_{c1}	t_{c2}	t_c	t_{c1}	t_c	_
1	Keel plate	A	13	Ballast tank/other	1	0.5	1.5	-	-	11.5
2	Bottom and bilge plate	A	11	Ballast tank/other	1	0.5	1.5	-	-	9.5
3	Side shell plate	A	10	Ballast tank/other	1	0.5	1.5	-	-	8.5
4	Shear strake plate	AH36	12	Ballast tank/other	1	0.5	1.5	-	-	10.5
5	Inner bottom plate 1	A	15	Ballast tank/other	1	0.5	1.5	-	-	13.5
6	Inner side shell plate 1	A	14	Ballast tank/other	1	0.5	1.5	-	-	12.5
7	Inner side shell plate 2	A	9	Ballast tank/other	1	0.5	1.5	-	-	7.5
8	Inner side shell plate 3	A	12	Ballast tank/other	1	0.5	1.5	-	-	10.5
9	Bulkhead plate stiffener	A	12	Ballast tank/other	1	0.5	1.5	-	-	10.5
10	Bulkhead plate	A	12	Ballast tank/other	1	0.5	1.5	-	-	10.5
11	Hatch coaming stay plate	AH36	10	other/other	0.5	0.5	1	-	-	9
12	Hatch coaming stiffener	DH36	12	other/other	0.5	0.5	1	-	-	11
13	Hatch coaming top plate	DH36	22	other/other	0.5	0.5	1	-	-	21
14	Hatch coaming plate	DH36	15	other/other	0.5	0.5	1	-	-	14
15	Main deck plate	AH36	15	Ballast tank/other	1	0.5	1.5	-	-	13.5
16	Inner bottom plate 2	A	12	Ballast tank	-	-	-	1	2	10
17	DB long girder CL	A	18	Ballast tank	-	-	-	1	2	16

Sr. No.	Parts Name	Material Grade	Gross thickness (mm)	Compartment type	sides	ctural	1	T _c for an internal member a compa		Net thickness (mm)
					t_{c1}	t_{c2}	t_c	t_{c1}	t_c	_
18	DB long girder 3786-OCL	A	12	Ballast tank	-	-	-	1	2	10
19	DB long girder 6325-OCL	A	9	Ballast tank	-	-	-	1	1.8	7.2
20	Bottom longitudinal	A	8	Ballast tank	-	-	-	1	1.6	6.4
21	Inner bottom longitudinal	AH36	10	Ballast tank	-	-	-	1	2	8
22	Side shell longitudinal	A	8	Ballast tank	-	-	-	1	1.6	6.4
23	Inner side shell longitudinal	A	8	Ballast tank	-	-	-	1	1.6	6.4
24	Main deck longitudinal	AH36	10	Ballast tank	-	-	-	1	2	8
25	Flat bar-side shell	A	8	Ballast tank	-	-	-	1	1.6	6.4
26	Web frame plate_side shell 1	AH36	8	Ballast tank	-	-	-	1	1.6	6.4
27	Web frame plate_side shell 2	AH36	11	Ballast tank	-	-	-	1	2	9
28	Web frame plate bottom 1	A	9	Ballast tank	-	-	-	1	1.8	7.2
29	Web frame plate _ bottom 2	A	11	Ballast tank	-	-	-	1	2	9
30	Flat bar-bottom	A	10	Ballast tank	-	-	-	1	2	8
31	Ordinary frame bracket	A	9	Ballast tank	-	-	-	1	1.8	7.2

3.5.6 Hull Girder Strength Check

The stress values are examined to ascertain if they fall within the rule requirements. Based on BV rules NR 467, Part B, Section 2, Chapter 4, Sec. 2, a hull girder yielding check was performed [36]. The hull girder normal stresses caused by vertical bending moments are calculated using the beam theory and the following formulae:

In Hogging condition

$$\sigma_1 = \left(\frac{M_{TH}}{Z}\right) 10^3 \,(\text{N/mm}^2)$$
 (3–24)

In Sagging condition

$$\sigma_1 = \left(\frac{M_{TS}}{Z}\right) 10^3 \,(\text{N/mm}^2)$$
 (3–25)

Checking criteria for hull girder stress are given by the following equation:

$$\sigma_1 = MAX (\sigma_H, \sigma_S) \le \frac{175}{K} (\text{N/mm}^2)$$
 (3-26)

where M_{TH} and M_{TS} are the vertical bending moments in the Hogging and Sagging conditions, respectively, Z is the section modulus and K is the material factor.

Table 3–10: Material factor [36].

Material yield stress, R_{EH} in N/mm ²	Material factor K
235	1.00
315	0.78
355	0.72
390	0.68

Table 3–10 presents the material factor corresponding to different steel grades, which holds significant importance in determining the mechanical characteristics of the steel. The material factor is closely associated with the specified minimum yield stress of the steel, effectively categorising steel grades based on their strength levels. For instance, steel boasting a specified minimum yield stress of 235 N/mm² is categorised as normal strength, whereas steel with a

higher yield stress is classified as higher strength. The material factor is applied for hull girder strength and scantling purposes in the construction of ships.

3.6 Design Loads

3.6.1 Overview

A ship at sea is subjected to various loads that produce structural deformation and stress. The initial step is to assume accurately defined loads acting on the structure to construct a design. The load is gradually transferred from a local structural member to a more significant supporting element [3]. Global or primary loads act on the ship as a beam (hull girder), and primary response loads affect the ship's structural behaviour. Alternatively, local loads are applied to limited structural models (stiffened panels, single beams and plate panels). Individual structural components, for instance plating panels, ordinary stiffeners and significant supporting members, are subjected to local loads, which are pressures and stresses applied directly to them [121]. In this analysis, only hull girder loads were applied to investigate this ship's longitudinal strength.

3.6.2 Hull Girder Loads

There are static and dynamic components to ship hull girder loads. More specifically, still water bending moments and shear forces are the most important of these components. The ship's hull girder can be considered a non-uniform beam subjected to variable loads along its length [123].

3.6.2.1 Still Water Bending Moments (SWBM)

Under one load condition, the still water bending moment at a given section of the ship is constant but varies from one load condition to the next. Each load condition's duration is likewise a random variable. According to the above load cases, classification society rules specifically provide formulations to evaluate still water bending moment values. The direct computation can also determine the bending moment of still water [124]. This study estimated the still water bending moment using the BV, NR 467 rules for the classification of steel ships [36].

3.6.2.2 Vertical Wave Bending Moment (VWBM)

An additional vertical bending moment induced by waves must be considered to estimate the total bending moment. This component depends on the ship's navigation range. In this investigation, the analysed ship's navigation range was unrestricted. The vertical wave bending moment was also determined according to BV and NR 467 rules for the classification of steel ships [36].

3.6.2.3 Horizontal Wave Bending Moment (HWBM)

A horizontal wave bending moment ensues when a ship is in a beam and oblique sea [125]. According to the BV, NR 467 rules for the classification of steel ships, the horizontal wave bending moment at any hull transverse section must be calculated [36].

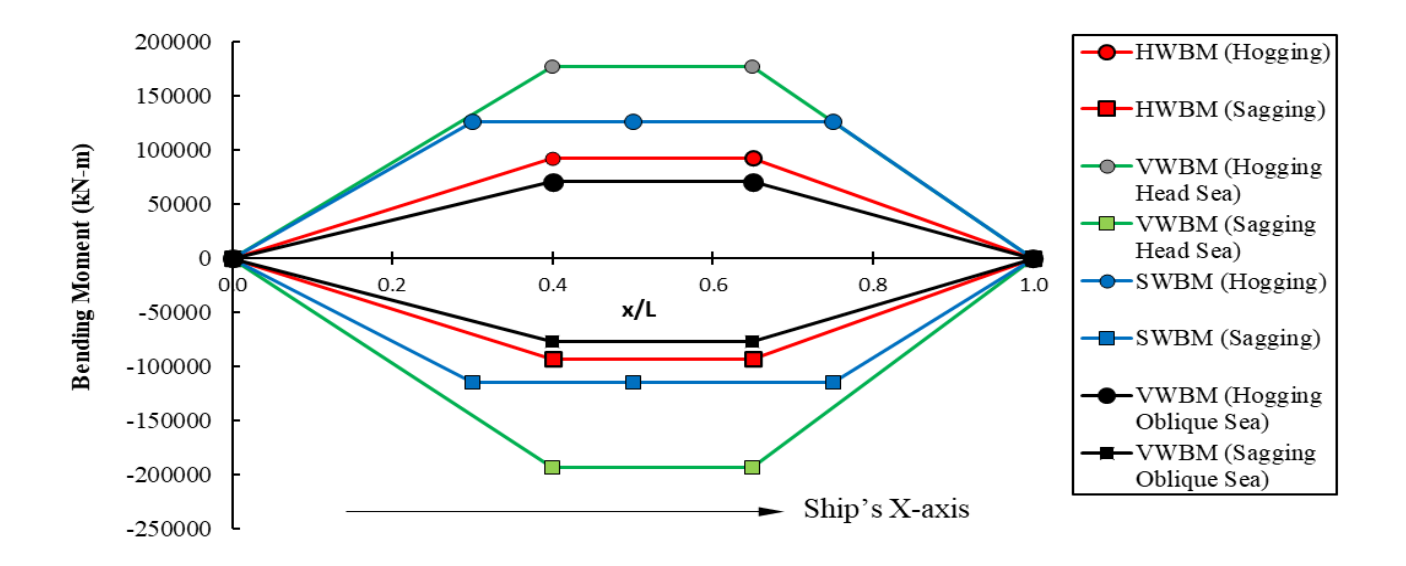


Figure 3-8: Comparison of the analysed ship's bending moments along the ship's length (*L*).

Figure 3–8 compares the ship's bending moments, illustrating the distribution and variation of bending moments along the ship's length (L). This graph provides details about how environmental factors influence the ship's structural integrity. It facilitates a better understanding of the ship's load-bearing capacity and offers valuable information for optimising design and operational decisions to enhance performance and safety.

3.6.2.4 Wave-Induced Torsional Moment

The wave-induced torsional moment occurs in oblique seas [126]. The wave-induced torsional moment at any transverse hull section is calculated using BV, NR 467 rules (Pt B, Chapter 5, Sec. 4) for steel ship classification [36].

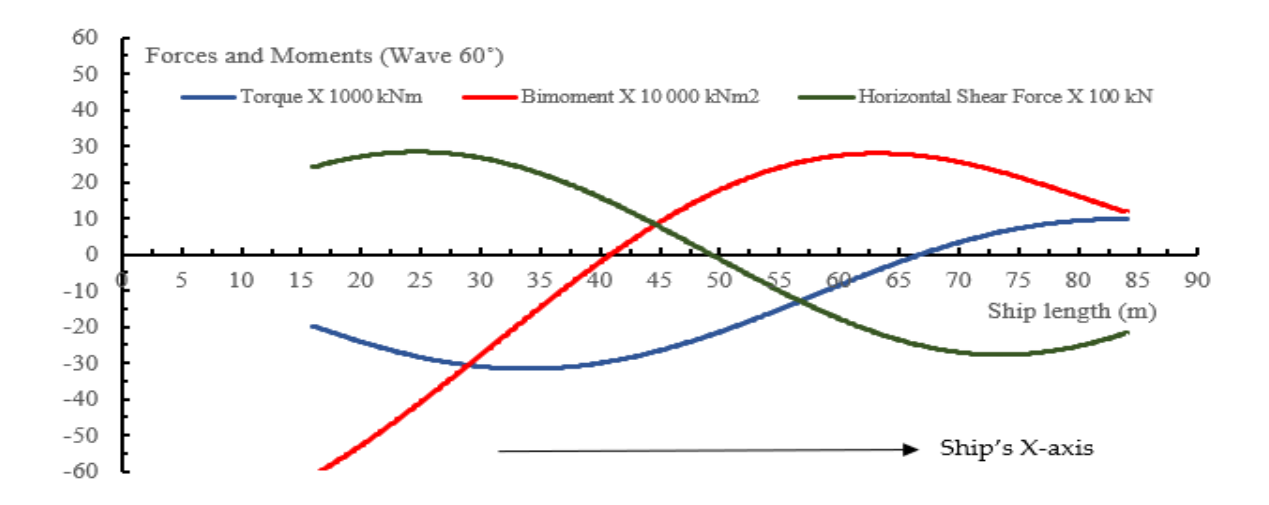


Figure 3-9: Wave-induced torsional moment of the analysed ship along the ship's length (L) (wave at 60°).

Figure 3–9 shows the distribution of horizontal shear force, bi-moment, and torque within the cargo hold of the ship when the ship's wave angle is 60°. The data reveals that these forces peak near the edges at both the aft and forward bulkheads, highlighting critical stress points that are vital for understanding the structural response of the cargo hold under load.

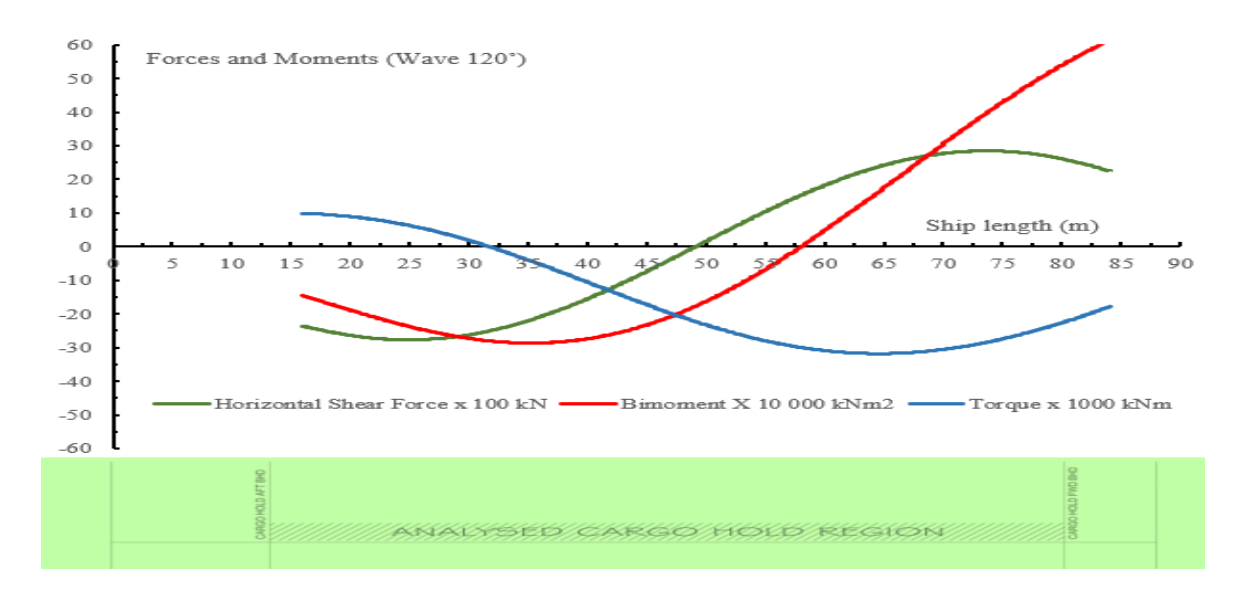


Figure 3-10: Wave-induced torsional moment of the analysed ship along the ship's length (L) (wave at 120°).

Figure 3–10 shows the distribution of maximum values for horizontal shear force, bi-moment, and torque along the entire length of the cargo hold when the ship's wave angle is 120°. This consistent application ensures that the structural analysis accurately represents operational conditions, facilitating effective design and safety evaluations.

3.6.3 Load Cases

When considering load cases for self-propelled multi-purpose cargo ships, it is crucial to account for still water and wave loads. These loads are chosen to identify the most significant impacts that can affect the ship's structural integrity [108]. According to BV, NR 467 regulations for the classification of steel ships [36], load cases can be divided into two categories:

1. Upright ship condition.

In this condition, hull girder loads are composed of still water bending and vertical wave bending moments.

2. Inclined ship condition.

When the ship is inclined, it experiences various hull girder loads, incorporating still water bending moment, vertical wave bending moment, horizontal wave bending moment, along with wave-induced torsional moment.

The hull girder loads to be considered in each load situation are provided in Table 3–11, according to BV Rules NR 467 (Part B, Chapter 3, Sec. 1). Table 3–11 shows the distinct contributions of vertical wave bending moments under different load conditions. In the upright load case, the vertical wave bending moment contributes fully. Nonetheless, its contribution is reduced to 40% in the incline load case. In contrast, the horizontal wave bending moment exhibits a different behaviour: it makes no contribution in the upright load case but is a full contributor in the incline load case.

Table 3–11: Wave hull girder loads in each load case [36].

Lood asso	Vertical way	ve bending moment	Horizontal wave bending moment			
Load case	Ref. value Combination factor		Ref. value	Combination factor		
Upright	M_{WV}	1	M_{WH}	0		
Incline	M_{WV}	0.4	M_{WH}	1		

This study applied the following load cases and loading conditions for structural analysis. Table 3–12 shows the loading conditions for ships, explicitly focusing on rule-based load cases for both upright and inclined conditions. The table presents scenarios for full load (Sagging) and ballast load (Hogging), which are crucial for assessing the structural integrity of the vessel and determining the longitudinal strength and ultimate stability of the ship's hull structure.

Table 3–12: Rule-based load cases and loading conditions [36].

	Loading conditions	
Load cases	Full Load (Sagging)	Ballast load (Hogging)
Upright condition	X	X
Inclined condition	X	X

3.7 Analysed Ship Structural Analysis

The global strength analysis aids in determining the stress and stiffness of a hull girder for specific load cases caused by loading conditions. Its goal is to assess the strength of the hull girder in a longitudinal direction rather than the local strength from local loads. When simple beam theory is unsatisfactory in relation to estimating the structural response of the hull girder, a global strength analysis may be required. Examples include the following [124]:

- Container ships have substantial deck openings that are susceptible to overall torsional deformation and stress responses.
- Certain ships, such as Ro-Ro and vehicle carriers, do not have transverse bulkheads running along the ship's length or may have limited bulkheads.
- On large passenger ships, there may be a partially functional superstructure or top hull girder.

This section undertakes a comprehensive analysis of the global longitudinal structural integrity of the investigated vessel. The assessment of structural robustness aligns meticulously with the stringent requirements stipulated by BV Rules. The midship section's plating and stiffeners are systematically checked as per (BV) rules using the MARS 2000 software. All structural components in the midship section undergo careful examination, with a thorough comparison with respect to the specified rules. Appendix A comprises a detailed report on the evaluation of

compliance with the rules, including the outcomes for all longitudinal stiffeners and plate strakes, presented by means of the results provided by the MARS 2000 software.

Furthermore, the structural adequacy assessment of primary supporting constituents is methodically executed by means of direct calculation. The computational process is smoothly combined with the FEMAP platform and connected with NX-NASTRAN. This analytical approach guarantees a meticulous evaluation of the primary structural members' resilience, corroborating their conformity with the exacting standards of strength and stability.

This section painstakingly examines the scantlings of plating and ordinary/secondary stiffeners using BV rules and guidelines. The Bureau Veritas MARS 2000 tool is exploited to conduct a detailed assessment to make certain that the stipulated dimensions comply with the strict requirements outlined in BV regulations. It is important to note that the values the MARS 2000 tool provides to evaluate plating and secondary stiffener dimensions are given in a gross context.

Subsequently, a meticulous process ensues whereby the scantling verification is executed based on net scantlings, effectively accounting for the corrosion allowance, which is deducted from the specified thickness values. This prudent method ensures that the measurement is accurate and complete in assessing the strength and alignment of the structure according to relevant standards. Following this strict process, all aspects of the vessel are methodically reviewed to assure compliance with important regulations. This proactive approach helps identify any hidden weaknesses in the structure, which can then be addressed to enhance the safety and reliability of the vessel, confirming its ability to operate consistently.

3.7.1 MARS 2000

The MARS 2000 software, developed by Bureau Veritas, is used for scantling calculations. This software can perform scantling calculations for plating and stiffeners on any transverse section of the vessel's parallel body. The strength of primary supporting members and transverse elements can be considered through direct calculations or finite element analysis. The Bureau Veritas MARS 2000 software has three modules that can be accessed from its main graphical user interface (GUI):

- Basic Ship Data
- Edit

• Rule

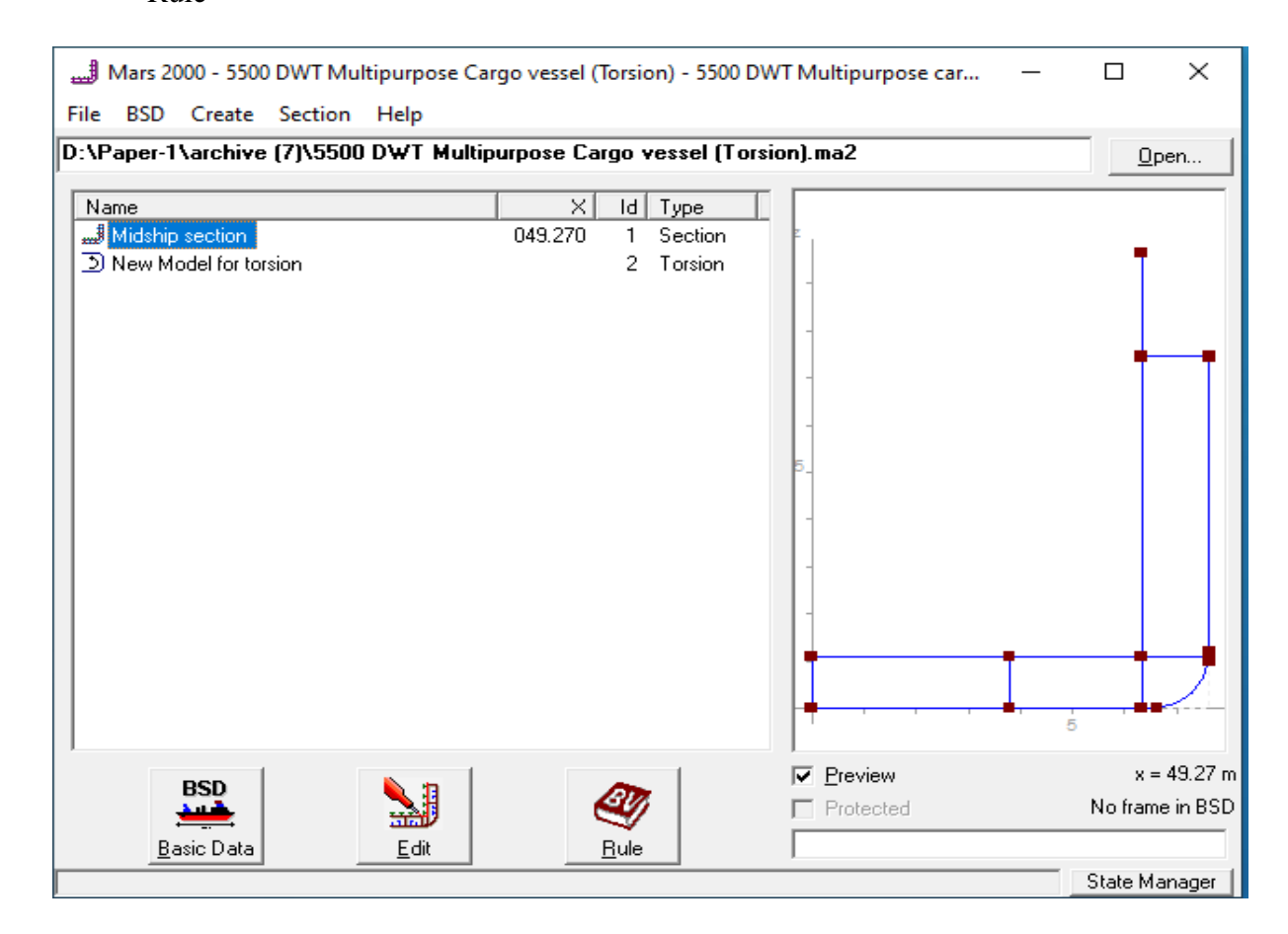


Figure 3-11: MARS Inland main interface.

The Basic Ship Data (BSD) module starts the process and establishes the main particulars of the ship. This essential module is further divided into six separate subsections, each of which focuses on documenting a particular piece of information that, taken together, creates an exhaustive representation of the ship's features. These subsections are essential building blocks in the assessment and design processes to ensure every significant detail is identified.

- 1. General
- 2. Notations & Main Data
- 3. Moment & Draughts
- 4. Materials
- 5. Frame Locations
- 6. Calculations & Print

Figure 3–11 shows the primary interface of BV Mars 2000 software, distinguished by its user-friendly and intuitive design, promoting effortless modelling and robust consistency and error checks. This software offers swift computations and grants immediate access to detailed results, allowing in-depth analysis. It is a valuable resource for evaluating ships' transverse cross-sections, transverse bulkheads, besides hull strength criteria. BV Mars 2000 is a 2D engineering tool enabling professionals to establish a fundamental ship model and conduct scantling calculations according to the Bureau Veritas and IACS regulations, making it an indispensable asset for ship design and assessment.

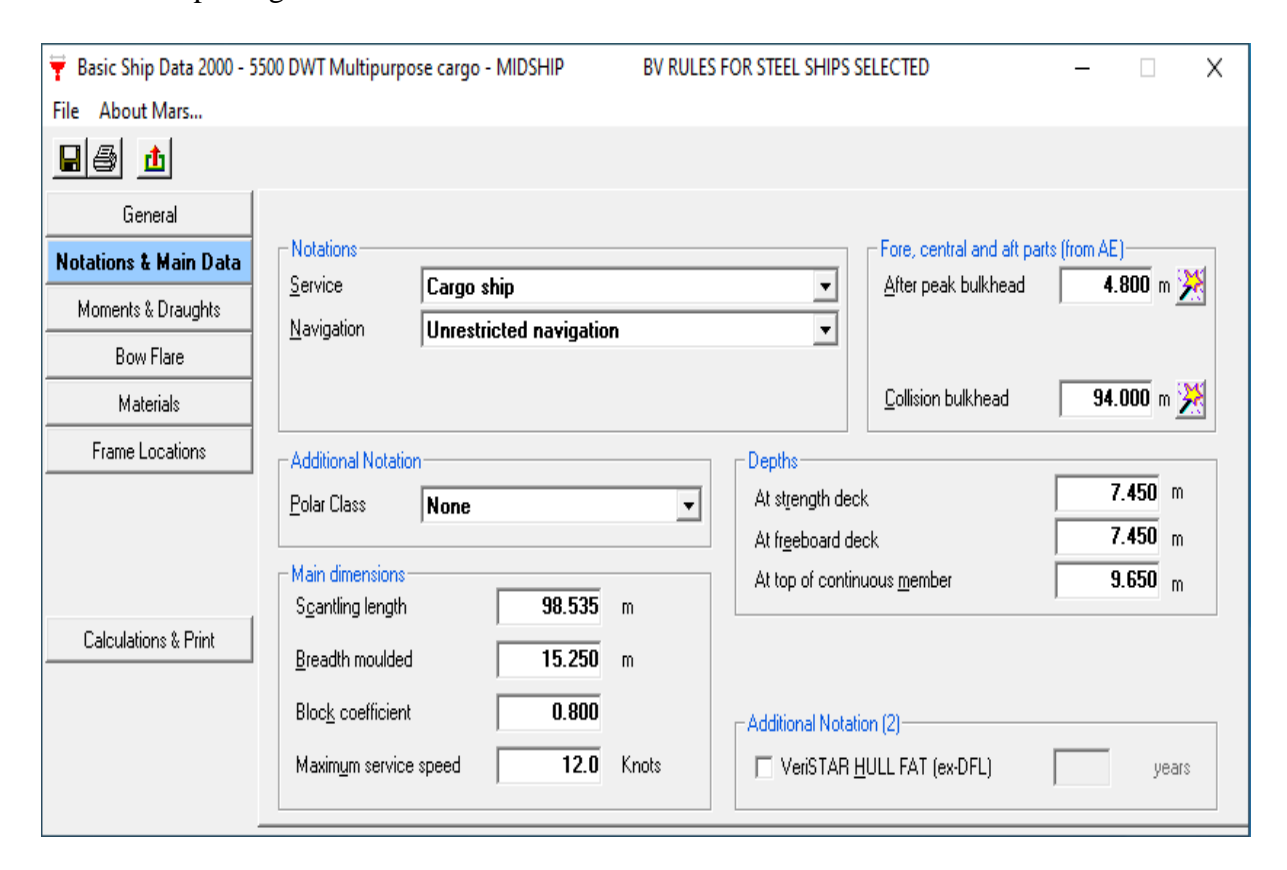


Figure 3-12: Basic ship's input data.

Figure 3–12 comprehensively shows the primary input data parameters utilised in the ship's analysis. After establishing the fundamental ship data, the section is constructed within the Edit module. Initially, the section's geometry is outlined by defining nodes and panels. Following this, various components such as plating strakes, longitudinal stiffeners, transverse stiffeners and compartments are meticulously defined. In the case of each element, it is imperative to input the gross scantlings as initial dimensions. The MARS 2000 software subsequently derives net scantlings, employing rules based on the specific compartment within which each element is positioned.

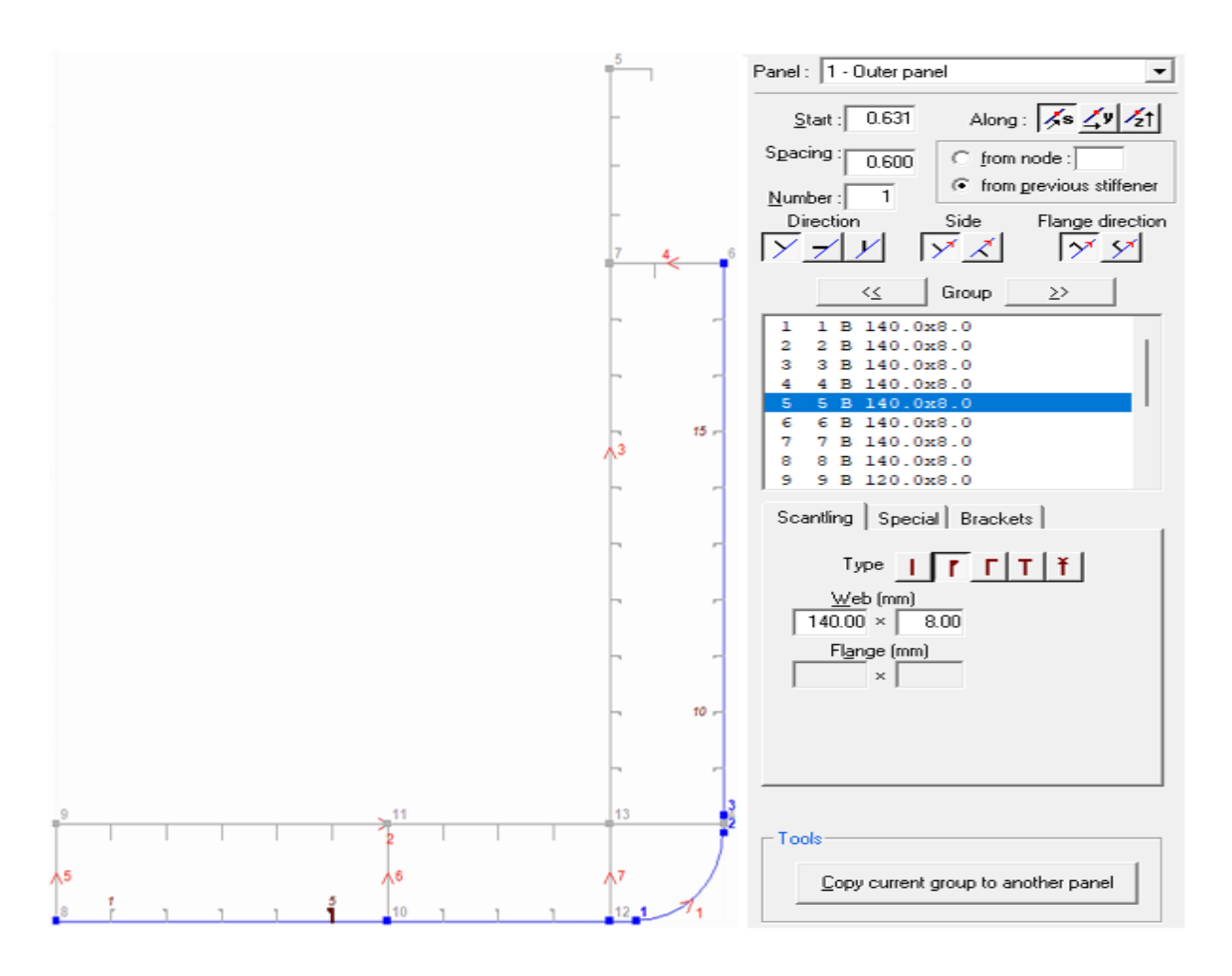


Figure 3-13: Midship section in MARS 2000.

Figure 3–1 shows the midship section of a ship within the BV Mars 2000 software. The BV Mars software will validate this midship to guarantee its structural integrity and safety. This validation process is fundamental to ensuring the ship's structural integrity and safety, encompassing critical assessments of transverse sections, geometric properties, hull girder strength, local strength criteria for plates and stiffeners, as well as the examination of side frames for single-sided bulk carriers and oil tankers. It confirms that the ship's design conforms to strict industry regulations and safety standards, demonstrating its commitment to excellence and safety in maritime engineering and shipbuilding.

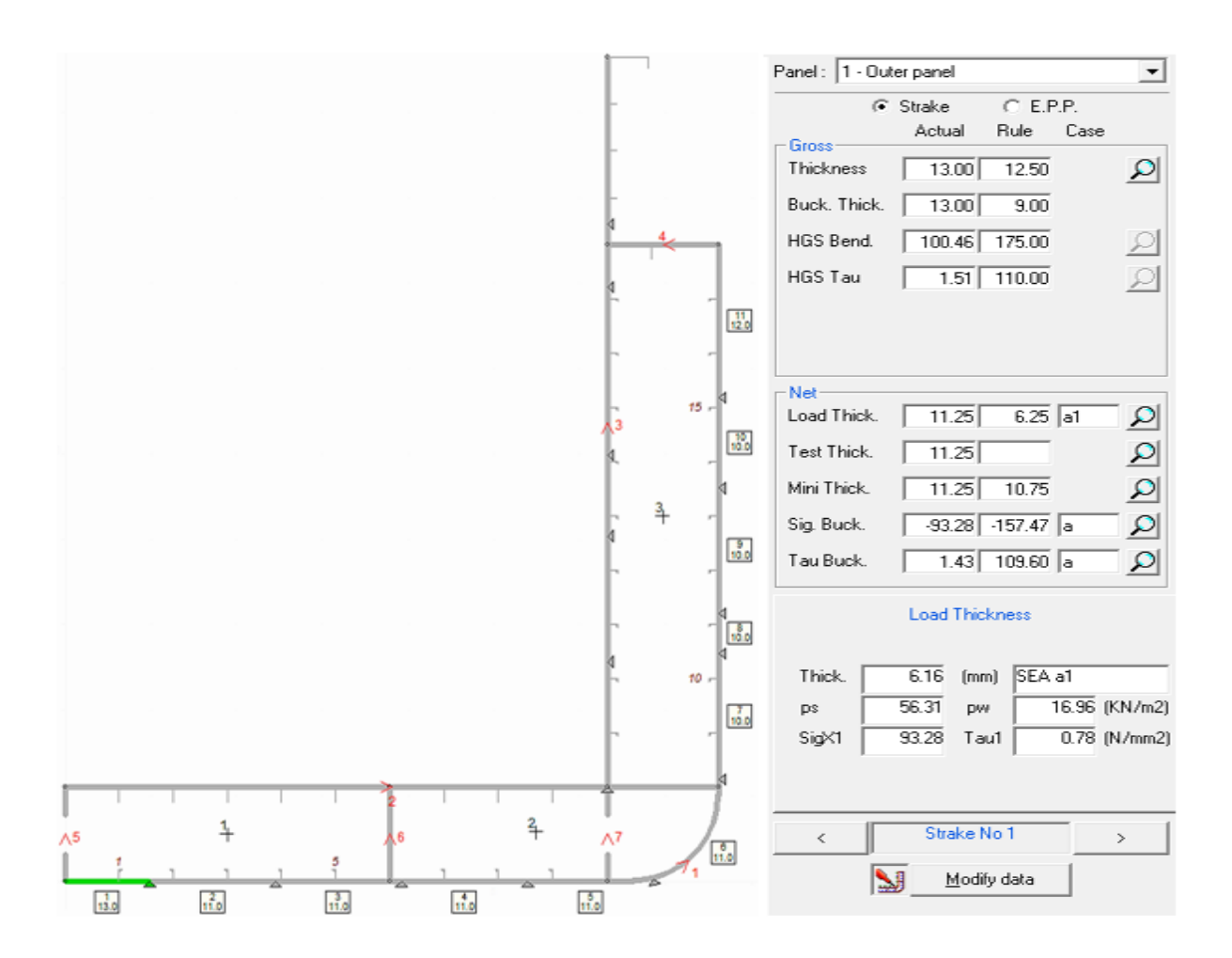


Figure 3-14: Calculations and rule check in MARS 2000.

Figure 3–14 shows the calculations and rule checks performed on the analysed ship's midship section within BV MARS 2000. The Rule module encompasses evaluations of yielding, ultimate strength, together with buckling tests for the longitudinal stiffeners. Moreover, this module generates output results that include cross-sectional characteristics for both gross and net scantlings.

3.7.2 Checking Criteria for Stress

A strength check was performed with FEMAP, utilising checking criteria from BV and NR 467 rules to classify steel ships [36].

The master allowable stress, σ_{Master} , in N/mm², was obtained from the following formula [36]:

$$\sigma_{Master} = \frac{R_y}{\gamma_R \gamma_M} \tag{3-27}$$

where

 R_y : is the yielding stress.

 γ_R : is the resistance partial safety factor and

 γ_M : is the material partial safety factor.

For mild steel (Grade A), the master allowable stress, σ_{Master} , is calculated as 219.42 N/mm². σ_{Master} , the maximum allowed stress for high tensile steel (Grade AH-36), is estimated to be 331.77 N/mm². It is crucial to confirm that the equivalent hull girder stress σ_{VM} is in keeping with the following formula for different types of analyses:

$$\sigma_{VM} \le \sigma_{Master}$$
 (3–28)

3.7.3 Hull Girder Strength Check

The section modulus at the deck and bottom is compared to the following rule requirements:

The analysis in Table 3–13 demonstrates that the specified rule requirements have been satisfactorily met, with the actual section modulus surpassing the specified threshold. Subsequently, a thorough comparison is conducted using gross and net scantling values to assess how closely the calculated values are in keeping with the predetermined acceptance criteria.

Table 3–13: Section modulus comparison.

Section modulus	Distance from baseline (m)	Rule	Actual
Bottom (m ³)	0.000	1.75244	3.02538
Deck (m ³)	7.450	1.26176	2.04909
Hatch coaming top (m ³)	9.578	1.26176	1.38528

After an in-depth examination of Table 3–14, it is evident that the modulus of the deck, bottom and hatch coaming top sections adheres well to the required standards for both the actual gross and net section modulus. The structural assessment was conducted with meticulous attention to detail and precision, ensuring that the vessel's crucial components met the regulatory criteria. This observation confirms the high level of alignment achieved.

Table 3–14: Gross/Net moduli.

Section modulus	Distance from baseline (m)	Actual gross	Actual net
Deck (m ³)	7.450	2.049091	1.837189
Bottom (m ³)	0.000	3.025378	2.603001
Hatch coaming top (m ³)	9.578	1.385278	1.235224

Table 3-15 confirms that the stress evaluations validate the structural strength of the ship's deck, bottom, and hatch coaming top under various loading conditions. The stress levels are well below the established thresholds, as outlined in Section 3.7.1.2. The scrupulous analysis of stress distribution further confirms that the hull girder of the vessel is subjected to bending stresses that comply with the permissible limits set by relevant regulations.

Table 3–15: Hull girder bending stress.

Items	Distance from baseline (m)	Sagging, σ_S (N/mm ²)	Hogging, σ_H (N/mm ²)
Bottom	0.000	101.61	100.46
Deck	7.450	150.02	148.33
Hatch coaming top	9.578	224.32	221.79

3.7.4 Scantling Check of Plating

A scantling check of plating is performed to confirm that the vessel's thickness values meet the rule's criteria. The net thickness values should be higher than the BV regulations, NR 467, Part B, Chapter 5's required values.

Mars 2000 calculates three different rule-based thicknesses. These thicknesses are:

 t_1 or $t_{Minimum}$: considers the minimum thickness of the vessel.

 t_2 or t_{Load} : considers local (external/internal) pressures owing to loads.

 t_3 or $t_{Buckling}$: considers the buckling strength check.

The net scantlings (scantlings adjusted for corrosion allowance) were compared to the required rule values. The results of the scantling checks for plating under Hogging and Sagging conditions are summarised in Tables 3–16 and 3–17, respectively. The net thickness values

were compared to the most stringent rule values (selected from $t_1/t_2/t_3$) to maintain compliance with all the requirements.

Based on the information in Table 3–16, Inner Bottom Plate-2 did not meet the required thickness outlined by regulatory standards. Similarly, DB Longitudinal Girder 3786 OCL and DB Longitudinal Girder 6325 OCL did not meet the required thickness, contravening the criteria set for buckling considerations (t_3). However, these components meet the minimum required rule values (t_2/t_1) during Hogging. Similarly, Table 3–17 pinpoints that Inner Bottom Plate-2 does not satisfy the thickness requirements associated with buckling considerations (t_3). Even so, it does meet the minimum required rule values (t_2/t_1) for the Sagging condition.

Table 3–16: Scantling check of plating (Hogging condition).

		Gross t	hickness	
Sr. No.	Plating	Actual thickness (mm)	Maximum rule thickness (mm)	Definition
1	Keel plate	13	12.5	1
2	Bottom & Bilge plate	11	9.5	3
3	Side shell plate	10	9.5	1
4	Shear strake plate	12	10.5	1
5	Inner bottom plate 1	15	12.5	2
6	Inner side shell plate 1	14	9	2
7	Inner side shell plate 2	9	8	2
8	Inner side shell plate 3	12	11	1
9	Hatch coaming plate	15	11	3
10	Main deck plate	15	13	3
11	Inner bottom plate 2	12	13	2
12	DB long girder CL	18	13.5	3
13	DB long girder 3786 OCL	12	14.5	3
14	DB long girder 6325 OCL	9	12.5	3

⁽¹⁾ Minimum rule thickness t_1 . Maximum of the values calculated on each EPP.

⁽²⁾ Thickness t_2 based on external or internal design pressure and on a stress factor λ_T or λ_L coming from the overall bending stress. The output value of load thickness t_2 is the maximum one.

⁽³⁾ Buckling thickness t_3 . Value calculated on critical EPP.

Table 3–17: Scantling check of plating (Sagging condition).

		Gross t	hickness	_	
Sr. No.	Plating	Actual thickness (mm)	Maximum rule thickness (mm)	Definition	
1	Keel plate	13	12.5	1	
2	Bottom & Bilge plate	11	9.5	3	
3	Side shell plate	10	9.5	1	
4	Shear strake plate	12	10.5	1	
5	Inner bottom plate 1	15	12.5	2	
6	Inner side shell plate 1	14	9	2	
7	Inner side shell plate 2	9	7.5	2	
8	Inner side shell plate 3	12	9	3	
9	Hatch coaming plate	15	11	3	
10	Main deck plate	15	13	3	
11	Inner bottom plate 2	12	13	2	
12	DB long girder CL	18	11.5	3	
13	DB long girder 3786 OCL	12	11.5	1	
14	DB long girder 6325 OCL	9	6.5	3	

- (1) Minimum rule thickness t_1 . Maximum of the values calculated on each EPP.
- (2) Thickness t_2 based on external or internal design pressure and on a stress factor λ_T or λ_L coming from the overall bending stress. The output value of load thickness t_2 is the maximum one.
- (3) Buckling thickness t_3 . Value calculated on critical EPP.

This research will focus on optimising multiple objectives, including weight and production costs. Granting Inner Bottom Plate-2, DB Longitudinal Girder 3786 OCL and DB Longitudinal Girder 6325 OCL do not currently meet the buckling criteria, after optimisation, the primary focus will be on verifying that the optimised model scantlings satisfy both yielding and buckling criteria.

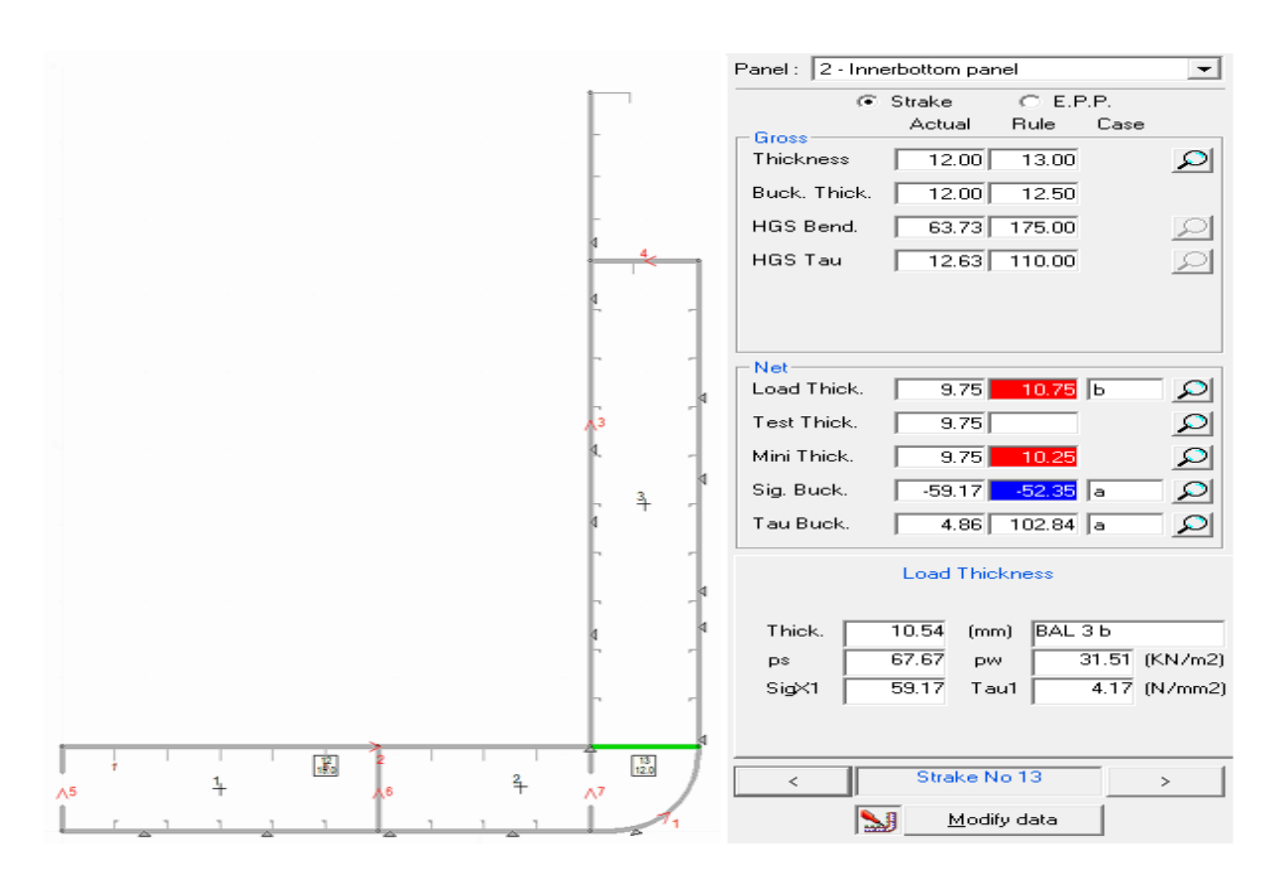


Figure 3-15: Inner bottom plate 2 (Hogging condition).

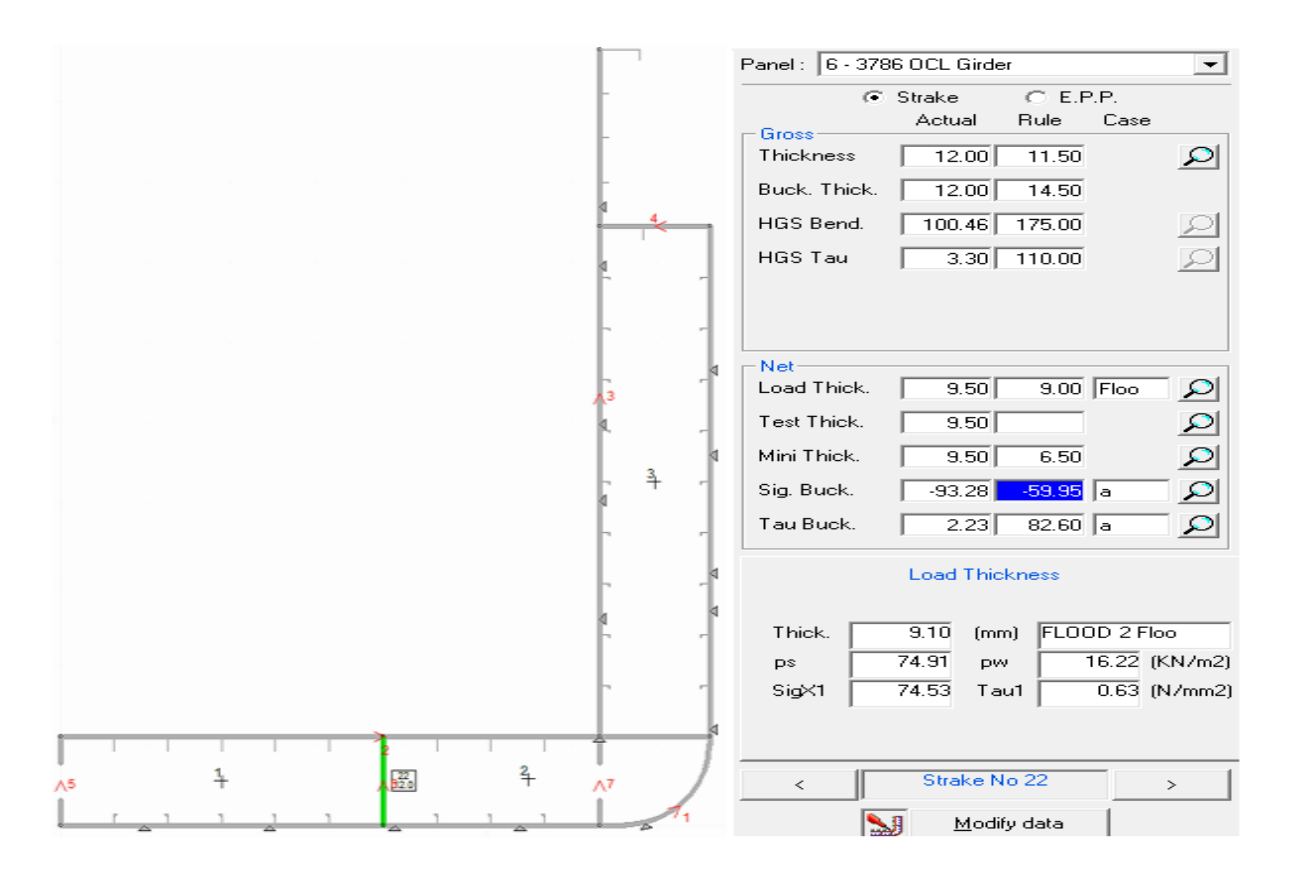


Figure 3-16: Double bottom longitudinal girder 3786 OCL (Hogging condition).

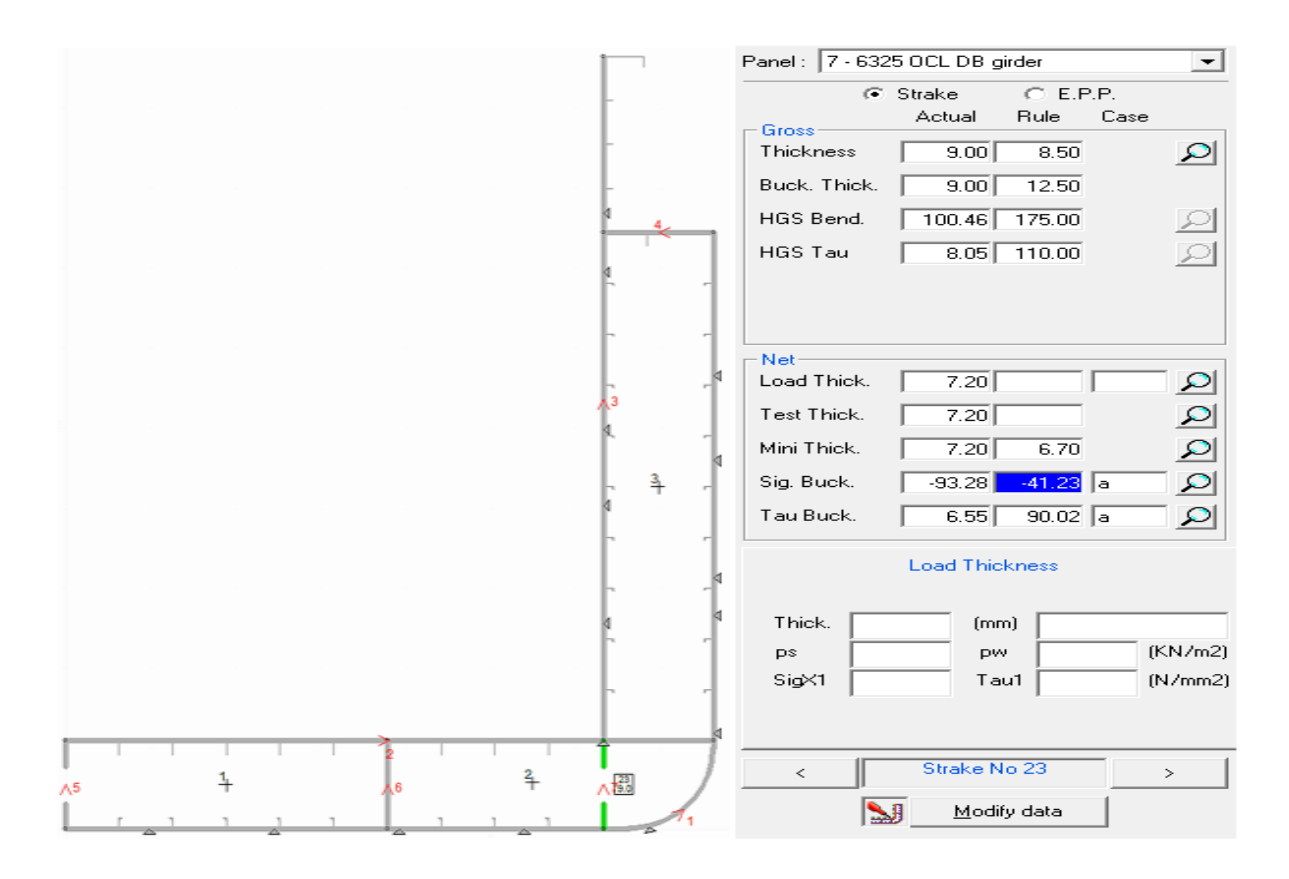


Figure 3-17: Double bottom longitudinal girder 6325 OCL (Hogging condition).

Figures 3–15, 3–16 and 3–17 in this study present a comprehensive comparative analysis of gross actual and gross rule thickness, as well as load actual and load rule thickness, in conjunction with buckling actual and rule thickness under Hogging conditions for Inner Bottom Plate 2, double bottom longitudinal girder 3786 OCL plate and double bottom longitudinal girder 6325 OCL plate. This analysis was carried out using BV Mars 2000 Software. The findings from this assessment offer valuable insights into the structural compliance of ship scantlings with design standards and real-world conditions.

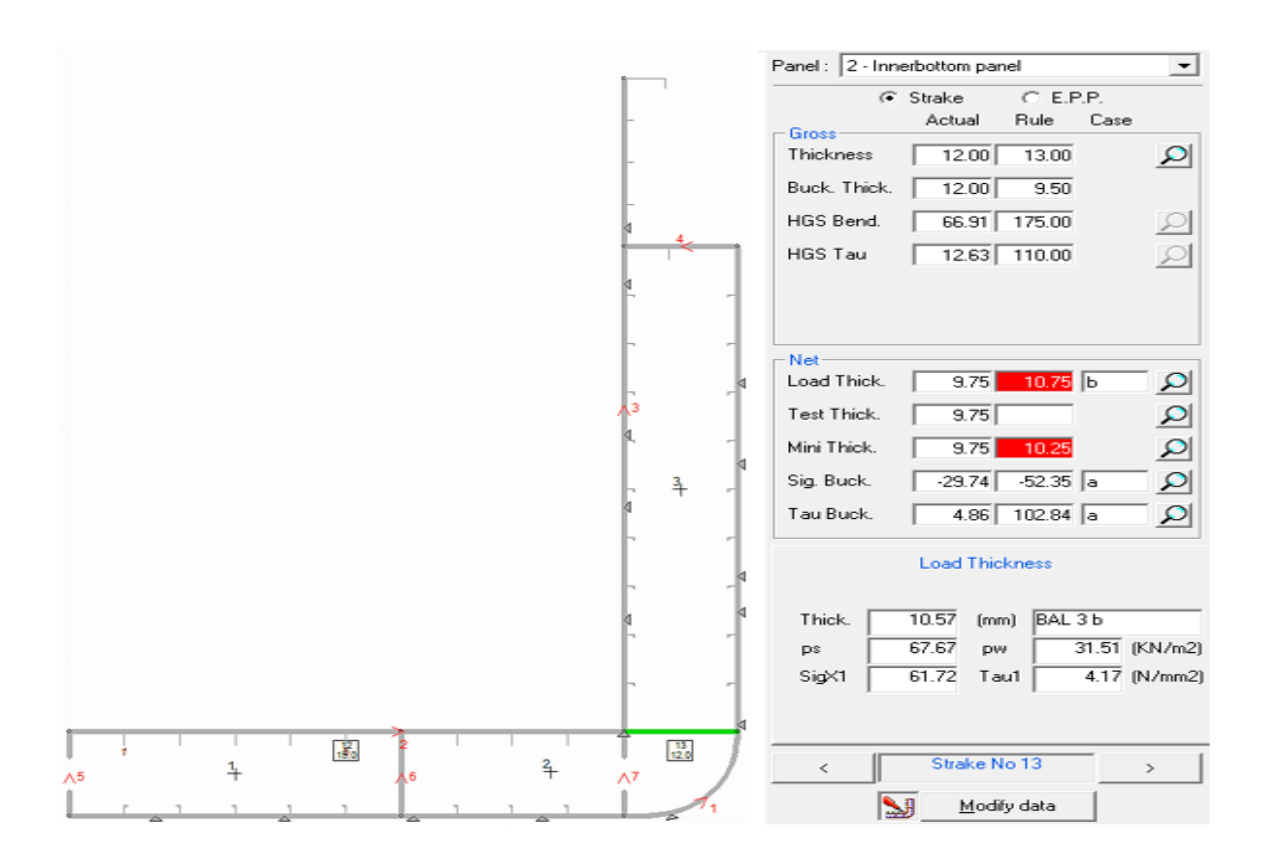


Figure 3-18: Inner bottom plate 2 (Sagging condition).

Figure 3–18 shows a comprehensive comparative study of critical parameters, including gross actual and rule thickness and net actual and rule thickness for Inner Bottom Plate-2. The analysis is unequivocally conducted under Sagging conditions relevant to structural assessments. This thorough examination significantly enhances the understanding of how ships respond to Sagging conditions, providing valuable insights into structural integrity and compliance with industry standards. These meticulous investigations support informed decision-making in ship design and operation.

3.7.5 Scantling Check of Secondary Stiffeners

The secondary stiffeners are checked for their scantlings to meet the required standards. This verification involves calculating the actual section modulus and shear area using the net scantling approach and comparing them to the required rule specifications. Net scantling measurements are compared to maximum rule values, similar to the plating procedure. This process ensures compliance with regulations by meticulously matching the computed section modulus and shear area with the stipulated requirements.

Tables 3–18 and 3–19 present valuable data pertaining to secondary members under Hogging conditions. Table 3–18 reveals that the thicknesses of the inner bottom and deck stiffeners are inadequate, while Table 3–19 complements this by detailing the shear area and section modulus of these secondary stiffeners, demonstrating that all items exceed the rule criteria. Despite the inadequate thicknesses, the ship's overall structural integrity is maintained, allowing it to endure challenging weather conditions and loading scenarios.

Table 3–18: The net thickness of the stiffener web (Hogging condition).

	T	Net thickness				
Sr. No.	Longitudinal	Actual thickness (mm)	Minimum thickness (mm)			
1	Bottom	8	6.5			
2	Inner bottom	10	13			
3	Side shell	8	6.0			
4	Inner side shell	8	6.0			
5	Main deck	10	13			
6	Hatch coaming	12	8			

Table 3–19: Shear area/Section modulus (actual v/s required); Net values (Hogging condition).

Sr. No.	Longitudinal	Shear (cm		Definition from rules	Section n (cm		Definition from rules
		Actual	Rule	from rules	Actual	Rule	from rules
1	Bottom	7.68	2.39	1	87.80	61.64	3
2	Inner bottom	13.47	4.82	1	112.93	95.05	3
3	Side shell	7.19	2.21	1	63.42	36.20	3
4	Inner side shell	7.19	3.01	1	66.49	48.49	3
5	Main deck	13.47	0.58	1	113.10	13.21	3
6	Hatch coaming	13.2	0.52	1	63.58	13.77	3

⁽¹⁾ Shear area based on external or internal design pressure (A_{SH} load)

⁽²⁾ Shear area based on test pressure (A_{SH} test)

⁽³⁾ Modulus based on external or internal design pressure and on a stress factor depending on the overall bending stress (W load)

⁽⁴⁾ Modulus based on test pressure (W test)

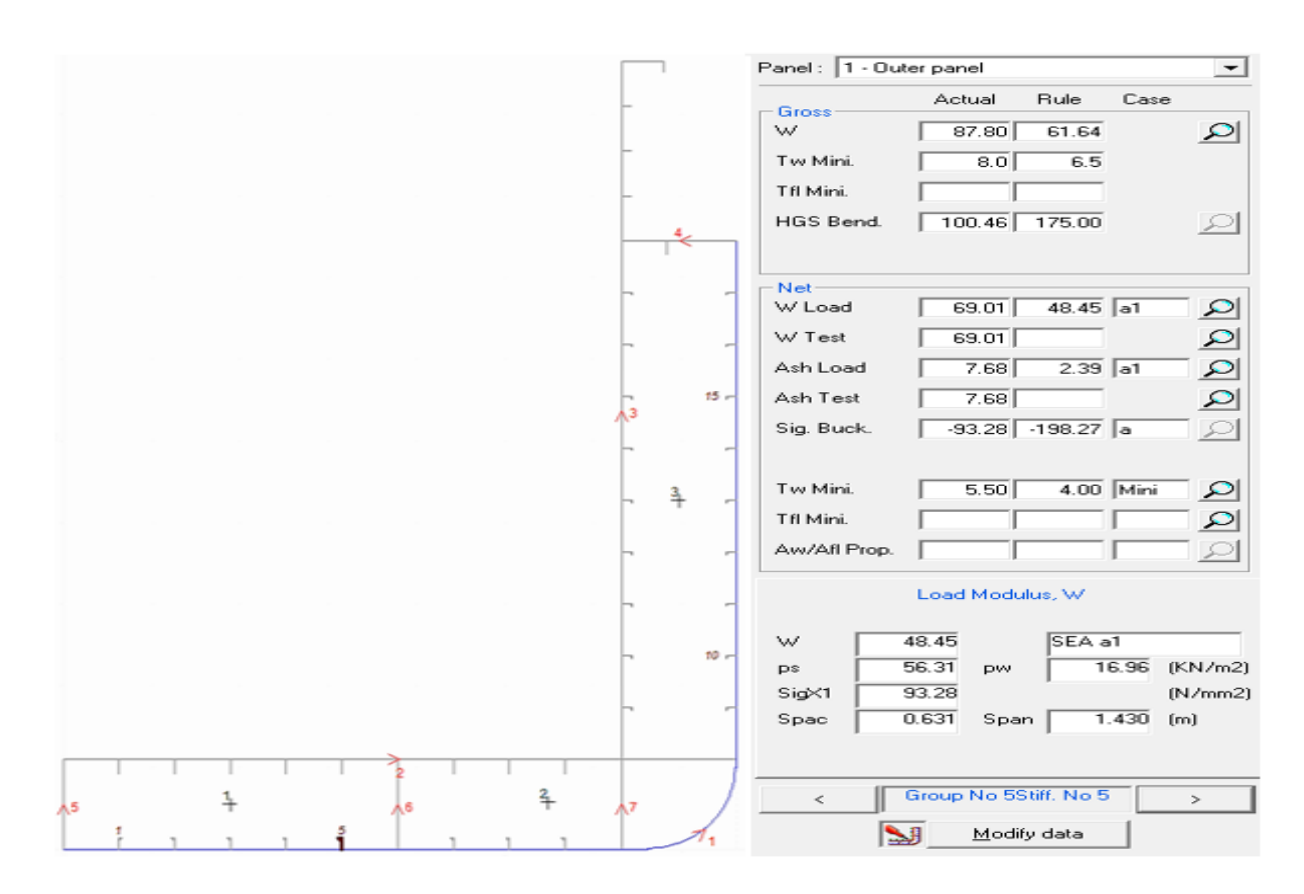


Figure 3-19: Bottom Stiffener (Hogging condition).

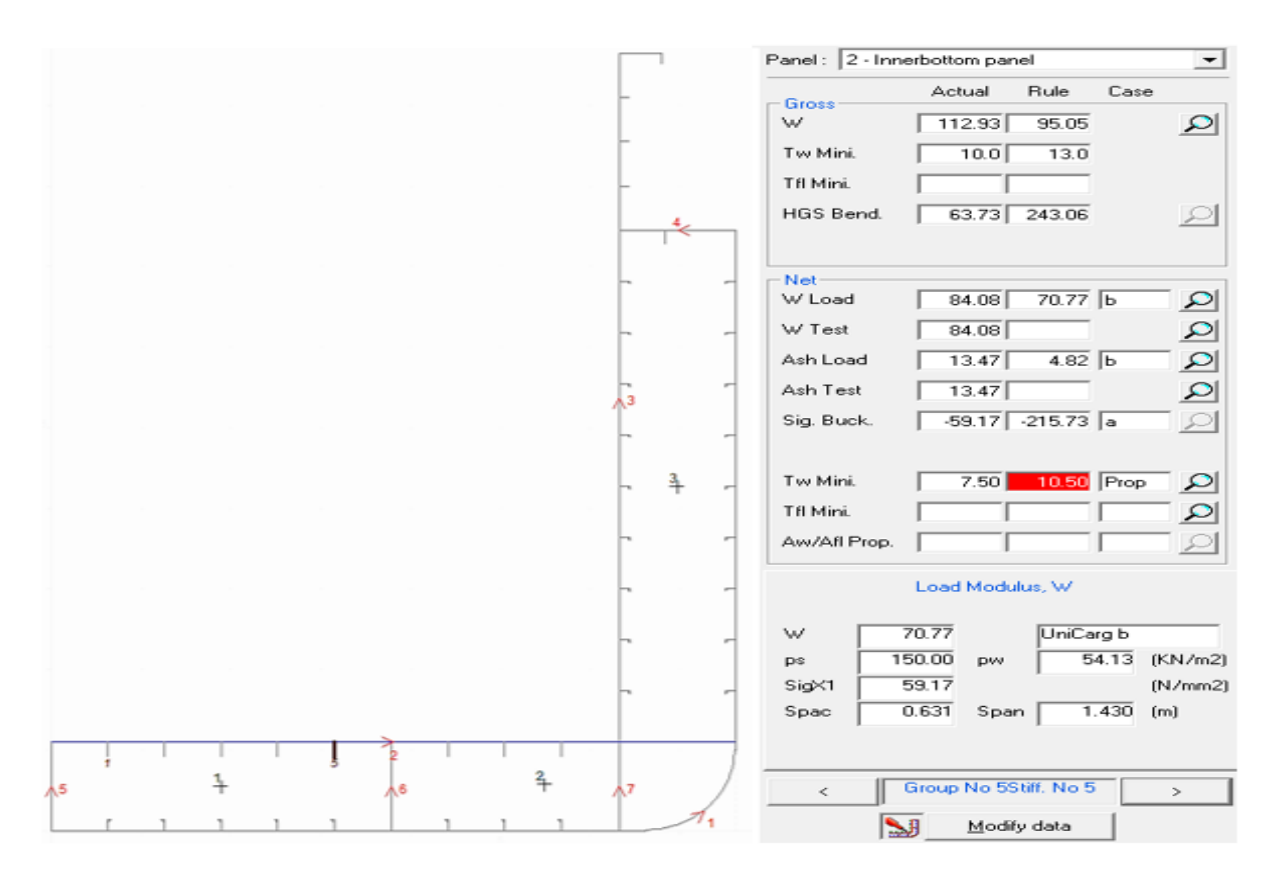


Figure 3-20: Inner Bottom Stiffener (Hogging condition).

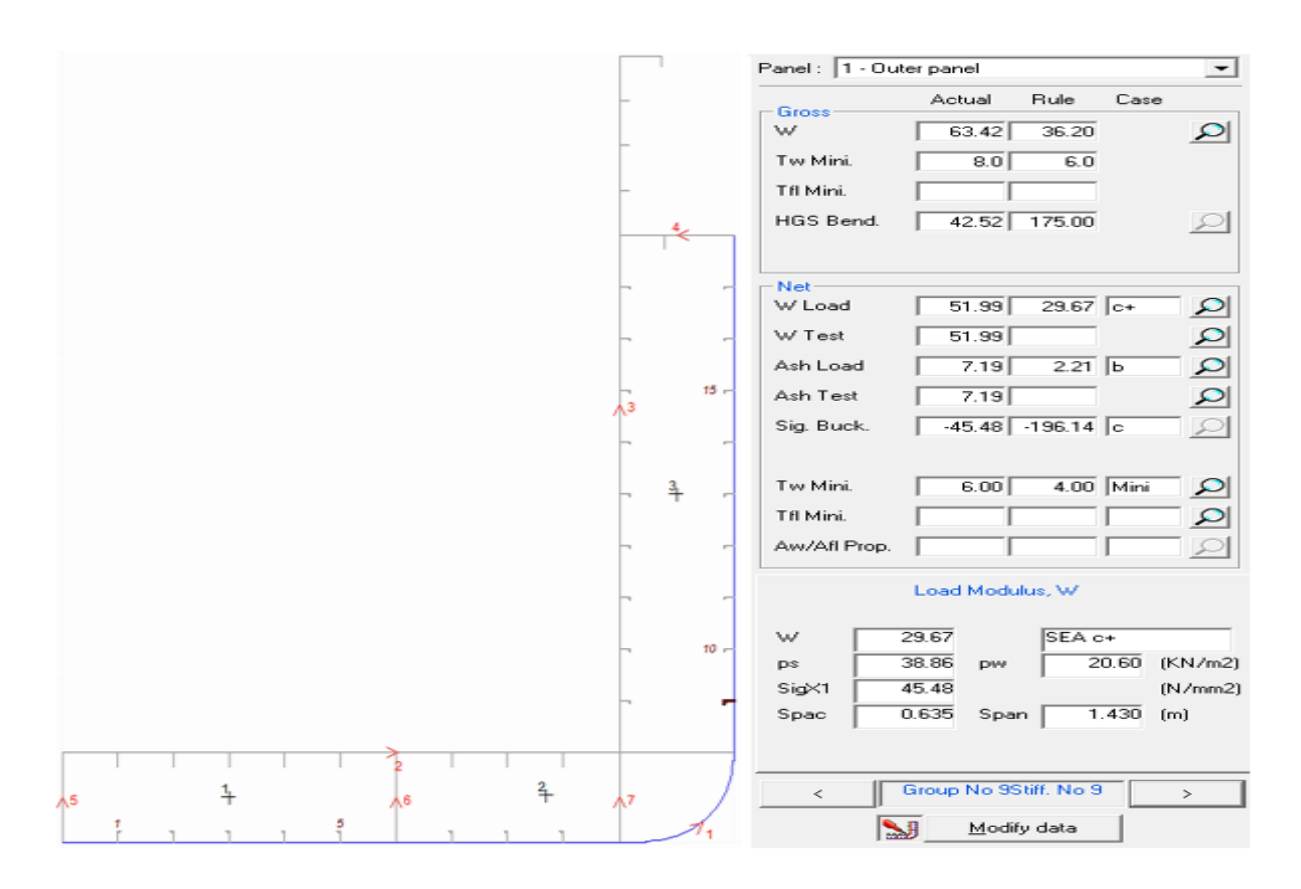


Figure 3-21: Side Shell stiffener (Hogging condition).

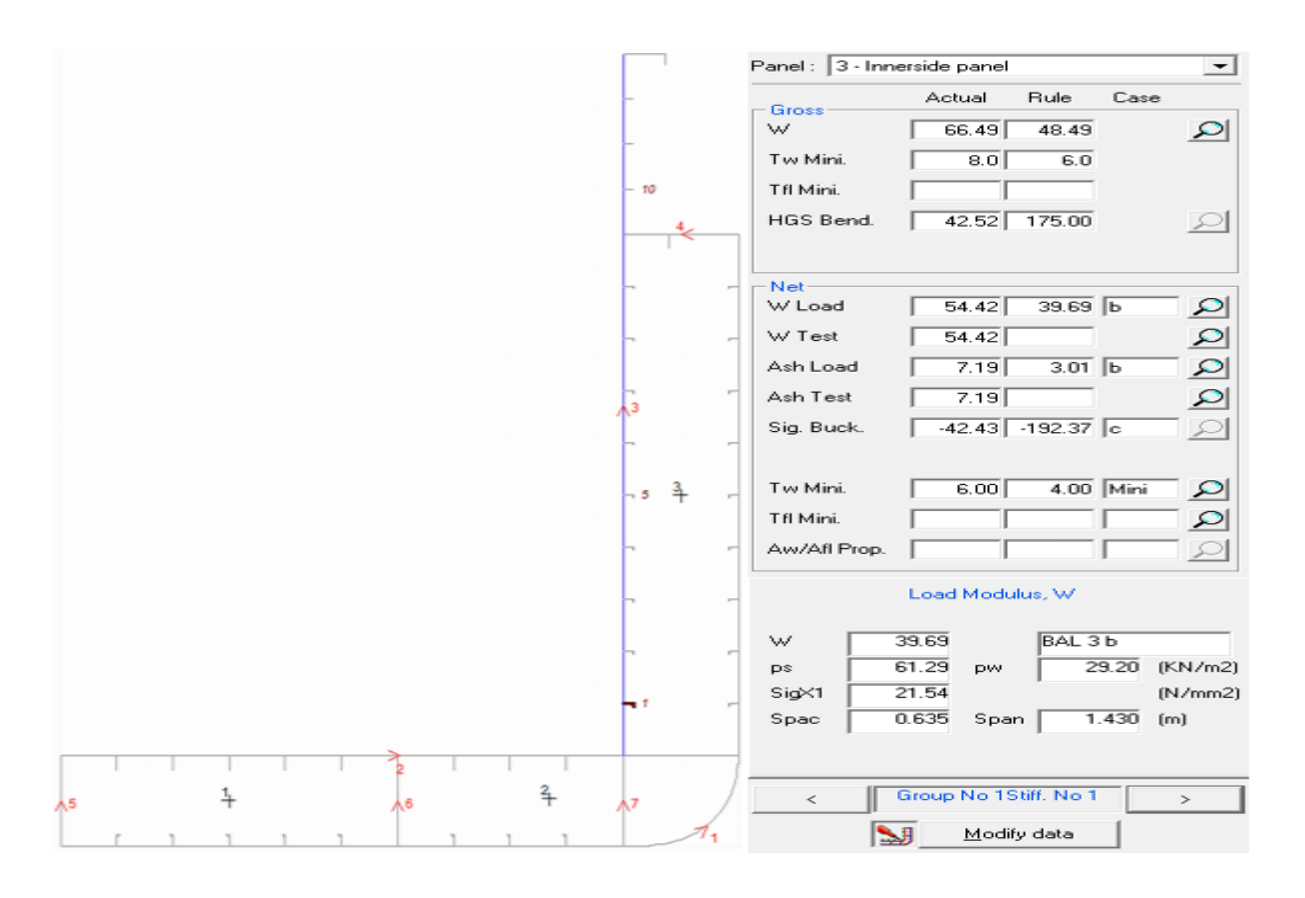


Figure 3-22: Inner side shell stiffener (Hogging condition).

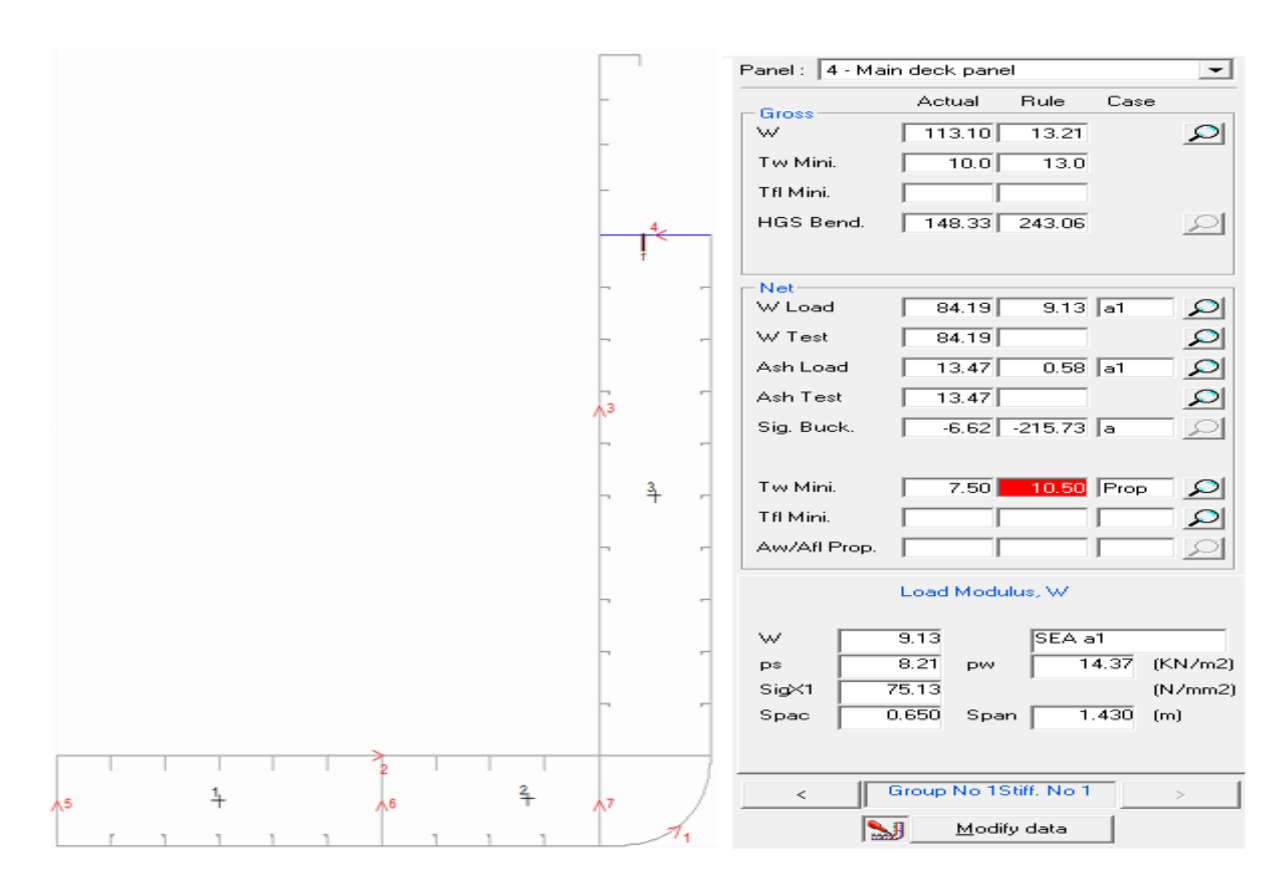


Figure 3-23: Main deck stiffener (Hogging condition).

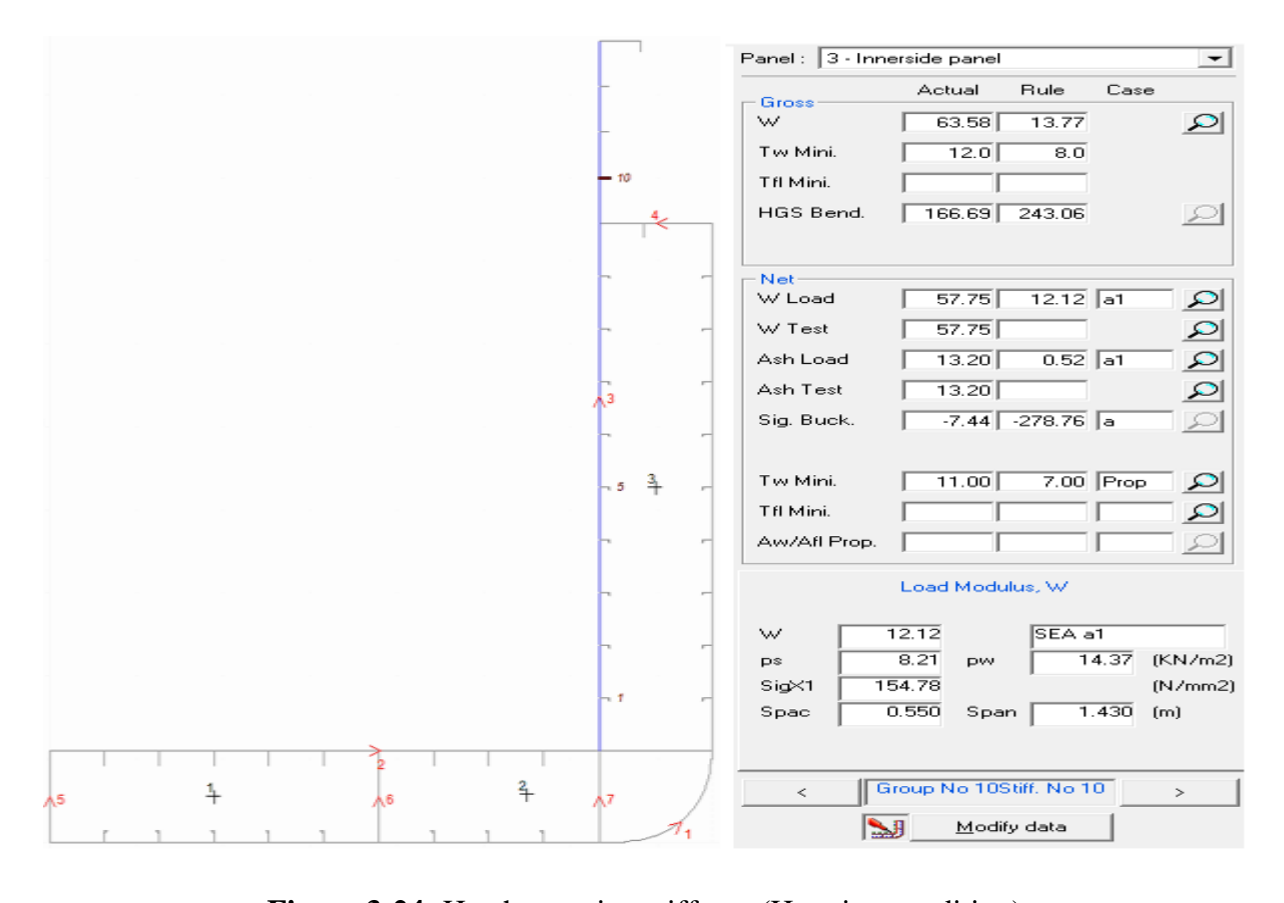


Figure 3-24: Hatch coaming stiffener (Hogging condition).

In Figures 3–19 to 3–24, an extensive comparative analysis of the ship's Hogging conditions is presented, focusing on the critical parameters associated with the ship's secondary structural members, which include the Bottom Stiffener, Inner Bottom Stiffener, Side Shell Stiffener, Inner Side Shell Stiffener, Main Deck Stiffener and Hatch Coaming Stiffener. The analysis incorporates Shear area assessments, where actual values under external or internal design pressure (ASH load) are compared to rule values, in addition to Shear area evaluations, where actual values under test pressure (ASH test) are juxtaposed with rule values. Additionally, the Section Modulus is examined based on external or internal design pressure, accompanied by a stress factor influenced by overall bending stress (W load) and Section Modulus derived from test pressure (W test). These findings provide valuable data pertaining into secondary members' structural integrity and performance in ship design and construction.

Tables 3–20 and 3–21 deliver a distinct perspective. Table 3–20 describes the net scantlings for secondary members but under Sagging conditions, providing insights into actual versus minimum net thickness parameters in this specific loading scenario. Table 3–21, in turn, explores the shear area and section modulus of secondary stiffeners under Sagging conditions, which is crucial to assess their structural integrity when exposed to bending loads in Sagging configurations. Tables 3–20 and 3–21 comprehensively understand how secondary members perform under Sagging conditions, encompassing data on net scantlings and section modulus to evaluate their behaviour effectively.

Table 3–20: The net thickness of the stiffener web (Sagging condition).

	Longitudinal	Net thickness				
Sr. No.	Longitudinal	Actual thickness (mm)	Minimum thickness (mm)			
1	Bottom	8	6.5			
2	Inner bottom	10	13			
3	Side shell	8	6.5			
4	Inner side shell	8	6.5			
5	Main deck	10	13			
6	Hatch coaming	12	8			

Table 3–21: Shear area/Section modulus (actual v/s required); Net values (Sagging condition).

Sr. No.			area 1 ²)	Definition	Sect modulus		Definition
		Actual	Rule	from rules	Actual	Rule	from rules
1	Bottom	7.68	2.39	1	87.80	45.66	3
2	Inner bottom	13.47	4.82	1	112.93	85.20	3
3	Side shell	7.19	2.21	1	63.42	39.26	3
4	Inner side shell	7.19	3.01	1	66.49	53.65	3
5	Main deck	13.47	0.58	1	113.10	17.21	3
6	Hatch coaming	13.2	0.52	1	63.58	9.74	3

- (1) Shear area based on external or internal design pressure (A_{SH} load)
- (2) Shear area based on test pressure (A_{SH} test)
- (3) Modulus based on external or internal design pressure and on stress, factor depending on the overall bending stress (W load)
- (4) Modulus based on test pressure (W test)

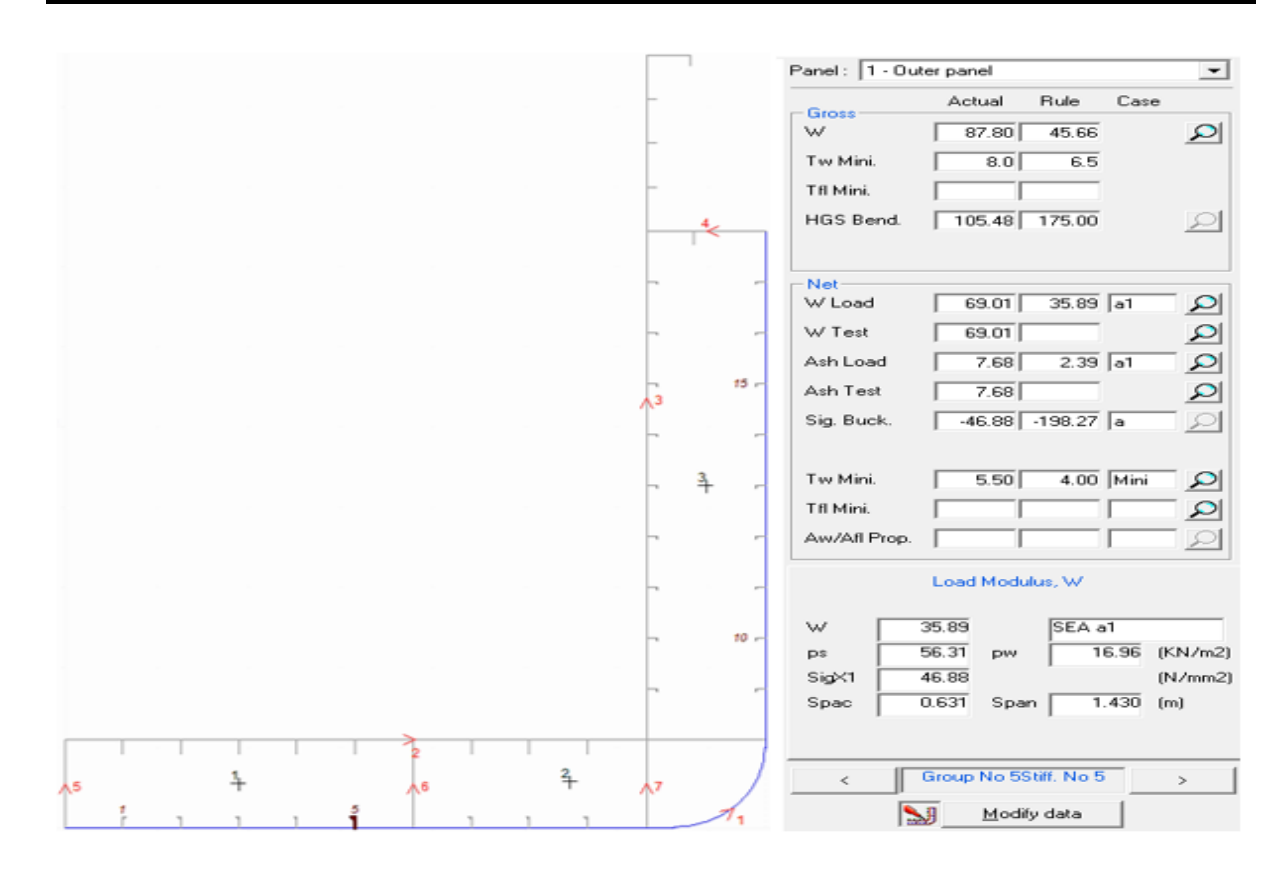


Figure 3-25: Bottom stiffener (Sagging condition).

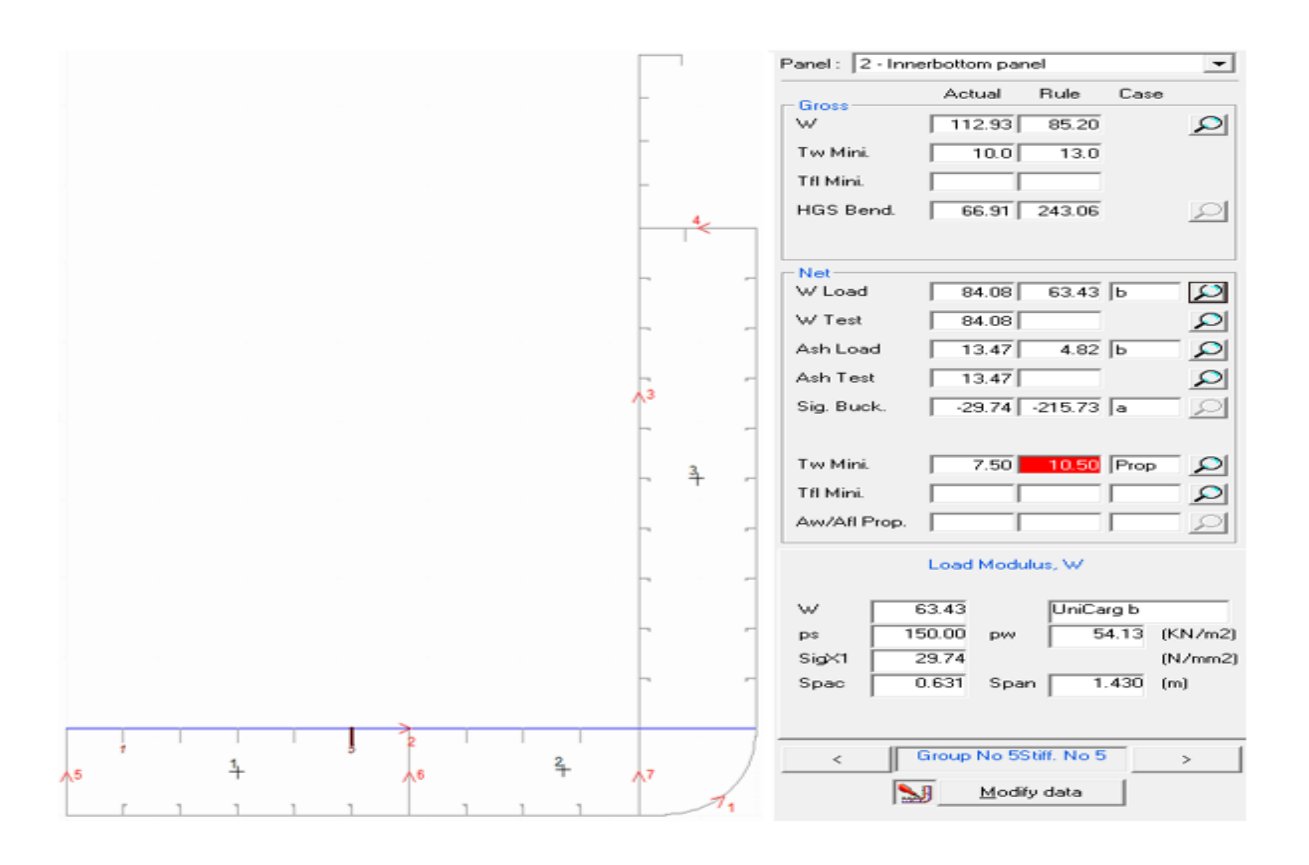


Figure 3-26: Inner Bottom stiffener (Sagging condition).

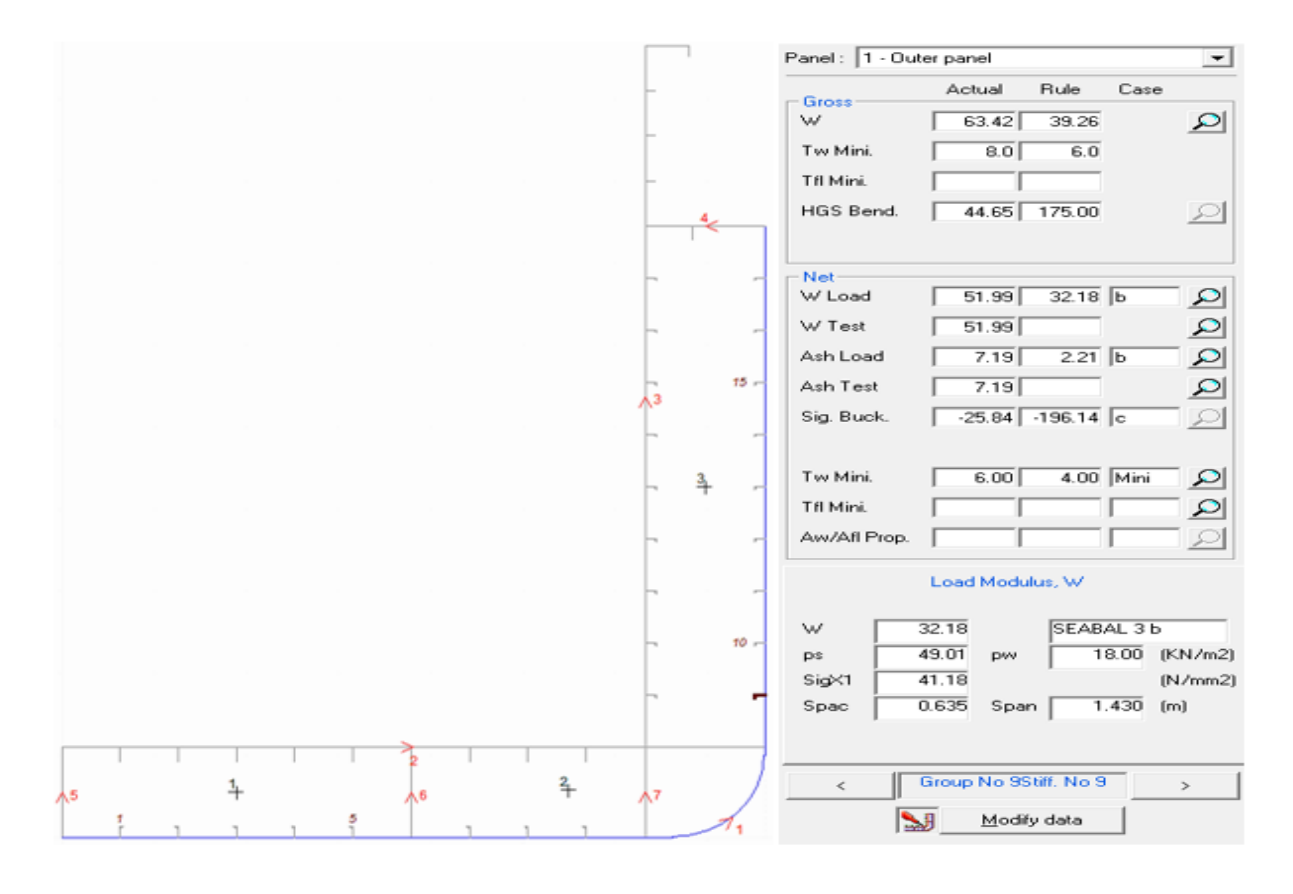


Figure 3-27: Side shell stiffener (Sagging condition).

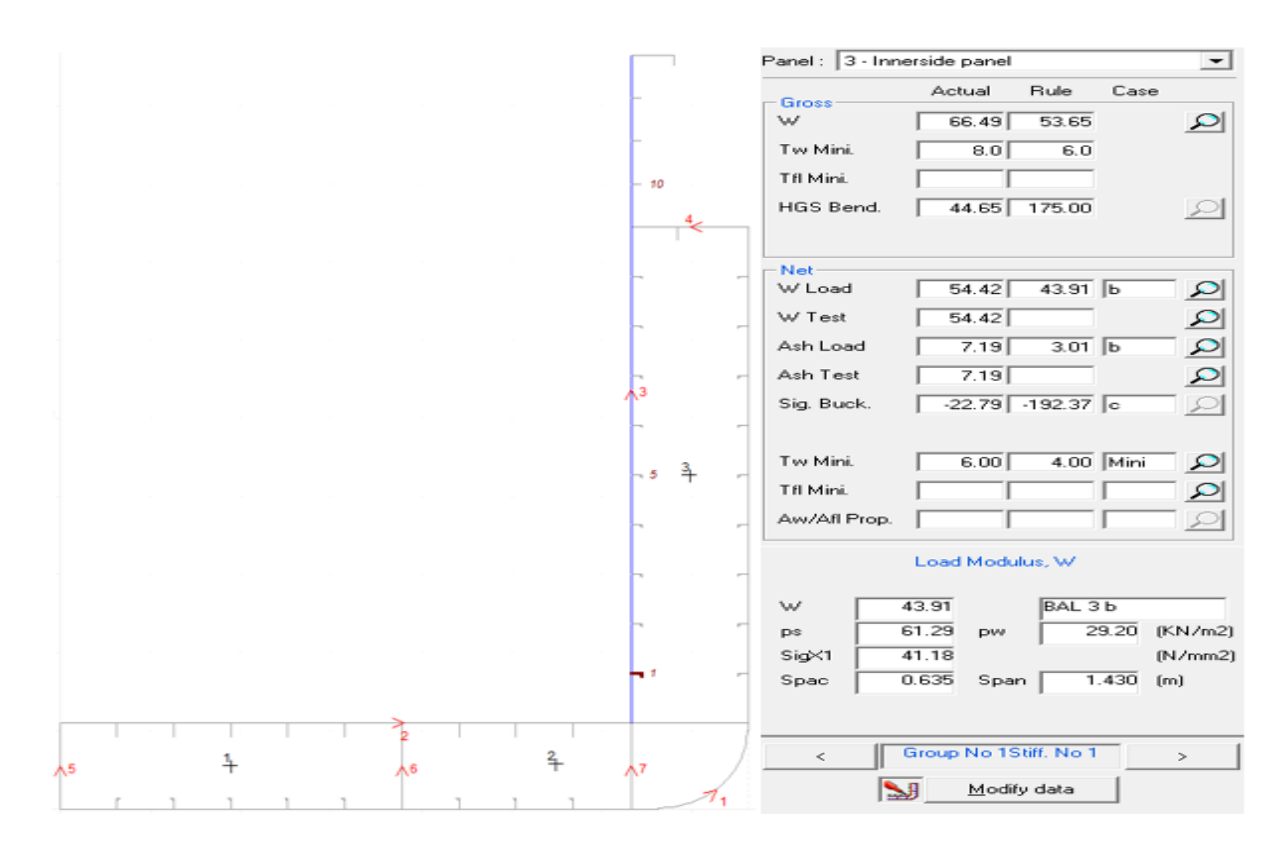


Figure 3-28: Inner side shell stiffener (Sagging condition).

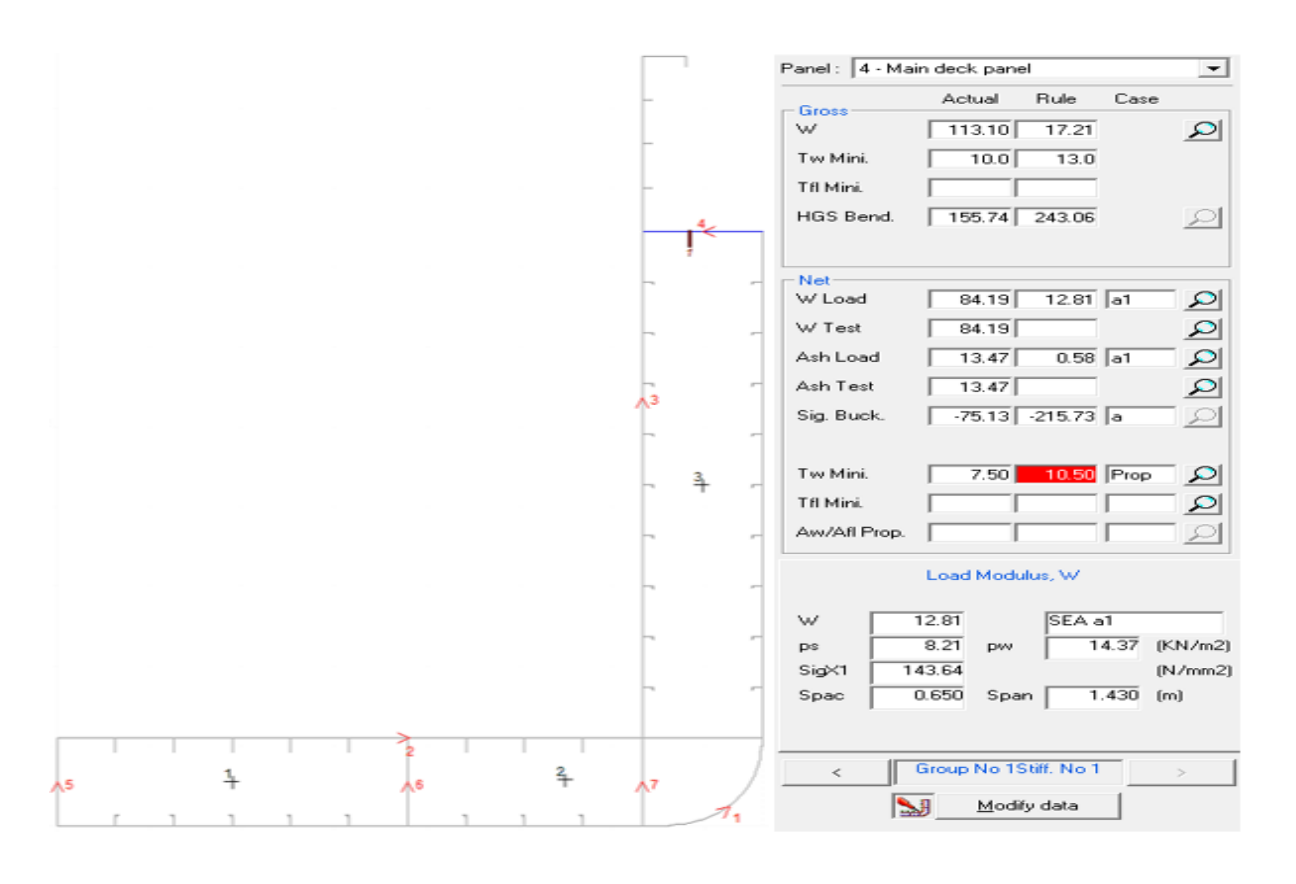


Figure 3-29: Main deck stiffener (Sagging condition).

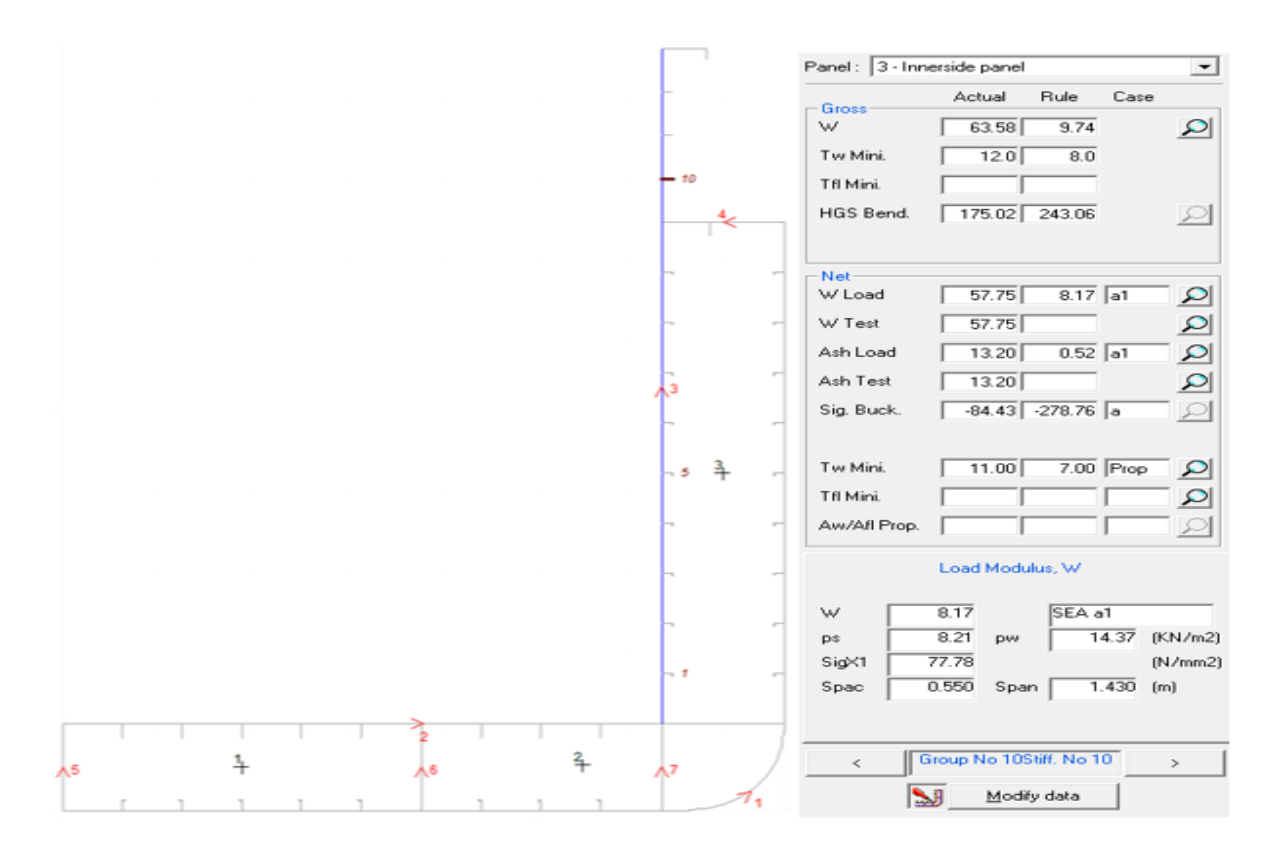


Figure 3-30: Hatch coaming stiffener (Sagging condition).

Figures 3–25 to 3–30 show a comprehensive comparative analysis of ships in Sagging condition, explicitly focusing on critical parameters related to secondary structural members. These parameters incorporate the Bottom Stiffener, Inner Bottom Stiffener, Side Shell Stiffener, Inner Side Shell Stiffener, Main Deck Stiffener and Hatch Coaming Stiffener. The analysis covers Shear area assessments, comparing actual values under external or internal design pressure (ASH load) to rule values and Shear area evaluations, comparing actual values under test pressure (ASH test) to rule values. Likewise, the examination of the Section Modulus includes concerns for external or internal design pressure, a stress factor dependent on overall bending stress (W load) and Section Modulus based on test pressure (W test). These findings provide beneficial information into secondary members' structural integrity and performance in ship design and construction, particularly under Sagging conditions, despite the insufficient thickness of the inner bottom and main deck stiffeners.

3.8 Strength Check of Primary Supporting Members

FEMAP presents a platform for conducting structural analysis through direct engineering calculations by integrating with NX-NASTRAN.

3.8.1 Coordinate System

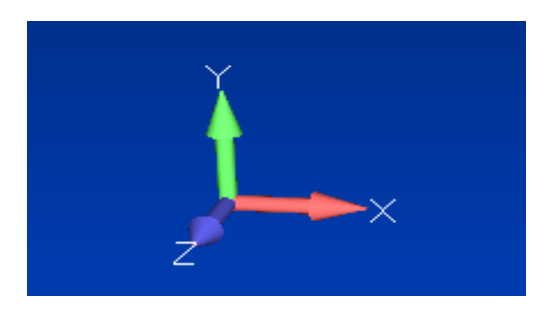


Figure 3-31: Coordinate system for modelling [36].

According to BV rules NR 467 (Part B, Chapter 1, Sec. 2), the coordinate system for the vessel is a right-hand coordinate system (refer to Figure 3–31) [36]:

Origin: where the longitudinal plane of symmetry intersects with the aft end of L and the baseline is where the vessel's intersection is situated

X-axis: longitudinal axis, positive forwards

Z-axis: transverse axis, positive towards portside

Y-axis: vertical axis, positive upwards

According to NR 467, the coordinate system is shown in Figure 3–31.

3.8.2 Modelling and Mesh Characteristics

Plate elements were employed in the structural modelling to represent the structures accurately. Figure 3–32 visually demonstrates the realisation of convergence between the elements' first edge and normal vectors. This convergence is key to attaining the desired outcomes. Careful consideration has been given to the dimensions and shapes of these elements. To achieve precise results, most components are modelled as quadrilaterals. Triangular elements are used only when they cannot be avoided in a given situation.

In addition, the shapes of all the elements have been carefully designed to maintain their proper aspect ratios. Finite element models are constructed using linear assumptions. In the process of finite element (FE) modelling, as shown in Figure 3–33, it is of the utmost importance to adhere to the recommendations provided by the Bureau Veritas (BV) standards (NR 467, Part B, Chapter 5, Appendix 1 and Sec. 3.4.1). The following guidelines provide a framework to make certain that the FE models are accurate and reliable [36].

- The quadrilateral elements must have an aspect ratio of no more than 4.
- The angles of the quadrilateral elements must be larger than 60 degrees and less than 120 degrees.
- The angles of the triangle elements must be larger than 30 degrees and less than 120 degrees.

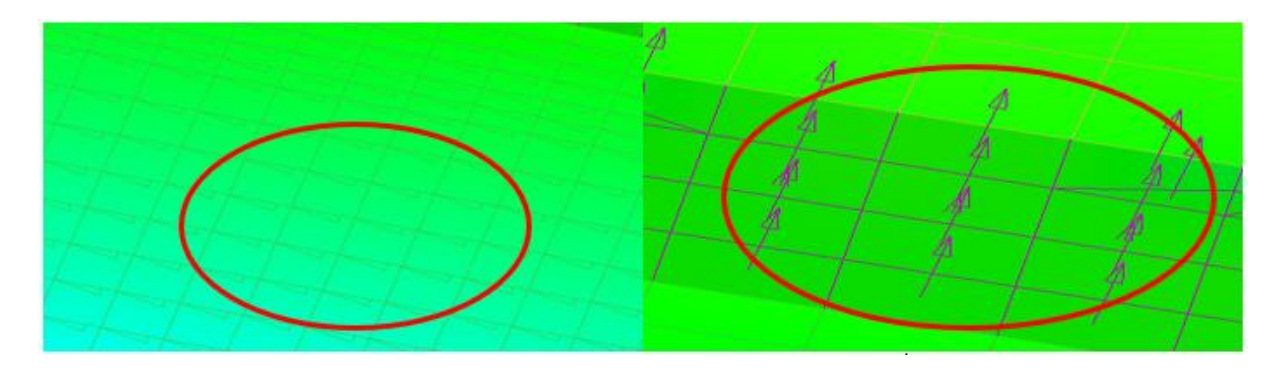


Figure 3-32: Harmonised first edge (left) and normal vectors (right) [36].

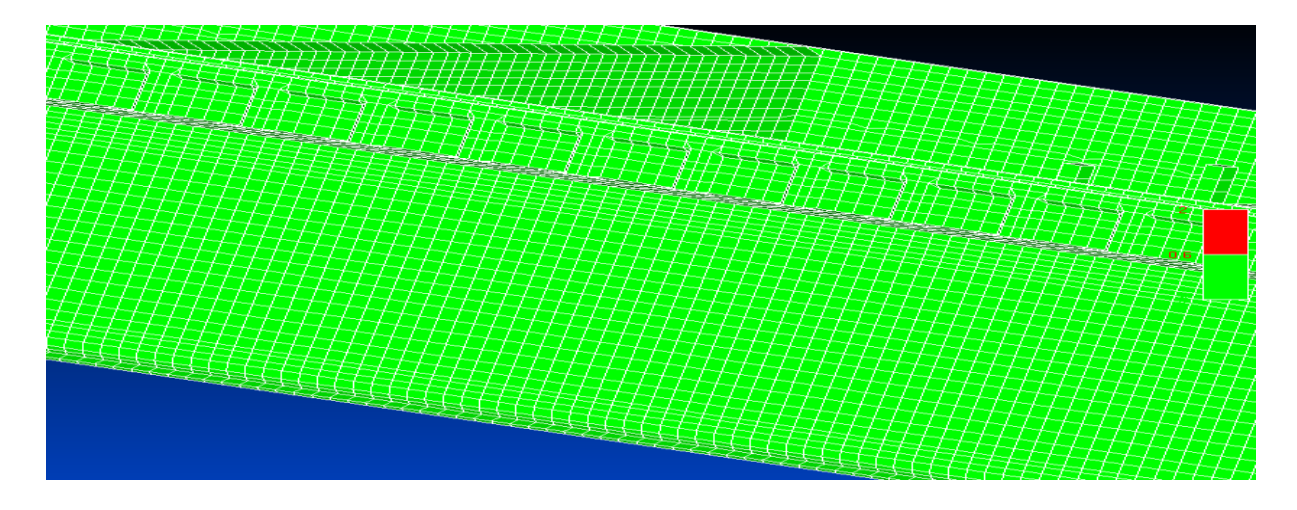


Figure 3-33: Mesh shapes [36].

3.8.3 Ship Hull Structural Analysis

The strength of the longitudinal hull girder members, primary supporting members and the transverse bulkhead is evaluated by way of analysing the strength of the cargo hold.

3.8.3.1 Structural Model

There are four primary steps involved in creating a finite element model:

- geometry creation.
- meshing and boundary conditions application.
- solution.
- examination of the findings.

To thoroughly investigate the ship's longitudinal strength, a detailed model encompassing three distinct cargo holds was developed. It was determined that adding an extended cargo hold model was necessary to avoid boundary effects despite the examined vessel only having one main cargo hold. The comprehensive model includes three different cargo holds. The main cargo hold stretches from frame 24 to frame 125. The aft hold, which acts as the engine room, is located between frame 8 and frame 24. Finally, the forward hold operates as a cofferdam and is positioned between frame 125 and frame 132. The cargo hold model is completed with relatively fine mesh using a quadrilateral orthotropic shell element with four nodes, each with six degrees of freedom and translations in the x, y and z directions and rotations about the axes. In order to obtain more accurate results, a relatively fine mesh is utilised in this analysis. In contrast, the coarse mesh model is primarily employed to verify the global stress levels of longitudinally effective plates [108].

The analysis was performed using the "Net" thickness method, where the strength analysis considered the corrosion deduction of the plate and stiffener thickness. The corrosion deductions for plating and stiffening were calculated according to the BV, NR 467 rules for steel ship classification. This method corroborates the structural integrity of the cargo ship in both "as-built" and "design life" conditions [36].

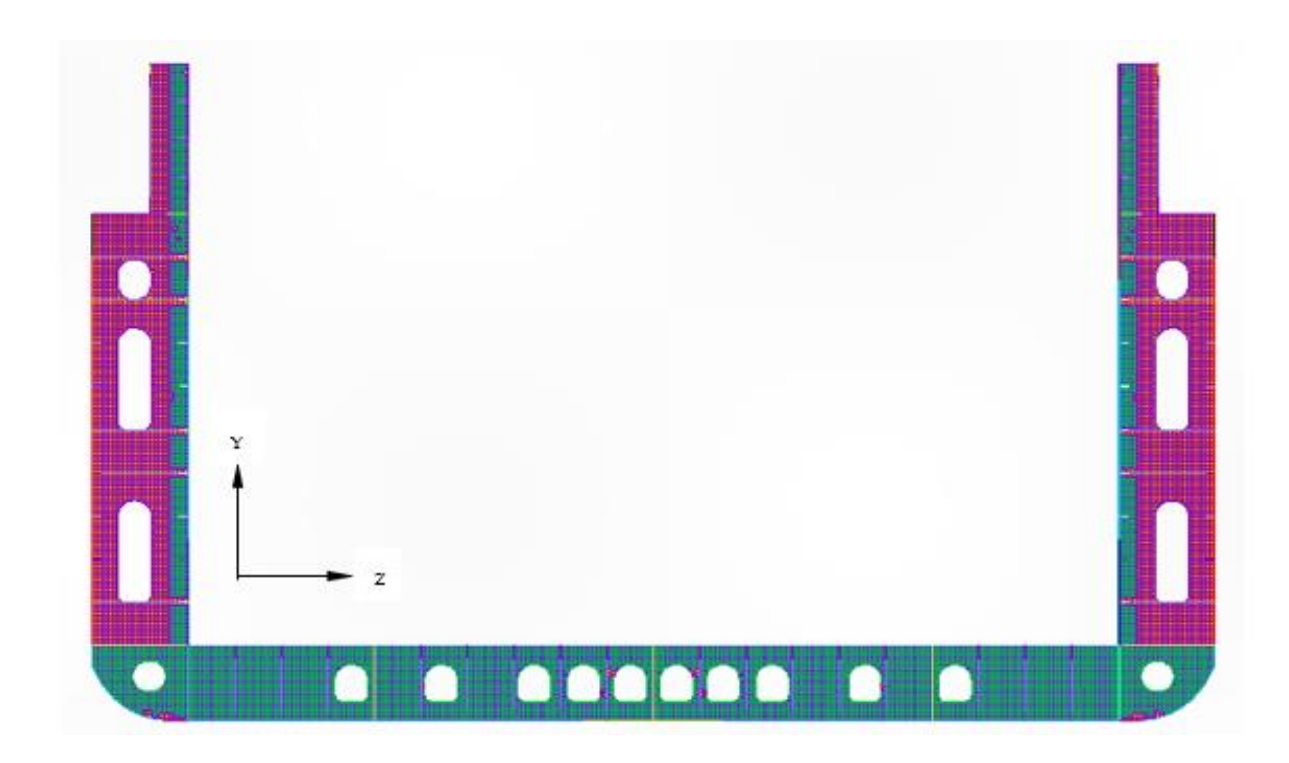


Figure 3-34: A typical mesh arrangement of the transverse web in FEMAP.

In Figure 3–34, the complex mesh layout demonstrates a transverse web structure. This structure is necessary for precise simulation and thorough analysis. The design and arrangement of the mesh are carefully thought out with the intention of creating a strong foundation, ensuring the cargo model's accuracy and dependability.

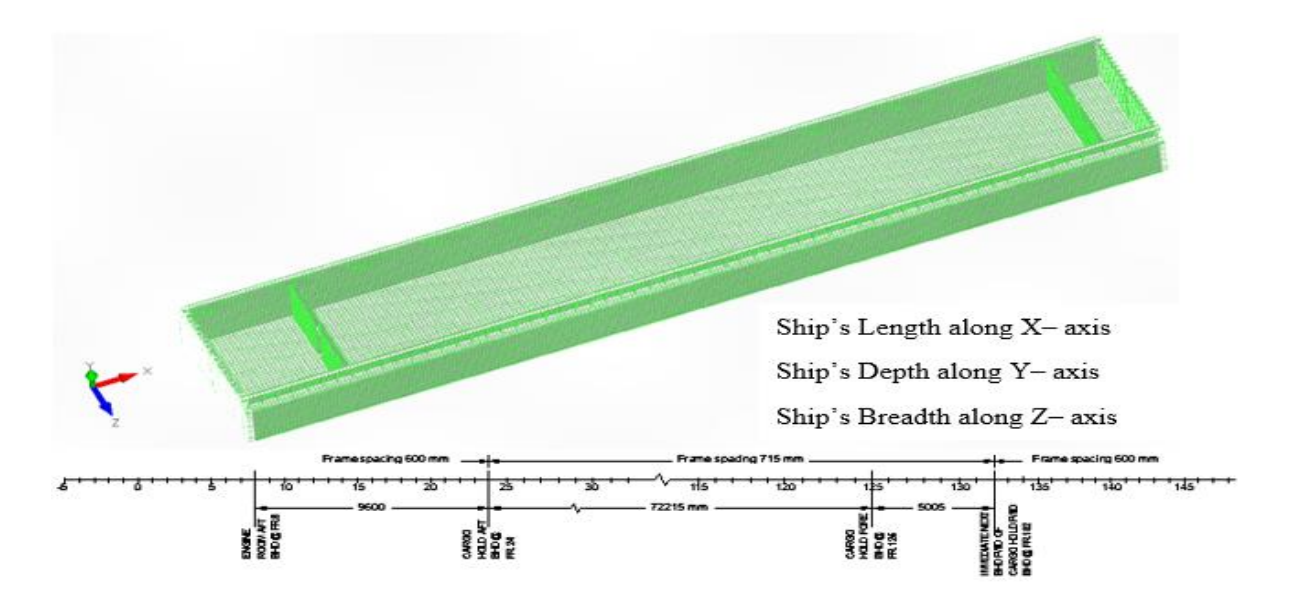


Figure 3-35: Generated FE model of the analysed ship in FEMAP.

Figure 3–35 shows a detailed representation of the cargo hold model, including various connected parts such as frames and longitudinal stiffeners. This complex structure highlights the strength and effectiveness of the analysis system. Key measurements of the model include an impressive, analysed cargo hold length of 72.215 metres, a forward hold length of 5.005 metres, an aftward hold length of 9.6 metres, a width of 15.25 metres and a height of 9.65 metres. It is constructed with a relatively fine mesh consisting of 167,949 nodes and 211,530 elements, exhibiting the precision and sophistication of the simulation.

Table 3–22 presents key material properties of mild steel and higher tensile steel, including elastic modulus, density, Poisson's ratio and yield stress values. These properties are crucial for material selection and structural analysis in ship design and structural engineering.

Table 3–22: Material properties of steel [127].

Properties	Symbols	Values
Elastic modulus	E	206 GPa
Density	ho	7850 kg/m^3
Poisson's ratio	ν	0.30
37' 11 .	D	235 MPa (for Mild steel)
Yield stress	R_e	355 MPa (for High tensile steel)

3.8.3.2 Boundary Condition, Applications of Loads/Moments and Results

If a cantilever beam has a bending moment on one side, the bending moment will be the same in all parts along the beam's length. The same concept was used in this FE model to explore the longitudinal strength of the hull girder. On one side of the FE model, bending moments were applied, while the other was restricted by fixed constraints (Table 3–23). Rigid elements were built beneath the main deck to transfer the load to the hull structure. A rigid element connects the nodes at the free edges of the structure to the other nodes on the same plane, allowing them to function as a single entity. To establish two boundary conditions, it was necessary to utilise two rigid components [128]:

- 1. Constraint: A rigid element was applied at the model aft with zero degrees of freedom to clamp.
- 2. Moment: To establish a Hogging/Sagging condition, a bending moment was applied in the positive y-direction to a rigid element in the fore part of the model [128].



Figure 3-36: Cantilever beam applied with constant bending moment [129].

Figure 3–36 shows the behaviour of a cantilever beam subjected to a constant bending moment. Within a cantilever beam, the bending moment experiences maximum magnitude at the fixed end while progressively diminishing to zero at the free end. The bending moment at any specific position, denoted as x, along the cantilever beam, can be determined by means of the equation $M_x = -P$. x, where P represents the applied load at the extremity of the cantilever, whilst x signifies the distance from the fixed end to the point of interest along the beam's length.

Table 3–23 provides a detailed summary of the boundary conditions to apply to the ship model during the analysis. This table summarises essential aspects of the model, including specific nodes at the aft and fore-ends and the constraints placed on translation and rotation along the X, Y and Z axes. These boundary conditions are crucial in simulating a cantilever configuration and play a key role in determining the structural behaviour and response of the ship to different loading scenarios.

Table 3–23: Boundary conditions (Cantilever).

Douglass on ditions	Transla	ations in di	rections	Rotation around axes			
Boundary conditions	X	Y	Z	X	Y	Z	
Node at the aft end	Fixed	Fixed	Fixed	Fixed	Fixed	Fixed	
Node at the fore end	Free	Free	Free	Free	Free	Free	

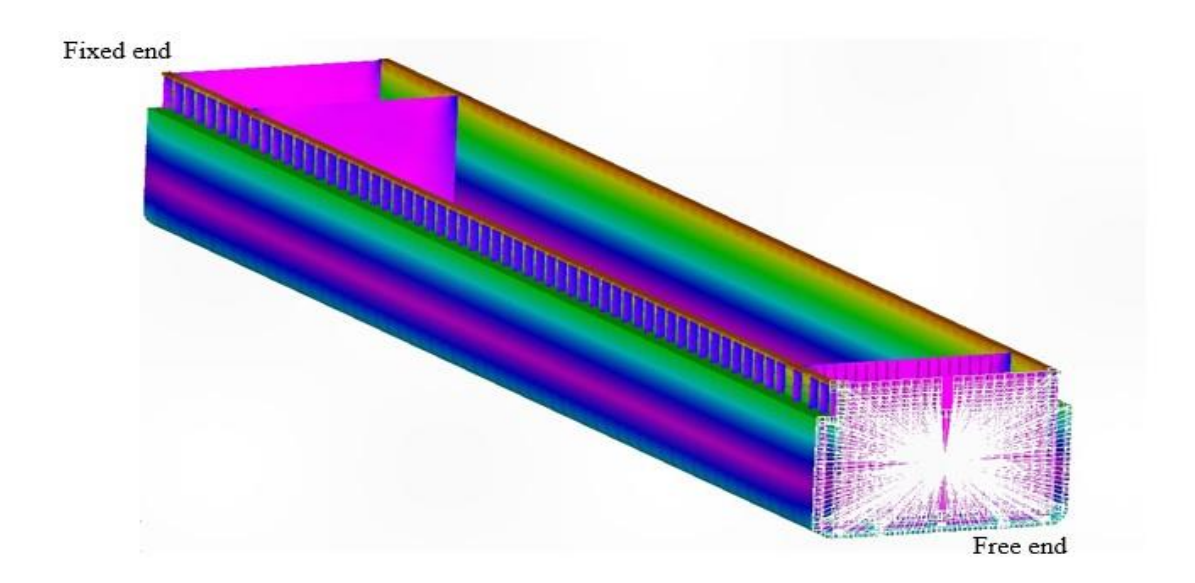


Figure 3-37: Rigid Element in FEMAP.

Figure 3–37 shows the cargo hold indispensable forward and aft rigid elements. These elements are vital in transferring and distributing loads within a ship's cargo hold, particularly in analysing its longitudinal strength. They are meticulously crafted to counteract any unnecessary deformations, buckling or potential failures caused by varying loading scenarios.

3.8.3.3 Grid Convergence Study

A grid convergence study is essential in numerical simulations to validate the results obtained. This study comprises simulations on two or more successively finer grids to assess the solution's sensitivity to grid refinement. The Grid Convergence Index (GCI) method, which requires at least three systematic mesh refinements to estimate the error between grids and ensure convergence, is commonly used for this purpose [130].

A grid convergence study aims to refine the mesh multiple times and compare solutions to estimate discretisation errors accurately. By comparing results from different mesh resolutions and guaranteeing that the solution is independent of mesh resolution, researchers can confidently select the best model for accurate and reliable simulation results. This technique is employed in ship modelling with the aim of studying the impact of mesh size and quality on the accuracy of the simulation results. By conducting mesh sensitivity analysis, the precision of the simulation can be enhanced, leading to a better understanding of the behaviour of the ship model under different conditions [131].

Table 3–24 compares Von Mises stresses comprehensively across five distinct ship models. The analysis encompasses variations in mesh refinement, incorporating coarse, fine and finer mesh configurations, with adjustments in element size and mesh density factor.

Table 3–24: Comparative analysis of Von Mises stresses across multiple ship models using varied mesh refinement levels.

Element size	Density	Max Von Mises Stress (MPa)
600	0.0017	247.46
500	0.0020	249.13
400	0.0025	259.61
357.5	0.0028	266
178.5	0.0056	266

The convergence curve portrayed in Figure 3–38 demonstrates that the Mesh Density factor of 0.0028 makes the results stable, confirming the chosen model's accuracy. This factor is crucial in determining the most suitable mesh size for a given simulation.

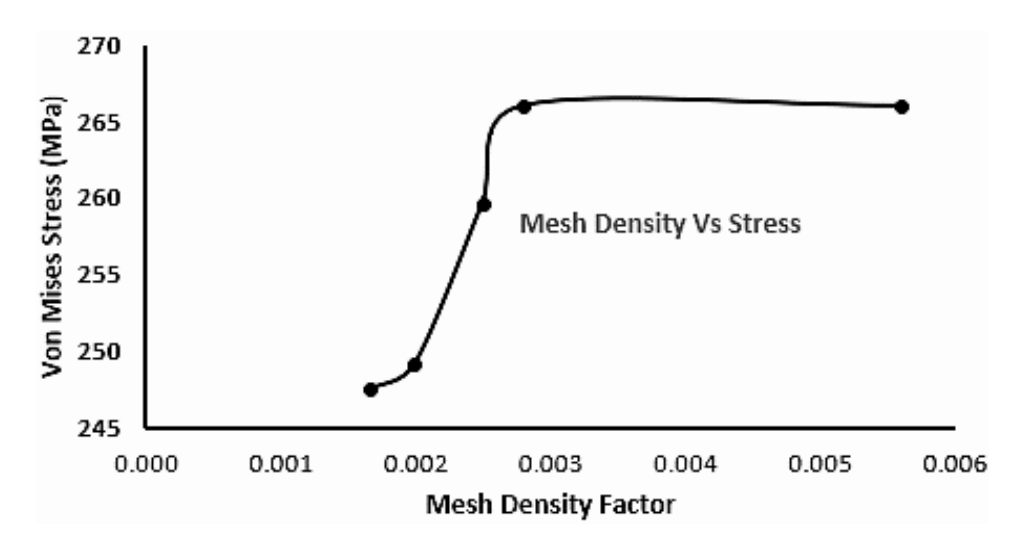


Figure 3-38: Convergence curve illustrating optimal mesh density for simulation accuracy.

In this study, five systematic mesh refinement models were developed. Surprisingly, among these models, the model characterised by an element size of 357.5 mm and a mesh density factor of 0.0028 demonstrated superior simulation results. This model achieved a balance, avoiding extremes of excessive refinement or coarseness. The study's emphasis on prioritising global load considerations over local loads is significant. Specifically, the coarse mesh model is primarily used to verify the global stress levels of longitudinally effective plates [108].

A comparison of normal longitudinal bending stress values obtained from beam theory and the finite element model is conducted for validation. The normal longitudinal bending stress on the side shell plating in the midship area is obtained from the MARS 2000 model, which is based on beam theory and the FE model for comparison. Both upright and inclined load cases have been investigated in this analysis.

3.8.3.4 Investigated Ship's Structural Analysis – Upright Condition

A ship will experience both still water and vertical wave bending while in an upright position. The stress values in the midship areas were studied because the applied maximum bending moment corresponded to the value in the midship section.

Table 3–25 displays the magnitudes of still water and vertical wave bending moments obtained from the results provided by the MARS 2000 software (refer to Appendix A). These moments are crucial contributions as regards assessing the longitudinal strength of the ship hull girder under both Hogging and Sagging loading conditions. The combined impact of these values is a vital factor in calculating the ship's structural strength.

Table 3–25: Still water and vertical wave bending moments.

Items	Hogging (kNm)	Sagging (kNm)
Design still water bending moment	125651	-113909
Design vertical wave bending moment	177581	-192769

Table 3–26: Comparison of normal stress between beam theory and FE model (Hogging-Upright load case).

	Normal vertical bending stress (MPa)	
Z (m)	Direct Calculation	Beam Theory
9.65	239	221.79
9.1	220	203.43
8.55	200	185.06
8	179	166.69
7.45	158	148.33
6.815	138	127.12
6.18	119	105.91
5.545	96	84.71
4.91	73	63.5
4.275	50	42.3
3.64	27	21.09
3	-8	-0.11
2.37	-32	-21.32
1.735	-55	-42.52
1.1	-76	-63.73
0	-111	-100.46

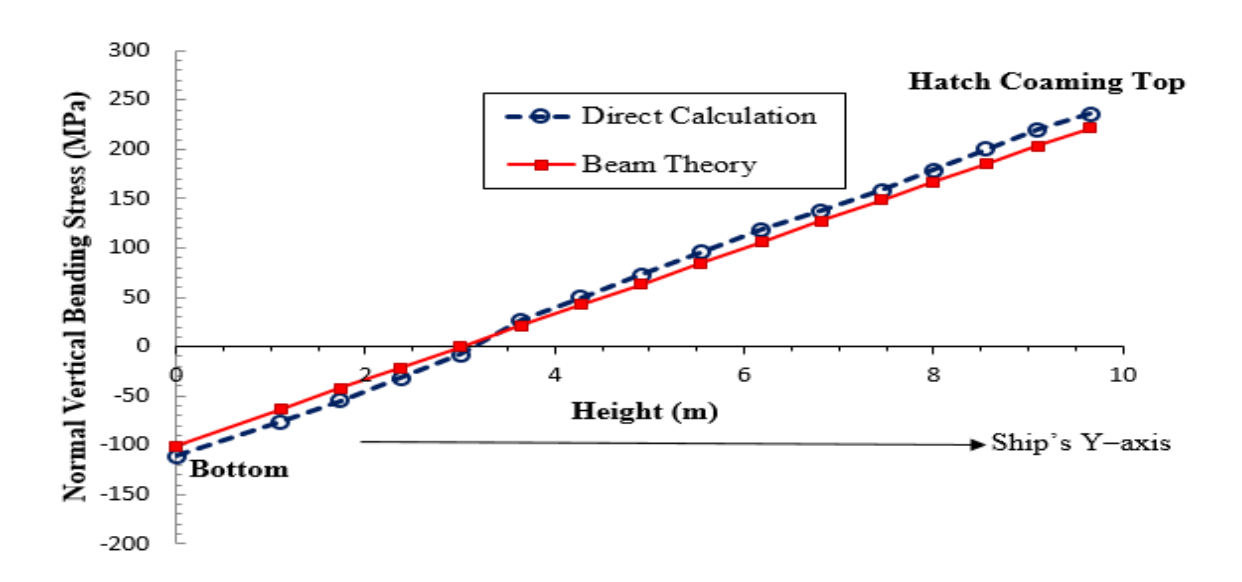


Figure 3-39: Comparison of normal longitudinal bending stress between beam theory and FE model (Hogging-Upright load case).

Table 3–26 and Figure 3–39 compared normal longitudinal bending stresses under Hogging conditions for upright load cases. Theoretical predictions derived from beam theory are compared with the results from the finite element (FE) model.

Based on the data displayed in Figure 3–39 above, there is a stress differential of approximately 5% between the results obtained from the beam theory calculations and direct computation. In the conceptual framework of beam theory, this difference can be considered an acceptable deviation [28].

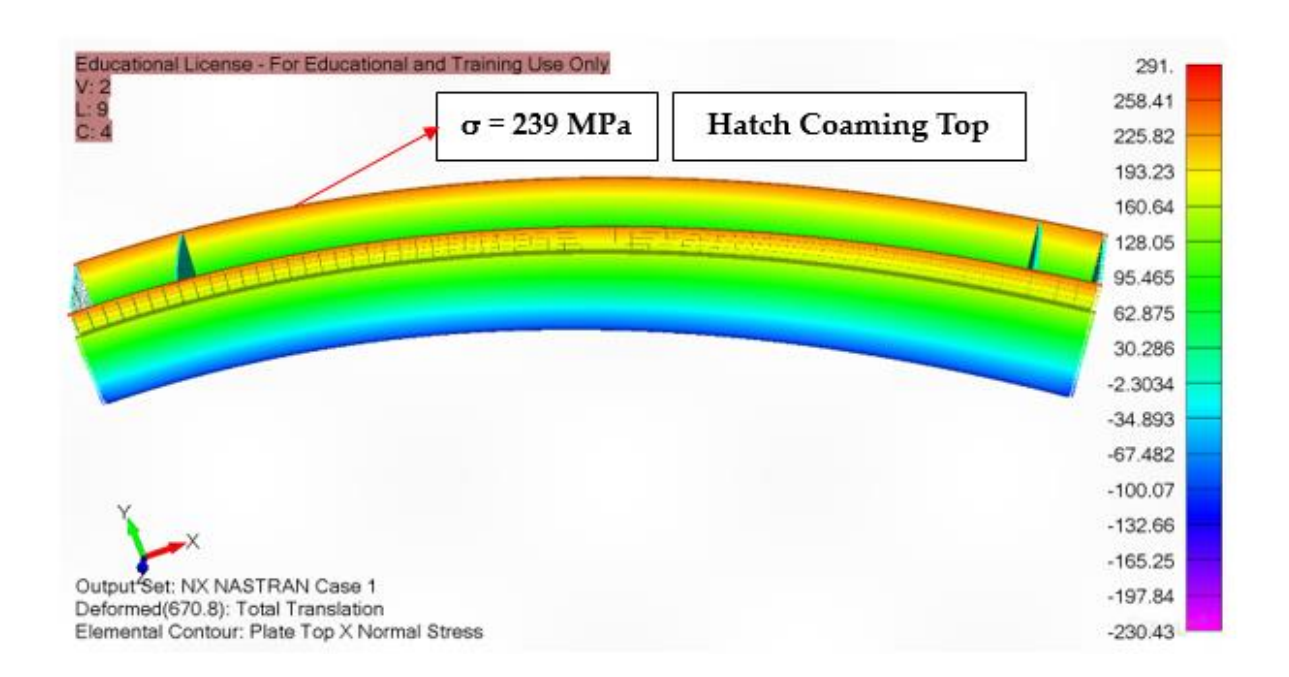


Figure 3-40: Hull girder normal stress at midship (Hogging—upright condition).

To meet the strength-checking criterion, the normal stress in critical areas had to be lower than the maximum allowed stress outlined in Sec. 3.7.1.2. As seen in Figure 3–40, the maximum stress generated at the top plate of the hatch coaming, made of high-tensile steel, has a maximum normal stress value of 239 MPa. It is apparent that this measurement is well below the stress threshold of 331.77 MPa that was set.

Table 3–27: Comparison of normal stress between beam theory and FE model (Sagging-Upright load case).

	Normal vertical bending stress (MP	
$\mathbf{Z}(\mathbf{m})$	Direct Calculation	Beam Theory
9.65	-242	-224.32
9.1	-221	-205.75
8.55	-201	-187.17
8	-181	-168.6
7.45	-160	-150.02
6.815	-138	-128.57
6.18	-120	-107.12
5.545	-97	-85.68
4.91	-73	-64.23
4.275	-50	-42.78
3.64	-27	-21.33
3	9	0.11
2.37	33	21.56
1.735	56	43.01
1.1	77	64.45
0	112	101.61

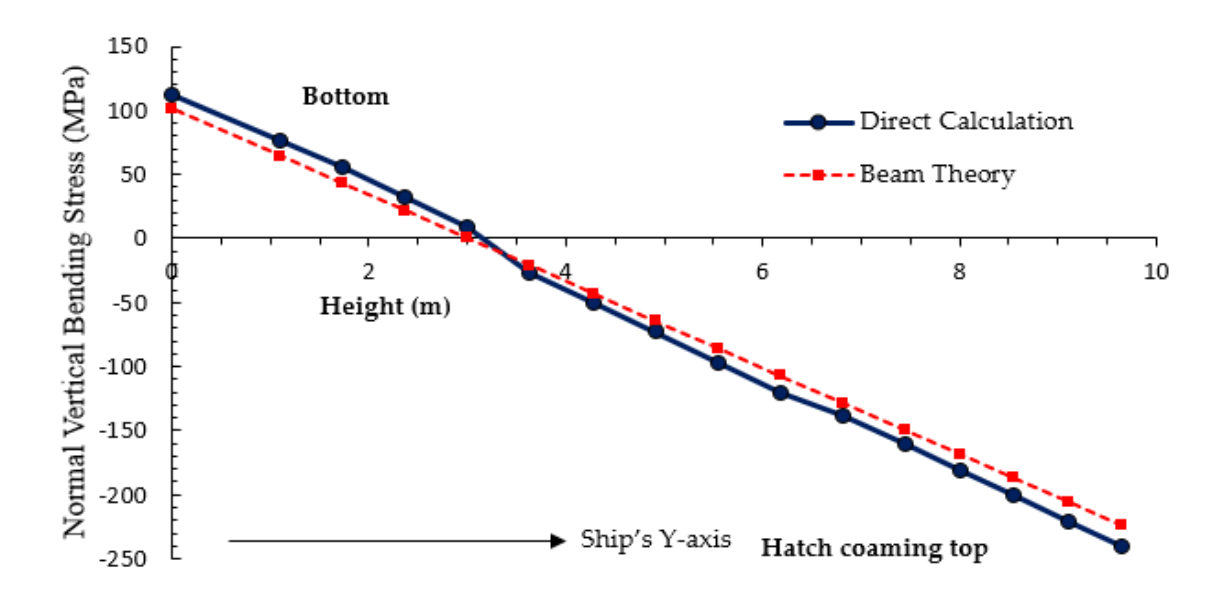


Figure 3-41: Comparison of normal longitudinal bending stress between beam theory and FE model (Sagging-Upright load case).

Table 3–27 and Figure 3–41 comprehensively compare the normal longitudinal bending stresses between the beam theory and the finite element (FE) model. This comparison is conducted under the Sagging condition for the upright load case. Visual and tabulated representations facilitate a rigorous analysis of the stress distribution and its variance across the structures.

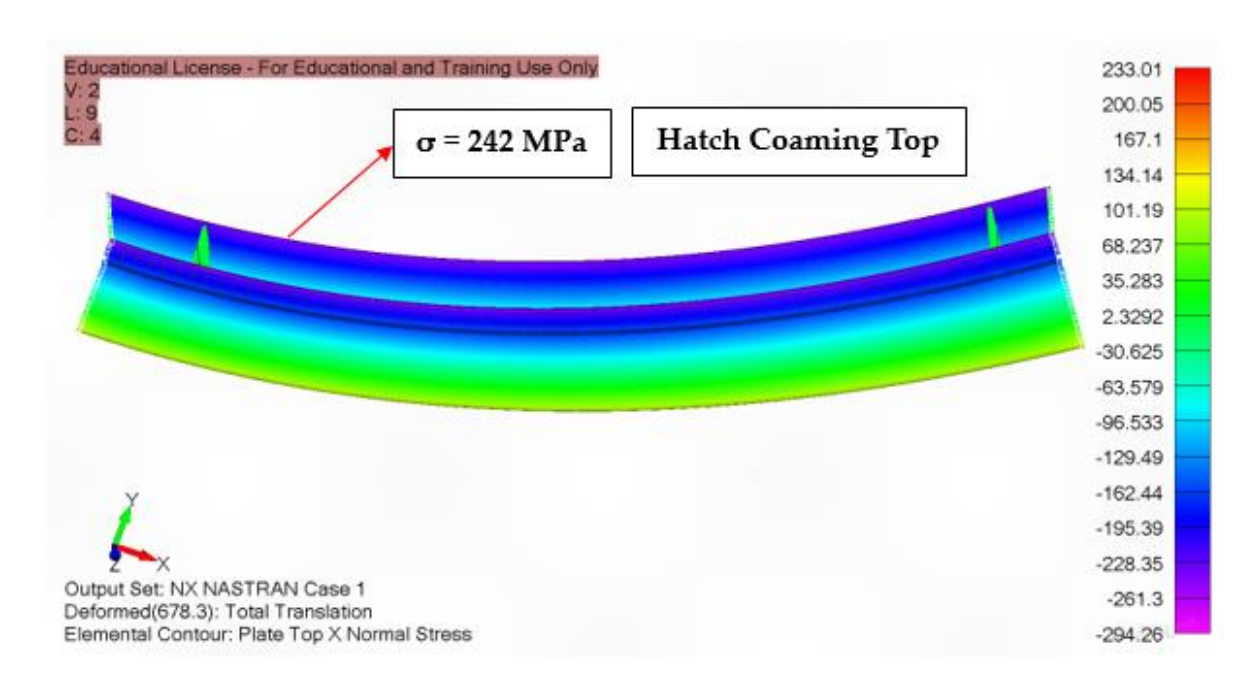


Figure 3-42: Hull girder normal stress at midship (Sagging—upright condition).

From the aforementioned Figure 3–41, it was observed that there was a stress difference of approximately 5% between the calculations obtained via beam theory and direct computation. This is acceptable in regard to the concept of beam theory [28]. Figure 3–42 shows that the maximum stress generated at the top plate of the hatch coaming, which is made of high-tensile steel (Grade DH36), has a maximum normal stress value of 242 MPa. This value notably falls below the established stress threshold of 331.77 MPa, as stipulated by the permissible stress constraint.

The selection of the Sagging condition for in-depth investigation in this study is substantiated by its position as the most critical scenario. This choice is supported by several factors, including the elevated hull girder stress levels perceived in the upright conditions, as shown in Figures 3–40 (Hogging—upright condition) and 3–42 (Sagging—upright condition), as well as the higher bending moments, as indicated in Table 3–25. Consequently, given its significance

in assessing structural performance and integrity, the Sagging condition emerges as the focal point for comprehensive analysis.

3.8.3.5 Structural Analysis of Ships under Combined Bending and Torsional Loads in Inclined (Oblique Sea) Conditions

When a ship is inclined, it experiences various types of moments, such as still water bending, vertical wave bending, horizontal wave bending and wave-induced torsional moments. However, this scenario does not fully account for the vertical wave bending moment. According to BV and NR 467 rules intended for the classification of steel ships, a load combination factor shows the amount of vertical wave bending moment that occurs in an inclined condition. In this situation, the load combination factor for the vertical wave bending moment was 0.4, indicating that only 40% would be effective [36]. Figure 3–16 explains the results of the hull girder's normal stress concerning an inclined condition.

Table 3–28: Normal stress in FE model (Sagging- Inclined load case).

Normal vertical bending stress (MPa)		
Height (m)	Direct calculation	
0	65.8	
1.1	47.9	
1.735	32.47	
2.37	16.23	
3	- 2.98	
3.64	- 22.36	
4.275	- 40.5	
4.91	- 59.75	
5.545	- 78.9	
6.18	- 97.6	
6.815	- 116.1	
7.45	- 140.8	
8	- 162.74	
8.55	- 177.56	
9.1	- 192.93	
9.65	- 210	

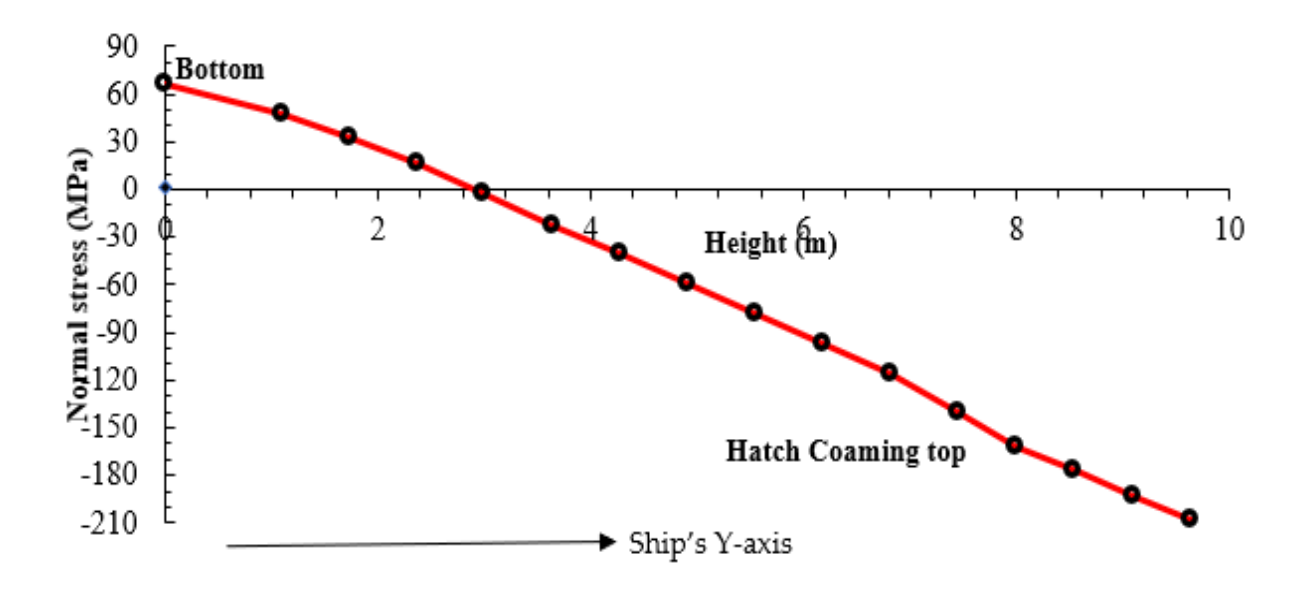


Figure 3-43: Hull girder normal stress at midship due to combined bending and torsional loads (Sagging—inclined conditions) along the depth (height) of the ship.

Table 3–28 and Figure 3–43 show the normal longitudinal bending stresses within the finite element (FE) model. This analysis is specifically carried out under the Sagging condition for the inclined load case. These visual and tabulated representations provide valuable tools that permit the comprehensive analysis of stress distribution across the structural components.

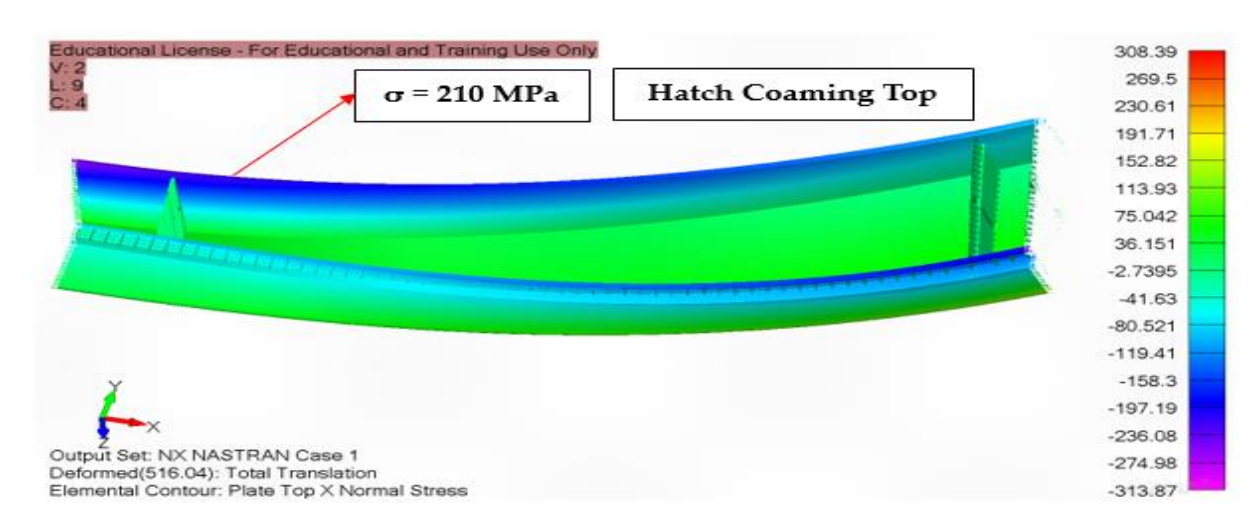


Figure 3-44: Hull girder normal stress at midship due to combined bending and torsional load (Sagging—Inclined condition).

Figures 3–43 and 3–44 show that the hatch coaming top plate had maximum hull girder normal stress values lower than the master allowable stress, as stated in Sec. 3.7.1.2. In an inclined state, the still water bending moment, the vertical wave bending moment, the horizontal wave

bending moment, together with the wave—induced torsional moment are all active. Therefore, it is crucial to ascertain each moment's contribution to hull girder stresses.

3.8.3.6 Impact of Still Water and Vertical Wave Bending Moment in an Inclined (Oblique Sea) Condition

Table 3–29 presents the normal stress of the still water and the vertical wave bending moment between the beam theory and direct calculation. As the study outlines, this assessment is performed under the Sagging condition for an inclined load case.

Table 3–29: Comparison of normal stress due to still water and vertical wave bending moment between beam theory and FE model (Sagging—Inclined load case).

	Normal vertical bending stress (M		
Z (m)	Direct Calculation	Beam Theory	
9.65	-150	-140	
9.1	-138	-128.33	
8.55	-125	-116.75	
8	-113	-105.16	
7.45	-100	-93.57	
6.815	-90	-80.2	
6.18	-75	-66.82	
5.545	-60	-53.44	
4.91	-47	-40.06	
4.275	-32	-26.68	
3.64	-17	-13.31	
3	5	0.07	
2.37	20	13.45	
1.735	36	26.83	
1.1	48	40.2	
0	70	63.38	

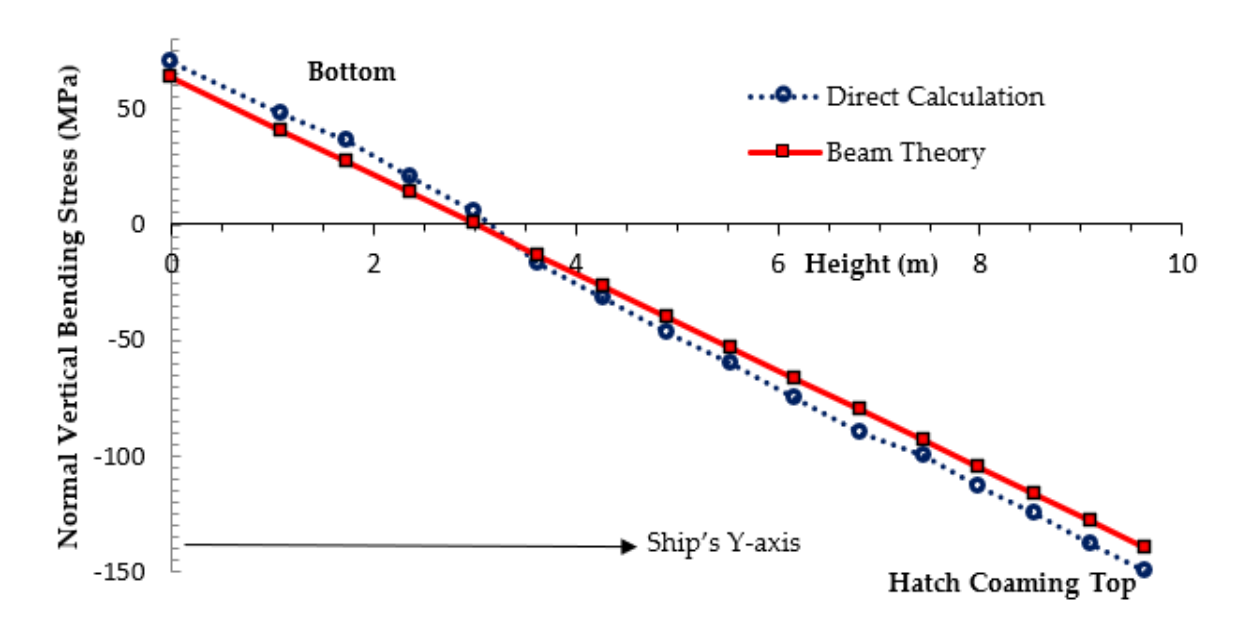


Figure 3-45: Comparison of hull girder stress between beam theory and direct calculation at midship due to still water and vertical wave bending moment (Sagging—inclined condition) along the depth (height) of the ship.

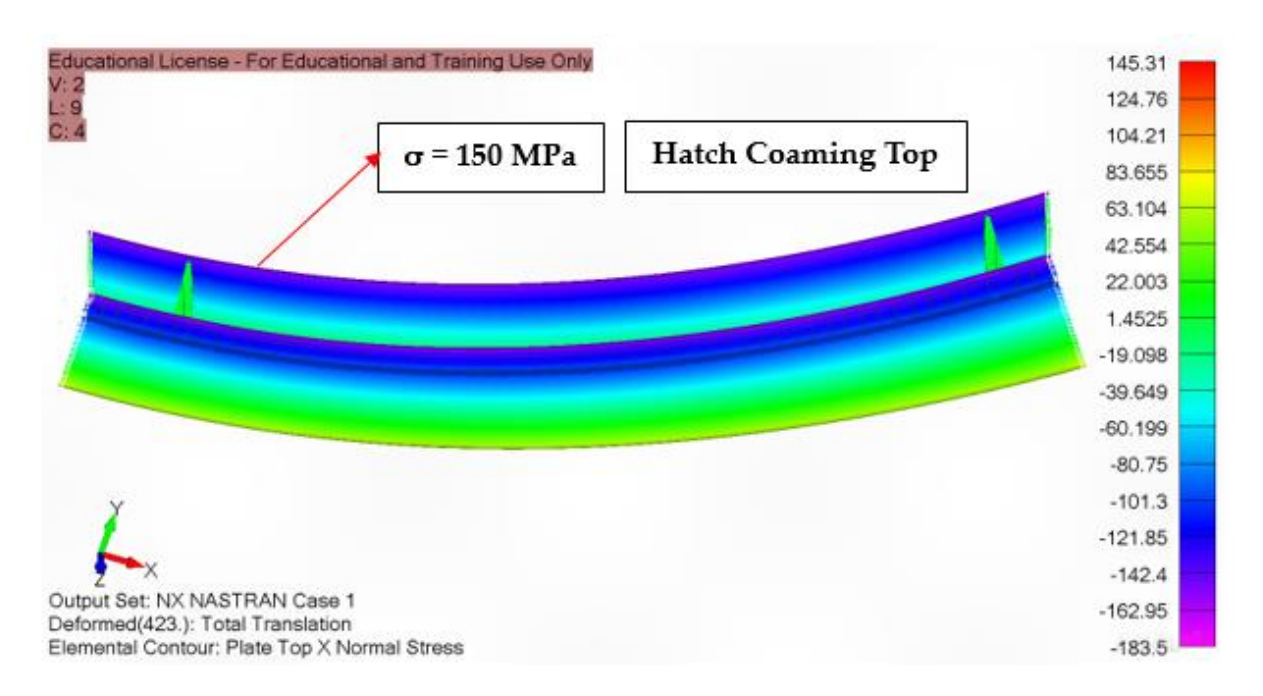


Figure 3-46: Hull girder normal stress at midship due to still water and vertical wave bending moment (Sagging—inclined condition).

Validation (Figure 3–45) was performed by comparing the hull girder normal stress values obtained from beam theory with those calculated exactly. Figure 3–45 shows a stress difference of approximately 5% between the calculations obtained through beam theory and direct computation. This level of discrepancy is considered acceptable within the context of beam

theory [132]. Figure 3–46 shows that the hull girder normal stress because of still water and vertical wave bending moment at midship (Sagging—inclined condition) occurs primarily at the hatch coaming top, accounting for approximately 70% of the total stress in inclined condition.

3.8.3.7 Impact of Horizontal Wave Bending Moment in an Inclined Load Case

Table 3–30 presents normal horizontal wave bending moment stress obtained through beam theory and direct calculation methods. As described in the study, this analysis is conducted under the Sagging condition for an inclined load case.

Table 3–30: Comparison of normal stress due to horizontal wave bending moment between beam theory and FE model (Sagging—Inclined load case).

	Normal horizontal bending stress (MPa)	
Height (m)	Direct Calculation	Beam Theory
9.65	21.5	22.42
9.1	21.5	22.42
8.55	21.5	22.42
8	21.5	22.42
7.45	21.5	22.42
6.815	21.5	22.42
6.18	21.5	22.42
5.545	21.5	22.42
4.91	21.5	22.42
4.275	21.5	22.42
3.64	21.5	22.42
3	21.5	22.42
2.37	21.5	22.42
1.735	21.5	22.42
1.1	21.5	22.42
0	21.5	22.42

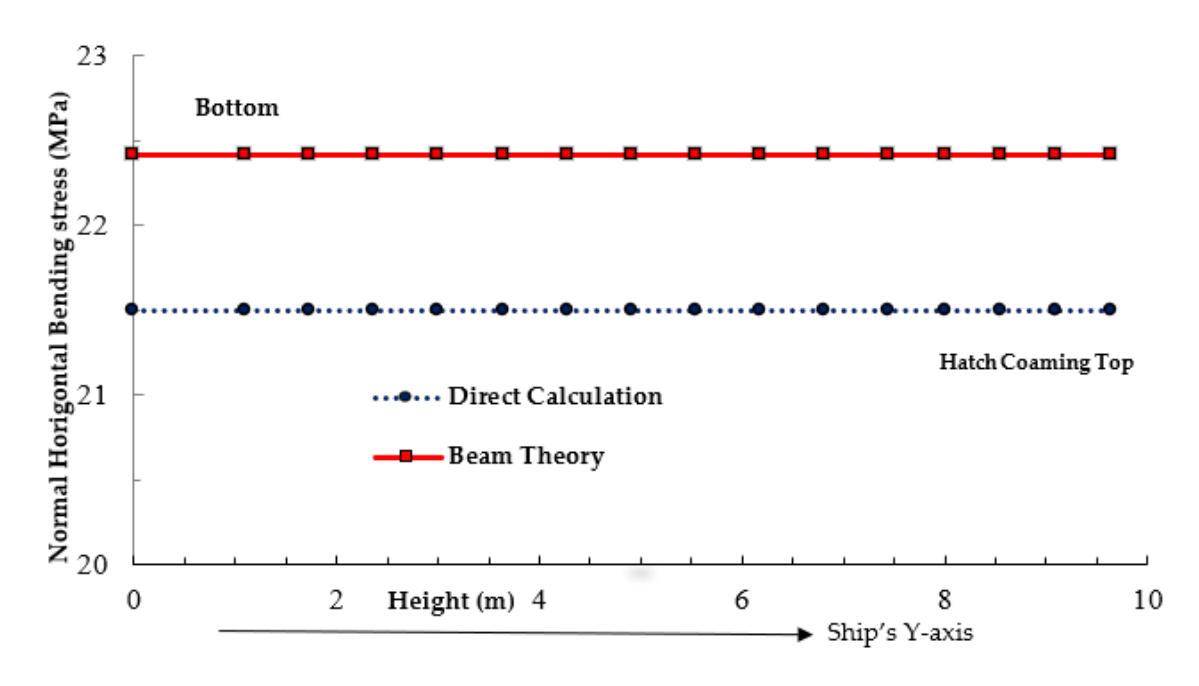


Figure 3-47: Comparison of normal longitudinal bending stress due to horizontal wave bending moment between beam theory and FE model.

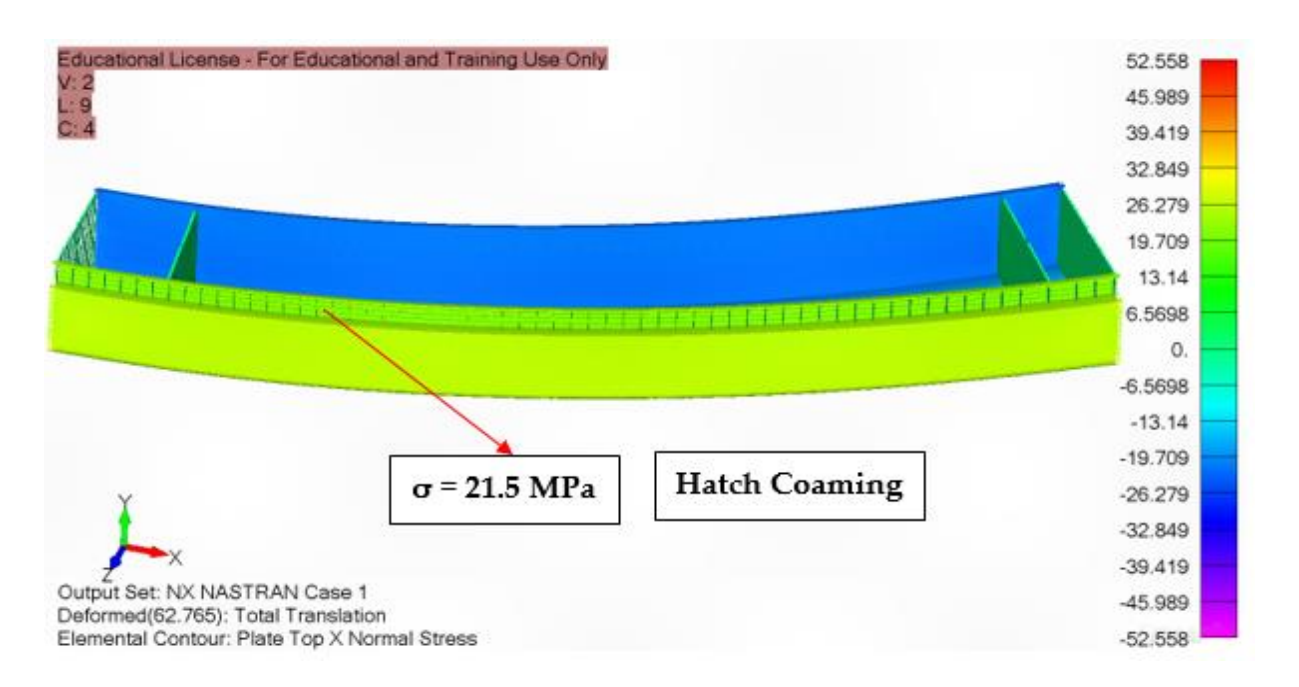


Figure 3-48: Maximum hull girder normal stress due to horizontal wave bending moment (Beam Sea condition).

Confirmation (Figure 3–47) was conducted by comparing normal stress values due to horizontal wave bending moment derived from beam theory and direct calculation. Figures 3–47 and 3–48 show that the maximum normal stress values as a result of horizontal wave bending moment would be the same as the vertical side plate, which was less than the master allowed stress defined in Sec. 3.7.1.2 and contributes roughly 10% in the inclined load case.

3.8.3.8 Impact of the Wave—Induced Torsional Moment in an Inclined (Oblique Sea) Condition

The normal warping stress from torsion values obtained from the thin-walled girder theory was compared to the direct calculation for validation. First, in the finite element model, only torsional moment is applied and normal stress due to torsion is checked. Then, a comparison of normal warping stress due to torsion values obtained from the thin-walled girder theory and the finite element model is undertaken for validation. The normal warping stress caused by torsion on the inner side shell in the midship area is taken from the MARS 2000 model (Torsion module) based on the thin-walled girder theory and FE model for comparison.

Table 3–31 and Figure 3–49 compare warping normal stress caused by wave-induced torsional moment between thin wall girder theory and direct calculation for inclined load case.

Table 3–31: Comparison of warping normal stress due to wave-induced torsional moment between thin wall girder theory and FE model (Inclined load case).

	Warping normal stress (MPa)	
Z (m)	Thin wall girder theory	Direct Calculation
9.65	27	35
9.1	24.235	29
8.55	23.031	25
8	20.123	22
7.45	19.897	21.5
6.815	16.7	18.9
6.18	12.3	14.7
5.545	9.1	11.2
4.91	5.3	7.7
4.275	2.1	3.1
3.64	0.1	-1
3	-1.6	-3.4
2.37	-5.7	-7.1
1.735	-8	-10
1.1	-10.6	-13
0	-19.5	-20.2

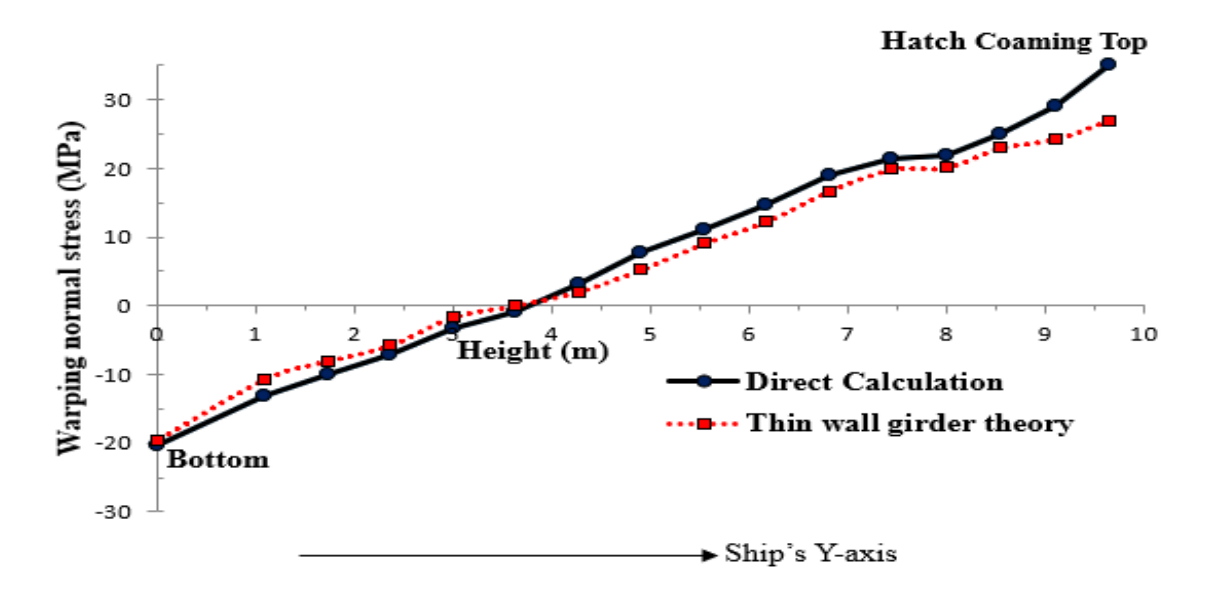


Figure 3-49: Comparison of hull girder warping normal stress due to wave-induced torsional moment between thin wall girder theory and direct calculation (Sagging—inclined condition) along the depth (height) of the ship.

Figure 3–49 shows a difference of around 10% in stress between thin wall girder theory and direct calculation. However, this difference could be considered acceptable based on the hypothesis of the thin wall girder theory. The most significant normal warping stress caused by torsion occurred near the cargo hold bulkheads, as shown in Figure 3–49.

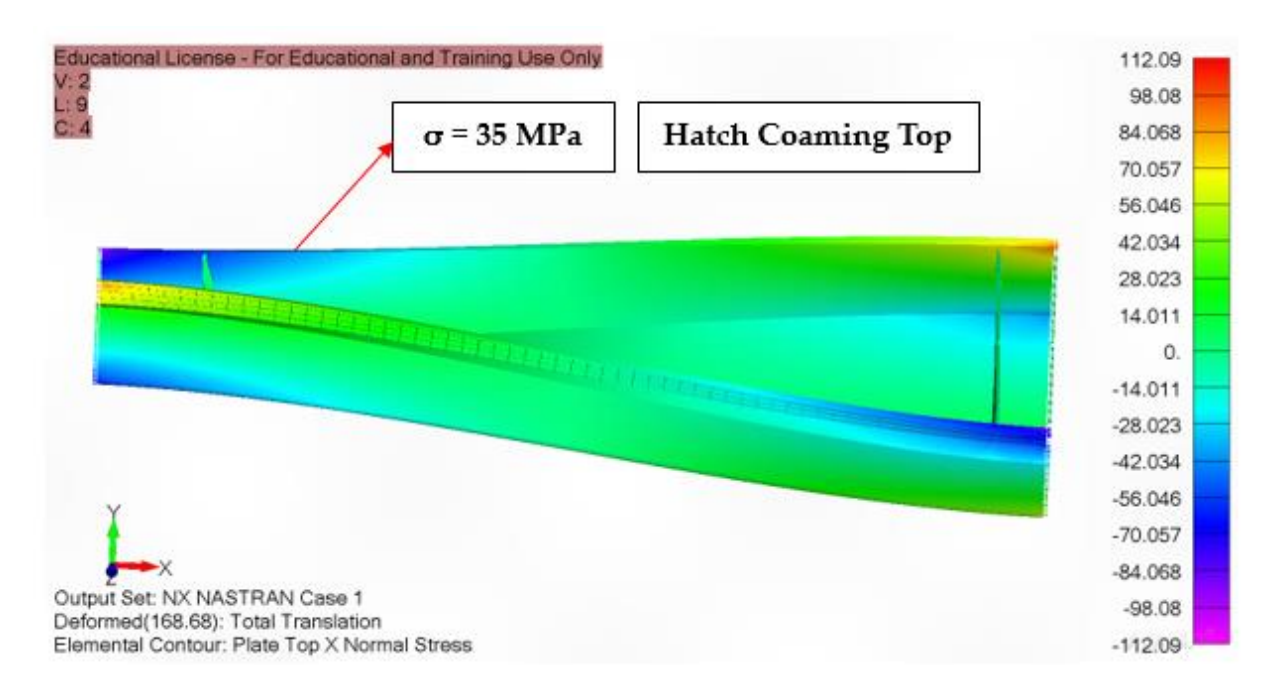


Figure 3-50: The hull girder warping normal stress due to torsion (open—deck ship).

Figure 3–50 shows that torsion generated the highest normal warping stress at the hatch coaming top, which accounted for approximately 20% of the total stress in an inclined load case.

3.8.3.9 Impact of Torsion between the Open—Deck and Closed—Deck Ships

Investigating the impact of torsion on open-deck vessels necessitates comparing open-deck and closed-deck ships concerning torsional loads. A main deck panel spanning from side to side within the open-deck ship under investigation has been introduced to allow this comparison. This panel simulates the structure of a closed deck, allowing for an assessment of the torsional behaviour of both open- and closed-deck ships under identical torsional loads. The preceding section has already addressed the influence of torsion on open-deck ships. A thorough examination of the hull girder, warping normal stress resulting from torsion, is conducted to validate the findings. This examination involves direct calculations for both open-deck and closed-deck ships, ensuring a comprehensive understanding of the torsion-related stress levels in each case.

It is vital to recognise the impact of torsion on both open- and closed-deck ships. Sec. 3.8.3.8 covers the effect of torsion on open-deck ships.

Table 3–32 and Figure 3–51 present a comparative analysis of warping normal stress resulting from wave-induced torsional moments, as calculated precisely, for both open and closed deck ships under inclined load conditions.

Table 3–32: Comparison of Warping Normal Stress for Open-Deck and Closed-Deck Ships, Calculated Directly Due to Wave-Induced Torsional Moments (Inclined Load Case).

	Warping norm	al stress (MPa)
Height (m)	Direct calculation (open deck)	Direct calculation (closed deck)
0	13.855	2.717
1.1	10.473	1.766
1.735	7.1	1.498
2.37	6.1	1.178
3	3.463	0.558
3.64	-0.257	-0.077
4.275	-3.97	-0.4
4.91	-7.692	-0.7
5.545	-11.206	-1.328
6.18	-14.681	-1.867
6.815	-18.139	-2.347
7.45	-21.483	-2.767

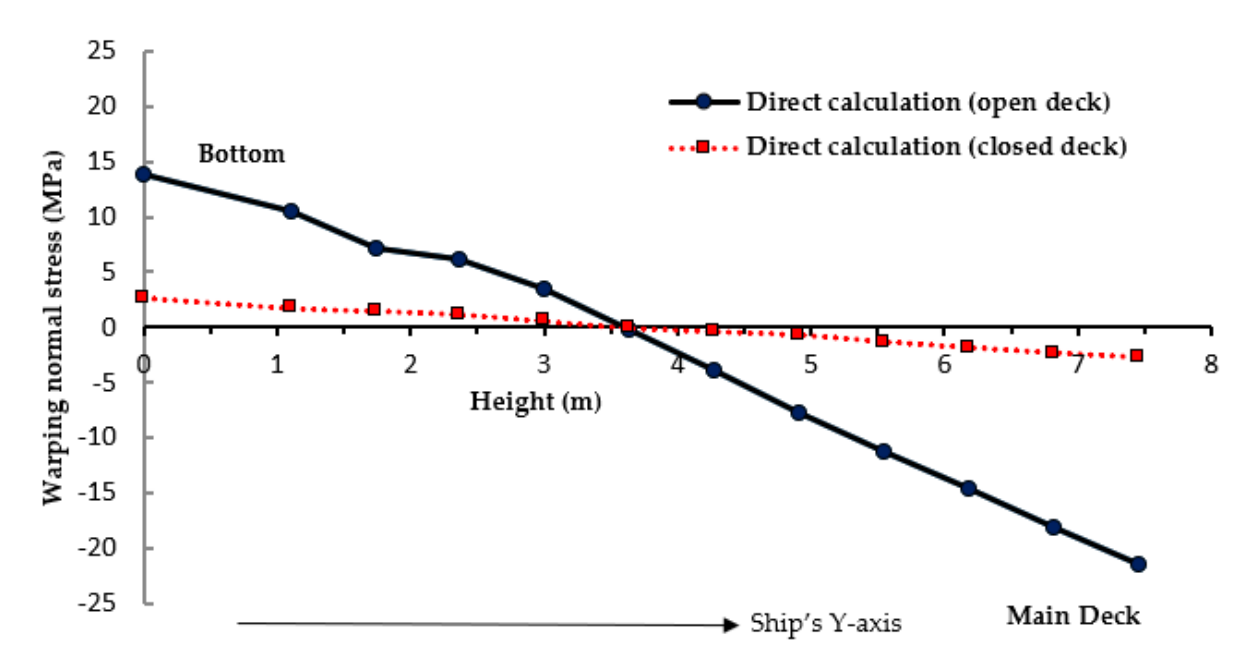


Figure 3-51: Comparison of hull girder warping normal stress between open—and closed—deck ships along the depth (height) of the ship.

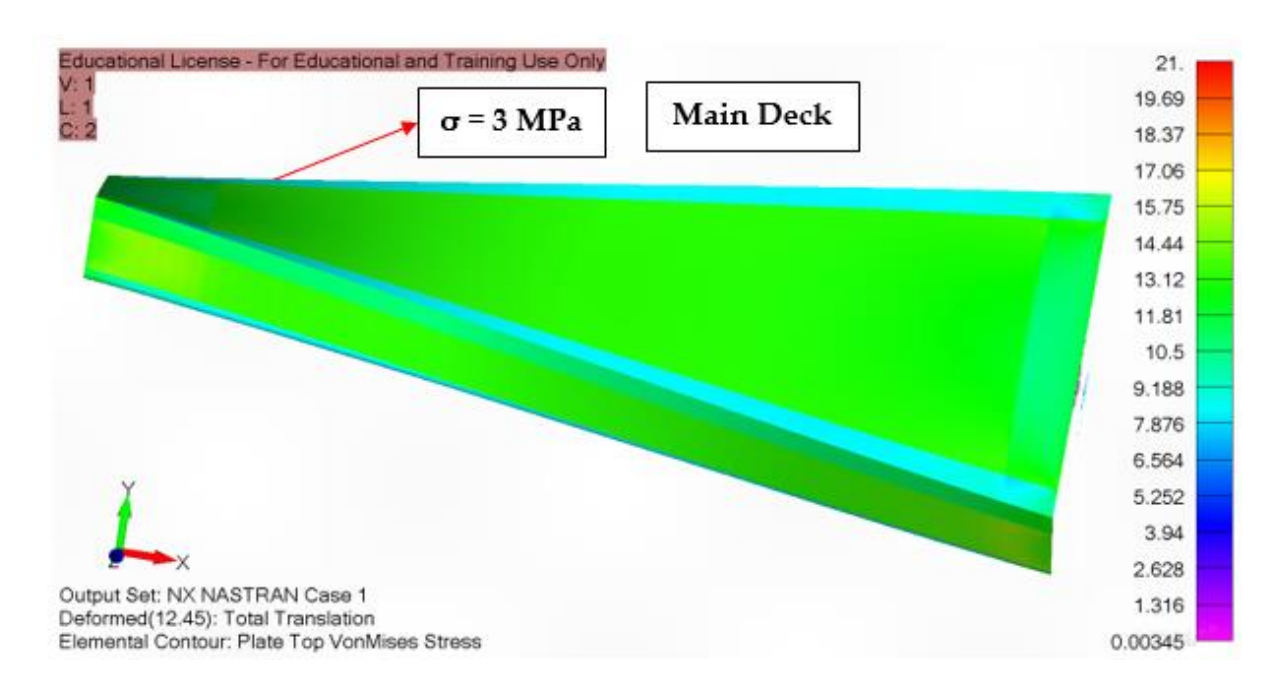


Figure 3-52: The hull girder warping normal stress due to torsion (closed—deck ship).

Figures 3–51 and 3–52 show that hull girder warping normal stresses were considerably less significant in closed-deck ships, whereas they accounted for roughly 20% of hull girder normal stresses in open-deck ships. In open-deck ships, the warping normal stress reaches zero at the shear centre point while registering higher values at the bottom and main deck levels, making these areas more critical regarding warping normal stress considerations.

3.9 Buckling Analysis

The ship's structural components experience compressive loads, which can cause buckling. This study investigated the impact of axial, bending and shear loads on the ship's structural components. The primary factors contributing to plate buckling in ship structural components include [67]:

- Elevated compressive and residual stresses.
- Heightened shear stresses.
- Combined stress conditions.
- Insufficient flexural rigidity.
- Inadequate stiffening.

- Notable initial imperfections.
- Extensive and improper utilisation of high-tensile steel.
- Excessive material degradation resulting from general and localised pitting corrosions.

The primary failure mechanisms observed in stiffened panels comprise:

- Lateral buckling of stiffeners.
- Torsional buckling of stiffeners.
- Flexural buckling of stiffeners.
- Flexural buckling of the plate-stiffener combination.
- Buckling of plate panels between stiffeners.

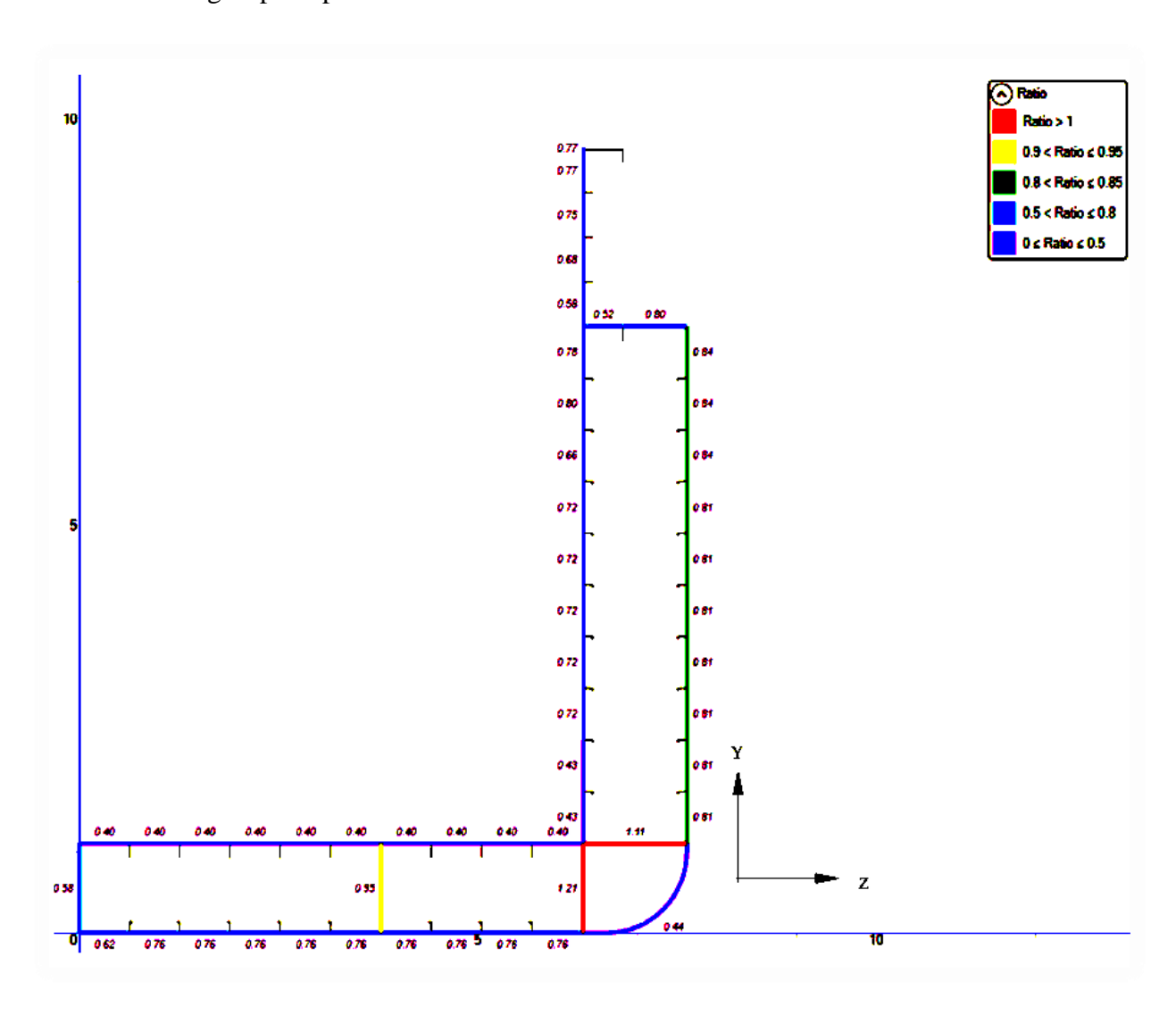


Figure 3-53: Buckling of plate panel in BV Mars, 2000.

Figure 3–53 shows the buckling capacity of the plate panel within the midship section. When the buckling factor exceeds one, it denotes non-compliance with the buckling criteria defined in the BV rule. This figure underlines the red lines, representing plate panels with a buckling factor exceeding one, signifying a failure to meet the criteria. The regulations established by classification societies are acknowledged for their conservative nature. Therefore, the following sensitivity analysis was conducted on this midship section using Femap software 2021.2 to assess whether the failure areas satisfied the buckling criteria.

Table 3–33 presents an extensive overview of the prescribed boundary conditions for the ship model during the analysis. Within this table, critical aspects of the model are detailed, specifying nodes located at the aft and fore-ends, in conjunction with the constraints governing translation and rotation along the X, Y and Z axes. These boundary conditions are imperative for copying a cantilever configuration and hold significant sway over the structural response and behaviour of the ship when subjected to various loading scenarios.

Table 3–33: Boundary conditions (Cantilever).

Down down oon ditions	Transla	ations in di	Rotation around axes			
Boundary conditions	X	Y	Z	X	Y	Z
Node at the aft end	Fixed	Fixed	Fixed	Fixed	Fixed	Fixed
Node at the fore end	Free	Free	Free	Free	Free	Free

3.9.1 Buckling of Inner Bottom Panel

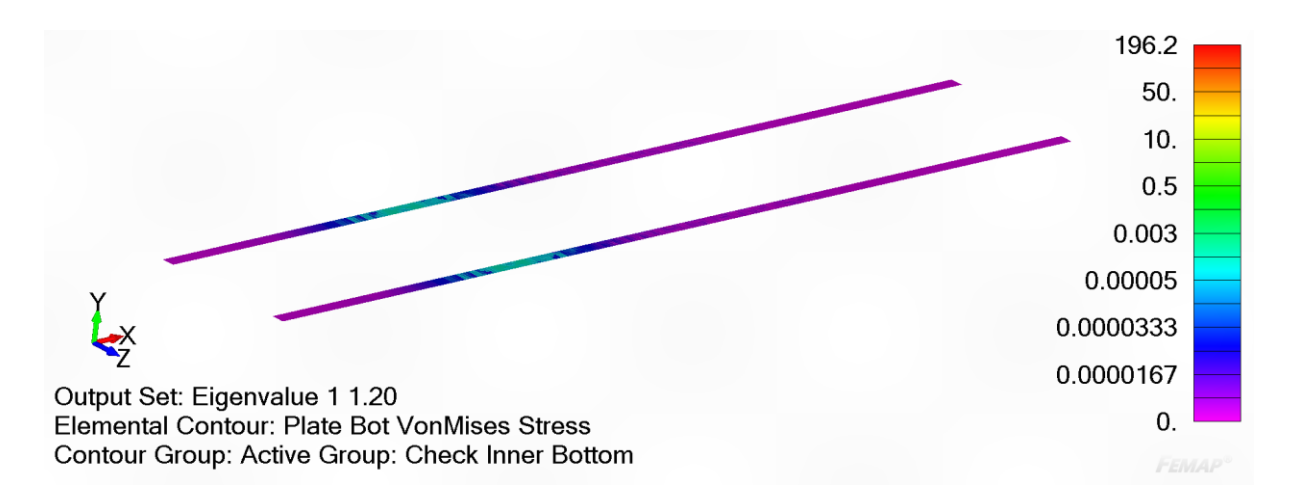


Figure 3-54: Inner Bottom Plate Panel Buckling under Hydrostatic and Inertia Loads in Femap.

Figure 3–54 shows the buckling behaviour of the inner bottom plate under hydrostatic and inertia loads. The analysis, conducted using BV Mars 2000, estimated hydrostatic and inertia loads of 204.13 kN/m². The eigenvalue from this analysis was 1.20, indicating that linear buckling occurs under these loading conditions. This result confirms that the inner bottom plate can withstand the specified loads without buckling failure, even under challenging scenarios.

3.9.2 Buckling of Inner Shell Panel

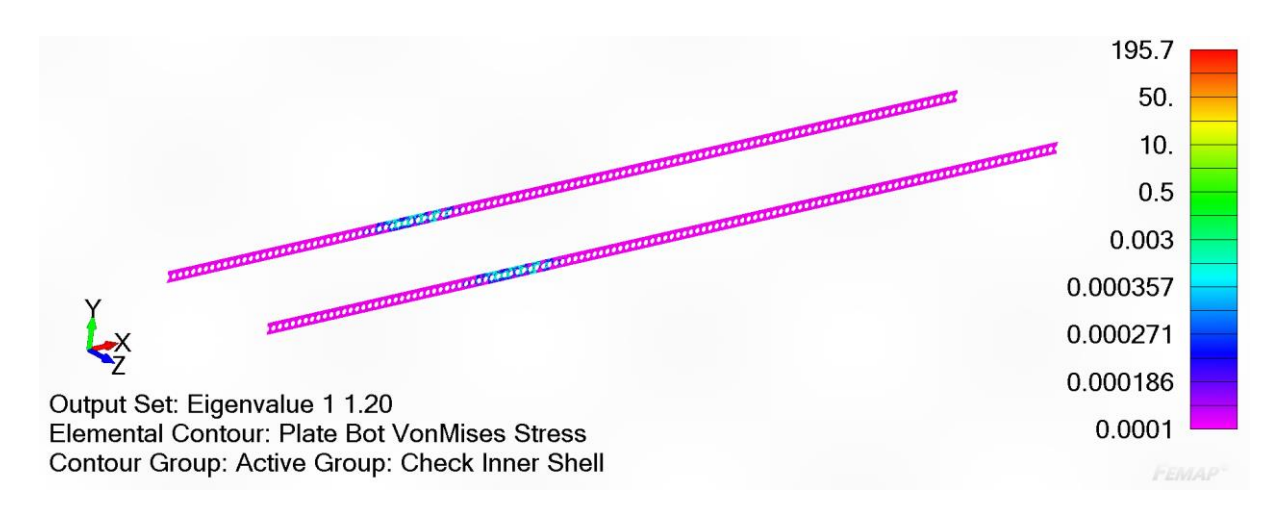


Figure 3-55: Inner Shell Plate Panel Buckling under Hydrostatic and Inertia Loads in Femap.

Figure 3–55 shows the performance of the inner shell plate under hydrostatic and inertia loads. The analysis, performed using BV Mars 2000, calculated these loads to be 204.13 kN/m². With an eigenvalue of 1.20, the study confirms that the inner shell plate satisfies the criteria for linear buckling under these conditions. This result highlights the plate's ability to maintain structural integrity when subjected to significant hydrostatic and inertia forces.

3.10 Discussion

This investigation is grounded on the Euler–Bernoulli beam theory to analyse a ship's strength under various loading conditions, including still water bending moment, vertical wave bending moment, and horizontal wave bending moment. Likewise, it is based on thin wall girder theory for a ship's strength calculations concerning wave-induced torsional moments. The hull girder normal stress discrepancy between beam theory and direct calculation was around 5% in both Sagging–upright and sagging–inclined conditions. Conversely, the warping stress difference

between the direct calculation and thin-wall girder theory was somewhere in the region of 10%. According to thin wall girder theory, up to 10% of discrepancies are allowable.

The strength of the hull girders was examined in this inspection. A relatively fine mesh was utilised in this analysis to validate the global stress levels of longitudinally effective plates, producing sufficient accuracy on a large scale. The upright and inclined load scenarios were examined in this analysis. In addition to the upright load condition, the inclined load condition is critical for open-deck ships. This is for the reason that open-deck ships are dependent on substantially higher hull girder warping normal stress in inclined conditions than closed-deck ships. Consequently, these stresses can significantly impact the structural integrity of the ship, particularly in the cargo hold end regions, where the highest hull girder warping normal stresses are regularly experienced.

The vessel under investigation is presently engaged in operational activities; however, certain sections of its structure do not conform to the prevailing rules and regulations. This circumstance has prompted the need for finite element (FE) analysis to be conducted with the aim of reviewing the vessel's structural integrity. In adherence to classification society standards, the wave load is predicated upon the North Atlantic wave spectrum, a conservative approach that consequently leads to prudent wave loads and similarly, careful consideration of the scantling.

The buckling analysis of the midship section using BV Mars 2000 software determined that the buckling criteria for the inner side shell panel and inner bottom plan in the bilge area did not meet the required standards. This is because classification societies' rules tend to be conservative. Nonetheless, after conducting a sensitivity analysis of the buckling using FEMAP software 2021.2, it was revealed that the eigenvalue exceeds one, confirming the occurrence of linear buckling even under such a demanding scenario.

Maximum torsional stiffness is required for ships to minimise vibration and maintain stability. A ship's design parameters can be optimised using the model generated and provided in this research. As this research progresses, work will focus on optimising several objectives (weight and production costs) and identifying the significant ship structural members that substantially impact the overall strength of ship structures. It is vital to reduce the steel weight of ships to save on manufacturing costs while maintaining standard safety criteria.

Literature reviews of pertinent previous works have been incorporated to better position the findings within the broader landscape of ship structural engineering research. For instance,

Jurišić et al. [133] previously emphasised the significant impact of understanding the effects of still water and wave load on midship structural integrity, agreeing with the current findings. Furthermore, the approach of emphasising the importance of conducting buckling analyses to evaluate structural integrity resonates with the work of Sun and Wang [134]. These findings are placed in the context of previous studies to demonstrate their relevance and contribution to improving ship structures' safety and reliability.

3.11 Conclusion

This investigation conducted a comprehensive analysis of a detailed cargo hold model to gauge the longitudinal strength of the hull girder structural members. The linear longitudinal strength of the ship was assessed using a 3D finite element model of the three distinct cargo holds. The hull girder stress values were substantiated by comparing the results against those obtained using Euler–Bernoulli beam theory and direct calculations. Additionally, the validity of torsional stress was confirmed by comparing the results with the results of the thin wall girder theory and direct calculation. The study examined the impact of various loading scenarios on the structural response, comparing the effect of torsion between closed-deck and open-deck ships. Lastly, buckling analysis was performed to assess the ship's buckling criteria, which were confirmed to be met as the eigenvalue exceeded one.

The structural investigation of the ship under consideration reveals the following:

Hull girder stresses at midship caused by still water bending and vertical wave bending moments contribute to approximately 70% of the total stress in an inclined condition.

Hull girder torsion stress is highest near the cargo hold bulkheads. Torsion induces the most typical warping stress near the top of the hatch coaming, representing approximately 20% of the total stress in inclined conditions.

In an inclined position, the maximum typical stress values from the horizontal wave bending moment are equivalent to those of the vertical side plate (hatch coaming plate) and contribute roughly 10%.

In closed-deck ships, hull girder warping normal stress is considerably less significant, accounting for around 20% of the total stress in open-deck ships.

Chapter 4

Hull Girder Deflection Analysis

4.1 Introduction

Ship structural deflection refers to the bending and deformation of a ship's hull, which occurs due to different loads, such as loading and unloading cargo and waves. When a ship encounters waves, the deflection of its hull increases significantly compared to when it is in still water. This extra deflection places additional stress on the ship's structure, emphasising the requirement for suitable design and upkeep to guarantee the safety and ability of the ship, particularly in challenging weather conditions [135]. The hull girder is a vital structural element of a ship that runs along its bottom and bears the weight of the machinery, cargo, along with other structures. Excessive deflection can result in structural failure, cargo damage, and even capsizing in extreme circumstances [136]. Lightship weight distribution, load distribution, and wave-induced global loads all contribute to the vertical bending moment that results in ship hull girder deflection [119]. During severe weather conditions, dynamic loads can also contribute to hull deflection [137]. An important task that must be performed beginning with the early design stages is the assessment of a ship's hull deflection in calm and turbulent waters [135]. The hull girder's bending moments caused by waves and shipload fluctuations can affect a ship's performance [138]. The propulsion shafting of the ship may also be impacted by hull deflection [139]. A ship's hull deflection can significantly impact its performance. Likewise, a ship's hull that has been deflected may experience positive displacement under Hogging conditions and a negative displacement under Sagging conditions [137]. Strength, deflection, and vibration are significant considerations in designing a ship's structure [3].

Niebylski (1970) introduced a mathematical model, that considers actual hull deflections during construction, currently used for manufacturing control and examining the impact of different factors on ship structures during sequential building stages [140]. Antoniou (1980) studied over 2000 observations of central deflection in shipyard plate panels, ascertaining that the plate slenderness ratio, stiffener thickness, plate aspect ratio, and weld throat thickness as significant factors in determining deflection. By means of regression analysis, the study determined the functional connection coefficients and proposed new formulas for predicting maximum

deflection in specific scenarios [141]. Ziha (2002) studied the impact of longitudinal deflections on bending moments and shear forces in merchant ship hulls, concluding that these effects were conservative and not of significant concern. Generally, more precise calculations of these quantities are optional [137]. Lee and Kim (2005) researched calculating hull deflection data in reverse using bending moments. They also examined ways to minimise bearing damage caused by hull deflection during the design phase. However, hull deflections from different loading scenarios significantly increased bearing offset [142]. Šverko (2005) conducted a study on multiple ships of various sizes and types to measure hull girder deflection accurately. The data collected was subsequently applied to evaluate the shaft alignment design and determine its susceptibility to changes during vessel operations through the ABS Shaft Alignment Optimisation program [143]. Naar (2006) completed a study on the prismatic hull girder of a post-Panamax passenger ship to analyse its maximum strength under Hogging and Sagging loading conditions. The coupled beam approach and the finite element method were utilised to evaluate the bending moment against the deflection of the hull girder. Both approaches yielded results that exhibited a significant correlation until the moment started to decrease [144]. Dardamanis (2022) studied shaft alignment in a standard 10,000 containership. Using automation in the process and minimal user pre-processing significantly reduced the time required to calculate hull deflections. This approach is dependable and efficient in determining hull deflections and bearing offsets due to its low time and experience requirements [145]. Farias et al. (2023) conducted research which confirmed that a ship's hull's deflection significantly affects its shaft's alignment in medium sized ships. The study used the Stiffness Method, Finite Element Analysis, besides the hull girder approach to identify the optimal alignment configuration for different operating conditions. The study achieved alignment configurations that met the approval criteria in 91.1% of the scenarios. Additionally, a reliability study proved that alignment optimisation improves the suitability and safety of the ship's propulsion system. The article highlights the importance of optimisation in achieving satisfactory alignment configurations, which ultimately enhances the reliability of both the system and the ship [146]. Zhou et al. (2023) investigated the effects of hull structural deformation on shaft alignment. The study divided hull deformation into global and local deformations and simplified them into single-span and grillage beam models. They then employed the matrix displacement method to calculate the effect of hull deformation on shaft alignment. The study established that hull deformation is a significant factor in shaft alignment and that the matrix displacement method is an effective tool for calculating hull deformation [147].

The contemporary hulls fitted to large oil carriers and cargo ships are designed to prevent bearing damage by minimising hull deflection. This is an important measure that ensures the safety and efficiency of these ships. Hull girder deflections significantly impact the bearing offset after the ship is constructed. Failure to consider hull deflection can result in a poorly designed alignment, leading to detrimental effects on bearing life. However, accurately forecasting and evaluating hull deflections poses a significant challenge. The ability to estimate hull deflection with adequate accuracy is essential to ensure a robust alignment design and, consequently, reduced alignment-related casualties [142].

Ships undergo deformation throughout their lifespans due to numerous factors such as local buckling, heat effects, global bending moment, and welding during construction. Controlling hull girder deflection within an acceptable range is essential to ensure the correct functioning of machinery and equipment. Excessive deflection can cause problems with shafting and pipework and increased torsional moment in the primary shaft owing to abnormalities and inefficiency. Moreover, pipe deflection can result in blockages and support-related issues with liquids. The deflection of the ship's hull, treated as a beam, can be obtained by performing a second integration of the bending moment and deflection relation (M_B/EI) curve and depends upon the moment of inertia (I) and elasticity (E). Excessive deflection reduces the structural efficiency of the ship. It is worth noting that while it may not give rise to structure failure, excessive deflection can misalign the ship's machinery and piping system, making these systems ineffective. Although classification standards do not set specific limits on hull girder deflections, the L/D (length to depth) ratio is related to the factors that help prevent excessive deflection [119].

Ship designers frequently consider the hull as a beam, where a discrepancy in the weight-buoyancy distribution causes a longitudinal bending moment. When designing the hull strength of a ship, it is typical to consider two extreme conditions: floating on a wave the same length as the ship and with the crest at each end, termed the "Sagging condition," and floating on a wave with the crest amidship, called the "Hogging condition." These two scenarios represent the most severe loading conditions of the ship [148].

The following factors need to be taken into account when considering the components of ships to control hull girder deflection. However, there are no strength-related restrictions. In the case of a ship with a higher L/D ratio, a greater hull girder deflection can be expected, and due attention should be given to this aspect [149].

- Longitudinally installed pipes and rods on the top deck or bottom can expand and contract.
- 2. An increase in draft results from the hull girder's deflection.
- 3. Hull girder deflection leads to the generation of secondary stress.
- 4. Flexural vibration, known as "whipping," can occur in the hull girder.

The study assesses the accuracy of an analytical technique in measuring a ship's hull girder deflection and compares it to the numerical approach. When designing a ship, designers must consider the hull girder's deflection, which helps maintain the ship's structural integrity and prevent potential failures. By examining all relevant aspects and utilising advanced modelling and simulation technologies, designers can construct a safe and effective ship capable of withstanding various loads and conditions throughout its service life.

4.2 Hull Girder Deflection

Deflections and stresses are standard parameters for measuring how ship hull structural elements respond to external loads. The term "strength" is related to structural performance standards and studies involving stresses, while "stiffness" considers deflection.

When analysing a structure, evaluating its strength and stiffness is vital to ensure it can effectively serve its intended purpose. Structural failure may occur if a structural component's material is compromised due to fracture, yielding, buckling, or other failure mechanisms caused by applied loads [119].

Several factors should be considered when considering ship components that limit hull girder deflection. It is important to note that there is no limitation from a strength perspective. However, ships with a larger L/D ratio (length-to-depth ratio) will likely experience more significant hull girder deflection, requiring attention. Ships that have been welded typically experience Sagging deflection, even without load. This deflection occurs because the deck is welded at the final stage. Moreover, the welded metal shrinks during cooling, causing the deck to contract. As a result of the Sagging, there is a loss of deadweight. To prevent this loss, ships are initially constructed with Hogging deflection, known as initial Hogging [149].

Once a ship is launched, it experiences Sagging deformation, equal to the initial Hogging. This creates tensile residual stress in the upper deck, while other areas of the ship, such as the bottom and side members, experience compressive residual stress [149].

From the perspective of longitudinal strength, it is not easy to restrict the hull girder's deflection. However, classification societies have developed rules based on their extensive experience to limit the deflection of the hull girder. This is because hull girder deflection strongly correlates with L/D and the tensile strength of steel, for example HT32 and HT36. The following equation evaluates the longitudinal strength to ensure that upper deck and bottom stresses remain below σ_a [149].

$$\delta = K \frac{WL^3}{EI} = \frac{K.WL.L^2}{E.\frac{I}{V}.y} = 2K.\frac{\sigma_a}{E}.\frac{L}{D}.L$$
(4-1)

where

 δ : Deflection of hull girder at midship

W: Load applied on hull girder

E: Young's modulus

I: The sectional moment of inertia of the hull girder

L: Ship length

D: Ship depth

y: Distance between the neutral axis and upper deck or bottom $(y \approx D/2)$

K: Constant

The above analysis determined that the deflection-to-ship length ratio (δ/L) is directly proportional to the ship length and depth (L/D) ratio.

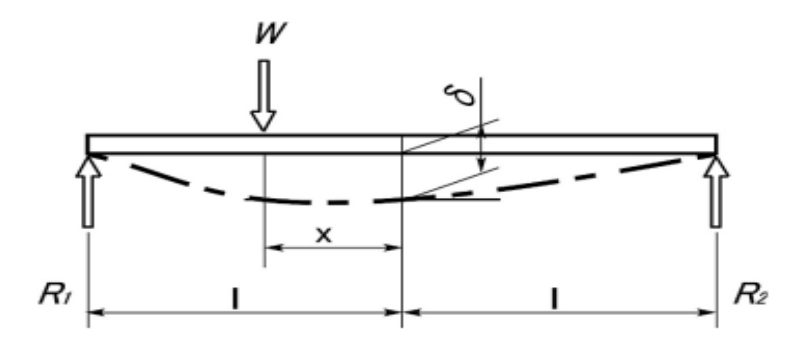


Figure 4-1: Deflection of both ends of the supported beam [149].

Figure 4–1 shows a beam that is supported at both ends. The equation below shows the deflection δ at midship resulting from applying load W [149].

$$\delta = \frac{W}{12EI} (2l^3 - 3lx^2 + x^3) \tag{4-2}$$

where

W: The amount of load

x: Distance between midship and loaded point

l: Half-length of ship

E: Young's modulus

I: The sectional moment of inertia of the midship section

The deflections at the midship caused by each load and buoyancy can be calculated using the formula provided [149].

4.2.1 Causes of Deflection

The deflection of the hull girder occurs when a ship is subjected to a vertical bending moment, horizontal wave bending moment, and wave-induced torsional moment. These moments can be caused by the distribution of the ship's lightship weight, the distribution of the load, together with the wave-induced global loads. In addition, the deflection caused by shear is combined with the deflection due to bending, albeit its amount is typically smaller in magnitude. The factors that gradually elevate nominal stress levels also lead to an incremental increase in flexibility. The hull girder deflection is of the utmost importance when designing a ship's

structure, guaranteeing the ship's structural performance, stability, safety, and efficiency [119]. To meet the intended goals, the hull girder is typically divided into three distinct categories: the primary hull girder as well as the internal structure and the superstructure. The primary hull girder is constructed to be sufficiently rigid to withstand the applied loads, the internal structure offers extra support and stiffness, while the superstructure is designed to provide additional space for crew and cargo while also contributing to the overall rigidity of the vessel [150].

4.2.2 Vertical and Horizontal Bending Moments

Many studies have concentrated on a ship's response to vertical longitudinal bending. However, lateral bending and twisting moments occur along with the vertical loads as a ship sails through rough waters and confronts waves from different directions directly in front or behind.

When a structure experiences vertical (M_v) and horizontal (M_h) bending moments, it dramatically increases the stress at its corners:

$$\sigma = \frac{M_v}{I_v/C_v} + \frac{M_h}{I_h/C_h} \tag{4-3}$$

where

M: Bending moment

I: Sectional moment of inertia about the neutral axis

C: Distance from the neutral axis to the extreme member

This study focuses on the vertical bending moment because it affects the ship's vertical reaction. Unlike in hull girder deflection analysis, horizontal bending does not interact with vertical bending. Therefore, the second part of the above-mentioned formula is not considered [119].

4.2.3 Boundary Conditions

The cantilever beam concept is implemented within the finite element (FE) model to comprehensively examine the hull girder's longitudinal strength attributes, aiming to obtain the results of the increased conservatism. In the deflection analysis, both sides of a supported beam have been subjected to bending moments and specific boundary conditions, which include moments. These conditions are applied on the forward and aft sides of the FE mode. They are

constrained by supported boundary conditions (refer to Tables 4–1 and 4–2). Under the main deck, rigid structural elements are constructed, transferring the load to numerous nodes. A rigid element connects free edge nodes to other nodes in the same plane, enabling them to function as a single unit. To establish two boundary conditions, two rigid components must be employed [128]:

- 1. Constraint: a rigid element at the model's aft and fwd. with zero degrees of freedom to clamp.
- 2. Moment: A bending moment is applied to a rigid element in the fore and aft parts of the model to establish the Hogging and Sagging conditions.

Table 4–1: Boundary conditions (For Head Sea).

Doundary conditions	Transla	tions in di	rections	Rotat	tion around	l axes
Boundary conditions	X	Y	Z	X	Y	Z
Node at the aft end	Fixed	Fixed	Fixed	Fixed	Fixed	Free
Node at the fore end	Fixed	Fixed	Fixed	Fixed	Fixed	Free

Table 4–2: Boundary conditions (For Beam Sea).

Doundour conditions	Transla	tions in di	rections	Rotat	ion aroun	d axes
Boundary conditions	X	Y	Z	X	Y	Z
Node at the aft end	Fixed	Fixed	Fixed	Fixed	Free	Fixed
Node at the fore end	Fixed	Fixed	Fixed	Fixed	Free	Fixed

4.2.4 Hull Girder Deflection Calculation

By equating the resistive moment to the bending moment, M, at section x, the elastic curve equation for a beam is obtained [119].

$$EI\frac{d^2y}{dx^2} = M(x) \tag{4-4}$$

In this equation, y is the deflection, E is the material's modulus of elasticity, whilst I is the moment of inertia of the beam's cross-section about a horizontal axis passing through its centroid.

Calculating a ship's bending-related deflection is similar to doing so for a beam. An intermediate M_B/I curve's second integration is used to calculate the deflection of a free-free supported ship with a variable moment of inertia [119].

$$\frac{M_B}{EI} = \frac{d^2y}{dx^2} \tag{4-5}$$

$$\frac{dy}{dx} = \frac{1}{E} \left[\int \frac{M_B}{I} \, dx \right] + a \tag{4-6}$$

$$y = \frac{1}{E} \left[\iint \frac{M_B}{I} \, dx dx \right] + ax + b \tag{4--7}$$

where

y is the deflection,

a is the first constant of integration of the M_B/I curve,

b is the second constant of integration of the M_B/I curve.

The change in slope is determined by the first integration of the M_B/I curve. The ordinates of the curve are equal to the areas under the M_B/I curve represented by [119]:

$$\frac{dy}{dx} = \frac{1}{E} \left[\int \frac{M_B}{I} \ dx \right] + a$$

The end slope is the integration constant, a. It is not zero since the ends of the hull girder are free. The total slope is equal to the sum of the end ordinates, and the axis of the slope curve is a line parallel to the baseline. The point of maximum deflection is typically close to the maximum ordinate of the M_B/I curve, at which the slope curve crosses the axis [119].

Depending on the loading, the bending moment may cross its baseline at one or more points. According to the size of the regions on the other side of the baseline, the slope curve would have matching points of a maximum or minimum slope. In this case, the M_B/I curve would have corresponding points of zero value [119].

The second integral of the M_B/I curve, which is the deflection curve, is represented by:

$$y = \frac{1}{E} \left[\iint \frac{M_B}{I} \, dx dx \right] + ax + b \tag{4-8}$$

The deflection curve's constant of integration, b, is equal to zero because the ends of the hull girder are free. The deflection curve will close at the ends of the baseline if the curve of the slope is integrated about the curve's axis [119].

The slope curve's constant of integration, a, is derived from the deflection due to the fact that when x = length L, y = 0 and:

$$a = \frac{-\frac{1}{E} \iint_0^L \frac{M_B}{I} \, dx \, dx}{I} \tag{4-9}$$

4.2.5 Analysing the Effects of Hull Girder Deflection

The deflection line of the ship's hull is frequently presented as a second-order symmetric parabola [137]:

$$w(x) = w_m \frac{x^2}{\left(\frac{L_{wl}}{2}\right)^2} \tag{4-10}$$

where w(x) is a general hull deflection at section x, w_m is a specific ship hull deflection at amidship, and L_{wl} is the length of the waterplane.

The deflection line of a ship's hull is neither symmetrical nor parabolic, but the deviations from the parabolic form are of minimal significance. It has been demonstrated experimentally and numerically that a parabola can satisfactorily fit the hull deflection data. However, it is impractical and often impossible to accurately determine the exact shape of the hull deflection on board. As the precise location is often unknown, assuming that the maximal deflection occurs at the longitudinal centre of flotation (LCF) can simplify the draft survey process without significantly impacting the accuracy of the displacement calculation [137].

4.2.6 Measurement of Deflection

Multiple draft readings, as in a lightship, can be taken to determine the hull girder longitudinal deflection. Freeboard measurements are taken at various points along the length of the vessel. These measurements are then plotted against the vessel's line plan, allowing the direction and magnitude of deflection to be observed through the waterline's curvature. To conduct a lightship survey, it is necessary to sound all tanks and evaluate their volume. A list of weights for non-

lightship items (cargo, fuel, or other operational items) on board must be prepared, documenting the mass and location of each weight. Similarly, the draught markings should be verified and recorded. Freeboard measurements indicate the distance from the water to the moulded deck edge and are taken at several locations along the vessel and recorded [119].

The hull deflections relevant for shaft alignment occur at the ship's stern, where the propulsion shafting is located. When the vessel's draught changes, the bearings supporting the propulsion shafting experience alterations in their offset due to changes in the ship's buoyancy. Hull deflections can be determined by measuring the difference between the bearing offsets in two ship situations [151].

To obtain the necessary data for defining hull deflections, at least five sets of measurements need to be taken at different ship draft conditions to assess the deflection of the ship's hull accurately [152]:

- 1. Docking
- 2. Light draft right after launch and before any bearing adjustments.
- 3. Light draft after bearing adjustment.
- 4. Ballast condition.
- 5. Fully loaded condition.

Installing strain gauges at various points along the line shaft is necessary to quantify the bending moments. Before or after the strain gauge measurements, measuring the engine crankshaft deflections, main engine bearing reactions, line shaft bearing reactions and forward stern tube bearing reactions is necessary. The bearing offset will be determined from the parameters measured using reverse analysis [152].

4.3 Serviceability

4.3.1 Limiting Tolerance

The regulations from classification societies often include specifications for local deflections to ensure they are reasonable. As an illustration, according to International Standards, there exists a restriction on the hull girder deflection, which is set at 1 mm per metre of a ship's length

in situ. Stiffeners also have additional criteria to meet [119]. To prevent buckling, it is important to scrutinise the stiffness of members under compressive loads. To achieve this, it is essential to ensure that the stiffener and its corresponding plate have a minimum moment of inertia [153].

It is reasonable to presume that the allowable stress has sufficient margin to accommodate any unforeseen heavy loads. The safety factor against yield failure is determined by comparing the Von Mises stress of the structure (σ_e) against the permissible stress (σ_o), giving the result [119]:

$$\sigma_e \le \sigma_0 = s_{1 \times} \sigma_v \tag{4-11}$$

where

 s_I : The classification society defines the partial safety factor and varies based on the loading condition and analysis method.

 σ_y : The minimum yield point of the steel being considered varies depending on the ship type. The specific parts of the hull structure and permissible stresses may also differ for each part.

4.3.2 Typical Potential Problems

4.3.2.1 In Shafting

Deflection in the hull girder can create shaft misalignment, resulting in vibration, noise, and wear and tear of the shaft and bearing. According to satisfactory crankshaft deflection readings, the engine position and bearing offsets are within the manufacturer's acceptable range. Engine manufacturers advise that crankshaft deflections should be near zero for the in-service situation with a warm engine and a loaded vessel. Each engine manufacturer establishes maximum allowable crankshaft deflections. Different deflection restrictions apply for new and old engines based on the manufacturer's guidelines and the condition of the engine [152].

4.3.2.2 In Piping

The installation of piping and equipment may encounter challenges due to hull girder deflection, leading to misalignment, stress and fatigue. However, longitudinally oriented bilge and ballast systems are less affected by significant hull girder deflection. This is because the materials used in these systems have a lower elastic modulus than conventional steel piping, making them less susceptible to deformation.

When compared to steel piping, aluminium piping can manage only one-third of the stress for the same amount of hull deflection. Similarly, fibreglass piping can hold only one-tenth to one-fifteenth of the stress compared to steel piping. As a result, increasing hull girder deflection is acceptable without subjecting the pipes to undue stress [154].

4.4 Safeguard against Excessive Deflection

Designing structures to meet deflection criteria typically requires heavier structural members than acceptable stress criteria. For instance, a vessel's stern must be designed to prevent excessive deflection that could interfere with the smooth rotation of the propeller and rudder. Simultaneously, the stress in the stern must also be kept within acceptable limits. The stern and engine room structures contain various rotating machines; hence, they must be designed to consider allowable stress and permissible deflection. When designing an engine room, ensuring that the structure does not cause misalignment of machines or pumps due to significant deflection is crucial. Similarly, limiting excessive deflection in the stern structure is essential, which requires careful consideration of its design [119].

The stress level of these members is significantly lower, practically one-tenth, compared to other structures when calculating the stress of the stern or stern frame with the appropriate external load assumption. This difference arises because the scantlings of these members are determined based on the permitted deflection requirements rather than allowable stress standards [119].

To develop a design based on allowable deflection, it is essential first to clarify the acceptable limits. Subsequently, the stiffness of structural members must be determined to ensure that the deflection of each member remains below the critical limit. However, concerning the stern, stern frame, and rudder, it is unfortunate that the allowable deflection criteria cannot be fully established at the initial stages of a project. The following criteria must be set to design more reasonable and sophisticated structures [119]:

- Allowable stress to prevent cracking or buckling.
- Acceptable amplitude to avoid vibration.
- Allowable deflection to prevent machinery damage.

4.5 Analytical Determination of Ship's Hull Girder Deflection as a Simply Supported Beam

The maximum bending moment in rule calculations is obtained through the analytical estimation of the highest deflection value. To analyse hull girder deflection, it is necessary to consider the total still water and vertical wave bending moments during both Head Sea Hogging and Sagging conditions. The horizontal bending moment should also be considered when experiencing a Beam Sea condition [147]. The distribution of bending moments is determined by measuring the moment of inertia (*I*) in multiple transverse sections along the ship's entire length. The midship area typically exhibits the highest moment of inertia. The cross-sectional areas decrease as the sections move closer to the ends of the ship because of its hull form, resulting in a corresponding decrease in the moments of inertia [155].

Tables 4–3 and 4–4 display the hull girder deflection analysis results conducted under specific conditions. Table 4–3 shows the results for the "Hogging Condition" obtained through analytical calculations, while Table 4–4 presents the results for the "Sagging Condition," which were similarly derived analytically. The comprehensive hull girder deflection analysis uses critical parameters, for instance still water bending moment, vertical wave bending moment, moment of inertia and the *M/I* equation.

Table 4–3: Hull Girder Deflection Analysis Results (Analytical Calculation, Hogging Condition).

Still water bending moment	=	126351 kNm	
Vertical wave bending moment	=	177581 kNm	
L	=	104.135 m	
E	=	206000000 KN/m ²	
a	=	-0.006037279	

	$X\left(\mathbf{m}\right)$	Still water bending moment (kNm)	Vertical wave bending moment (kNm)	Total Bending moment M (kNm)	Moment of inertia, I (Y axis) (m ⁴)	M/I	<i>M/I</i> equation	Deflection z (mm)
0	0	0	0	0	0.5	0	0	0.00
0.1L	10.4135	42117	44395.25	86512.25	4.3	20119.13	353796.6667	61.15
0.2L	20.827	84234	88790.5	173024.5	9.1	19013.68	2310214.409	114.52
0.3L	31.2405	126351	133185.8	259536.75	9.1	28520.52	6818571.296	155.51
0.4L	41.654	126351	177581	303932	9.1	33399.12	14445719.38	181.35
0.5L	52.0675	126351	177581	303932	9.1	33399.12	25504876.94	190.54
0.6L	62.481	126351	177581	303932	9.1	33399.12	40126311.31	182.43
0.65L	67.688	126351	177581	303932	9.1	33399.12	48767842.1	171.91
0.7L	72.8945	126351	152212.3	278563.286	9.1	30611.35	58269872.31	157.22
0.8L	83.308	84234	101474.9	185708.857	9.1	20407.57	79679376.36	116.16
0.9L	93.7215	42117	50737.43	92854.4286	4.3	21594.05	103778841.1	62.04
L	104.135	0	0	0	0.5	0	129510570.6	0.00

Table 4–4: Hull Girder Deflection Analysis Results (Analytical Calculation, Sagging Condition).

			Moment
a		=	-0.006044328
E		=	206000000 KN/m^2
L		=	104.135 m
Vertical wave bending	moment	=	192769 kNm
Still water bending mo	ment	=	114633 kNm

	X (m)	Still water bending moment (kNm)	Vertical wave bending moment (kNm)	Total Bending moment M (kNm)	Moment of inertia, I (Y axis) (m ⁴)	M/I	<i>M/I</i> equation	Deflection z (mm)
0	0	0	0	0	0.5	0	0	0.00
0.1L	10.4135	38211	48192.25	86403.25	4.3	20093.78	351722.2386	-61.24
0.2L	20.827	76422	96384.5	172806.5	9.1	18989.73	2296855.284	-114.74
0.3L	31.2405	114633	144576.8	259209.75	9.1	28484.59	6791200.617	-155.86
0.4L	41.654	114633	192769	307402	9.1	33780.44	14416540.8	-181.79
0.5L	52.0675	114633	192769	307402	9.1	33780.44	25499121.77	-190.93
0.6L	62.481	114633	192769	307402	9.1	33780.44	40173046.21	-182.64
0.65L	67.688	114633	192769	307402	9.1	33780.44	48849303.6	-171.99
0.7L	72.8945	114633	165230.6	279863.571	9.1	30754.24	58388578.07	-157.16
0.8L	83.308	76422	110153.7	186575.714	9.1	20502.83	79865358.15	-115.84
0.9L	93.7215	38211	55076.86	93287.8571	4.3	21694.85	103990530.8	-61.68
L	104.135	0	0	0	0.5	0	129661781.7	0.00

Table 4–5 presents the outcomes of the hull girder deflection analysis conducted under Beam Sea conditions, employing analytical calculations. This comprehensive analysis considers essential factors, including horizontal wave bending moment, moment of inertia and the *M/I* equation. Its significance lies in rigorously evaluating a ship's structural integrity, yielding invaluable data to support and adhere to maritime safety and engineering standards.

Table 4–5: Hull Girder Deflection Analysis Results (Analytical Calculation, Beam Sea Condition).

Horizontal wave bending moment	=	93037 kNm
L	=	104.135 m
E	=	206000000 KN/m^2
a	=	-0.000493239

	$X(\mathbf{m})$	Horizontal wave Bending moment M (kNm)	Moment of inertia, I (Z axis) (m ⁴)	M/I	<i>M/I</i> equation	Deflection y (mm)
0	0	0	0.5	0	0	0.00
0.1L	10.4135	23259.25	13.5	1722.9074	28417.46501	5.00
0.2L	20.827	46518.5	31.63	1470.7082	182231.1029	9.39
0.3L	31.2405	69777.75	31.63	2206.0623	542320.8191	12.78
0.4L	41.654	93037	31.63	2941.4164	1163353.992	14.90
0.5L	52.0675	93037	31.63	2941.4164	2076602.916	15.60
0.6L	62.481	93037	31.63	2941.4164	3291538.043	14.84
0.7L	72.8945	69777.75	31.63	2206.0623	4796197.03	12.67
0.8L	83.308	46518.5	31.63	1470.7082	6556329.588	9.26
0.9L	93.7215	23259.25	13.5	1722.9074	8513318.133	4.90
L	104.135	0	0.5	0	10580874.24	0.00

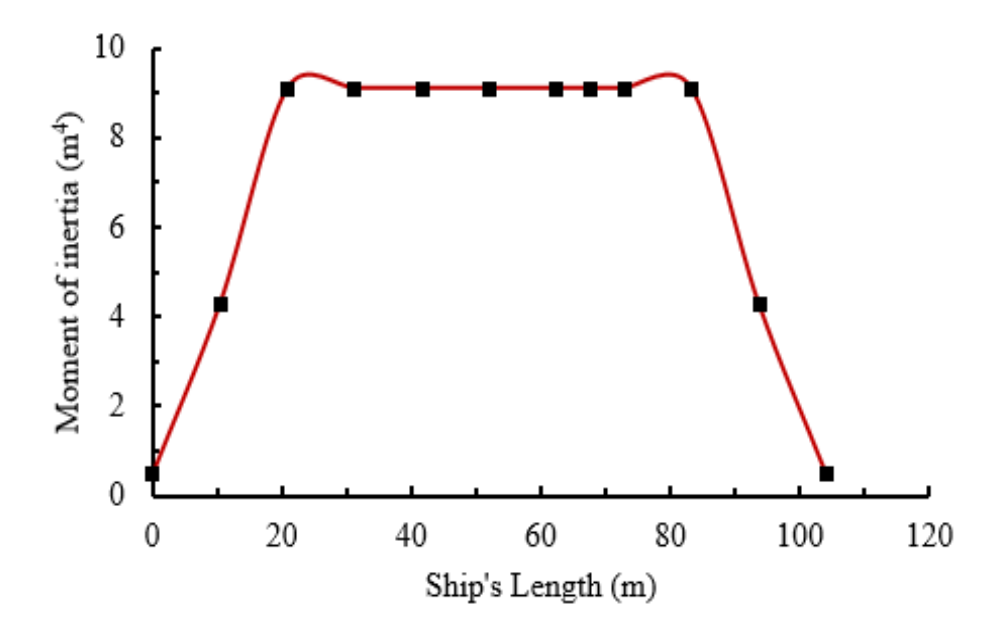


Figure 4-2: Distribution of the moment of inertia (*Y* axis) along the ship's length.

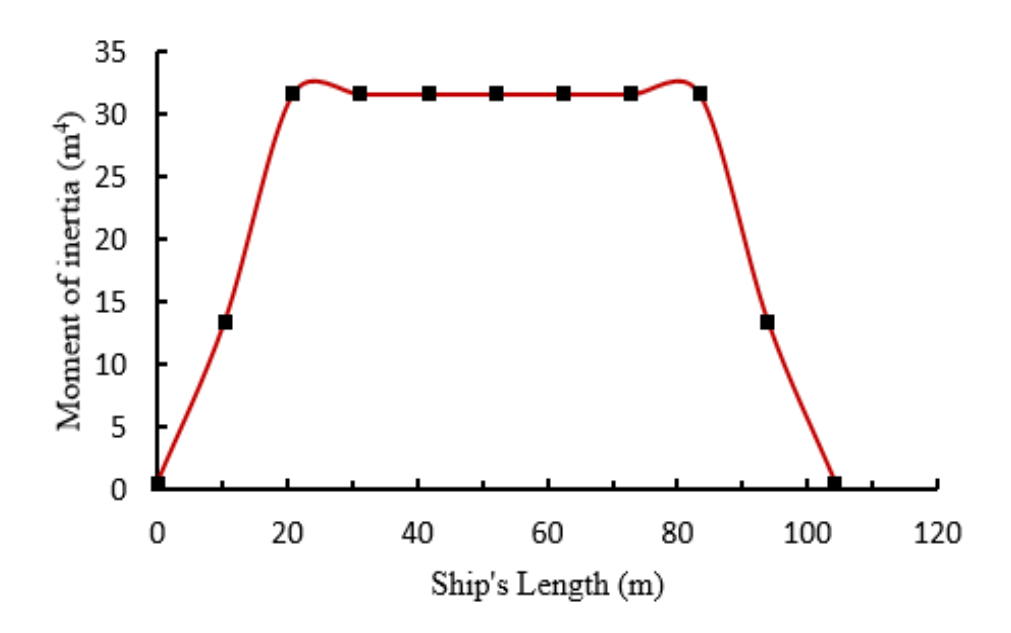


Figure 4-3: Distribution of the moment of inertia (Z axis) along the ship's length.

Figures 4-2 and 4-3 show the moment of inertia distribution along the ship's length, with the X-axis representing the ship's longitudinal position and the Y-axis showing the moment of inertia values. The midship section typically exhibits higher values due to its fuller shape and concentrated structural elements, while lower values are observed at the bow and stern due to smaller cross-sections. This distribution significantly impacts the ship's resistance to bending and rotational forces, influencing structural integrity and seakeeping performance. The variation arises from differences in hull shape, structural design, and load distribution along the vessel.

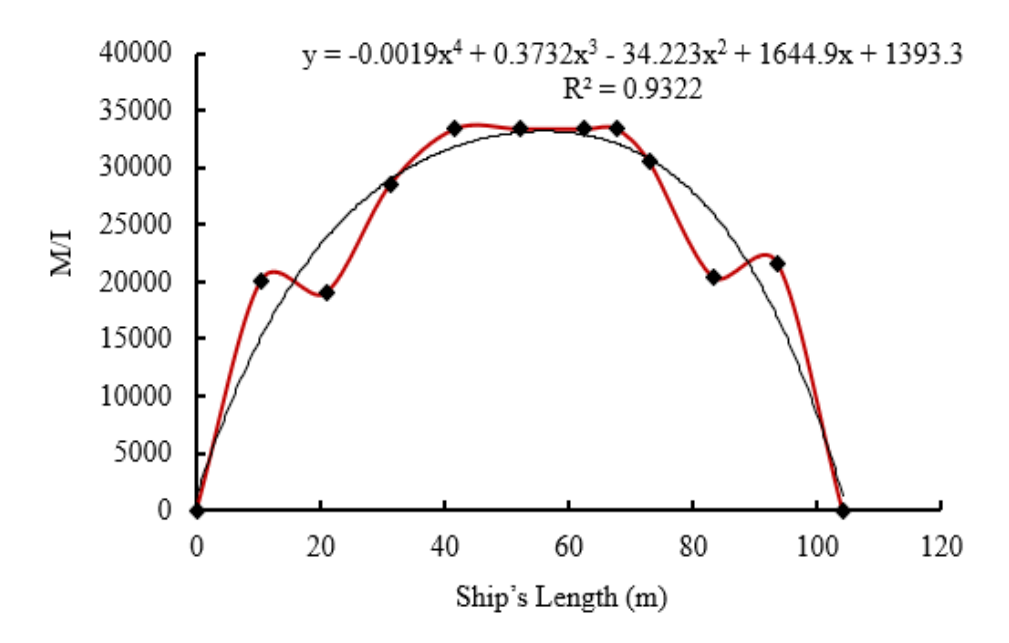


Figure 4-4: M_B/I curve along the ship's length (Hogging-Head Sea).

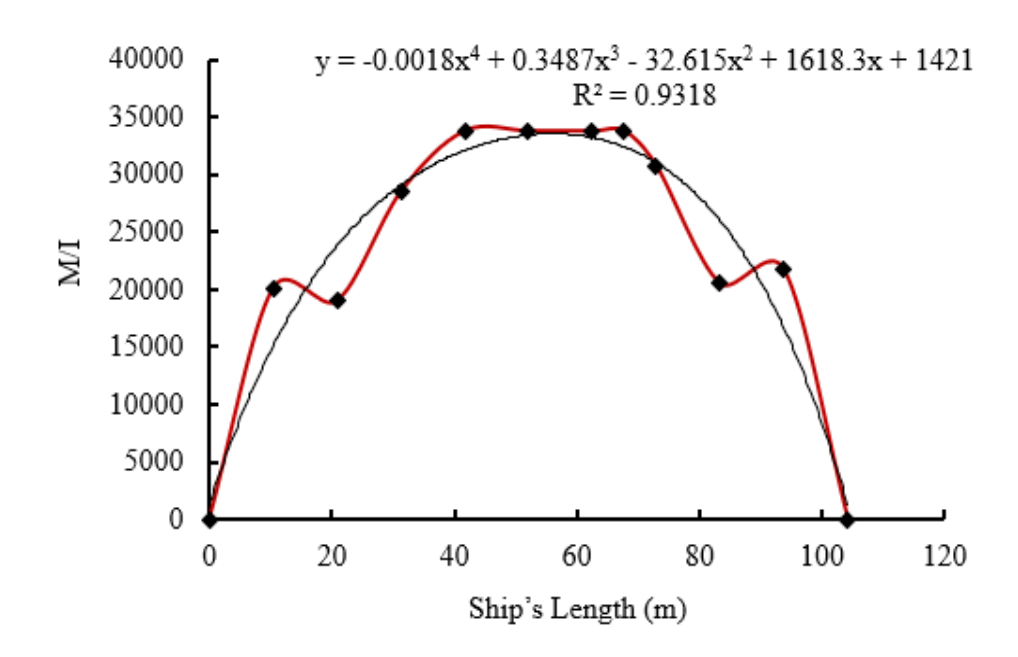


Figure 4-5: M_B/I curve along the ship's length (Sagging-Head Sea).

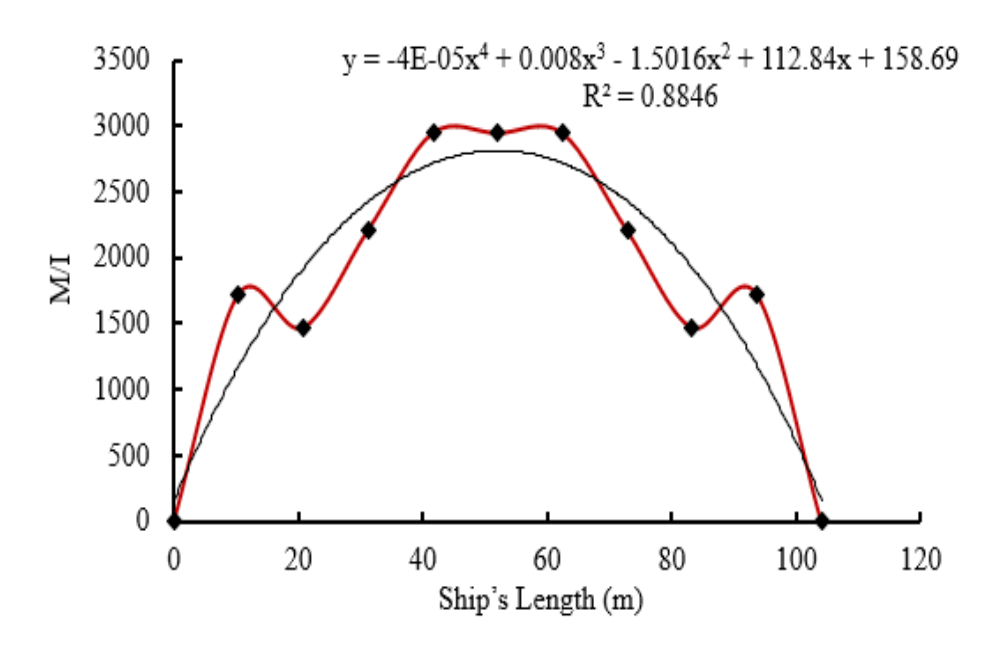


Figure 4-6: M_B/I curve along the ship's length (Beam Sea).

A parabolic equation has been derived to obtain a mathematical representation of the moment of inertia distribution near the ship's ends. The second integration of the M_B/I curve determines the deflection. This mathematical operation integrates the function twice. This is typically obtained using Microsoft Excel software when a trend line is added to the M_B/I curve. Figures 4–4 and 4–5, derived from the data presented in Tables 4–3 and 4–4, illustrate the M_B/I curve along the ship's length for Hogging and Sagging loading scenarios during Head Sea conditions,

respectively. Figure 4–6, generated from Table 4–5, represents the M_B/I curve along the ship's length for the Beam Sea conditions.

The MB/I function approximates the original curve, yielding R-squared values of 0.9322, 0.9318, and 0.8846 for the Hogging-Head, Sagging-Head and Beam Sea conditions, respectively. The R-squared value, also known as the coefficient of determination, measures how well the data fits the curve. A higher R-squared value indicates that the data fits the curve better, signifying a more accurate approximation. Hull girder deflections for the analysed ship's loading can be calculated using the equations in Figures 4–4, 4–5 and 4–6. These figures show hull girder deflection under various loading conditions, especially Head Sea Hogging, Sagging and Beam Sea conditions. The data used to generate these figures is presented in Tables 4–3, 4–4 and 4–5.

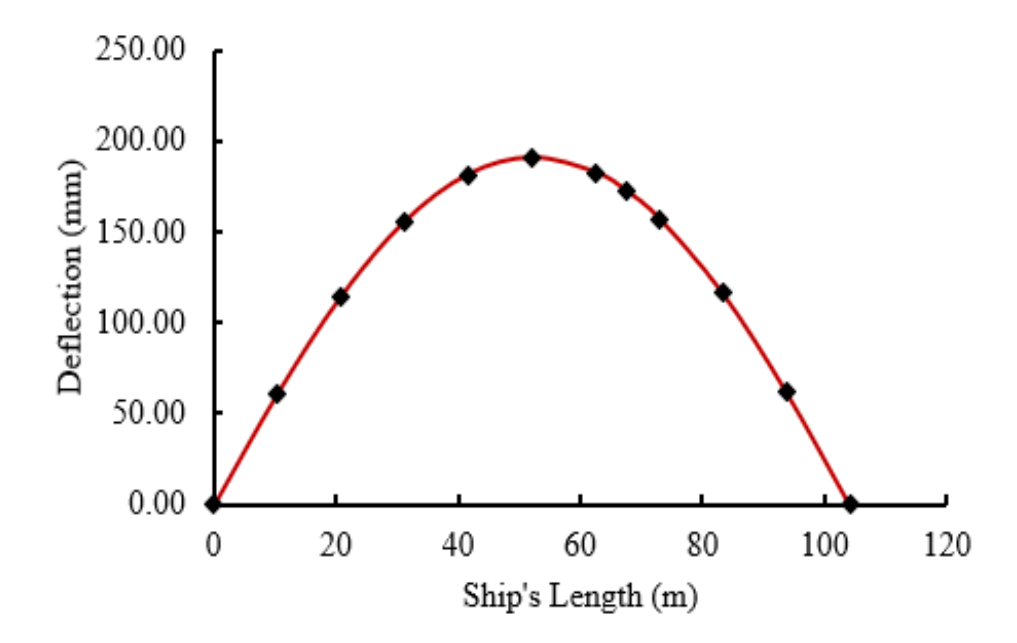


Figure 4-7: Longitudinal hull girder deflection (mm) along the ship's length (Hogging-Head Sea).

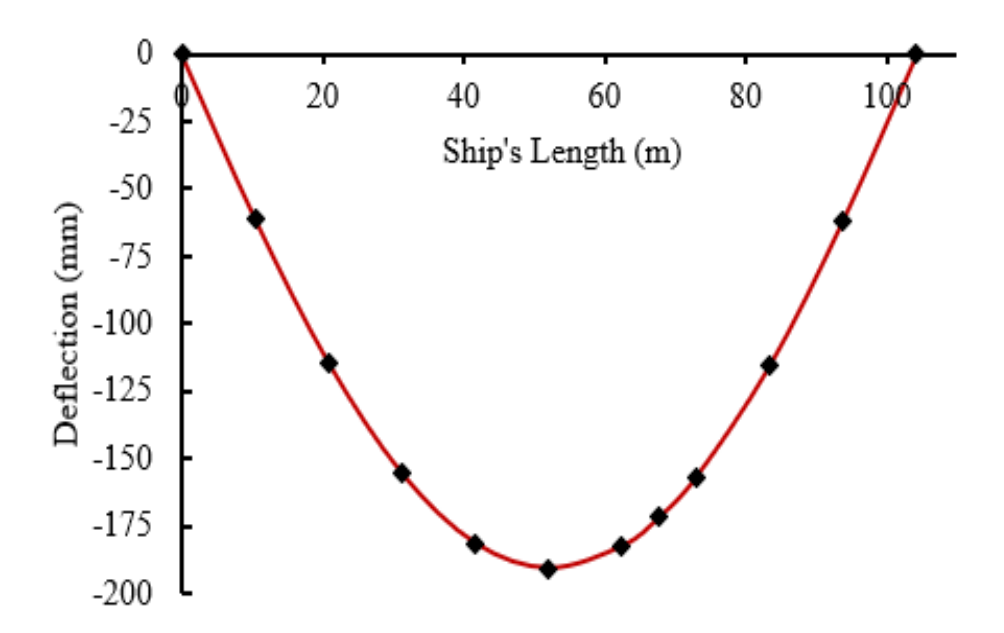


Figure 4-8: Longitudinal hull girder deflection (mm) along the ship's length (Sagging-Head Sea).

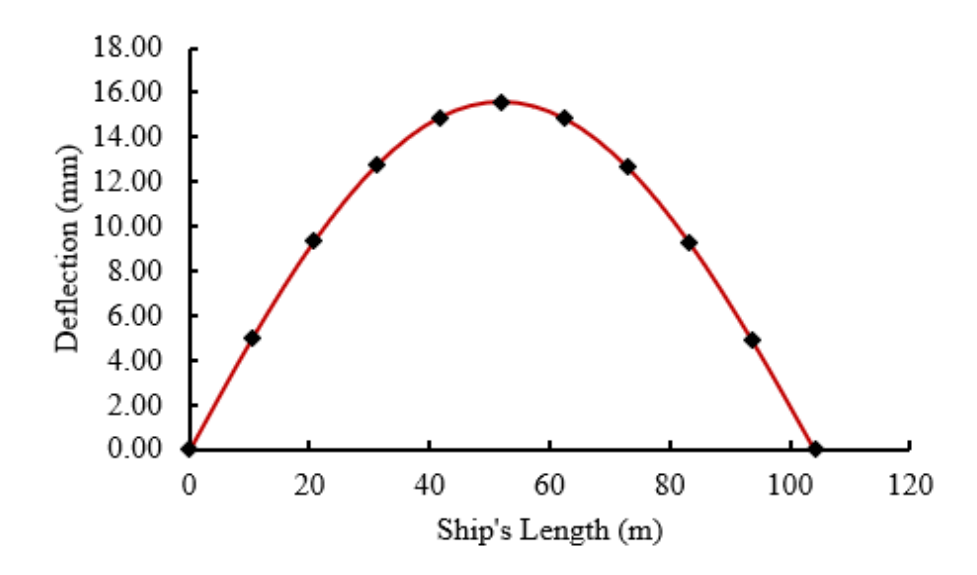


Figure 4-9: Transverse hull girder deflection (mm) along the ship's length (Beam Sea).

Figures 4–7 and 4–8, generated using data from Tables 4–3 and 4–4, show a notable resemblance in longitudinal hull girder deflection between Hogging and Sagging loading scenarios, with the peak value occurring at approximately 190 mm in the midship region. Conversely, Figure 4–9, based on data from Table 4–5, shows that the maximum transverse hull girder deflection at the midship measures approximately 16 mm.

4.6 Numerical Determination of the Ship's Hull Girder Deflection as a Simply Supported Beam

To verify the accuracy of the analytical deflection calculation, a Finite Element (FE) model of the cargo hold was utilised to determine the ship's hull girder deflection. In this analysis, the ship was treated as a simply supported beam. Subsequently, various loads were applied, including the combined still water and vertical wave bending moments under both Head Sea Hogging and Sagging conditions. The horizontal bending moment during the Beam Sea condition was also considered. To perform the analysis, the Femap software with the NX Nastran solver was employed to conduct the static analysis.

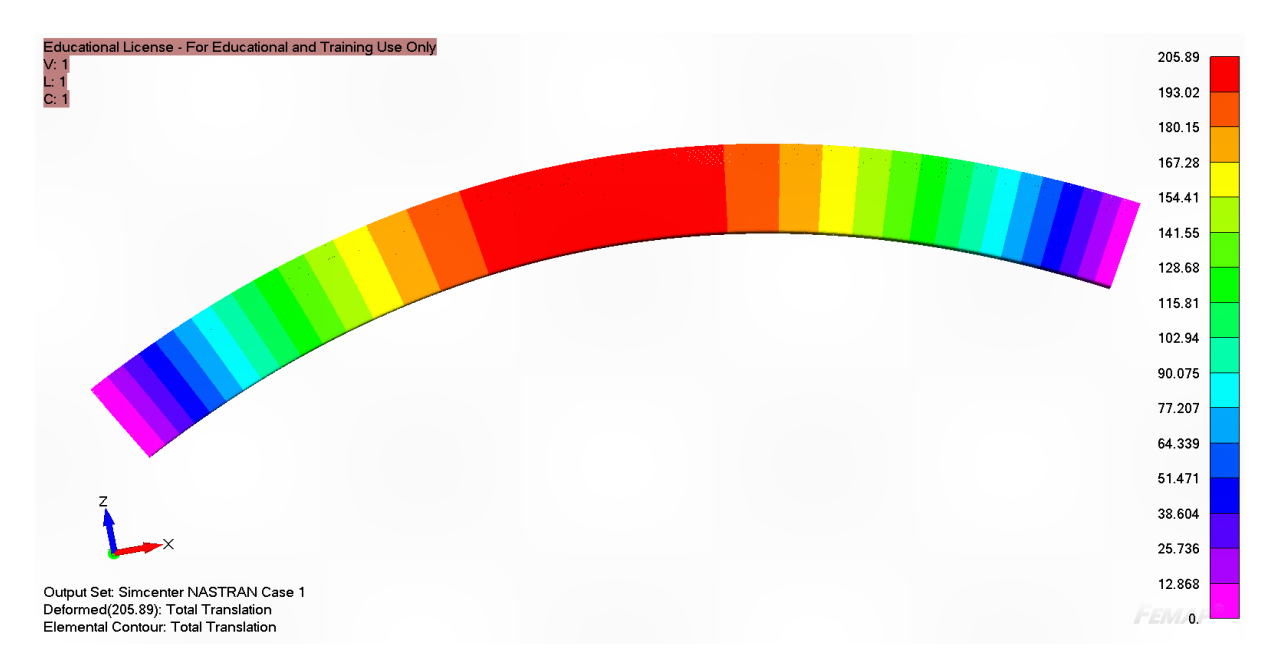


Figure 4-10: Longitudinal hull girder deflection (mm) along the ship's length (Hogging Head Sea).

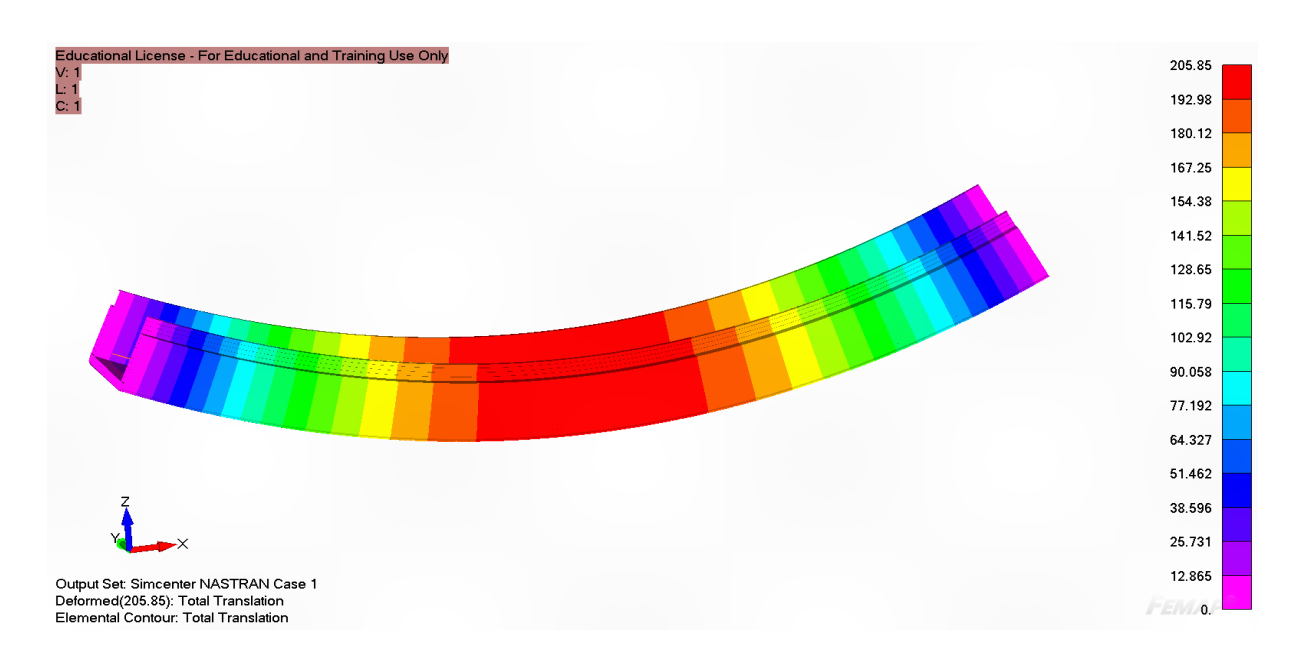


Figure 4-11: Longitudinal hull girder deflection (mm) along the ship's length (Sagging Head Sea).

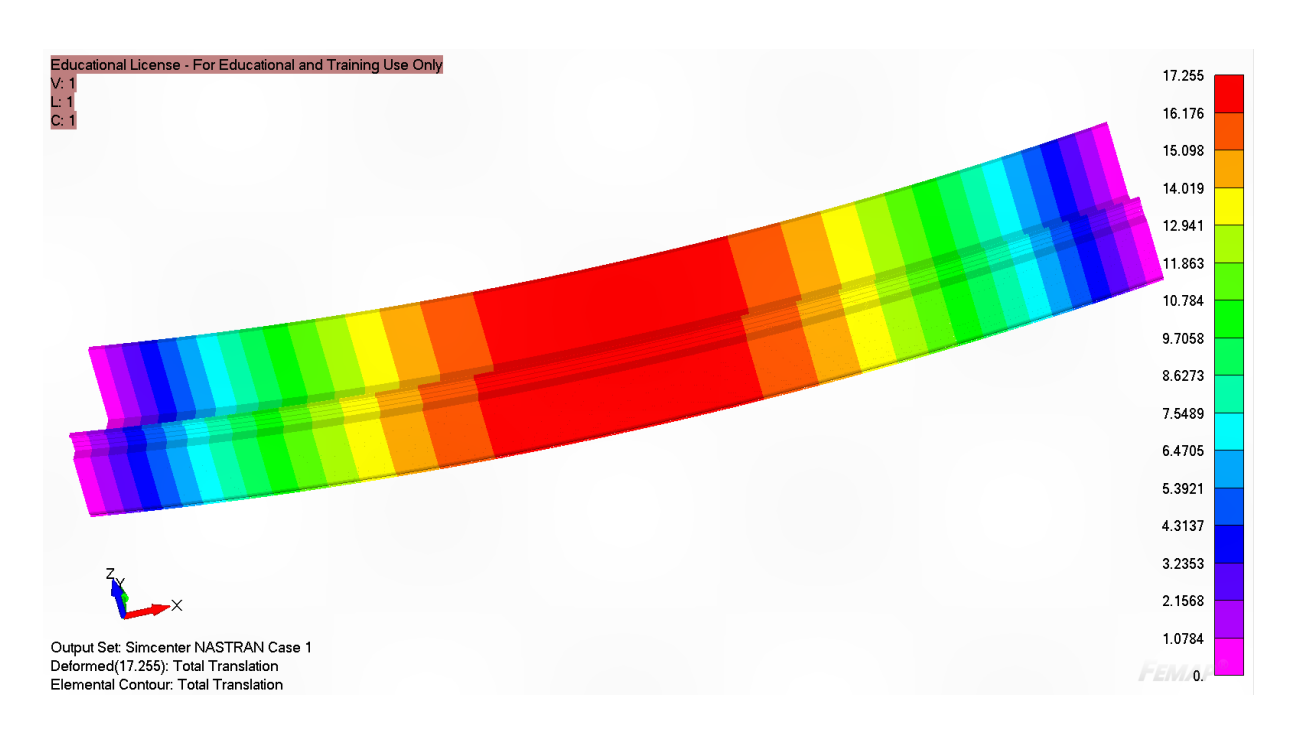


Figure 4-12: Transverse hull girder deflection (mm) along the ship's length (Beam Sea).

The results obtained for the longitudinal deflection in both Hogging and Sagging under Head Sea conditions are presented in Figures 4–10 and 4–11, respectively. Figure 4–12 displays the transverse deflection of the hull girder under Beam Sea conditions. These figures visually represent the deflection patterns under various sea conditions, making them essential for analysing ship deflections. They illustrate the hull's response, including longitudinal deflections

in hogging and sagging under head seas and transverse deflections under beam seas. By identifying potential stress points and assessing structural integrity, these insights play a crucial role in guiding effective design and safety improvements.

4.7 Mesh Sensitivity Analysis

Mesh sensitivity analysis is a technique used in numerical simulations to determine the optimal mesh size and quality for accurate results. It involves varying the mesh size and comparing the results to determine the optimal mesh size for the simulation. This technique is employed in ship modelling to investigate the effects of mesh size and quality on the accuracy of the simulation results. The analysis can help improve the accuracy of the simulation and provide insights into the behaviour of the ship model under varying conditions [156].

To address discrepancies between numerical and analytical determinations of ship hull girder deflection, a mesh sensitivity analysis was conducted to ensure accurate comparisons. The convergence curves and their respective data tables are as follows:

Table 4–6 provides a detailed comparison of the impact of different mesh sizes on the behaviour of a ship under Head Sea Hogging conditions. The table includes data on various mesh sizes used in the analysis and presents deflection data from analytical and numerical sources. Analytical deflection values represent theoretical calculations, while numerical deflection values are derived from the simulations. This table helps to directly evaluate the influence of different mesh sizes on deflection outcomes, allowing for a comparison between analytical predictions and numerical simulations. It also highlights the significance of modelling methodologies in analysing the ship's performance.

Table 4–6: Analytical and Numerical deflections data for Head Sea Hogging condition.

	Head Sea Hoggin	g
	Deflection	ons (mm)
Mesh Density	Head Sea Hogging Analytical	Head Sea Hogging Numerical
1	190.5	1
5	190.5	197.65
10	190.5	205.885
50	190.5	205.885
100	190.5	205.885
500	190.5	205.885
1000	190.5	205.885
5000	190.5	205.885
10000	190.5	205.885

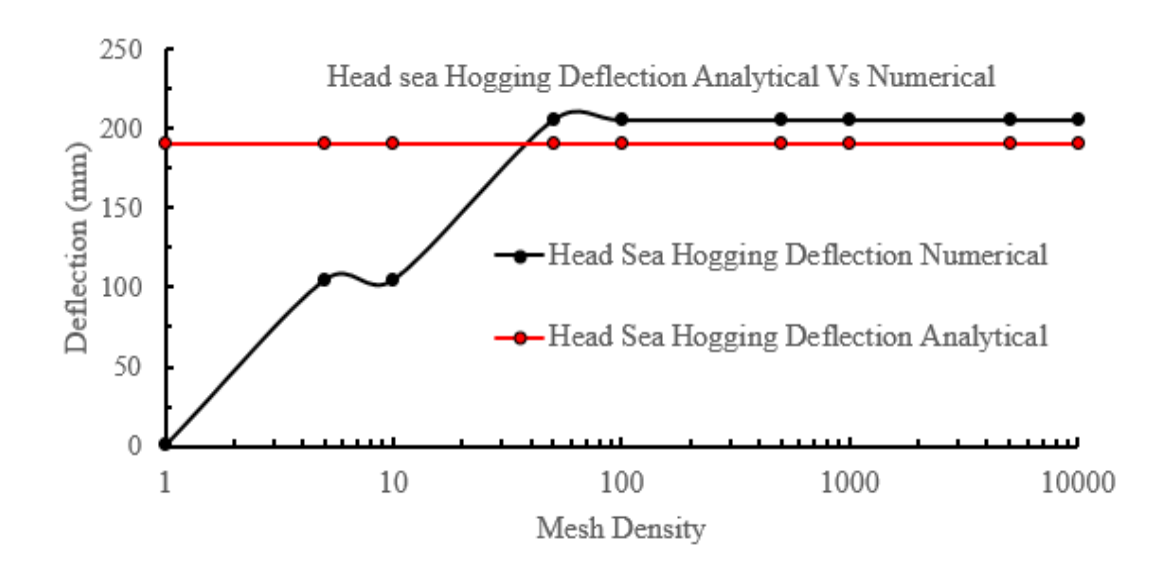


Figure 4-13: Comparison of Analytical vs. Numerical deflection (Hogging Head Sea).

Figure 4–13 presents a comparison of the analytical and numerical evaluations of the deflection of the Hull girder under the Head Sea Hogging condition. The results demonstrate that the deflection reaches a stable point at a mesh density of 100 and remains constant as the mesh density increases.

Table 4–7 presents a variety of mesh sizes used in the analysis and thoroughly investigates deflection data under Head Sea Sagging conditions from both analytical and numerical sources. It is a crucial resource for understanding the impact of different mesh sizes on deflection results

in Head Sea Sagging conditions. It enables the evaluation of the accuracy and convergence of analytical predictions versus numerical simulations.

Table 4–7: Analytical and Numerical deflections data for Head Sea Sagging condition.

	Head Sea Sagging		
	Deflection	ons (mm)	
Mesh Density	Head Sea Sagging Analytical	Head Sea Sagging Numerical	
1	190.9	1	
5	190.9	105.35	
10	190.9	105.351	
50	190.9	205.846	
100	190.9	205.846	
500	190.9	205.846	
1000	190.9	205.846	
5000	190.9	205.846	
10000	190.9	205.846	

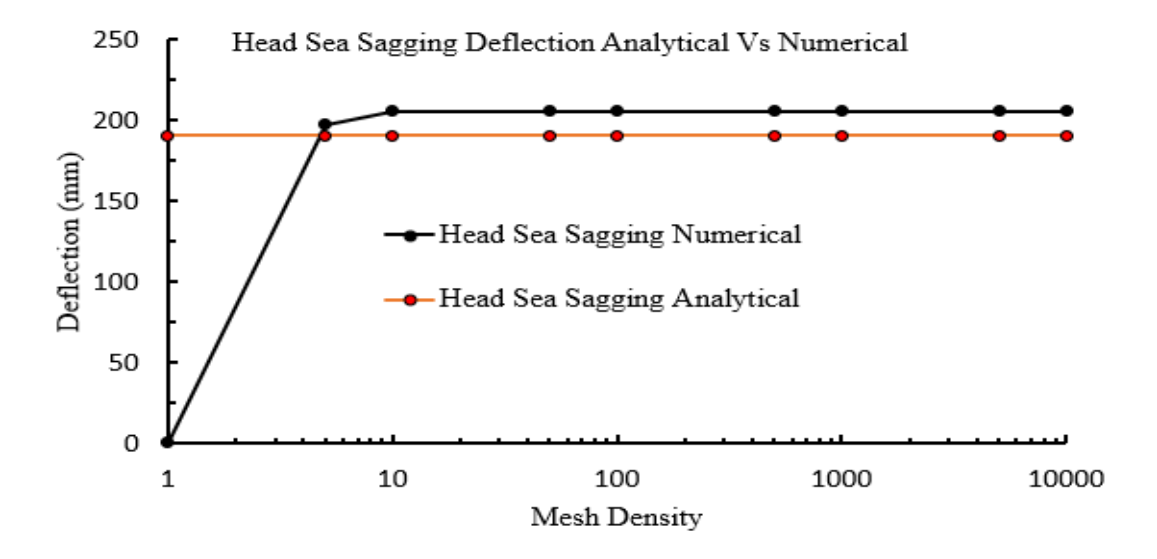


Figure 4-14: Comparison of Analytical vs. Numerical deflection (Sagging Head Sea).

In Figure 4–14, a comprehensive comparison is presented, contrasting analytical and numerical hull girder deflection responses under the challenging Head Sea Sagging condition. Notably, the findings reveal a significant trend: deflection stabilises at a mesh density of 10 and remains constant as mesh density increases.

Table 4–8 compares the Beam Sea condition's analytical and numerical deflection data across various mesh sizes. This table enables a comprehensive assessment of how different mesh sizes influence deflection outcomes under Beam Sea conditions, facilitating a comparison between analytical predictions and numerical simulations.

Table 4–8: Analytical and Numerical deflections data for Beam Sea condition.

	Beam Sea				
Mesh	Deflection	Deflections (mm)			
Density	Beam sea Analytical	Beam sea Numerical			
1	15.6	1			
5	15.6	16.56			
10	15.6	17.254			
50	15.6	17.254			
100	15.6	17.254			
500	15.6	17.254			
1000	15.6	17.254			
5000	15.6	17.254			
10000	15.6	17.254			

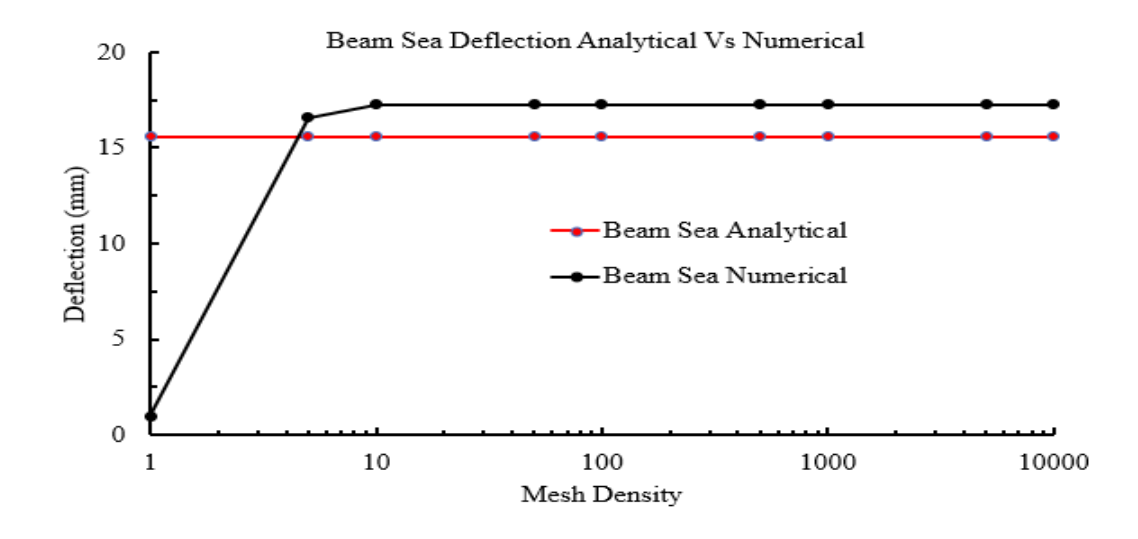


Figure 4-15: Comparison of Analytical vs. Numerical deflection (Beam Sea).

Figure 4–15 compares analytical and numerical hull girder deflection under Beam Sea conditions. The results indicate stabilisation at a mesh density of 10, remaining constant as the mesh density increases. This finding suggests an optimal balance between mesh density and computational resources for ship design and analysis.

Table 4–9 prominently presents numerical data related to deflection for various sea conditions, featuring Head Sea Hogging, Head Sea Sagging, and Beam Sea alongside their corresponding mesh size parameters. These data columns thoroughly examine the ship's deflection responses in distinct sea states and mesh resolutions.

Table 4–9: Numerical comparison of hull girder deflections in various sea conditions.

	Deflections (mm)					
Mesh Density	Head Sea Hogging Numerical	Head Sea Sagging Numerical	Beam sea Numerical			
1	1	1	1			
5	105.35	197.65	16.56			
10	105.351	205.885	17.254			
50	205.846	205.885	17.254			
100	205.846	205.885	17.254			
500	205.846	205.885	17.254			
1000	205.846	205.885	17.254			
5000	205.846	205.885	17.254			
10000	205.846	205.885	17.254			

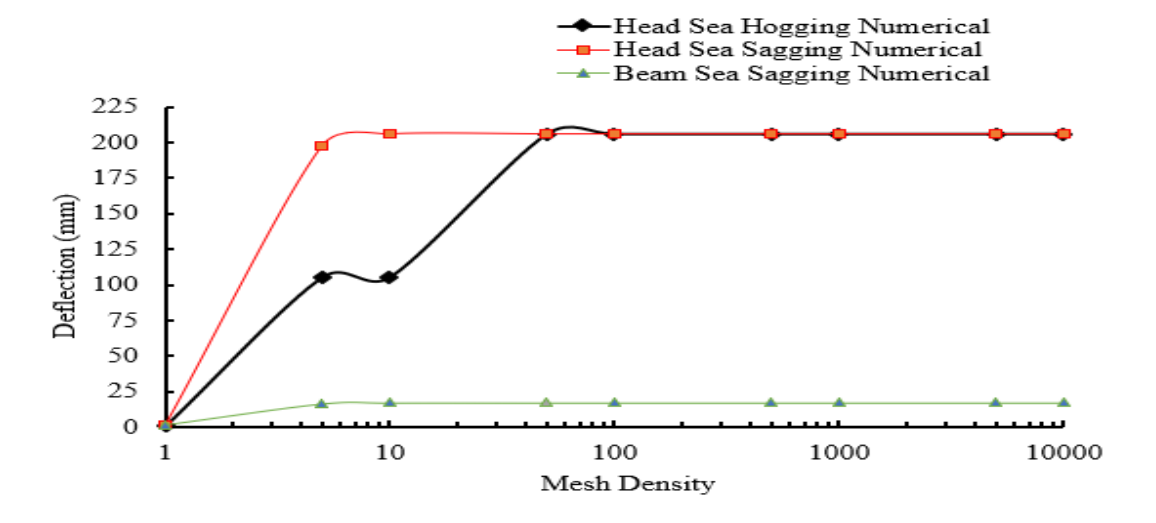


Figure 4-16: Comparison of different Numerical deflection for Head Sea Hogging, Sagging and Beam Sea conditions.

Figure 4–16 comprehensively compares the numerical hull girder deflection under Head Sea Hogging, Sagging and Beam Sea conditions. The findings reveal that the deflection stabilises at a mesh density of 100 for Head Sea conditions and 10 for Beam Sea conditions. Despite increasing the mesh density, the deflection remains constant in both cases.

4.7 Numerical Determination of the Ship's Hull Girder Deflection as a Complex Structure

This study used the cargo hold Finite Element (FE) model to calculate the hull girder deflection. The calculations involved the combined still water and vertical wave bending moments under both Head Sea Hogging and Sagging conditions and the horizontal bending moment during the Beam Sea condition. Subsequently, the ship is analysed by implementing the constraints outlined in Sec. 4.2.3 and applying all relevant loads. This analysis applies the NX Nastran solver to create a new static analysis within the Femap software.

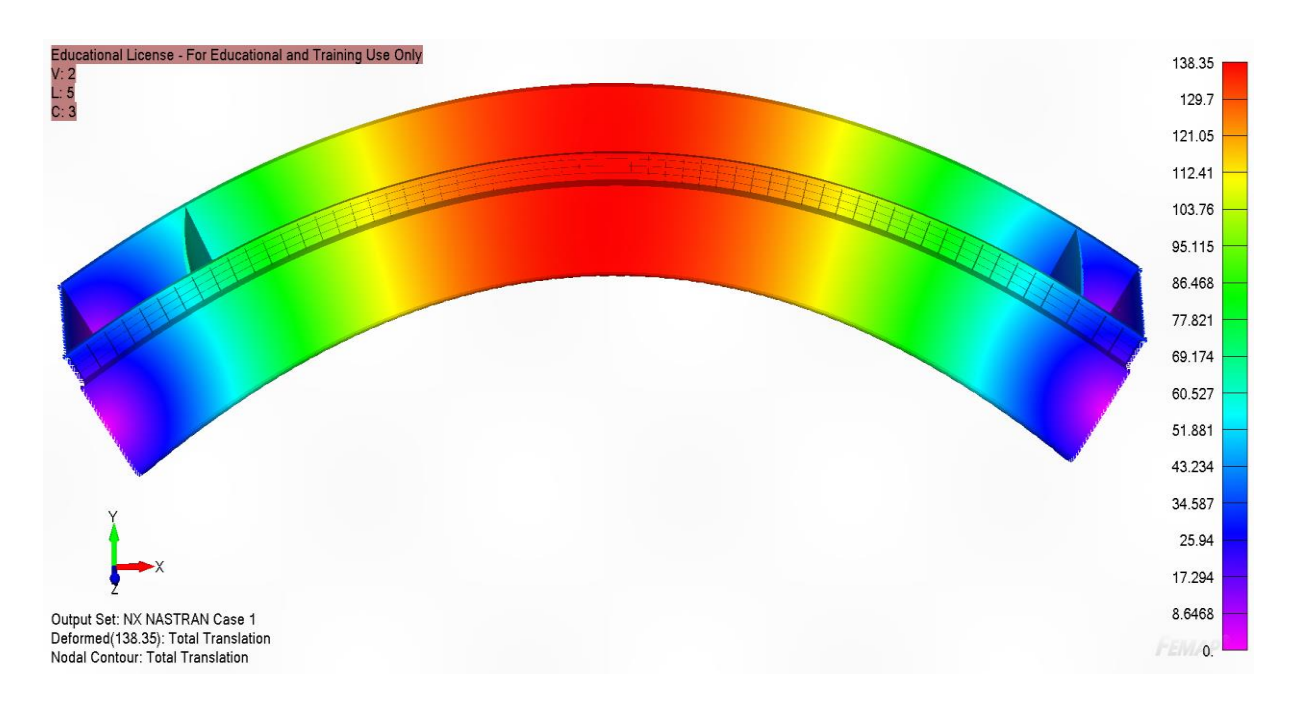


Figure 4-17: Longitudinal hull girder deflection (mm) along the ship's length (Hogging Head Sea).

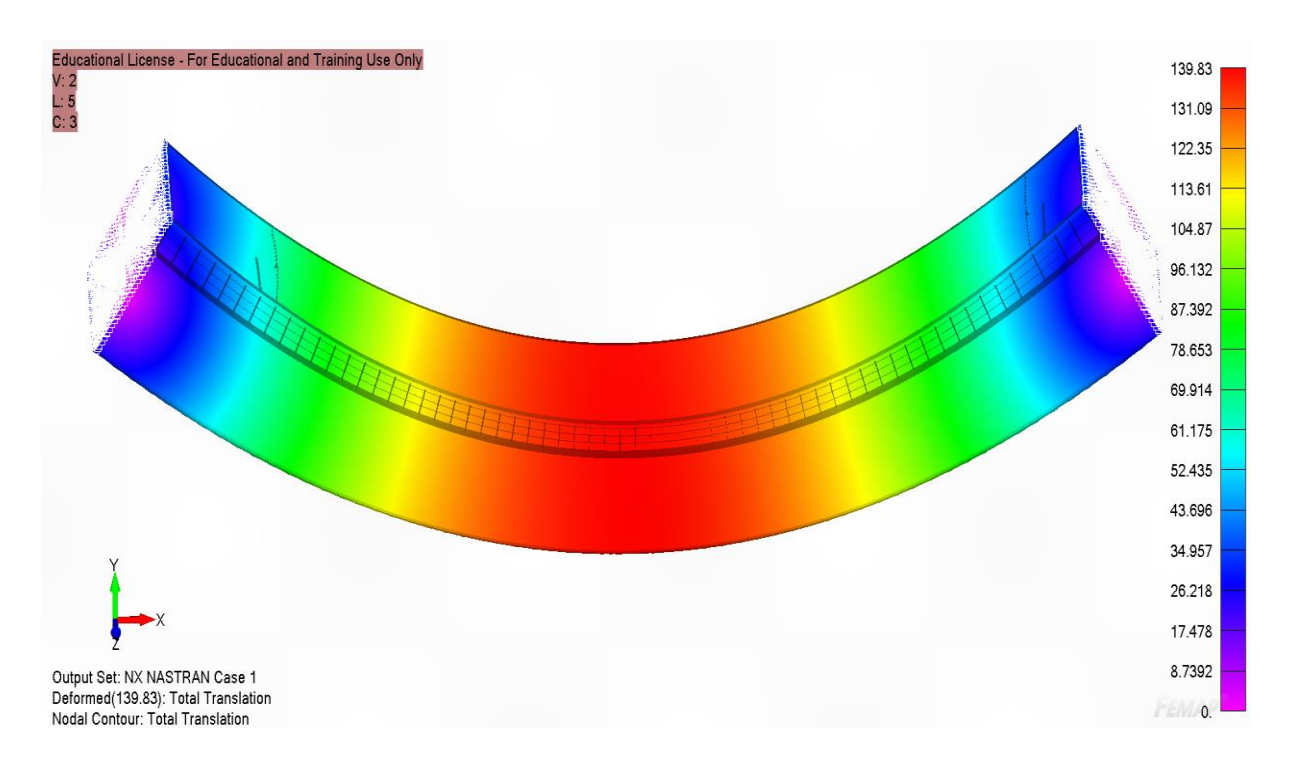


Figure 4-18: Longitudinal hull girder deflection (mm) along the ship's length (Sagging Head Sea).

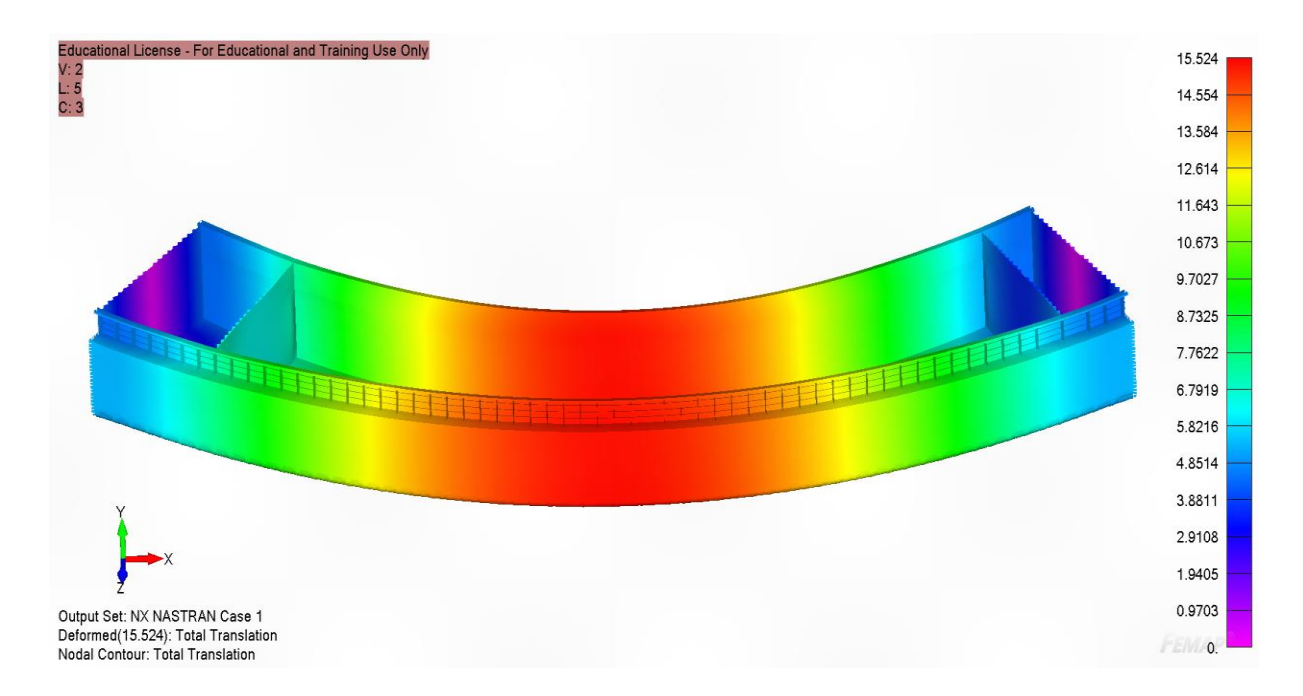


Figure 4-19: Transverse hull girder deflection (mm) along the ship's length (Beam Sea).

The resulting hull girder longitudinal deflection for Head Sea conditions (Sagging and Hogging) is presented in Figures 4–17 and 4–18, respectively, while the transverse hull girder deflection at Beam Sea is shown in Figure 4–19. In the midship region, there is a significant longitudinal hull girder deflection, as portrayed in Figures 4–17 and 4–18. During Head Sea

Sagging, the maximum deflection recorded is approximately 140 mm, while Head Sea Hogging results in a peak deflection of 138 mm. Additionally, Figure 4–19 indicates that the maximum transverse hull girder deflection midship is approximately 16 mm.

4.8 The Difference Between the Analytical and Numerical Determination of Hull Girder Deflection

The midship scantlings of the ship provided the necessary properties to calculate the analytical hull girder deflection for the entire analysed ship, treating it as a simple beam. The underlying assumption is that the ship behaves like a simply supported beam at its ends. The numerical hull girder deflection was obtained for the same conditions using the Finite Element Analysis (FEA) environment (FEMAP/NASTRAN). This analysis considered the ship to be a simple beam while considering the complex geometry of the detailed cargo hold model.

Table 4–10 presents a detailed dataset that exhibits the deflection characteristics of a ship's hull girder under different sea conditions. The table thoroughly compares the results of rigorous analytical techniques and sophisticated numerical simulations. Furthermore, the table carefully shows the differences in the deflection patterns considering the overall ship length and the intricate details of its cargo hold length. This data provides valuable insights for maritime engineers, researchers and industry professionals, assisting them to make informed decisions regarding ship design, maintenance and operational safety in various naval environments. Its inclusion highlights its significant contribution to maritime engineering and safety standards.

Table 4–10: Difference between the analytical and numerical determination of hull girder deflection.

		Hull girder deflection (mm)				
		The analysical	The englished	The numerical values		
Sr. No.	Load cases	The analytical values for the analysed ship	ues for the values for the		Detailed cargo hold model	
1	Hogging (Head Sea)	190.5	138.16	205.89	138.35	
2	Sagging (Head Sea)	190.9	138.78	205.85	139.83	
3	Beam sea	15.6	11.47	17.25	15.5	

The numerical method determines the hull girder deflection, enabling more precise results for intricate ship geometries. After reviewing Table 4–10, it is evident that the numerical deflection value in the analysis of the ship's hull girder is slightly higher than the analytical value. However, this discrepancy is within an acceptable range. Moreover, the values for hull girder deflection in both the analytical and numerical analysis of the cargo hold align, confirming the analytical study's accuracy. Therefore, the goal of this study has been accomplished.

4.9 Discussion

Euler-Bernoulli's beam theory is employed in this study to evaluate the stress and deflection resulting from vertical or lateral hull bending moments. The method assumes a consistent cross-section along the hull's length and relies on Euler-Bernoulli's beam theory.

This study has revealed a variation between the analytical and numerical deflection values when considering a ship as a supported beam. This difference is allowable according to Euler-Bernoulli's beam theory concept. However, due to the complex geometries of ship structures, the numerical determination of deflection yields more precise results. The numerical deflection calculation is used to achieve more accurate outcomes for intricate geometries.

The deflection of the hull girder is limited to 1 mm per metre of the ship's length as per International Standards [119]. Although the classification rules do not explicitly mention any restrictions on hull girder deflections, the standard opposed to excessive deflection is linked to the L/D (Length to Depth) ratio. Based on the analysis, the ship's numerical deflection exceeds the International standard value of approximately 105 mm for the analysed ship. The numerical deflection is greater because of two reasons:

- 1. The application of net scantlings affects the stiffness of the ship's structure and generates increased deflection.
- The use solely of the cargo hold model instead of considering the entire ship's model.
 This simplification can result in a less accurate depiction of the ship's actual behaviour and higher deflection values.

To address these issues, applying the gross scantlings and considering the entire ship model will undoubtedly decrease the numerical deflection, resulting in more reliable predictions.

Table 4–10 confirms the convergence of the analytical hull girder deflection value for the cargo hold model to the numerical value for the complex model. This convergence affirms the accuracy of the analytical analysis.

To ensure safe and secure transport, it is imperative to evenly distribute cargo and use robust materials, such as steel, to mitigate hull stresses like Hogging, Sagging, and Shearing and reduce hull girder deflection.

This study has developed a model aimed at optimising ship design parameters, focusing on achieving multiple objectives, such as weight reduction and production cost efficiency, and identifying critical ship structural components that significantly impact the overall strength of the ship structure. The main objective is to reduce production costs by minimising the steel used in the ship's construction while ensuring compliance with all essential safety standards. The optimisation process will be conducted to strike a balance between various design parameters and constraints, leading to an efficient and cost-effective ship design.

4.10 Conclusion

This investigation aimed to assess the longitudinal strength and deflection of a ship's hull girder. To achieve this, a 3D finite element cargo hold model was used to examine and calculate the ship's linear longitudinal strength and deflection.

To validate the findings, numerical and analytical methods were used to evaluate the strength of the hull girder. The hull girder's longitudinal deflection was estimated for both upward bending (Hogging) and downward bending (Sagging) scenarios. The ship was represented as a beam in the analytical technique, with the deflection calculated based on the bending of the hull girder. In contrast, the numerical approach applied finite element analysis to determine the hull

girder's deflection precisely. The deflection of the transverse hull girder is significant for the deflection of the hatch during open-deck ship operations. The ship undergoes transverse hull girder deflection in Beam Sea conditions, while longitudinal hull girder deflection occurs in Head Sea conditions. After analysing analytical and numerical estimations, the study confirms that longitudinal deflection is more significant than transverse deflection in the hull girder.

Calculating hull girder deflection can be time-consuming; hence, evaluating it analytically early in the ship design process is more effective. Ensuring precision and reliability requires validating analytical results with numerical results. Combining both approaches offers a comprehensive understanding of the ship's hull girder strength and deflection behaviour, enhancing its overall structural integrity and safety.

Chapter 5

Analysis of Ship Components Applying the Design of Experiments Method

5.1 Introduction

The structure of a ship is a crucial component that requires extensive research and development ahead of operation. This research ensures that the ship's structure remains strong and durable throughout its lifespan. An integrated approach that combines analytical, numerical and empirical analysis is used to create safe, affordable and ergonomic ship structures. This approach involves a methodical examination of research papers, case studies, and review articles, in combination with creative engineering applications covering various ship types and configurations [150]. Identifying fundamental structural elements within a ship is pivotal to confirming the ship's enduring structural integrity and operational lifespan, requiring a comprehensive investigation of the ship's design and construction details, essential for ship designers, builders and operators [157].

Carefully selecting influential structural components is crucial in relation to a ship's cost, strength, building expenses, performance, safety and optimisation. Designers can enhance a ship's effectiveness, cost-efficiency and security by judiciously choosing materials and optimising the placement of structural components. To reduce the weight of a structure, it is vital to strategically improve critical structural components, for instance hull designs, decks, bulkheads, floors and web frames [158]. By carefully improving their placement, designers can significantly reduce weight, leading to better fuel efficiency, lower operational costs and a smaller environmental footprint [6]. Moreover, the economic dimension of this undertaking is significant, given that optimising structural placement facilitates reasonable material selection and conformation, which, in turn, directly influence financial outlays. This alignment streamlines ship construction, saving costs and reducing the financial burden [51]. This optimisation approach also addresses the fundamental principles of resilience and safety intrinsic to a ship's structural framework. By judiciously positioning these components, the foundational robustness of the ship is strengthened, enhancing its capacity to withstand stress, fatigue and external forces. This is particularly essential for ships navigating challenging

environments or carrying heavy loads [1]. The precise optimisation of structural placements enhances labour efficiency and temporal efficacy. It decreases ship construction timelines by reducing the required work, promoting quicker progress and timely delivery. Recognising and optimising important structural components in the design of a ship contributes significantly to weight reduction, cost savings, enhanced robustness and safety, improved labour efficiency and temporal expediency. By way of these attempts at optimisation, designers develop ships that personify heightened efficiency, fiscal prudence and environmental alignment [158].

Analysing a ship's structure is significant in regard to naval architecture and maritime engineering. The primary goal is to ensure that marine structures are stable, durable and effective. This analysis requires advanced computational simulations and empirical testing in conjunction with theoretical models to understand how ships respond to various loads and weather conditions. By considering factors such as material properties, geometry and dynamic forces, ship structural analysis dramatically improves the safety and efficiency of marine transportation [2]. Ship structural analysis methods evaluate the performance and integrity of marine ships [159]. Finite Element Analysis (FEA) is a technique that accurately calculates stress and strain on a ship's structure under varying loads and situations by breaking it into smaller elements [160]. When designing and building ships, Classification Societies have strict rules and specifications to meet safety and operational criteria. Nonetheless, ship structural analysis encounters various challenges such as accounting for uncertainties in material properties and environmental factors and accurately replicating complex real-world conditions like wave-induced and dynamic loads. To improve ship safety, longevity and performance, it is essential to constantly strive for more accurate computer models, incorporate sensor data for real-time structural health monitoring and balance structural robustness with cost-effectiveness [2].

This method helps identify which factors significantly impact the response variable and how they interact with each other. When replicating a full factorial design becomes impractical or unfeasible, researchers turn to a statistical experimental technique termed fractional factorial design. These designs are effective in various contexts, such as pilot studies and screening tests where efficiency and precision are essential [161].

The reason for using the fractional factorial design method to determine the essential structural components of a ship is due to its ability to identify the key factors that effectively influence the ship's behaviour and performance. By conducting fractional factorial design experiments,

researchers can systematically manipulate various structural elements, known as factors, within the ship and observe corresponding changes in the response variable, such as speed, stability and fuel efficiency. This method helps identify influential factors while minimising the need for excessive experimentation [162]. When analysing ships, using the fractional factorial design method can assist researchers in identifying the key structural elements that determine a ship's characteristics. This approach allows for this finding without needing to test every possible combination, saving time, resources and costs compared to the more extensive, complete factorial design approach [161]. Using the fractional factorial design method, information can be gained to direct future studies, improvements, or adaptations to a ship's design. This can result in a better performance or effectively meeting specific requirements. Therefore, utilising the fractional factorial approach in analysing ship structures can be a strategic framework that improves the efficiency of the research process and promotes developments in maritime engineering [162].

In their study, Vizzari et al. (2020) recommended using fractional factorial designs for efficient trial creation and evaluation, particularly in developing semi-transparent layers for solar road applications. This method systematically explores the impacts of multiple factors on layer performance while minimising the required trials by means of reduced factor combinations [163]. Natoli (2018) explored the practical implications of fractional factorial designs in engineering research, focusing on their application in analysing the optical and mechanical traits of a semi-transparent layer used in solar roadways. The author emphasised the importance of selecting an appropriate fractional factorial design based on factors, levels and the required resolution using main effects plots, interaction plots and regression models [164]. Hester and Usher (2017) highlighted the effectiveness of fractional factorial designs in experimental planning, particularly in resource-constrained situations or when multiple factors are involved. By employing fractional factorial methods, researchers can gain valuable knowledge leading to further studies, system improvements or enhanced overall performance [165]. Pamnani et al. (2017) conducted a study using a design of experiments (DOE) approach, utilising response surface methodology, to optimise the welding parameters. Their primary objective was to enhance the penetration depth achievable in a single pass during gas tungsten arc welding (GTAW). This optimisation aimed to improve the quality and efficiency of the welding process, specifically for naval-grade steel applications [166]. Kuo and Wu (2009) presented an innovative method for an experimental design by integrating fractional factorial and full factorial experiments. This approach was effectively implemented in designing a

containership's hatch corner, underlining its capability to identify the global optimum with fewer trials compared to conventional techniques. The research also compared the proposed methodology and the Taguchi Technique, explaining its superiority in prioritising design parameters and providing greater awareness for designers. The results indicate that this novel approach presents a compelling and efficient optimisation method through the design of experiments, with promising applicability in addressing multi-objective challenges [167]. Gorshy et al. (2009) proposed a novel ship optimisation approach employing multi-disciplinary design optimisation (MDO), integrating response surface methodology (RSM) and particle swarm optimisation (PSO) to minimise the daily running costs of fully loaded ships. This approach incorporates the design of experiments (DOE) to sample influential inputs. Despite computational expenses, results from a case study demonstrate the approach's potential to enhance ship design and performance, addressing the computational challenges of integrating DOE [168]. Allen et al. (2009) observed that fractional factorial designs facilitate the organisation and evaluation of experiments aimed at identifying significant variables. This approach enables efficient analysis of how distinct factors influence the outcome variable and reduces the required number of tests by focusing on a smaller range of factor combinations. The strategies utilised in designing and analysing fractional factorial experiments can serve as a beneficial guide for conducting and interpreting study results [169]. Hawkins and Lye (2006) examined the utilisation of the Design of Experiments (DOE) methodology to explore the factors impacting tension in marine risers for FPSO (Floating Production Storage and Offloading) vessels. Their study stresses the importance of incorporating design parameters and environmental factors in the analysis of riser tension. The results emphasise the efficacy of the DOE method in clarifying the intricate relationships among the variables influencing riser tension in FPSO applications, offering valuable insights for both research endeavours and practical engineering applications [170].

The factorial design represents a significant experimental technique used throughout diverse fields such as agriculture, pharmaceutical research and engineering. This method can potentially optimise manufacturing processes, enhance product quality and reduce engineering costs. A fundamental advantage lies in its capacity to yield a greater volume of data at comparable or even reduced costs compared to conventional research approaches. Furthermore, factorial design facilitates the study of multiple variables without increasing expenses [161]. Despite the criticality of comprehending ship structures, the utilisation of this methodology still needs to be improved among researchers. To address this gap, the present study employs a

fractional factorial design approach to discern the fundamental structural components within ships that significantly influence their overall structural integrity. This statement improves ship construction, presenting significant implications. Given the limited investigation of this domain by others, this finding is a unique and compelling contribution to the field.

5.2 Development of the Models

5.2.1 Overview

When applying the Design of Experiments (DOE) technique to evaluate the strength of ship structures, carefully choosing the structural factors and their corresponding levels is essential. This selection process includes considering critical features, for example, the thickness of crucial components:

- Keel Plate
- Bottom Plate
- Side Shell Plate
- Shear Strake Plate
- Inner Side Shell Plate
- Hatch Coaming Plate
- Main Deck Plate
- Hatch Coaming Top Plate
- Inner Bottom Plate
- Double Bottom Longitudinal Girder, CL (Centre Line)

Additionally, the spacing of:

- Web Frame
- Stiffener

This approach focuses on two levels of detail, recognising the significant impact structural components have on the overall integrity of ship structures. The fractional factorial design

method is a practical and systematic approach that increases understanding of ship engineering and is the foundation for empirical research in ship structure analysis.

Table 5–1 provides the lower and upper limits of ship structural factor variables. These variables will be meticulously analysed using the fractional factorial design framework to determine the most significant factors.

Table 5–1: Variables Ranges.

Sr. No.	Variables	Values in mm
1	Keel plate thickness	(8.5, 14.5)
2	Bottom plate thickness	(7.5, 12.5)
3	Side shell plate thickness	(6.5, 11.5)
4	Shear strake plate thickness	(8.5, 13.5)
5	Inner side shell plate thickness	(7.5, 13.5)
6	Inner bottom plate thickness	(9.0, 14.5)
7	Hatch coaming plate thickness	(10.0, 16.0)
8	Main deck plate thickness	(11.5, 15.5)
9	Hatch coaming top plate thickness	(17.0, 23.0)
10	Double Bottom Longitudinal Girder, CL	(7.0, 11.0)
11	Web frame spacing	(1430, 2145)
12	Stiffener spacing	(631, 700)

5.2.2 Significance of the Parameters

The selection and optimisation of various structural parameters significantly impact a ship's resilience and production costs. In this context, the chosen thicknesses of critical components have a crucial role to play in determining the ship's ability to withstand stress and environmental conditions while also affecting the overall production costs [22]. The identified structural parameters include:

- 1. **Bottom Plate**: The thickness of the ship's bottom plate affects its ability to withstand grounding and obstacles, contributing to its resilience against external impacts [12].
- 2. **Side Shell Plate**: The ship's ability to endure lateral stresses from waves and collisions is crucial to maintaining the overall structural integrity. This ability is affected by the thickness of side shell plates [12].

- 3. **Shear Strake Plate**: The thickness of the topmost strake affects the ship's ability to withstand waves and navigate different sea conditions smoothly [12].
- 4. **Inner Side Shell Plate**: The thickness of the ship's inner shell plates contributes to its longitudinal strength, stability and resilience against torsional forces [12].
- 5. **Hatch Coaming Plate**: The thickness of the hatch coaming plates is crucial to maintaining the structural integrity of cargo access points, ensuring durability and preventing potential cargo handling issues [171].
- 6. **Main Deck Plate**: The thickness of the main deck plate affects the ship's capacity to transport cargo and resist external loads from equipment and machinery [171].
- 7. **Hatch Coaming Top Plate**: The thickness of the top plate on the hatch coaming impacts the ship's ability to secure and protect cargo during transportation, ensuring resilience against impacts and external forces [171].
- 8. **Inner Bottom Plate**: The thickness of the inner bottom plates affects the ship's strength, as it impacts load and pressure distribution [12].
- 9. **Keel Plate**: The thickness of the keel plate is crucial to maintaining the ship's structural integrity along the keel line, enhancing its ability to tolerate vertical stresses [12].
- 10. **Double bottom longitudinal girder (CL)**: The longitudinal girder CL comprises an integral component of the double bottom structure, playing a crucial role in ensuring the structural integrity and crashworthiness of the ship. It contributes to the ship's longitudinal strength and assists in mitigating upward pressure and bending stresses [2].

Apart from thicknesses, the spacing of the following elements is also essential:

- 1. **Web Frame**: The spacing between web frames affects the ship's structural integrity, rigidity and ability to resist bending and torsional stresses [172].
- Stiffener: The correct spacing of stiffeners on the ship is essential for distributing loads, preventing stress concentrations and improving overall resilience against deformation [172].

Optimising the ship's structural parameters is a complex task that involves balancing resilience, operational needs and production costs. The selected configurations directly affect the ship's ability to navigate challenging maritime conditions while maintaining economic viability [17].

5.2.3 Boundary Values

To meet the Bureau Veritas (BV) classification requirements, the maximum and minimum values of specific structural parameters depend on several factors, such as the type of ship, its size, together with the spacing of its stiffeners. BV and other respected classification bodies have established regulations and standards that govern these parameters, tailored to the ship's intended use, operational zone and other relevant factors. Adhering to these guidelines is crucial to ensure that ships meet safety standards and are fit for their intended purpose.

Following established shipbuilding practices and expert advice, it is recommended to maintain a minimum plate thickness of at least 5 mm as a precautionary measure to prevent distortion and warping during welding. In most cases, there is no upper limit in relation to plate thickness, but high-grade plates are frequently used to avoid excessive thickness. Maintaining a minimum plate thickness ensures structural integrity while balancing weight considerations.

The variable ranges of the twelve (12) factors for the analysed ship were carefully selected. This approach ensures the study aligns with classification requirements, promoting a comprehensive evaluation of the ship's structural integrity. Considering several factors and their potential interactions, the analysis provides a valuable understanding of the ship's performance and durability, helping shipbuilders and operators make informed decisions throughout the design and construction process.

5.2.4 Design Matrix Construction

A preliminary model was established to assess the ship's longitudinal hull girder strength and overall performance for a multi-purpose cargo ship equipped with three cargo holds. This model sets the foundation for future developments, integrating twelve structural parameters that impact ship resilience and production costs. Careful consideration was given to establishing these parameters' upper and lower limits to meet the strict requirements associated with BV classification standards. Employing Minitab software's fractional factorial design methodology, a comprehensive design matrix includes 128 combinations of the identified twelve parameters.

This matrix effectively captures the complex relationships and cumulative consequences of parameters on a system that covers all aspects. This process generates 128 combinations by defining parameter ranges for twelve variables in two distinct levels, spanning the designated parameter spectrum. After the matrix is set up, Minitab's strong statistical abilities become prominent, allowing for a detailed analysis of each parameter's impact on the system's response variables. This method systematically explores essential configurations, enabling a total evaluation of the main effects and intricate interactions. The software has user-friendly visual aids and analytical tools that simplify complex data, making it easier for users to make informed decisions based on empirical data. Minitab's dependable computational algorithms guarantee precise execution of the fractional factorial design, resulting in reliable outcomes that help optimise processes, products and overarching systems.

5.2.5 Parameter Modification and New Model Generation

To comprehensively investigate the significance of specific design factors, a thorough selection process identified the twelve parameters exerting the most significant influence. These parameters were systematically modified across all 128 models comprising the design matrix. Through these deliberate adjustments, a novel combination of 128 models emerged, each characterised by a distinct configuration of parameter values, resulting in various designs. This systematic approach enables a detailed examination of how each design part affects the outcome. It allows a holistic assessment of their collective effects on the overall performance and behaviour of the system under study. This research aims to build a solid foundation so as to understand the complex interplay between design parameters and their implications for practical engineering applications by creating an extensive set of models.

5.3 Integrated Structural and Stress Analysis Methods

In this study, 128 design permutations are thoroughly analysed to determine the Von Mises and torsional stress in a cantilever beam model that represents a ship subjected to bending and torsional loads. The technique involves altering the base model's twelve key parameters to create the 128 new models submitted for stress analysis. The objective is to investigate the factors that influence torsional and Von Mises stress the most. By examining a wide range of design permutations, this study aims to provide comprehensive insights into the structural behaviour of ships under bending and torsional loads.

When assessing the structural integrity of a ship, it is imperative to consider both Von Mises stress and warping stress as critical factors. Von Mises stress is a pivotal measure that predicts material yielding under intricate loading scenarios derived from combining individual stresses within the material. In ship design, Finite Element Analysis (FEA) is frequently employed to ascertain Von Mises stress across diverse sections of the ship's structure, such as the hull girder. This analysis is fundamental in verifying the material's capability to endure anticipated operational loads [173]. Conversely, warping stress pertains to the twisting or warping tendencies exhibited by the ship's structure under varying loading conditions [174]. Detailed understanding and analysis of these stresses are imperative for evaluating the structural robustness of the ship and safeguarding its operational safety.

5.3.1 Von Mises Stress Analysis

A detailed investigation into Von Mises stress analysis was undertaken, entailing the generation and examination of 128 models. Each model underwent rigorous stress analysis, incorporating precisely defined boundary conditions (refer to Table 3–23) and exposure to bending moments (as explained in Table 3–25). To accurately emulate the structural behaviour of the ship under scrutiny, the model was simulated as a cantilever beam. In contrast to the conventional approach of modelling ships as supported beams, the selection of the cantilever beam configuration in this study was deliberate, with the intention of ensuring conservative results. This decision was in accordance with the primary objective of optimising the ship's structural design. Notably, the sagging condition, particularly in head sea conditions, emerged as the most critical scenario in this study (refer to Table 3–25 and Figure 3–42); therefore, sagging is considered for all analyses.

The cantilever beam analogy facilitates the determination of Von Mises stresses at critical junctures within the structure. These stresses are a cornerstone in forecasting the structure's flexural behaviour and strain distribution under bending loads. By means of the comprehensive assessment of these stresses, significant information about the structural integrity and performance of the ship can be obtained, thereby facilitating the refinement and optimisation of its design.

5.3.2 Warping Stress Analysis

A rigorous torsional stress examination was conducted in analysing each of the 128 models, similar to Von Mises stress analysis. Torsional moments were applied to each model sourced from the BV Mars 2000 software's torsional analysis module.

Torsional stress analysis is paramount in evaluating the structural integrity of the ship's components under twisting forces. It provides a greater understanding of how the structure reacts to torsional loads, essential for ensuring the robustness of the ship's design.

A comprehensive dataset was compiled after completing Von Mises stress and torsional stress analyses across all 128 models. This dataset encompasses stress values and warping stress values for various combinations of parameters. The collected stress data will be analysed using Minitab software, employing factorial design techniques. The primary objective of this analysis is to identify the most influential factors impacting both Von Mises and torsional stress. Given that the principal focus of this study revolves around optimising the ship's structural design, the regression equation (refer to Appendix B) obtained from the analysis of Von Mises stress will be used to optimise the ship's weight reduction strategies. This systematic approach to data analysis and optimisation procedures demonstrates the commitment to enhancing the structural efficiency and performance of the ship, contributing to its operational effectiveness and safety.

5.4 Evaluating the Production Costs

The ship's production costs are estimated using weights obtained from Finite Element models in FEMAP software. Employing a top-down strategy, production costs are based on comprehensive parameters, including the hull weight, block coefficient and ship's length. This method implements empirical, statistical and close-form equations derived from extensive ship data. A thorough cost-benefit analysis is conducted to maintain economic feasibility and ensure adherence to quality benchmarks by incorporating engineering simulation, cost estimation and data analytics by way of the top-down approach.

The cost calculations are performed using an Excel spreadsheet that compiles and analyses weight data obtained from FEMAP models. This tool is instrumental in calculating the production costs for the base and 128 models within the design matrix. Weight data for each model, sourced from FEMAP, is inputted to calculate the costs associated with a range of factors. These costs are then categorised and totalled to estimate the overall cost for each model.

The production costs of the analysed ship were assessed using empirical formulas [175] within Microsoft Excel. Various factors were considered, for instance the cost of steel plates and preparing the work. The cutting, transport, forming, assembly and welding costs were also taken into account. Data related to these costs were collected from several shipyards in Bangladesh, including Ananda Shipyard and Slipways Limited, Three Angle Marine Limited, Western Marine Shipyard Limited, Radiant Shipyard Limited and Karnafully Shipyard Limited. Ananda Shipyard and Slipways Limited were the reference points for comparison on account of their involvement in constructing the analysed ship. The applicability of the production costs within the context of Europe and other regions of the world acknowledges the potential variations in cost structures and regulatory frameworks.

The production cost data for 128 models were calculated and analysed by way of Minitab software using regression analysis. This analysis aims to identify the most influential factors related to production costs. The regression equation (refer to Appendix B) obtained from the study will be employed in the optimisation procedure to minimise ship production costs.

5.5 Design of Experiments (DOE)

Design of Experiments (DOE) is a structured method applied across various domains, such as engineering, manufacturing, and scientific research, to conduct experiments systematically. It entails carefully planning experimental setups to ensure reliable and valid results while optimising resource utilisation. By controlling sources of variation, DOE enables researchers to understand the relationship between input factors and output responses. Statistical methods used in DOE aid in process optimisation, quality improvement and cost reduction. Additionally, DOE is crucial for identifying significant factors and their interactions, contributing to the development of robust and efficient systems [176].

DOE aims to optimise the model by selecting the optimal elements and levels. Project teams can apply different values to important model factors to acquire more model information. The DOE results provide maximum information with minimal resources. Depending on how factor levels affect DOE outcomes, variables can be categorised to identify which affect the average, both average and variability or have no effect on the quality attributes of DOE. DOE experiments may yield [177]:

1. Identification of critical variables affecting the outcome (s) of the DOE.

- 2. Establishment of factor(s) levels for important components optimising the intended result.
- 3. Selection of the optimal or most cost-effective configurations for insignificant elements.
- 4. Validation (confirmation) of responses and incorporation into production or design.

5.5.1 Factorial Designs

The factorial design is a powerful research method that allows for the simultaneous examination of multiple independent variables or dimensions. This unique capability enables researchers to uncover both the main effects and complex interactions. A complete factorial experiment includes every combination of factor levels. This versatile investigative approach is regularly applied in various fields, including nursing research, clinical trials, animal experimentation, as well as research into mechanical properties [178]. In the manufacturing industry, it is commonly accepted that experimental designs, particularly full and fractional factorial designs are frequently utilised at both 2 and 3 levels [161]. In studies concerning mechanical properties, factorial design is frequently utilised to assess the significance of various factors and comprehend their interactions [179].

The number of experiments *N* necessary for a thorough factorial design examination is provided as [180]:

$$N = L^F (5-1)$$

where the number of levels is L and the number of factors is F.

Consequently, the Finite Element Method (FEM) model requires a lot of computations. But, by using fractional factorial designs, it is possible to reduce the workload. These designs only include some combinations of elements. Plackett and Burman's screening plans evaluate only a subset of combinations. For primary analyses, the Plackett/Burman methodology is sufficient. However, full and fractional factorial designs are necessary to investigate interaction factors [181].

5.5.2 Plackett/Burman Design

The Plackett-Burman design (PBD) is an effective screening technique to identify significant elements from many variables influencing a given process [182]. This research focused on twelve variables, including primary and secondary structural members and overall structural strength, which were analysed, highlighting key factors for detailed investigation.

The growing fascination with Plackett-Burman designs with run sizes that differ from the powers of the two indicates a shift towards more flexible and customisable experimental designs. Traditionally, the run size in experimental designs was limited to being a power of 2, but recent developments have allowed for greater flexibility in choosing the run size, such as multiples of 4 or other arbitrary values [183].

The two-level factorial design pioneered by Plackett and Burman has found application in analysing diverse medium elements and environmental conditions. At its core, the first-order model forms the foundation of the Plackett-Burman framework:

$$Y = \beta_0 + \sum \beta_i X_i \tag{5-2}$$

where Y is the predicted response, β_0 is the model intercept, β_i is the linear coefficient and X_i is the level of an independent variable. In the scope of this current research, a comprehensive investigation encompassing twenty distinct experimental designs, each featuring twelve assigned variables, was conducted. The assessment of the significance of these factors centred on the criterion that their confidence intervals attain a threshold of 90% or higher [184].

Run	Block	A	В	C	D	E	F	G	Н	J	K	L	M
1	1	-	-	+	+	ı	+	+	-	-	_	-	+
2	1	+	+	ı	-	+	+	ı	+	+	_	-	-
3	1	+	-	ı	+	+	-	+	+	-	_	-	-
4	1	-	+	+	+	+	_	ı	+	+	-	+	+
5	1	+	_	-	_	-	+	ı	+	_	+	+	+
6	1	+	_	+	+	-	_	-	_	+	_	+	_
7	1	_	+	-	+	-	+	+	+	+	_	_	+
8	1	+	+	ı	-	ı	_	+	-	+	-	+	+
9	1	+	+	-	+	+	_	ı	_	_	+	_	+
10	1	_	_	-	_	+	_	+	_	+	+	+	+
11	1	+	+	+	-	ı	+	+	-	+	+	-	-
12	1	-	+	+	-	ı	-	ı	+	-	+	-	+
13	1	-	_	ı	-	ı	_	ı	-	-	-	_	
14	1	-	_	ı	+	ı	+	ı	+	+	+	+	
15	1	-	+	+	-	+	+	ı	-	-	-	+	
16	1	+	+	+	+	ı	_	+	+	-	+	+	
17	1	+	_	+	_	+	+	+	+	_	_	+	+
18	1	_	_	+	_	+	_	+	+	+	+	_	_
19	1	+	_	+	+	+	+	-	_	+	+	_	+
20	1	_	+	_	+	+	+	+	_	_	+	+	_

Figure 5-1: Plackett and Burman's Screening Scheme for Investigating Twelve (12) Factors.

Figure 5–1 shows the Plackett and Burman screening approach to investigate twelve factors through twenty experimental runs. These factors are evaluated at two levels: higher (+) and lower (–). The primary goal of this method is to identify and measure the effects of each factor on the target parameter. Interaction effects could occur if more than one element is changed. Full or fractional factorial designs can be used further to research the impact of interactions between specific factors.

Pareto Chart of the Standardised Effects (Response is Von Mises Stress, $\alpha = 0.05$) Term Factor Name н Keel Plate Α В Bottom Plate C Side Shell Plate D D Shear Strake Plate G Ε Inner Bottom Plate Inner Side Shell Plate Main Deck Plate R Hatch Coaming Plate Hatch Coaming Top Plate м DB Longitudinal Girder, CL Web Frame Spacing Stiffener Spacing L c

Figure 5-2: Plackett-Burman Screening Plan for Identifying Main Effects of Stress on Ship Hull.

10

The Pareto chart shows bars and a line graph, with individual factors represented by the bars in descending order of importance, while the line shows the cumulative total. Utilising a thorough screening process, Figure 5–2 portrays how hull girder stress significantly impacts the strength of the ship's hull structure. The outcomes of this comprehensive analysis are briefly presented in a Pareto diagram, emphasising the key findings. This diagram shows the most critical factors, including:

- Hatch Coaming plate
- Hatch Coaming Top plate
- Shear Strake plate
- Main Deck plate
- Inner Side Shell plate

All converge precisely at 2.36 on the reference line, underlining their substantial impact on the examined models. It is important to mention that these variables have undergone rigorous validation, adhere to established standards, and achieve a confidence level of 95%. The precise crafting of the models, encompassing all critical factors seamlessly, emphasises the precision and intricacy of their construction, underscoring the pivotal role of these factors in determining

the observed outcomes. Furthermore, these factors undergo extensive evaluation using a fractional factorial design on two levels, enabling interaction between the components.

5.5.3 Fraction Factorial Designs

Researchers can use fractional factorial design techniques to investigate direct and desired interaction effects with fewer trials. These designs are consistently applied and demonstrate effectiveness in analysing multiple factors. This approach scrutinises all potential combinations of components within each trial or replication. Factorial plans are advantageous when dealing with numerous factors. In every experimental trial or replication, all conceivable combinations of factor levels are evaluated. For instance, if factor *A* has "*a*" levels and factor *B* has "*b*" levels, each replicate includes "*ab*" combinations. Factorial designs effectively reveal factor interactions and prevent erroneous conclusions. However, as the number of variables increases, the potential combinations in factorial designs grow exponentially. In contrast, fractional factorial designs replicate a subset of these points, estimating the main effects and low-order interactions with diminished computational demands compared to full factorial methods [185].

Fractional factorial studies employ established design principles to reduce the size of an experiment while minimising the loss of essential information by not examining all levels of variables. These experiments provide informed assessments of the results of ad hoc strategies to reduce the experiment's size. This knowledge-based decision on the ultimate configuration of the investigation forms the scientific basis for selecting fractional factorial designs over other options to reduce the size of the experiment [180].

5.5.3.1 Identification of Influential Factors and Interactions Affecting Ship Hull Girder Stress

The variation in thickness across critical components is essential in ship stress analysis. Several different elements, including the Keel plate, Bottom plate, Side Shell plate, Shear Strake plate, Inner Side Shell plate, Hatch Coaming plate, Main Deck plate, Hatch Coaming Top plate, Inner Bottom plate and Double Bottom Longitudinal Girder (CL), impact the structural reaction of the ship. The stress distribution inside the ship's structure is also strongly influenced by the spacing of critical components like web frames and stiffeners. The combination of these parameters shapes the ship's overall structural robustness and safety. The key variables that

have a discernible impact on stress patterns have been identified using a systematic fractional factorial design investigation.

A comprehensive study was conducted on the dataset to ascertain the Von Mises stresses from applying bending moments to a dataset with 128 models. These Von Mises stresses underwent an exhaustive analysis using the Minitab statistical program to determine the factors that significantly impact their behaviour. This study contributes to understanding the Von Mises stress patterns in ship structures. It underlines the essential elements and their interactions that affect stress distribution throughout the ship.

Table 5–2 presents a detailed overview of the regression model's key performance metrics in this research.

Table 5–2: Model Summary (Hull Girder Stress).

S	R-squared	R-squared (adj)	R-squared (pred)
2.24154	99.66%	99.17%	97.94%

- **Standard Error** (**S**): The model's average error is around 2.24 units, indicating consistent and accurate predictions with minimal deviation.
- R-squared (R²): The model can account for 99.66% of the observed variability in Von Mises stress. This high R-squared value signifies the model's exceptional ability to explain the variation in Von Mises stress.
- Adjusted R-squared: The model's adjusted R-squared value remains strong at 99.17% despite its complexity. This value demonstrates the model's resilience in providing relevant explanations, as the included independent variables are significantly influential in elucidating Von Mises stress.
- Predicted R-squared: The model's predicted R-squared value of 97.94% specifies its potential to predict approximately 97.94% of Von Mises stress variations for new data points. This value indicates that the model has solid predictive capabilities.

This thorough analysis confirms the regression model's efficacy in explaining and predicting Von Mises stress. Its robust fit, minimal error and solid predictive capacity make it a reliable tool for this research.

5.5.3.1.1 Pareto Chart

The Pareto chart is vital as regards assessing the magnitude of the standardised effects within a study. This graphical representation allows researchers to pinpoint the significant main effects and interactions, revealing instances where specific factors wield considerable influence over the response variable. By employing bars to represent these effects, the chart effectively distinguishes statistically substantial effects that surpass or equal the reference line, providing researchers with a clear visual indication of their significance.

Likewise, the vertical arrangement of bars on the Pareto Chart, organised in descending order of magnitude, presents a brief overview of the standardised effect values for individual factors and interactions. The length of each bar directly correlates with the effect's relative strength, facilitating the identification of the most influential factors within the studied framework. Consequently, factors associated with longer bars emerge as critical determinants, stressing their pronounced impact on the response variable and guiding further consideration of their underlying mechanisms. The Pareto chart is a vital analytical instrument that enriches researchers' understanding of the intricate relationships inherent in empirical inquiries and informs strategic decision-making processes [186].

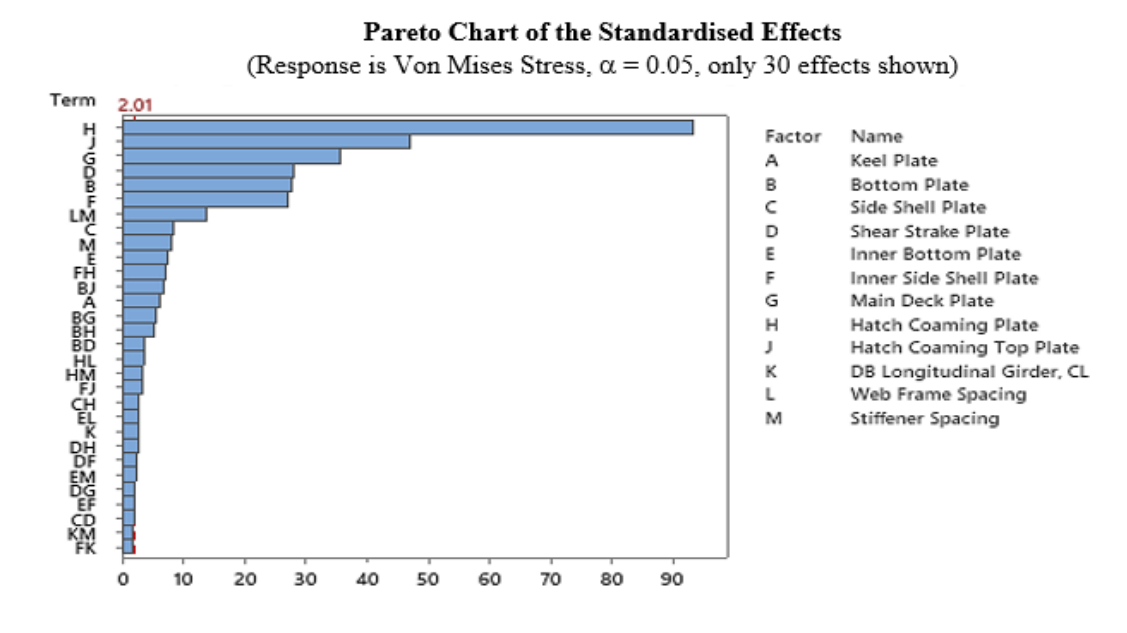


Figure 5–3: Standardisation Effects on Stress Response: Pareto Chart Analysis.

In Figure 5–3, several key factors intersect the reference line at a value of 2.01. These factors include both the main effects and interactions, which substantially influence the terms of the model. These factors intersect with the reference line, signifying they are essential within the

research framework and are crucial in determining the observed outcomes. This graphical representation highlights the essential features of the analysis and guides further exploration into the intricate dynamics underlying the observed phenomena.

The study has identified the top five factors that significantly impact ship stress.

- Hatch Coaming plate
- Hatch Coaming Top plate
- Main Deck plate
- Shear Strake plate
- Bottom plate

This study carefully investigates various factors that influence the Von Mises Stress associated with ship structures, both individually and collectively. By analysing the empirical data and practical implications, this research provides significant information pertaining to the importance of these factors. These insights are beneficial for ship designers and builders to improve the structural integrity of ships. Equally, the main effects of these factors significantly impact the model's outcomes.

In addition to the top five factors, this research emphasises the importance of the interaction between the Web Frame and Stiffener spacing in influencing the Von Mises stress. The statistical significance of these interactions provides vital knowledge concerning the complex relationships within the model terms, enriching the understanding of the underlying phenomena and their implications within the maritime domain.

Furthermore, the significant main effects shown in Figure 5–3 closely match those identified in the screening plan presented in Figure 5–2. This comparison underlines the usefulness of screening plans as crucial tools for conducting preliminary assessments, further strengthening their relevance in facilitating effective assessments within ship structural analysis.

5.5.3.1.2 Residual Plots

The residual plot is an effective tool in statistical analysis that helps to visualise the differences between the observed data points and the predicted values of a model. It does this by displaying the residuals, the differences between the observed and predicted values, compared to the predictor variables or fitted values. Examining the residual plot allows a statistical model's

assumptions and identifies patterns, trends, or heteroscedasticity in the residuals to be evaluated. This information guides the iterative model refinement process, generating a more robust and reliable statistical analysis. Additionally, the residual plot helps detect outliers, influential data points, or nonlinear relationships, allowing for informed decisions in model development and interpretation. Overall, the residual plot is an essential diagnostic tool for assessing the validity of model assumptions and ensuring the accuracy of statistical analyses [187].

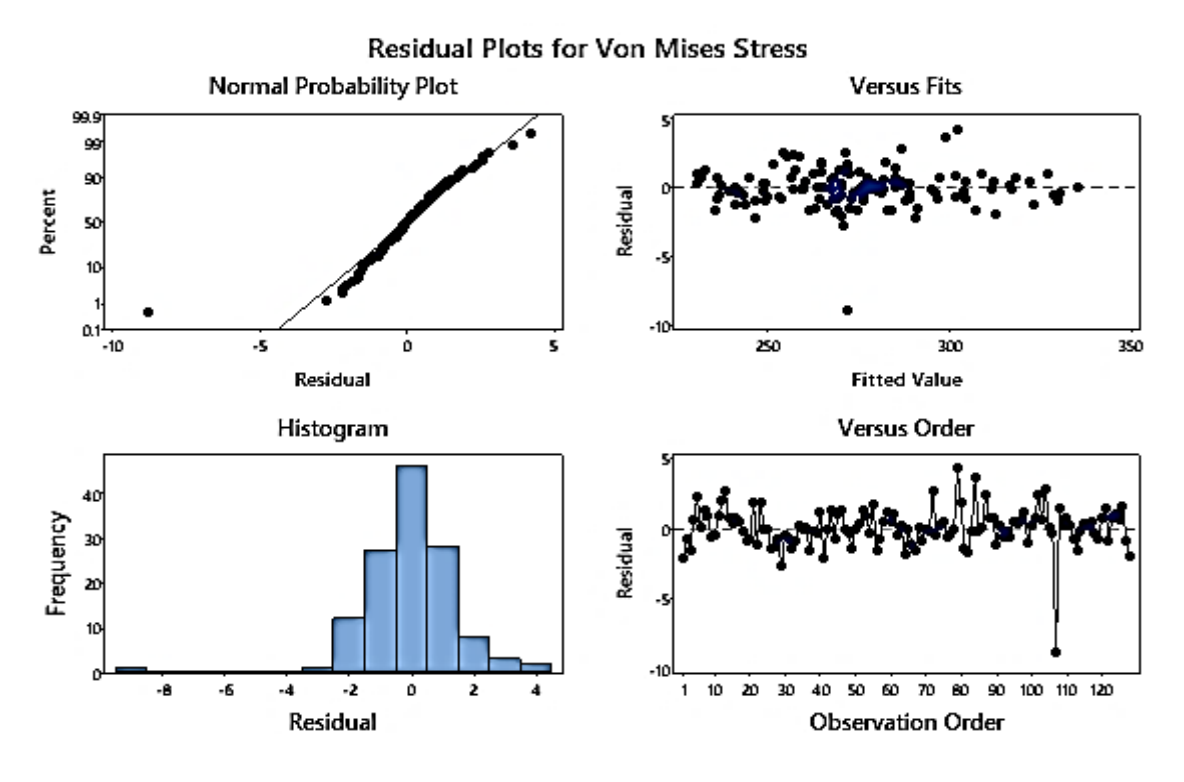


Figure 5–4: Residual Plots for Von Mises Stress Analysis.

Figure 5–4 shows a fundamental understanding of the normalcy assumption via the normal probability plot of the residuals. The plot proves the validity of the normality assumption, as the residuals closely adhere to a linear pattern. However, for a comprehensive examination of the distribution characteristics and potential deviations from normality, a histogram is employed to show the frequency distribution of residual values. The histogram reveals a noticeable skewness to the left or right in this figure, implying a departure from the normal distribution. Nevertheless, despite an extreme outlier on the left side, it remains within an acceptable range.

To evaluate the linearity assumption, the residuals versus fits plot is used. In Figure 5–4, this plot demonstrates that the residuals exhibit a scattered distribution around the horizontal reference line (zero), indicating the validity of the linearity assumption.

Conversely, the residuals versus order plot supports detecting any discernible patterns or trends within the residuals based on their order or sequence of observation. As shown in Figure 5–4, the residuals versus order plot shows that the residuals are randomly dispersed around the horizontal reference line, which is typically indicative of a zero residual value. This comprehensive analysis validates the assumptions underlying the statistical model.

5.5.3.2 Identification of Influential Factors and Interactions Affecting Warping Stress

Understanding the factors and interactions that affect warping stress is essential in ship stress analysis. Several critical components influence the warping stress in a ship's structure, including the Keel plate, Bottom plate, side shell plate, shear strake plate, inner side shell plate, Hatch Coaming plate, Main Deck plate, Hatch Coaming Top plate, Inner Bottom plate, besides the Double Bottom Longitudinal Girder plate. The spacing of web frames and stiffeners also plays a significant role in the distribution of torsional stress. These complex parameters combine to shape the structural integrity and safety of the ship against torsional forces. Using a fractional factorial design, it is possible to identify the key variables and their interactions that impact warping stress patterns.

A study was conducted on 128 models to understand torsional stress in ship structures. The study applied torsional moments to create warping stresses, which were subsequently analysed using Minitab software to identify the key factors impacting warping stress. The investigation identifies the critical factors and their interactions significantly influencing warping stress patterns. This detailed examination not only helps acquire an understanding of the complexities inherent in ship torsional stress analysis but also contributes to developing strategies for optimising structural design and ensuring vessel safety and longevity.

Table 5–3 presents the key metrics used to assess the efficacy of regression models in analysing warping stress within this study.

Table 5–3: Model Summary (Warping Stress).

S	R-squared	R-squared (adj)	R-squared (pred)
1.52334	99.25%	98.17%	95.45%

- **Standard Error (S):** The model consistently yields highly accurate predictions with minimal error, maintaining an average prediction error of approximately 1.52 units.
- **R-squared** (**R**²): An impressive R-squared value of 99.25% underscores the model's exceptional capacity to explain roughly 99.25% of the variance in warping stress. This metric reveals the model's efficacy in clarifying this critical parameter.
- Adjusted R-squared: Despite the complexity of the model, the adjusted R-squared score remains influential at 98.17%. This value underscores the significance of the incorporated independent variables in capturing warping stress and strengthens the model's ability to provide meaningful justifications.
- Predicted R-squared: The model is predicted to capture approximately 95.45% of warping stress variations in novel data instances, as indicated by the estimated R-squared value of 95.45%. This attribute enhances the model's potential as a reliable tool for predictive analysis.

This study highlights the importance of regression models in warping stress analysis, characterised by high concordance, minimal error margins and robust predictive capabilities, thereby affirming their reliability in enhancing the understanding of the phenomena associated with warping stress.

5.5.3.2.1 Pareto Chart

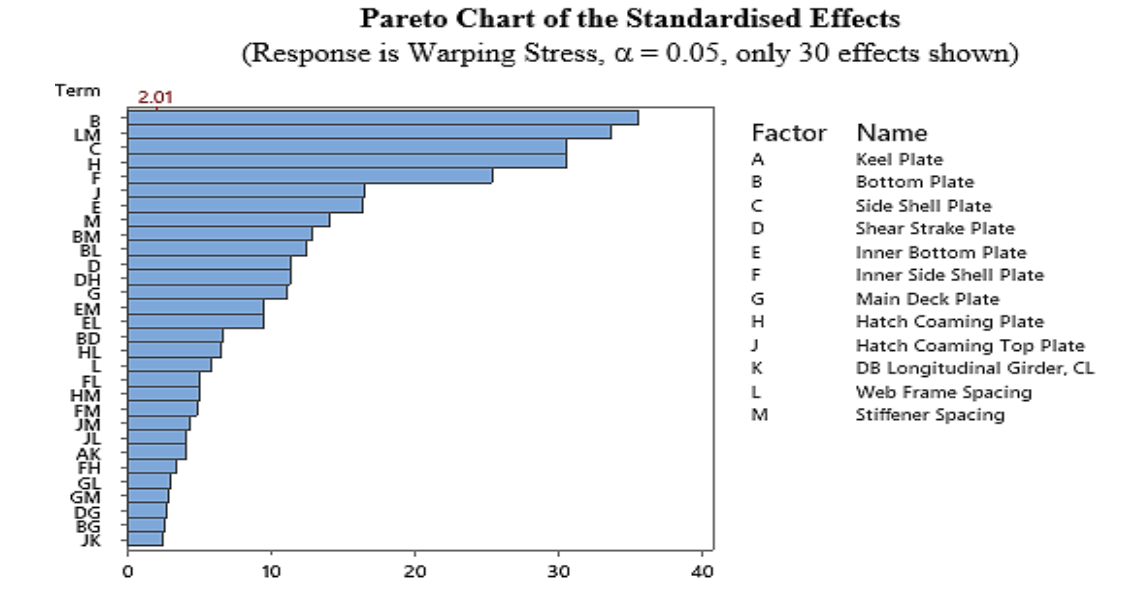


Figure 5–5: Standardisation Effects on Torsional Stress Response: Pareto Chart Analysis.

Figure 5–5 confirms that several key factors intersect with the reference line at a value of 2.01, indicating their importance in the model's terms. These factors include the main effects and interactions significantly influencing the model's dynamics. Moreover, Figure 5–5 acts as a clear reference point that visually highlights the significant factors and their functions in the research framework.

The study has identified six main factors that significantly impact the warping stress of a ship. These factors are:

- Bottom plate
- Side Shell plate
- Hatch Coaming plate
- Inner Side Shell Plate
- Hatch Coaming Top plate
- Inner Bottom Plate

The study has individually and collectively examined these factors to assess their influence on the structural integrity of a ship. Through empirical data analysis and practical implications, this research has provided crucial information about these factors' central role in defining warping stress dynamics. These findings are advantageous for ship designers and builders, providing actionable knowledge to enhance the robustness of ship structures.

Furthermore, this study has explored the intricate relationship between Web Frame and Stiffener spacing, highlighting its profound influence on warping stress. The study has established that the interaction effects between these variables surpassed the significance of the main effects observed for the Side Shell Plate, Hatch Coaming Plate, Inner Side Shell Plate and Hatch Coaming Top Plate. This underlines the complex nature of ship warping stress and emphasises the need for a comprehensive understanding of its contributing factors to optimise structural design and performance.

5.5.3.2.2 Residual Plots

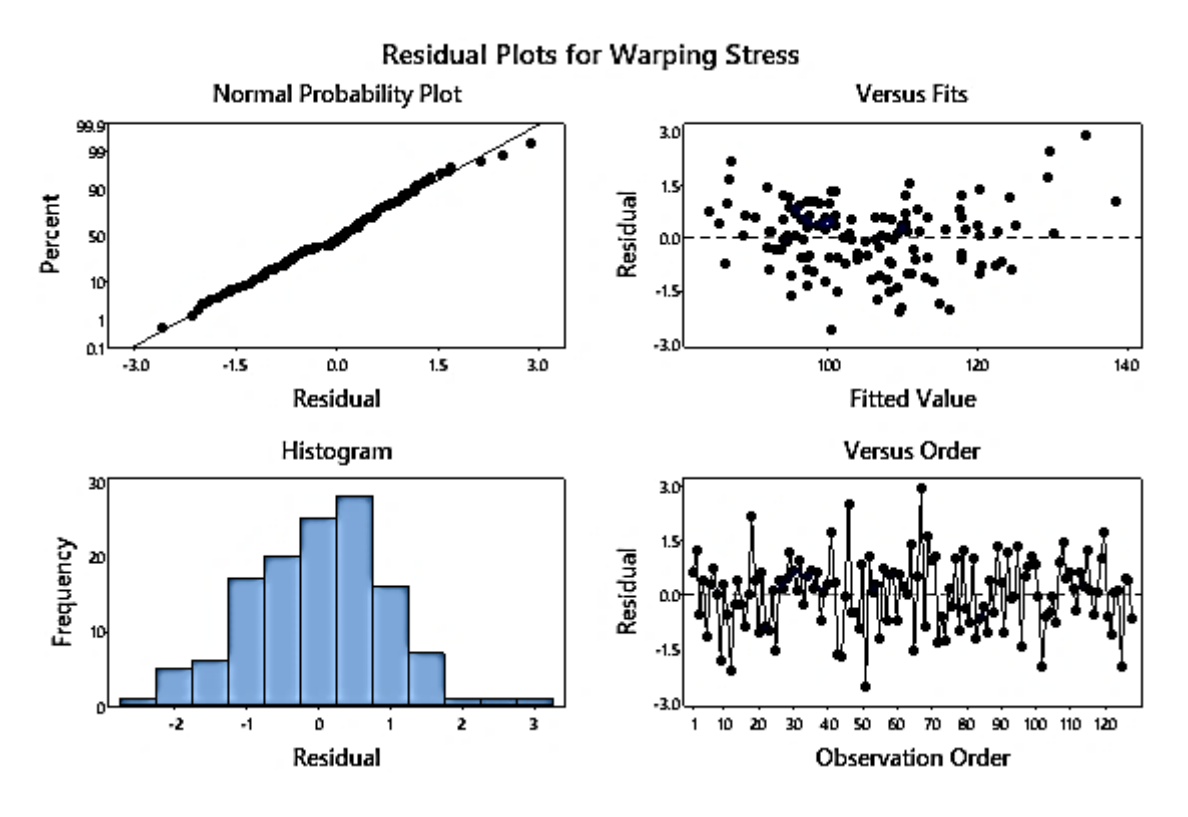


Figure 5–6: Residuals Plot for Warping Stress Analysis.

The warping stress residual plot is comprehensively described in Figure 5–6, offering important information regarding its distribution and connection with specific parameters. The figure comprises four essential components:

- 1. **Normal Probability Plot:** This plot indicates the distribution of stress residuals compared to the expected normal distribution. In Figure 5–6, the normal plot displays a linear pattern validating the normality assumption for the residuals.
- 2. **Histogram:** The histogram demonstrates the frequency distribution of torsional stress residuals within predetermined ranges, promoting an understanding of their concentration and spread. In this figure, the histogram suggests a skewness in the residuals but also identifies an acceptable outlier on the left side.
- 3. **Versus Fit:** This component reveals how torsional stress residuals differ with specific parameters. Versus File explores variations across different file instances, indicating in Figure 5–6, the residuals' linear dispersion around zero.
- 4. **Versus Order:** Conversely, Versus Order examines changes in residuals concerning the order of data points, revealing random arrangements around zero in Figure 5–6.

In brief, Figure 5–6 effectively presents the warping stress residual plot. It confirms the normality assumptions and demonstrates the distribution and parameter-based variations of the residuals.

5.5.3.3 Identification of Influential Factors and Interactions Affecting Production Costs

A ship's production costs are paramount regarding ship design and construction and are intricately linked to the dimensions and specifications of its various components, such as plate thickness and structural element spacing. Various factors contribute to shipbuilding production costs, encompassing the thickness of the bottom plate, side shell plate, shear strake plate, inner side shell plate, hatch coaming plate, main deck plate, hatch coaming top plate, inner bottom plate, keel plate, and hatch coaming stay plate. The spacing between structural elements, including web frames and stiffeners, also impacts costs. Understanding these intricate correlations among components is essential with regard to assessing the economic feasibility and effectiveness of ship construction. Rigorous fractional factorial design methods assist with identifying significant variables and their interactions that impact production costs, leading to a better understanding of the financial aspects of ship design and construction.

Minitab software has rigorously assessed and analysed one hundred twenty-eight (128) model production costs. This comprehensive analysis has yielded significant results, clarifying influential factors in relation to production costs, ship design and construction efficiency.

Table 5–4 displays key metrics for evaluating the effectiveness of the regression model used to analyse the production costs of ships in this study.

Table 5–4: Model Summary (Production Costs).

S	R-squared	R-squared (adj)	R-squared (pred)
1518.24	100.00%	99.99%	99.97%

- Standard Error (S): The model consistently produces highly accurate predictions with a low value of 1518.24 units, demonstrating precise estimations with minimal error on average.
- R-squared (R²): The regression model's excellent fit is confirmed by the high 100.00%
 R-squared value, indicating a practical explanation of about 100.00% of production costs variance in the dataset.
- Adjusted R-squared: Despite the model's complexity, the adjusted R-squared value remains high at 99.99%, denoting the effectiveness of the independent variables in explaining the dependent variable.
- Predicted R-squared: A predicted R-squared value of 99.97% suggests that the model will perform well on new data, strengthening its predictive capability.

The regression model's effectiveness in ship production costs analysis is strengthened by its strong fit, minimal error and robust predictive potential, emphasising its reliability in predicting production costs in the shipbuilding industry.

5.5.3.3.1 Pareto Chart

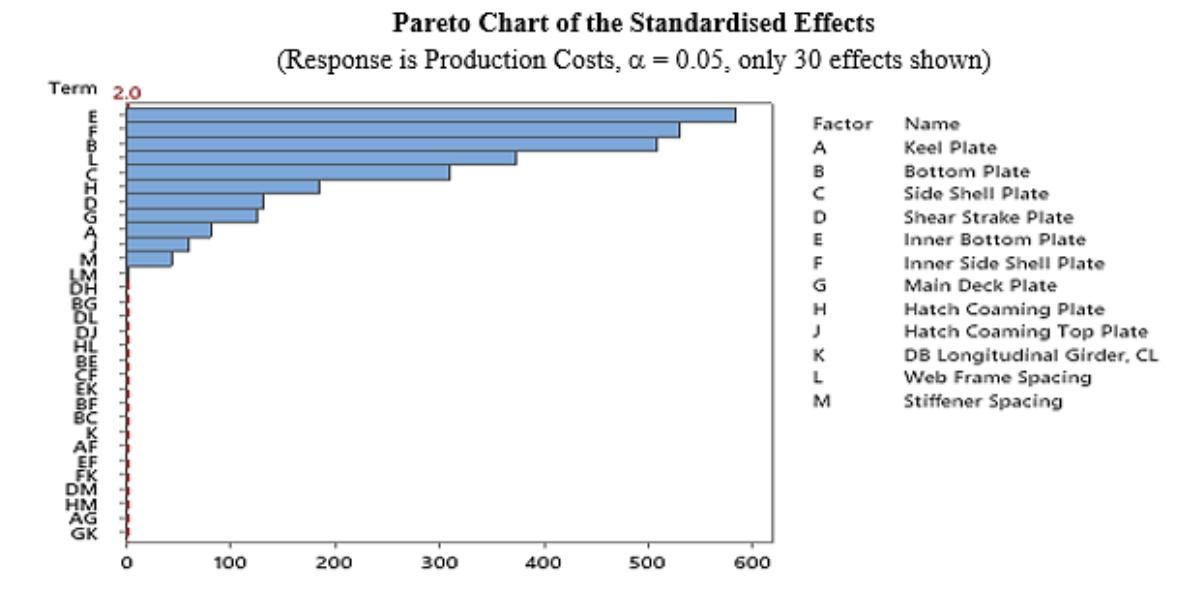


Figure 5-7: Standardisation Effects on Production Costs Response: Pareto Chart Analysis.

Figure 5–7 shows numerous critical factors intersecting with the reference line at a value of 2.0, profoundly impacting the ship's production costs. These factors incorporate the main effects and interactions, significantly influencing the model's dynamics. The figure stresses the discernible impact of each factor on production costs, with an absence of notable interactions among components, thereby reinforcing the primary importance of the identified main effects on ship production costs.

According to the analysis, the five factors that have the most significant impact on ship production costs are:

- Inner Bottom plate
- Inner Side plate
- Bottom plate
- Web Frame spacing
- Side Shell plate

The study painstakingly examines the factors that impact ship production costs. Rigorous analysis of empirical data provides knowledge pertaining to how these factors shape the overall cost dynamics of ship production. These findings hold significant implications for ship

designers and builders, offering actionable knowledge to enhance the cost-effectiveness of ship structures.

Additionally, the study examines the complex relationships among various production cost factors, pointing out their substantial influence on the overall cost of ship production. This influence underscores the elaborate nature of ship production costs and emphasises the importance of understanding these factors in detail to optimise structural design and achieve cost efficiency in performance.

Overall, the research contributes to a more comprehensive understanding of the factors affecting ship production costs and provides practical implications for stakeholders in the maritime industry.

5.5.3.3.2 Residual Plots

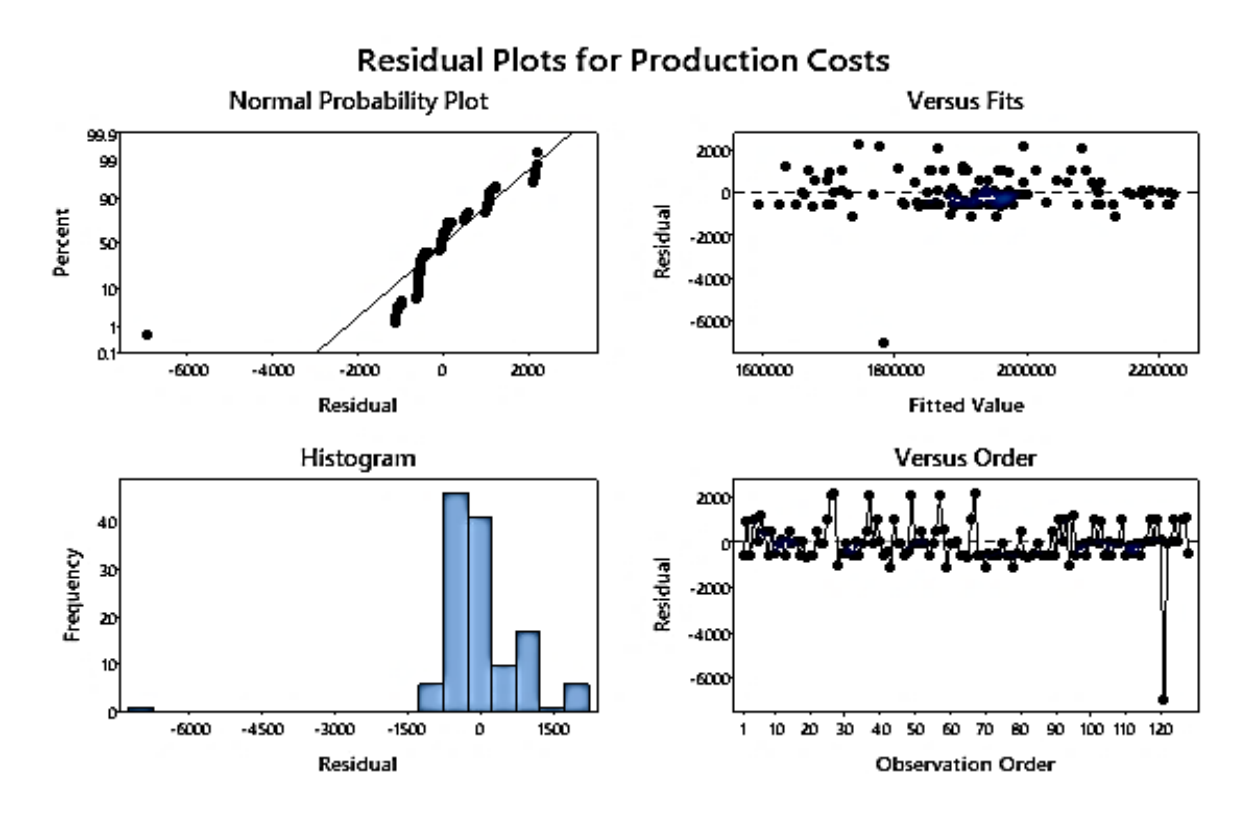


Figure 5-8: A Residual Plot for Production Costs Analysis.

In Minitab's analysis of ship production costs, Figure 5–8 shows the residual plots. These plots are essential for assessing the model's goodness of fit and identifying any patterns or trends in the residuals. Residual plots help verify that the statistical models' assumptions are met.

1. **Normal Probability Plot of Residuals:** This graph analyses whether the residuals follow a normal distribution, a crucial assumption in many statistical models. The

normal probability plot in Figure 5–8 confirms the normality assumption, as the residuals closely follow a linear pattern.

- 2. **Histogram of Residuals:** Figure 5–8 visually represents the distribution of residuals. The histogram indicates that there may be noticeable skewness to the left or right, which suggests a deviation from the normal distribution. However, it is important to point out that there is an extreme outlier on the right side, although it still falls within an acceptable range.
- 3. **Residuals versus Fitted Values Plot:** The plot in Figure 5–8 exhibits that the model effectively captures the underlying data patterns. The residuals are scattered around the horizontal reference line at zero, indicating the validity of the linearity assumption.
- 4. **Residuals versus Order Plot:** This graph helps identify any patterns or trends in the residuals over time or order. Figure 5–8 reveals a plot that compares the residuals to their order. It indicates that the residuals are randomly distributed around the horizontal reference line, meaning their value is typically near zero.

5.6 Discussion

The findings presented in this study offer a significant understanding of the elaborate relationship between ship structural design and production costs, providing extremely useful information for stakeholders in the maritime industry. By employing the Design of Experiments (DOE) methodology, this research systematically investigates the influence of crucial ship components on structural integrity and cost dynamics, addressing a critical need for comprehensive analysis in ship design.

One of this study's notable contributions is identifying critical factors affecting Von Mises stress, a key indicator of structural performance. Using the Plackett-Burman screening method, components such as Hatch Coaming plate, Hatch Coaming Top plate, Shear Strake plate, Main Deck plate and Inner Side Shell plate emerge as significant determinants of stress distribution within ship structures. This highlights the importance of considering specific structural elements during the design phase to mitigate stress concentrations and ensure optimal performance under varying operational conditions.

Furthermore, the study explores the complex interactions between these factors, revealing insights into the synergistic effects that shape structural behaviour. The analysis uncovers the

convoluted relationships between component variations and their combined impact on Von Mises stress, warping stress and production costs by employing fractional factorial design techniques. This comprehensive approach enhances understanding of the multifaceted nature of ship design, emphasising the need for complete consideration of interrelated factors to achieve optimal outcomes.

In addition to structural performance, the study addresses the critical aspect of production costs in ship construction. By examining factors influencing cost dynamics, for example, plate thickness selection and component spacing, a better understanding of opportunities concerning cost optimisation without compromising structural integrity is gained. This aligns with the industry's ongoing efforts to balance economic considerations with safety and performance requirements, bringing to light the importance of informed decision-making in ship design and construction processes.

The structural integrity of ships substantially depends on their significant components, which play a crucial role in determining the overall strength of the ship. This research prioritises optimising multiple objectives, particularly weight reduction and production cost efficiency. Utilising regression equations (refer to Appendix B) derived from fractional factorial design, principally focusing on Von Mises' stress and production costs, is an initial approach for optimisation strategies. Minimising the steel weight during ship construction is essential to reduce manufacturing costs and ensure adherence to established safety standards.

Overall, the findings of this research stress the significance of adopting a systematic and datadriven approach to ship design optimisation. By exploiting the empirical data and statistical analysis, stakeholders can make informed decisions to enhance structural integrity and cost efficiency throughout the lifecycle of a ship. Continuing research in this area can further refine optimisation techniques and incorporate emerging technologies to drive innovation and sustainability in the maritime industry.

5.7 Conclusion

By rigorously applying the Design of Experiments (DOE) approach within the Minitab software environment, this research has uncovered important insights into the critical aspects of ship design and production cost optimisation. The study, which focused on twelve longitudinal components of ship structural elements, has produced significant findings that contribute to advancing knowledge in the maritime industry.

- Efficacy of Screening Plans: Using the Plackett-Burman screening method and the subsequent comparison with main effects highlighted the efficacy of screening plans as crucial tools for preliminary assessments in ship structural analysis. This underlines the importance of systematic approaches in identifying key structural integrity factors.
- Identification of Critical Components: The study identified several crucial
 components, including the Hatch Coaming plate, Hatch Coaming Top plate, Shear
 Strake plate, Main Deck plate, Inner Side Shell plate, Bottom plate, Inner Bottom plate
 and others, which exert substantial influence on Von Mises stress, warping stress,
 besides production costs.
- 3. Complex Interactions: The research revealed intricate interactions between ship components, emphasising the multifaceted nature of structural dynamics. Notably, the interaction between Web Frame and Stiffener spacing emerged as a significant determinant of Von Mises stress, warping stress and production costs, emphasising the need for a comprehensive understanding of related factors.
- 4. Impact on Structural Integrity: Analysis of Von Mises stress and warping stress provided a greater understanding of the factors determining structural integrity. Recognising the influence of specific components and their interactions is paramount as regards enhancing the robustness of ship structures and ensuring safe operation under varying conditions.
- 5. **Regression Equations:** One notable achievement concerning this study is the development of regression equations (refer to Appendix B), particularly for Von Mises Stress and production costs. These equations serve as the foundation for creating a Python-based optimisation code. This optimisation code (refer to Appendix C) is poised to revolutionise the efficiency and cost-effectiveness of multipurpose cargo ship design by improving ship weight optimisation while simultaneously minimising production costs.
- 6. **Cost Optimisation:** Examination of production costs explained vital drivers impacting the overall cost dynamics of ship construction. By identifying factors such as the Inner Bottom plate, Inner Side plate, Bottom plate, Web Frame spacing and Side Shell plate, the study offers actionable knowledge to enhance cost-effectiveness in ship production.

The research findings emphasise the significance of using systematic methods to identify crucial components and comprehend their interactions with the aim of enhancing structural performance and cost-effectiveness in shipbuilding. As the maritime industry evolves, the knowledge obtained from this study will support well-informed decision-making, innovation, together with sustainability in the design and production of ships.

Chapter 6

Ship Structural Optimisation: Procedure and Analysis

6.1 Introduction

Ship structural optimisation is integral to efficiently arranging components within a ship, reducing the utilisation of steel and ensuring structural integrity [55]. It is crucial for improving stress distribution, lowering maximum stress levels and boosting resistance in rough sea conditions while mitigating corrosion and structural failure risks. Optimising the deadweight of a transport ship is vital for financial and operational viability. Lighter vessels are more advantageous for cost-effective construction [51]. The focus of ship design optimisation is on lowering structural weight while preserving fundamental parts and is aimed at decreased fuel consumption, augmented deadweight capacity, improved freeboard, reduced initial costs, increased speed, and greater accessibility to channels and ports [70].

6.1.1 Objectives of Ship Structural Optimisation

The main objectives of optimising ship structures are threefold [6]:

- 1. **Mitigation of Greenhouse Gas Emissions:** A primary objective is to significantly reduce greenhouse gas emissions within the maritime industry, thereby contributing to a more environmentally sustainable future.
- 2. **Enhancement of Fuel Efficiency:** Another key objective is to enhance fuel efficiency by minimising energy consumption and improving propulsion systems, ultimately leading to greater economic efficiency.
- 3. **Augmentation of Vessel Safety and Performance:** Equally critical is improving ship safety and performance, encompassing stability, seakeeping capabilities, in conjunction with structural resilience.

6.1.2 Exploring the Benefits

This study explores the numerous potential advantages and applications of optimising ship construction, offering considerable promise to the marine industry. The following points outline some of the benefits that will be explored in this chapter:

- 1. **Emission Reduction:** Optimising ship structures can reduce greenhouse gas (GHG) emissions by lowering steel weight and production costs [6].
- 2. **Cost Reduction:** Improving a ship's structural design can also save costs, reducing material and labour expenses [51].
- 3. **Enhanced Durability:** Structural optimisation can decrease the likelihood of structural failures and damage. Carefully planned and optimised construction can extend a ship's longevity and reduce maintenance costs [188].
- 4. **Variable Scantlings:** Ship structural optimisation can result in different optimal structural scantlings based on the design objectives chosen, such as mass and vertical centre of gravity (VCG) [189].
- 5. **Multi-Objective Decision-Making:** This study also explores how a multi-attribute decision-making approach to ship design can be adapted to consider several objectives for different scenarios simultaneously [10].

This study's analysis of ship structural optimisation sheds light on its economic and environmental advantages. Likewise, it underscores the fundamental role of ship structural optimisation in enhancing the integrity, efficiency and adaptability of ship designs, ushering in a new era of innovation and sustainability within the maritime sector.

6.1.3 Optimisation Types and Challenges

There are different categories of structural optimisation based on design variables [70]:

- **Topology optimisation:** Topology optimisation is a mathematical technique that enhances the material arrangement within a designated design domain to diversify the range of structural topologies [51].
- **Shape optimisation:** It focuses on a fixed topology, with the structure's geometry (shape) as the optimisation goal [51].

- **Property optimisation:** Property optimisation is a commonly utilised concept in the maritime sector, involving the assessment of optimisation parameters such as plate thickness and profile section dimensions for a specific topology and shape [51].
- Choice of material: The selection of the appropriate material is a critical component of
 the structural optimisation process, where the integration of structural design and
 material choice is imperative to attain the most efficient solution for mechanical
 parts [190].

Topology and shape optimisation are vital for developing unique ships and developing local structures. Most traditional ship topologies are almost fixed after decades of ideal design, with safety and practicality dictating their shapes. Therefore, property optimisation is the most crucial and influential aspect [51].

Marine structures, for instance ships and offshore platforms, are complex and consist of components with residual stress prior to assembly. During the construction process, these structures may experience unexpected deformations, stresses and strains. Once launched and implemented in the demanding marine environment, analysing and optimising their structural integrity is especially challenging. Even with advanced structural optimisation algorithms, they may only be suitable for designing marine structures in some cases [22].

Exploring production costs and weight optimisation in ship design regularly involves addressing multi-objective optimisation problems. Thus far, extensive research efforts have been dedicated to achieving diverse optimisation objectives, leading to the development of various computational tools. Most prior research in structural optimisation has focused on comparing multiple optimisation strategies. However, this study introduces a novel approach by being the first to investigate the influence of structural components on ship Von Mises stress, torsional stress and production costs. This exploration is accomplished by applying fractional factorial analysis within the framework of common structural rules (CSR), explicitly optimising the structure about key ship variables rather than considering all possible factors. Critical ship characteristics are significantly identified by analysing structural element thicknesses, web frame locations and longitudinal stiffener locations. Employing the Design of Experiments (DOE) methodology minimises finite element calculations for the ship under investigation. To conduct this optimisation process, the Non-dominated Sorting Genetic Algorithm II (NSGA-II), implemented in Python, is utilised to iteratively refine the ship's structure based on the aforementioned pivotal factors.

6.2 Optimisation Strategy

The choice of the optimisation algorithm is key in evaluating the objective function for ship structural optimisation and providing enhanced design variables for subsequent structural enhancements. In this research, the NSGA-II is considered the preferred strategy for hull structural optimisation in ships. It is responsible for identifying the optimal ship structural scantlings and the production costs. The NSGA-II is an improvement over conventional Genetic Algorithms (GAs) and other optimisation techniques. By using a fast, non-dominated sorting approach, it effectively reduces computational complexity [191].

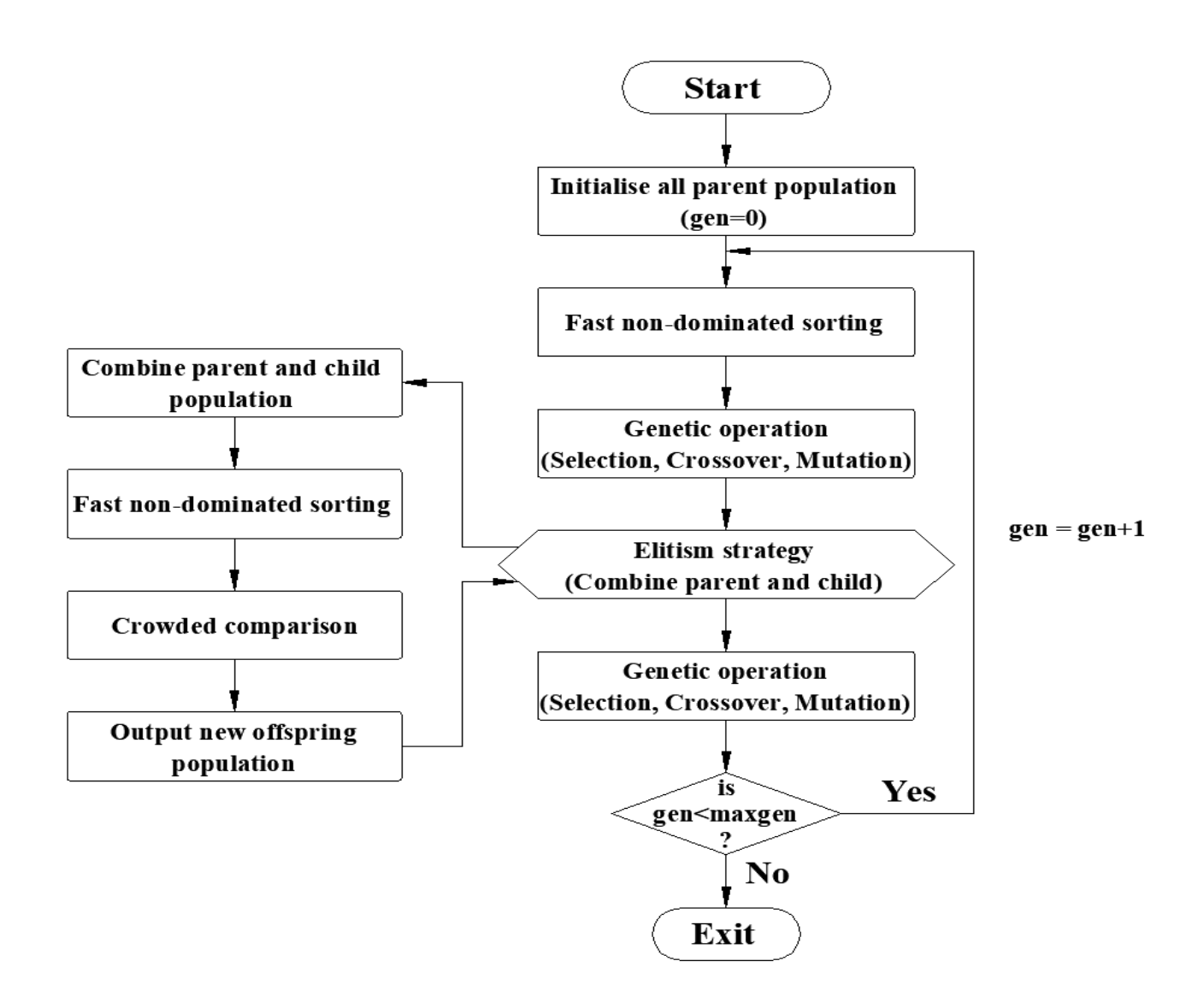


Figure 6-1: Flow chart for the NSGA-II [191].

This study employed the widely recognised multi-objective optimisation algorithm NSGA-II (Non-dominated Sorting Genetic Algorithm II), which is crucial in enhancing ship structural design. The Pareto optimal solutions, which represent a fine line between several competing objectives, are expertly found by this multi-objective optimisation technique. These Pareto-optimal results represent the best possible outcomes for the reason that improving one goal necessitates sacrificing another. NSGA-II is designed as a generational genetic algorithm. It incorporates a strict dominance ranking system to promote convergence and a crowding distance density mechanism to maintain variety [192].

Numerous academic studies in ship structure optimisation have utilised NSGA-II. For instance, NSGA-II outperformed vector optimisation problem (VOP), a straightforward genetic algorithm, in one study where the two were compared in various research studies focusing on multi-objective optimisation of ship structures, NSGA-II demonstrated significant advantages, specifically when optimising all objectives simultaneously [193].

The Stop-Sweep framework uses the NSGA-II algorithm for multi-objective optimisation to produce Pareto-optimal solutions. This algorithm proposes several crucial parameters, including 'pop_size' for controlling the population size and 'n_gen' to specify the number of generations. Modifying these parameters can significantly influence the density of the solution set [194].

Owing to NSGA-II's proficiency in finding Pareto-optimal solutions, its inherent capability to illustrate trade-offs between each objective and its demonstrated superiority over competing optimisation algorithms, as demonstrated in numerous academic works, it is an appropriate choice for enhancing ship structures [195].

6.3 Mathematical Framework for Ship Structural Optimisation

To optimise the structural design of a ship, it is necessary to define the objective functions, design variables and constraints, as in various optimisation methods.

6.3.1 Objective Functions

Objective functions exhibit explicit or implicit dependencies on design factors and are evaluated using numerical or mathematical expressions. Standard objective functions include weight, production cost, life cycle cost and safety indices [87].

This study's two objectives pertain to reducing weight and production costs.

6.3.1.1 Weight Function

Optimising the structural topology of a ship is a complex task that requires addressing several factors. One of the critical aspects of the problem is finding the right balance between the number of structural components in the longitudinal and transverse orientations and their dimensions. These variables significantly impact the overall weight of the ship's structure. Additionally, it is essential to bear in mind various constraints related to the ship's construction and operational needs. The objective function f(x) for optimising the weight of the hull structure is expressed as follows [10]:

$$f(x) = \sum_{j}^{r} w_j SW_j \tag{6-1}$$

where

r – number of structural regions

 SW_j – the weight of the j-th structural region

 w_i – relative weight coefficient

6.3.1.2 Cost Function

Production costs (PC) can be categorised into three distinctive components [52]:

- 1. **Raw materials costs (MC)**: The first step in assessing material costs is quantifying the required construction volume and obtaining price quotations from suppliers and subcontractors. This is crucial to accurately estimate material expenses.
- 2. **Labour costs (LC):** When assessing labour costs, it is best to make use of an analytical approach using empirical formulations. This involves thoroughly understanding the time required to complete each labour task associated with a workstation and dividing the construction process into separate stations.

3. **Overhead costs (OC)**: Overhead costs contain all of the expenses associated with construction that cannot be directly attributed to a specific workstation within the construction process [52].

$$PC = MC + (LC \times HC) + OC \tag{6-2}$$

where

PC is the production costs (\in)

MC is material costs (€)

LC is labour costs (man-hours)

HC is hourly costs (€/hour)

OC is overhead costs (€)

The shipbuilding process invariably proceeds by way of well-defined phases, each in conjunction with its associated costs. These phases include [175]:

- 1. Contract Signing
- 2. Basic Project Development
- 3. Detailed Production Project Planning
- 4. Ship Hull Construction
- 5. Outfitting (including piping, electrical systems, machinery and auxiliary systems)
- 6. Sea Trials and Certification
- 7. Ship Owner Delivery

It is essential to implement several stages pertaining to quality control, transportation, supervision and plan approvals during the ship construction process. Approvals must be acquired from various organisations such as the shipyard, marine design office, ship owner, classification societies and maritime flag authorities. These rigorous processes ensure the successful construction and certification of ocean-going ships [175].

A comprehensive examination and categorisation of six discrete components contributing to the cost of manufacturing a steel hull for a ship, exclusive of the steel material procurement costs was conducted. Consequently, the cost structure for the construction of a steel hull can be segregated into the following six cost centres, each aligning with a particular phase within the production process:

- 1. Costs of work preparation.
- 2. Expenditure associated with material cutting.
- 3. Costs related to material transportation.
- 4. Expenses incurred during the shaping procedure.
- 5. Expenditure linked with the assembly of components.
- 6. Costs arising from the welding process.

The following generic formula should be applied to each of these cost centres [175]:

$$C_{Process} = [Labour cost + Energy cost + Consumable materials cost + Equipment depreciation cost] [€]$$
(6–3)

The energy cost refers to the electricity required to power the equipment, while the material cost includes the expenses incurred in purchasing supplies and materials vital for the process. Depreciation costs cover the maintenance, amortisation and depreciation of used equipment. These three costs are more affordable compared to labour costs [175].

6.3.1.2.1 Work Preparation Costs

During the work preparation phase, it is fundamental to reflect on several cost elements. These are outlined below [175]:

- 1. Cost of Personal Computers (Depreciation Cost).
- 2. Energy Costs.
- 3. Cost of Software Licenses (to be integrated into the equipment depreciation cost).
- 4. Labour Costs of Work Preparers.
- 5. Training Costs (included within the labour cost category).

These components collectively contribute to formulating a cost equation that resembles the one presented [175]:

$$CPRE = \left[\left(n_p \times S_p \times h_p \right) + \left(K_e \times P_e \times h_p \right) + \left(C_d \times h_p \right) \right] \in$$
 (6-4)

 n_p – Number of Work preparers [M]

 S_p – Work preparer wage [\in /Mh]

 h_p – Work preparation time [h]

 K_e – Electricity consumption [kW/h]

 P_e – Electricity price [\in /kW]

 C_d – Depreciation cost [\in /h]

The equation is modified to simplify and connect expenses with block weight [175]:

$$C_p = P_b. \left(\gamma_b. CER_p. MDO_p + CEQ_p \right) [\in]$$
 (6-5)

 P_b – Block weight [t]

γ_b – Block complexity coefficient

 CER_p – Work preparation cost estimate relationship [Mh/t]

MDO_p – Work preparation labour cost [€/Mh]

 CEQ_p – Work preparation equipment costs $[\ell/t]$

6.3.1.2.2 Cutting Costs

When calculating expenses associated with cutting costs, the following factors should be included: cutting equipment (purchase/rental, amortisation, lease, devaluation and maintenance), energy, cutting gases, cutting operators and training. This produces a new set of equations that generate costs similar to those shown below [175].

Concerning the plasma cutting:

$$C_{PLA} = (n_{tc} \times S_{tc} \times h_c) + (K_e \times P_e \times h_c) + (K_{Ar} \times P_{Ar} \times h_c) + (C_d \times h_c) \in$$

$$(6-6)$$

 n_{tc} – Number of Cutting technicians [M]

 S_{tc} – Cutting technicians wage [\in /Mh]

$$h_c$$
 – Cutting time [h] $(h_c = \frac{d_c}{v_c})$

 v_c – Cutting speed [m/h]

 d_c – Cutting length [m]

 K_{Ar} – Plasma gas consumption [kg or m³/h]

 P_{Ar} – Plasma gas price [\notin /kg or m³]

The following costs formula can be applied in the case of an automatic oxy-gas cut [175]:

$$C_{OXI} = \begin{bmatrix} (n_{tc} \times S_{tc} \times h_c) + (K_e \times P_e \times h_c) + (K_o \times P_o \times h_c) + (K_A \times P_A \times h_c) \\ + (C_d \times h_c) \end{bmatrix} [\in] \quad (6-7)$$

 K_o – Oxygen consumption [kg or m³/h]

 P_o – Oxygen price [\notin /kg or m³]

 K_A – Acetylene consumption [kg or m³/h]

 P_A – Acetylene price [ϵ /kg or m³]

The following costs equation can be utilised in the case of manual oxy-gas cut [175]:

$$C_{MOXI} = \begin{bmatrix} (n_{tc} \times S_{tc} \times h_c) + (K_e \times P_e \times h_c) + (K_O \times P_O \times h_c) + (K_A \times P_A \times h_c) \\ + (C_d \times h_c) \end{bmatrix} [\in]$$

$$(6-8)$$

The majority of previous cost-cutting efforts have typically been related to labour. Therefore, it is advisable to separate labour costs from other expenses and combine them in a single lump sum, including equipment acquisition costs, maintenance, equipment depreciation, plus electricity/gas cutting costs. Using the following simplified equation, these costs will be directly calculated by way of the steel weight variable produced [175]:

$$C_c = P_b \cdot (\gamma_b \cdot CER_c \cdot MDO_c + CC_c + CEQ_c) [\in]$$
(6-9)

CER_c – Cutting cost estimate relationship [Mh/t]

 MDO_c – Cutting labour cost [\in /Mh]

 CC_c – Cutting consumables cost [€/t]

 CEQ_c – Cutting equipment costs [\in /t]

6.3.1.2.3 Transport Costs

Determining the costs associated with transportation equipment can be a complicated task. These costs comprise several factors, including equipment-related costs, for instance acquisition, renting, leasing, depreciation and maintenance, operators' labour costs, together with energy costs (whether electric or fuel). The total rental cost may already include several of these expenses.

Overhead gantry cranes (whether magnetic or not), cranes and small forklifts are examples of electric transport vehicles [175].

$$C_{PON} = \left[(n_{ot} \times S_{ot} \times h_t) + (K_{\rho} \times P_{\rho} \times h_t) + (C_d \times h_t) \right] [\in]$$
 (6–10)

 n_{ot} – Number of transport workers [M]

*S*_{ot} − Transport worker wage [€/Mh]

 h_t – Transportation time [h]

Transport vehicles fuelled by fossil fuels, such as shipyard dollies, mobile cranes, floating cranes and forklifts, allocate a segment of their costs to fuel, which is a substitute for electricity cost [175]:

$$C_{VEI} = \left[(n_{ot} \times S_{ot} \times h_t) + (K_C \times P_C \times h_t) + (C_d \times h_t) \right] [\in]$$
 (6–11)

 K_C – Fuel consumption [1/h]

 P_C – Fuel price [\in /1]

Welding costs are influenced by various factors, including the costs of welding equipment (acquisition/rental, leasing, depreciation and maintenance), welding speed (linked to consumption), and the number of welders (involving training and labour costs), consumable costs, as well as energy costs [175].

The cost of submerged arc welding (SAW) is:

$$C_{SAW} = \begin{bmatrix} (n_s \times S_s \times h_s) + (K_e \times P_e \times h_s) + (K_{fio} \times P_{fio} \times d_{sol}) \\ + (K_{flu} \times P_{flu} \times d_{sol}) + (C_d \times h_s) \end{bmatrix} [\in]$$
 (6-12)

 n_s – Number of welders [M]

 S_s – Welder's wage [\in /Mh]

 K_{fio} – Cored wires consumption [kg/m]

 K_{flu} – Protection flux consumption [kg/m]

P_{fio} – Cored wires price [€/kg]

 P_{flu} – Protection flux price [€/kg]

The following costs are associated with using flux-cored arc welding (FCAW) with gas protection [175]:

$$C_{FCAW} = \begin{bmatrix} (n_s \times S_s \times h_s) + (K_e \times P_e \times h_s) + (K_{fio} \times P_{fio} \times d_{sol}) \\ + (K_{pro} \times P_{pro} \times d_{sol}) + (C_d \times h_s) \end{bmatrix} [\in]$$
 (6–13)

 K_{pro} – Protection gas consumption [kg or m³/m]

*P*_{pro} – Protection gas price [€/kg or m³]

Finally, there is the utilisation of coated electrode SMAW welding, as seen in Eq. 6–12, with the only difference being the replacement of welding time with assembly time within the labour cost parcel [175].

$$C_{ELE} = \left[(n_s \times S_s \times h_s) + (K_e \times P_e \times h_s) + (K_{ele} \times P_{ele} \times d_{sol}) + (C_d \times h_s) \right] [\in] \quad (6-14)$$

Costs will be estimated for the produced weight of steel in the simplified equation [175]:

$$C_s = P_b \times \left(\gamma_b \times CER_s \times MDO_s + CC_s + CEQ_s \right) [\in]$$
 (6-15)

*CER*_s – Welding cost estimation ratio [Mh/t]

 MDO_s – Labour costs for welding [\in /Mh]

 CEQ_s – Equipment costs for welding $[\pounds/t]$

To sum up, the total simplified cost for constructing a ship's steel hull combines the costs from all previously discussed cost centres and an additional component associated with costs that still need to be addressed [175].

$$C_{TOTAL} = C_p + C_c + C_t + C_e + C_m + C_s + C_{EXTRAS}$$

$$(6-16)$$

Typically, cutting and welding tasks demand significant labour hours and the selection of technology can result in considerable non-productive costs [175].

6.3.2 Design Variables

The principal structural dimensions can act as design variables and localised characteristics, for instance the stiffener web thickness within a given structural area, whether applied to the entire structure or just a particular segment. 'Design variables' refer to various characteristics, including material type, grade, stiffener configurations (bulb, T and L), overall deck section and other relevant elements.

The optimisation objectives and the particular design process stage must be considered when choosing these factors. A ship typically consists of several stiffened panels, including bulkheads, bottoms, side shells and sub-elements of the deck.

The scantling of these stiffened panels is a crucial design factor. Despite widespread attempts to standardise production efficiency, there are differences among panels in the scantlings. The particular panel scantling, for example, HP200 or FB100x10, impacts plate thickness, frame spacing, stiffener spacing and stiffener dimensions [87].

6.3.3 Design Constraints

Constraints can be categorised as either explicit or implicit functions of design variables, which may take on linear or non-linear forms. These constraints are mathematical expressions that encapsulate user-imposed limitations on design variables, encompassing aspects, such as displacement, stress, ultimate strength, etc. [52].

Several types of constraints are considered in structural optimisation:

- Technological Constraints (or Side Constraints): These constraints set the upper and lower boundaries for design variables and guide optimisation [52].
- Geometrical Constraints: Geometrical constraints create connections between design variables to ensure the structural design is practical, realistic and reliable. They utilise specialised knowledge to prevent problems with local strength, such as web or flange buckling and stiffener tripping. Furthermore, they endeavour to guarantee welding

quality and accessibility, as welding a 30 mm thick plate to a 5 mm thick plate, for instance, is not recommended [52].

- Structural Constraints: To prevent yielding, buckling and fractures, in addition to other structural problems, restrictions are placed on deflection, stress and related factors. These constraints are determined using rational equations that are based on the principles of solid mechanics. Rational equations refer to analytical techniques that are logically consistent and not based on empirical or parametric formulations. They incorporate concepts from fundamental physics, for instance solid mechanics, strength, stability principles, and other related concepts. These structural constraints may limit variables such as deflection, stress levels in structural elements, tripping, buckling and ultimate strength [52].
- Global Constraints: Global constraints limit the ship's centre of gravity for stability, fabrication costs for producibility and flexural inertia for classification compliance [52].
- **Equality Constraints**: Design variables are frequently kept continuous through equality constraints. For instance, panels on the same deck have uniform thicknesses, whilst standardisation is applied to stiffener spacing [52].

The following is an example of a general structure optimisation problem [196]:

$$(SO) = \begin{cases} \text{minimise } f(x, y) \text{ with respect to } x \text{ and } y \\ \text{Subject to } \begin{cases} behavioural constraints on } y \\ \text{design constraints on } x \\ \text{equilibrium constraints} \end{cases}$$
 (6–17)

6.3.4 Single Criterion Problem

The typical formulation of the single criterion optimisation problem is:

$$min_x F(x) = F_1(x),$$
 $x = [x_1, x_2, \dots x_N]^T$

subject to the equality and inequality constraints

$$h_i(x) = 0,$$
 $i = 1, ..., I$
$$(6-18)$$
 $g_i(x) \ge 0,$ $j = 1, ..., J$

where the N unidentified design independent variables in the vector x rely on the single optimisation criterion or objective function $F_1(x)$. In general, the problem is subject to I equality constraints and J inequality constraints, respectively, $h_i(x)$ and $g_j(x)$, which are contingent on the vector x design variables for a feasible engineering solution. The minimisation form is universal because a maximisation problem can be resolved by minimising the inverse or negative of the cost function [197].

6.3.5 Multi-Criterion Problem

The multi-criterion optimisation problem involves more than one criterion (K > 1) and can be formulated as follows [197]:

$$min_x F(x) = [F_1(x), F_2(x), ..., F_K(x)],$$
 $x = [x_{1,x_{2,...,x_N}}]^T$

subject to equality and inequality constraints

$$h_i(x)=0, \qquad i=1,...,I$$

$$(6-19)$$
 $g_j(x) \ge 0, \qquad j=1,...,J$

where there are now K different optimisation criteria, numbered $F_1(x)$ through $F_K(x)$, each dependent on the N unidentified design factors in the vector x. A vector represents the total objective function F at this time. As a result of conflicts between the K criteria, there is generally no single solution to this problem [197].

6.3.6 Global Criterion Optima

Engineering design necessitates a particular outcome to be implemented, not a collection of options as the Pareto optimal set offers. The weighted sum, the min-max, and the closest to the ideological solutions are among the more logical strategies to establish a practical compromise among opposing requirements. The following global criteria can be utilised to obtain these solutions [197]:

$$P[F_k(x)] = \left\{ \sum_{k=1}^K \left[w_k \left| \frac{F_k(x) - F_k^0}{F_k^0} \right| \right]^{\rho} \right\}^{\frac{1}{\rho}}$$
 (6–20)

$$\sum_{k=1}^{K} w_k = 1$$

The best result that can be achieved using only that criterion is represented by F_k^0 , which is the value of criterion F_k obtained when it is the sole criterion utilised in the optimisation process. The scalar preference function $P[F_k(X)]$ replaces F(X) in Eq. 6–18 for a numerical solution.

When $\rho = 1$, Eq. 6–20 gives the weighted sum solution; when $\rho = 2$, it provides the closest-toutopian solution; when $\rho = \infty$, it offers the min-max solution. The numerical version of Eq. 6–20 with $\rho = \infty$ implements the minimax solution.

$$P[F_k(X)] = \max_k [w_k | (F_k(X) - F_k^0) |]$$
(6-21)

Moreover, solutions can be determined for a range of values for ρ . Subsequently, the design team can select the solution that best aligns with the design objective [197].

6.3.7 Pareto Optimal Solution

A Pareto-optimal solution is one where no individual can be improved without exacerbating the position of at least one other participant. In simpler terms, it means reaching a point where no more improvements can be made without harming someone [198]. The set of Pareto-optimal solutions in multi-objective optimisation is called the Pareto-optimal front, also termed the Pareto front or Pareto frontier. The Pareto front is an effective tool in engineering and other disciplines requiring the simultaneous optimisation of multiple objectives. It demonstrates the trade-offs of pursuing different goals, where achieving one objective may mean sacrificing another. This makes it an essential resource for decision-making [199].

NSGA-II is an evolutionary algorithm that makes use of an elitist approach to identify Pareto-optimal solutions by eliminating dominated alternatives. The Pareto front, which represents the trade-offs among multiple objectives, is constructed through this process [200]. Graphically, the Pareto front can be described as a curve or surface in the objective space, with each point on the curve signifying a Pareto-optimal solution. To preserve population diversity, NSGA-II utilises a crowding distance metric and a non-dominated sorting procedure to rank solutions based on non-dominance. Genetic operators, such as crossover, mutation and tournament selection, generate new candidate solutions. The algorithm extracts the Pareto-optimal front

from the final population of solutions, which can be portrayed as a curve or surface in the objective space [201].

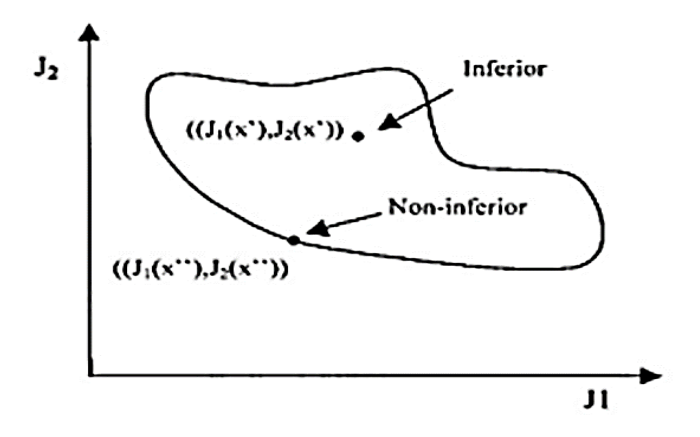


Figure 6-2: Feasible Solution Space [198].

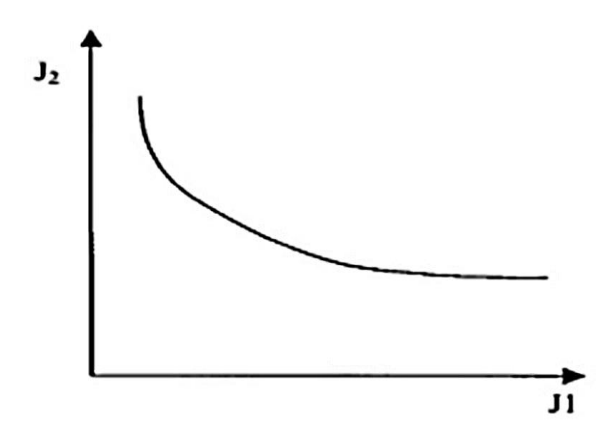


Figure 6-3: Pareto Optimal Curve [198].

Figures 6–2 and 6–3 show the "Feasible Solution Space," encompassing all viable solutions meeting specified constraints and objectives, as well as the "Pareto Optimal Curve," which identifies the optimal compromise solutions where no objective can be improved without sacrificing another. These visuals are vital tools in multi-objective optimisation, enabling decision-makers to navigate scenarios concerning multiple, potentially conflicting objectives effectively and make informed choices that strike an ideal balance.

6.4 Optimisation Algorithm

The optimisation algorithms are divided into two primary types: deterministic and heuristic approaches [6].

6.4.1 The Purely Deterministic Approaches

Optimisation aims to identify the most effective direction from an initial design, whether feasible or not. Methods such as Simplex, steepest descent, BFGS, SQP and the dual approach are possible [6].

- It seems that they tend to converge towards a local maximum.
- Evaluating the first derivative of constraints takes considerable time and effort.
 However, certain techniques do not require this evaluation, though they may require more iterations.
- The success of the optimisation solution relies on the initial design given that it is part of the convergence process.
- Issues involving continuous design variables are well-suited to these methods, while discrete design variables pose challenges.
- Excellent quality gradients cannot be used with noisy or non-derivable functions.
- These methods require accurate and reliable approximations of functions and their derivatives, with minimal resilience in this aspect.
- They typically converge quickly (5-10 iterations), offsetting gradient calculation time.

6.4.2 The Heuristic Approaches

This algorithm incorporates randomness in the search for an absolute optimum, increasing the possibility of success with each trial [6].

- Executing them is straightforward, but calibration may speed up convergence.
- They are generic and applicable to various domains, which explains their popularity.
- If the number of design variables is reduced, solutions become highly effective.
- Independent of the basic design.
- This algorithm excels at discovering a suitable global optimum solution at a reasonable computational cost.
- A precise determination of the Pareto front is essential for multi-objective optimisation.

- Discrete design variables are frequently more efficient than continuous design variables.
- They exhibit high resistance to inaccuracies and failures in their analysis.

6.5 Data Collection and Implementation

This study focuses on a multi-purpose cargo ship currently operating in Germany. The ship was built by Ananda Shipyard & Slipways Limited in Bangladesh and met the strict standards set by the Bureau Veritas (BV) classification society. The FEMAP software platform was employed to conduct a detailed assessment to create models of the ship's three cargo holds based on BV-approved designs. The scantlings of crucial parameters for the ship have been gathered from the BV-approved Midship Section drawing of the ship. Adhering to BV regulations and employing expert knowledge, a comprehensive spectrum of vital parameters encompassing lower and upper bounds for the ship was precisely ascertained. The development of a mathematical model for the cargo holds of this analysed ship, referred to as the 'base model', has been initiated. Twelve (12) vital parameters significantly influencing the ship's longitudinal strength were meticulously selected, drawing upon expertise and knowledge. Employing the robust fractional factorial design method available in the Minitab software suite, a comprehensive design matrix comprising 128 distinct ship configurations was constructed. A rigorous engineering process was applied to refine the twelve parameters mentioned earlier within this sophisticated matrix.

To conduct a methodical and reliable analysis, this study exploits a different approach than traditional maritime practice by treating the ship as a cantilever beam rather than a simply supported beam during the investigation. To simulate actual conditions, bending moments were carefully applied to each of the 128 model variants, resulting in data on Von Mises stress. Subsequently, a comprehensive analysis was undertaken to determine the distribution of Von Mises stress throughout the structural framework of the ship.

After performing a hull girder stress study, the Minitab software was utilised to conduct a comprehensive regression analysis. This analysis generated a regression equation (refer to Appendix B) that accurately describes the behaviour of hull girder stress. A complete assessment of the production costs of each of the 128 ship variants was also performed. The process entailed the incorporation of empirical formulas inside the Microsoft Excel platform, including several cost factors, such as steel plate cost, work preparation cost, cutting cost, transport cost, forming cost, assembly cost, along with welding cost. The data concerning these

costs were systematically collected from multiple shipyards in Bangladesh, specifically Ananda Shipyard and Slipways Limited, Three Angle Marine Limited, Western Marine Shipyard Limited, Radiant Shipyard Limited and Karnafully Shipyard Limited. Ananda Shipyard and Slipways Limited was selected as the reference point for comparison on account of its involvement in the ship's construction under analysis. In conclusion, Minitab's advanced regression analysis capabilities were employed to construct a regression equation to model production costs.

Python is employed for optimisation via the utilisation of the NSGA-II algorithm. The objective is to determine the optimal stress levels and related thicknesses for a set of twelve (12) distinct components while also optimising the production costs of the ship. The integration of regression equations for stress and production costs (refer to Appendix B) has been implemented within the NSGA-II algorithm, utilising the Python programming language to achieve this objective. The equations were derived from the statistical software program Minitab. The utilisation of random output data is employed to enhance the precision of the results. This study includes conducting multiple iterations to ascertain the most optimal results.

6.6 Assumptions and Constraints Used for the Optimisation Model

When optimising the structure of a ship, it is essential to consider various assumptions and constraints judiciously. This consideration ensures that the ship model accurately reflects the real-world problem and is manageable for analysis and optimisation. These assessments and constraints are critical in defining the scope of the optimisation model and identifying its limitations. The following list emphasises some of the key assumptions and constraints considered throughout the optimisation process:

6.6.1 Assumptions

This study deemed several assumptions compulsory to optimise ship structural components and simplify intricate problems. These assumptions encompass:

• **Ship Geometry:** The ship is considered a rigid body. Its geometry, comprising its shape and main dimensions (Length, Breadth and Depth), are assumed to be fixed and unmodifiable throughout the optimisation process [202].

- Material Properties: A ship is a complex structure that requires different plate thicknesses and grades in various sections to ensure its strength. The structural materials (e.g., steel and aluminium) are presumed to possess these requisite properties consistently throughout the entire ship. This assumption streamlines material selection and minimises the challenges connected with material variability [203].
- **Linear Elasticity:** Structural materials are assumed to exhibit linear elastic behaviour, thereby simplifying stress analysis [204]. This analysis does not consider non-linear behaviours, such as plastic deformation.
- **Simplified Geometry:** Simplified geometric shapes are used for structural elements, such as beams, plates and shells to accelerate the production and analysis procedures [205].
- **Static Loading:** It is recognised that the ship experiences primarily static loads during its operational life. This simplifies the analysis but may only partially account for the dynamic effects of waves and vibrations [206].
- **Discrete Material Choices:** A finite set of materials with established properties is assumed instead of considering a continuous range of options. This methodology enables the development of material selection and plate thickness optimisation for ship structures, resulting in improved efficiency [76].
- Manufacturing Efficiency: It is supposed that manufacturing processes are efficient and do not result in significant variations in material properties or production costs [207].

6.6.2 Constraints

Constraints are integral to optimising ship structures, as they define the problem space, guide the search for the optimal solution and ensure that the final design is in accordance with the objectives and limitations [22]. In this study, the following constraints have been applied:

• Stress constraint: It is crucial to avoid exceeding the maximum allowable stress in the ship's components to ensure that structural components meet safety and performance requirements while avoiding excessive weight [10].

- **Production Costs Constraint:** A maximum budget for production costs is set, considering material costs, labour, fabrication processes, together with other relevant expenses [208].
- Safety Regulations: Safety regulations and standards established by relevant maritime authorities, such as classification societies, are followed. These regulations may exert influence on design choices and material selection [18].
- **Technological Constraints**: The design variables' upper and lower bounds were assessed according to Bureau Veritas (BV) regulations [6].
- **Structural Constraints**: These constraints have been employed on the panels to mitigate yielding and buckling, ensuring that the maximum stresses experienced by the panels remain below the permissible threshold [10].
- Equality Constraints: To create a streamlined yet detailed scantling design, constraints are judiciously applied section by section. Panels within each section are consistently thick and standardisation principles are used for stiffener and frame spacing [10].
- **Geometrical constraints**: Constraints are implemented to ensure welding quality, prevent local strength failures and provide easy access to weld joints [6]. For instance, welding a 12 mm keel plate to a 6 mm bottom plate is averted.
- **Discrete Thickness Constraints:** In optimisation, obtaining specific plate thicknesses that are not commercially available can present challenges. In such scenarios, adhering to the constraint involves selecting the nearest higher available thickness [209]. For example, if the optimised plate thickness falls between 6 mm and 6.5 mm, a rounded-up plate thickness of 6.5 mm is used.

This rigorous approach optimises ship structures by considering a comprehensive set of assumptions and constraints, giving rise to practical and safe design solutions that accurately represent complex engineering challenges.

6.6.3 Detailed Steps for Implementing the Python Code

This section provides a detailed presentation of the implementation steps for the Python code (refer to Appendix C) used in the study. The Python code exploits the NSGA-II algorithm to optimise multiple objectives for a particular problem. The problem involves finding the optimal

thicknesses and spacing of web frames and stiffeners to reduce the weight and production costs of a multi-purpose cargo ship while meeting specific constraints. The following is a comprehensive breakdown of how the code is implemented:

1. Importing Required Libraries: The code begins by importing the necessary libraries to support various functionalities. This library includes DEAP for evolutionary computation, numpy for numerical operations, and random for generating random numbers. Matplotlib is used for visualisation, which is crucial for performance monitoring through visualising statistical data from DEAP. The warnings library manages warnings during code execution.

2. **Defining Helper Functions:**

This section defines important helper functions that are employed throughout the code.

- semiround (f): This function rounds a floating-point number, 'f,' based on certain conditions.
- plot_pareto_frontier (Xs, Ys, maxX = True, maxY = True): A function that plots the Pareto frontier using X and Y value lists. It helps to visualise the trade-off between stress and cost in optimisation results.
- 3. **Defining the Main Optimisation Function run_nsga:** This crucial function undertakes the main optimisation process, which takes in a range of input parameters. These include the design variable ranges, optimisation parameters (like crossover and mutation probabilities, population size and number of generations), in addition to threshold values for constraints.
 - def run_nsga(KeelPlate, BottomPlate, SideShellPlate, ShearStrakePlate, InnerBottomPlate, InnerSideShellPlate, MainDeckPlate, HatchCoamingPlate, HatchCoamingTopPlate, dblgcl, WebFrameSpacing, StiffenerSpacing, thresholdval, crossover_prob=0.7, mutation_prob=0.3, gen=500, pop=128)
- Defining Individual Evaluation Function evaluation: This function calculates and returns stress and cost objective values using current plate thicknesses and spacing as inputs.
- 5. **Defining Feasibility Function Feasible:** This function verifies if current design variables meet specified threshold constraints.

- 6. **Defining Distance Function distance:** A distance metric is calculated by measuring the deviation from the threshold values of the constraints.
- 7. **Defining Mutation Function myMutate:** A customised mutation function randomly revises specific design variables based on a specified probability.

8. Creating DEAP Creator and Toolbox Objects:

This section defines the essential objects and structures required for DEAP (Distributed Evolutionary Algorithms in Python).

- creator. create ("FitnessMax", base. Fitness, weights = (1.0, -1.0)): This line of code explains a fitness function with two objectives: minimise cost and maximise stress.
- creator. create ("Individual", list, fitness = creator. FitnessMax): An individual is defined as a list with a specified fitness level.

9. Registering Design Variables and Functions in the Toolbox:

- The toolbox is updated by recording the design variables, their ranges, as well as the custom mutation function.
- This process involves creating a series of design variable functions that will be applied to generate an individual.
- To begin the process, registers are used to initialise the population, assess their fitness,
 facilitate mating and introduce individual mutations.
- 10. **Setting Optimisation Parameters:** This step involves defining key optimisation parameters such as crossover probability (CXPB), mutation probability (MUTPB), the number of generations (NGEN) and the population size (POPSIZE).
- 11. **Evaluating Initial Population:** The fitness of the initial population is evaluated and fitness values are assigned to each individual.
- 12. **Main Evolutionary Loop:** The primary evolutionary loop runs for a set number of generations (NGEN). The process consists of the following steps:
- Selection of the best individuals using the NSGA-II algorithm.
- Application of crossover and mutation to create a new population.
- Calculation of fitness values for the new population.

- Updating the population with unique individuals.
- Recording the stress and cost values of the best individual at each generation.
- 13. **Displaying Results:** This section is responsible for presenting the following:
- The optimised values of design variables.
- The final fitness values.
- Plots illustrating the stress and cost values over iterations.
- A plot of the Pareto frontier which provides a visual representation of the trade-offs between stress and cost.
- 14. **Running the Optimisation:** The code's central part specifies input ranges, threshold values, besides optimisation parameters and calls the run_nsga function to perform multi-objective optimisation.

This section provides a detailed overview of implementing Python code for the multi-objective optimisation problem addressed in this study.

6.7 Case Study 1

The structure is represented by stiffened panels (plates and cylindrical shells). Each panel may be connected to up to nine (9) design variables. The following design parameters are listed:

- Plate thickness.
- For longitudinal members (stiffeners, crossbars, longitudinal, girders, etc.):
 - o web height and thickness,
 - o flange width,
 - o spacing between two longitudinal members.
- For transverse members (frames, transverse stiffeners, etc.):
 - o web height and thickness,
 - o flange width,
 - o spacing between two transverse members.

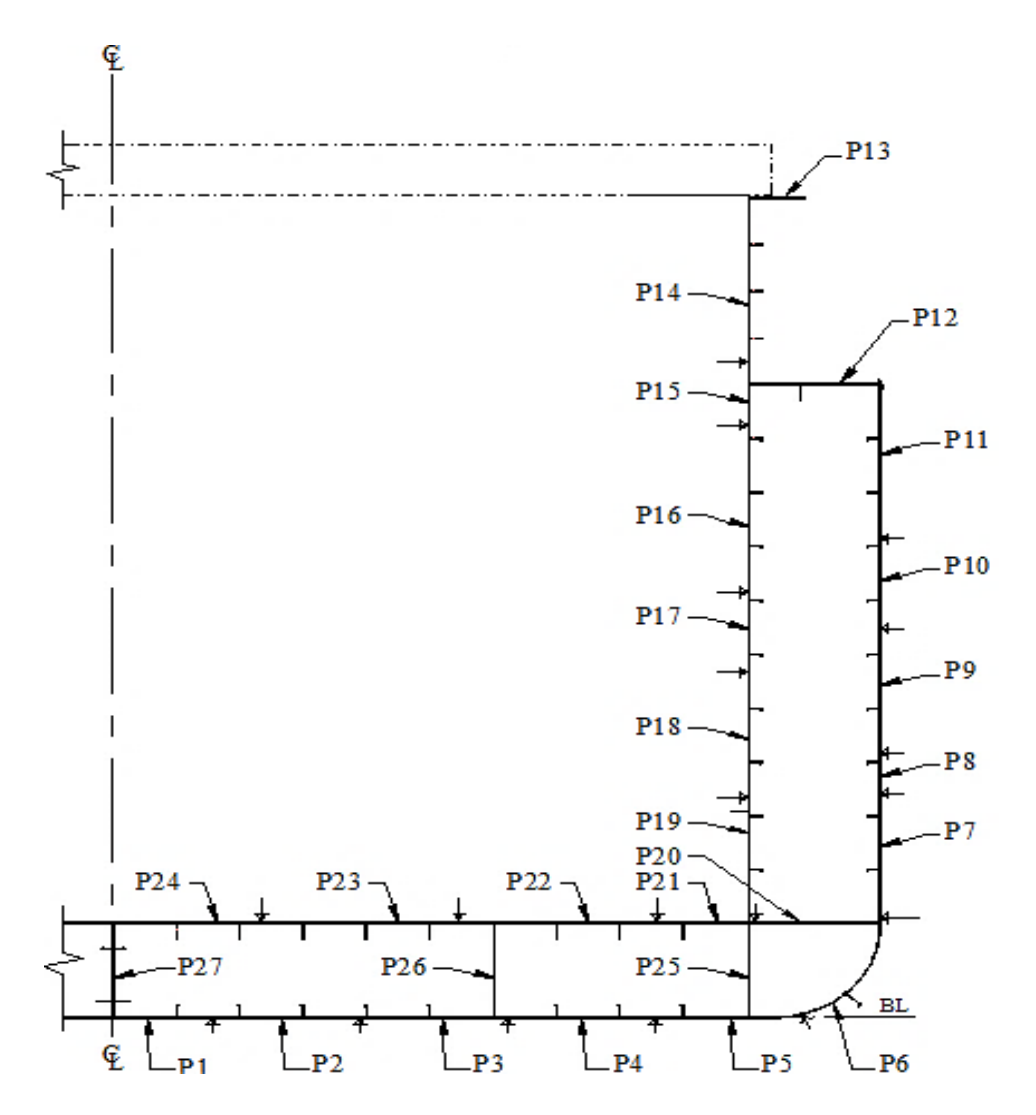


Figure 6-4: Panel definition of midship section.

Figure 6–4 shows the panel definition of the midship section, a critical aspect of the investigation within this study, highlighting 27 stiffened panels within the section. This visual representation is vital for structural optimisation, offering crucial information for hull design and construction. Engineers and designers can exploit this figure to comprehensively understand the ship's structural features and performance, influencing the overall design and construction process. It is an elementary reference for optimising the ship's structural integrity and guaranteeing an efficient and effective performance at sea.

The mesh model of the multipurpose cargo ship unit consists of the following elements:

- 27 stiffened panels in all, each with 9 different design variables.
- 2 additional panels to represent the symmetry axis (or boundary conditions).
- 243 design variables (9 x 27 panels).

- 54 equality constraints between design variables.
- 243 geometrical constraints (9 x 27 panels).
- 486 structural constraints (243 by load case).
- 2 constraints on hull ultimate strength.

The study revolves around the intricate mesh model of a multipurpose cargo ship unit comprising several crucial elements:

- 1. **27 Stiffened Panels:** These panels function as the model's core components. Each panel is identified by nine distinct design variables, resulting in 27 panels and a corresponding 243 design variables.
- 2. **Symmetry Axis Panels:** In addition to the 27 primary panels, two extra panels represent the ship's symmetry axis. These panels help define essential boundary conditions within the model.
- 3. **Equality Constraints:** A network of 54 equality constraints links various design variables, guaranteeing that the model meets specific requirements and standards.
- 4. **Geometrical Constraints:** The model incorporates 243 geometrical constraints originating from the nine design variables associated with each of the 27 panels. These constraints are fundamental to maintaining the structural integrity and shape of the ship.
- 5. **Structural Constraints:** To account for different load cases, 486 structural constraints are introduced, effectively two constraints for each of the 243 design variables. These constraints are essential in considering the ship's performance under varying conditions.
- 6. **Hull Ultimate Strength Constraints:** Finally, two constraints specifically target the hull's ultimate strength, ensuring that the model accurately reflects the ship's structural limitations and safety considerations.

The detailed breakdown of the mesh model's elements provides a solid research foundation. It allows analysis of the multipurpose cargo ship unit's structural behaviour, performance and optimisation in a complex and dynamic framework. This contribution to naval architecture and engineering adds to the existing body of knowledge.

6.8 Case Study 2

This study investigated the costs associated with the production processes of cutting, forming, welding, assembly and transportation in the manufacturing of steel hulls.

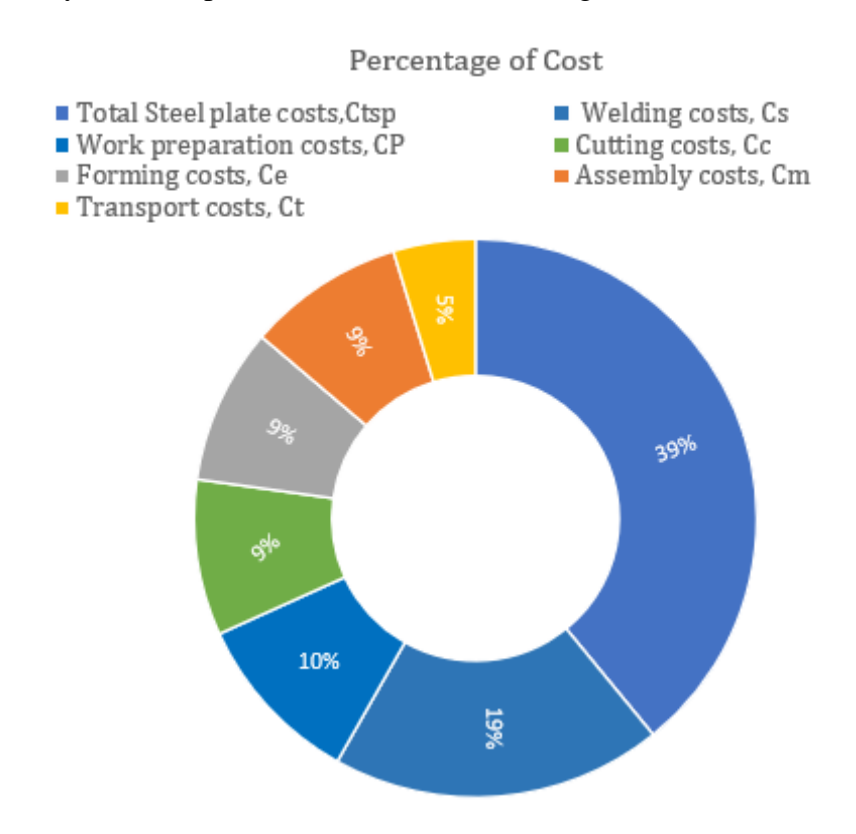


Figure 6-5: Distribution of production costs for the analysed ship.

The detailed analysis in Figure 6–5 provides a comprehensive breakdown of the costs of manufacturing steel hulls. This research explores the financial intricacies, expounding how resources are allocated within this crucial industry. The comprehensive assessment of these cost allocations divulges several observations that are worth mentioning.

The allocation of 39% of production costs for procuring steel plates highlights the crucial role of high-quality steel in constructing the hulls. This allocation underlines the significance of sourcing first-rate materials to ensure the structural strength and durability of the final product. It also raises concerns regarding potential cost-saving strategies or alternative materials that could be explored to reduce this significant expenditure.

Welding and work preparation costs account for significant costs in hull construction, accounting for 19% and 10% of the overall costs, respectively. This highlights the importance of the precision and skill required during this crucial phase. Exploring ways to optimise welding

techniques and automate the process could help costs to be reduced while maintaining highquality standards.

Moreover, the fact that forming, assembly, and cutting costs contribute 9% to the production process highlights their significance in converting raw materials into the ultimate steel hull structure. By identifying the areas where these processes can be streamlined or made more efficient, costs can be reduced and production timelines can be amended.

Finally, it is essential to note that while transportation expenses may only account for 5% of the total production costs, they should not be overlooked. The research indicates that improving logistics and supply chain management can help reduce costs and improve operational efficiency.

This detailed cost allocation breakdown is fundamental for decision-makers in the steel hull fabrication industry. It undoubtedly explains how financial resources are allocated and proposes ways to optimise costs and improve processes. These findings are essential for developing knowledge in this field and guiding industry professionals and researchers towards more efficient and sustainable practices in regard to steel hull fabrication.

6.9 Optimised Results and Pareto Front

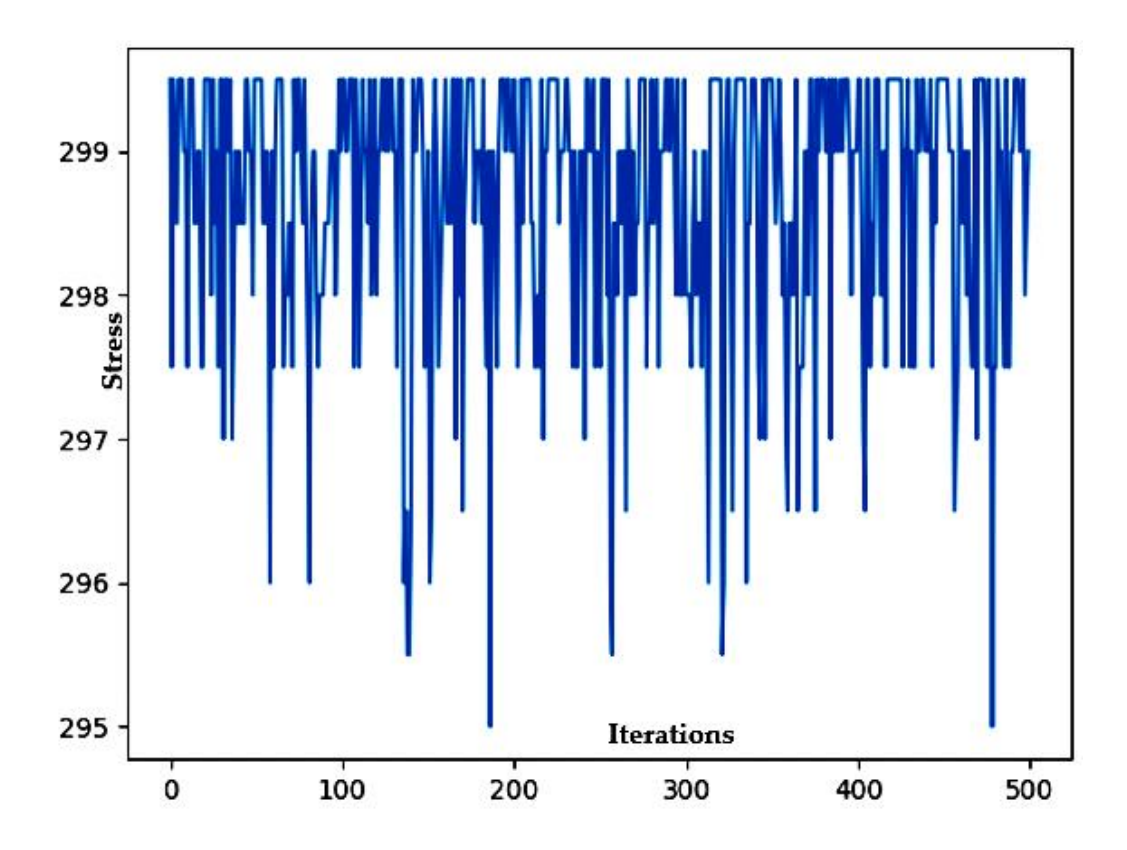


Figure 6-6: Number of Iterations vs. Best Individual Stress Value.

Figure 6–6 is a multi-history chart confirming the relationship between the number of iterations and the ideal hull girder Von Mises stress parameter values in ship optimisation. This visual representation provides a valuable resource for researchers, engineers, and designers optimising ship scantlings. The analysis shows two significant optimisation milestones, one around the 190th iteration and another around the 490th iteration. At these points, the carefully adjusted dimensions of the ship's structure achieve a remarkable balance. Within this balance zone, the hull girder Von Mises stress values remain consistent between 295 MPa and 299.8 MPa, which it is worth mentioning, is quite remarkable. This achievement reflects the precision and effectiveness of the optimisation process, striking a harmonious balance between ensuring structural integrity and optimising the application of materials. Hence, Figure 6-6 provides a critical reference point for future research, permitting data-driven decisions in ship design that prioritise safety and resource efficiency, ultimately progressing sustainable and cost-effective maritime engineering.

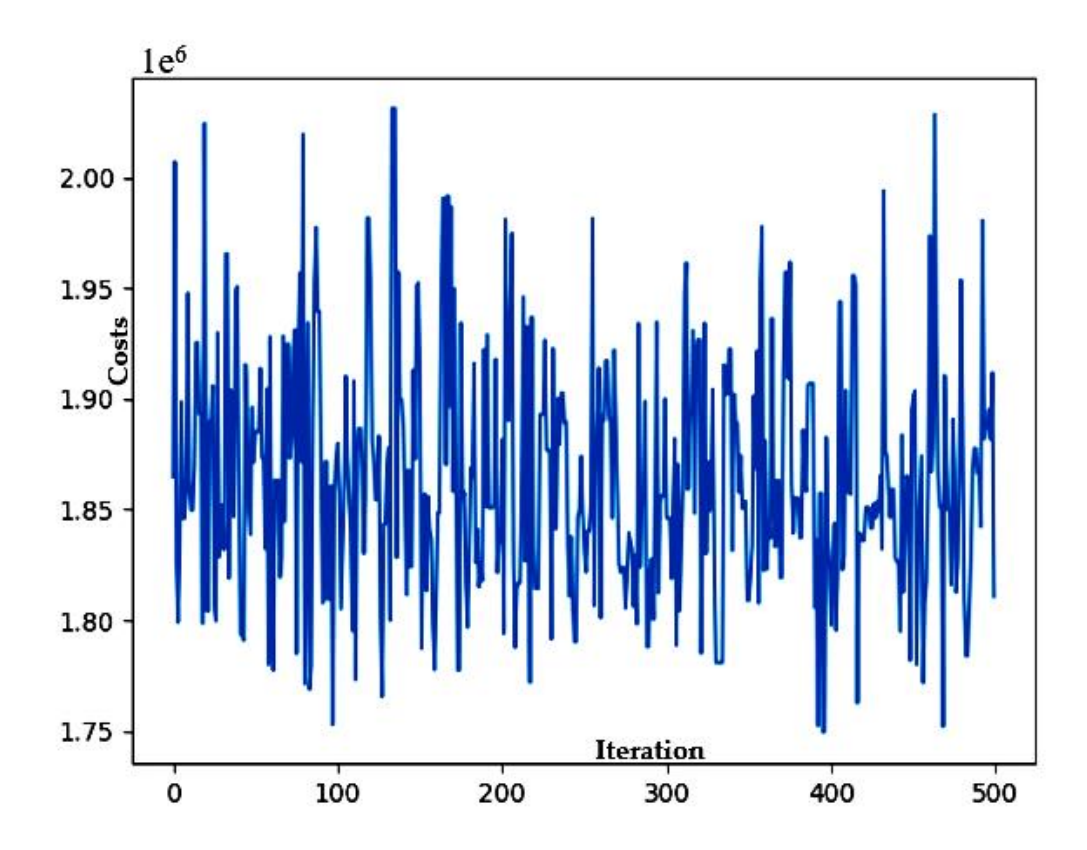


Figure 6-7: Number of Iterations vs. Best Individual Production Cost Value.

Figure 6–7 shows a comprehensive visual representation of the iterative optimisation process and its impact on the ideal production costs of the analysed ship, providing valuable insights into the convergence and variation patterns. The chart exhibits a multi-history perspective, tracking the relationship between the number of iterations and the corresponding ideal production cost values. Remarkably, the research reveals specific milestones within the iterative process where distinct trends emerge. Around the 140^{th} and 480^{th} iterations, the production cost estimates for the optimised ship reach a convergence point, stabilising at an upper threshold of approximately €2,035,000. These points signify a saturation in cost reduction benefits, implying that further iterations may yield diminishing returns regarding cost optimisation.

Conversely, the above figure demonstrates a noticeable decline at approximately the 100th, 400th and 480th iterations, reaching a minimum threshold of approximately €1,750,000. These inflexion points represent key junctures in the optimisation process, denoting extensive improvements in cost-effectiveness and highlighting the efficacy of the applied methodology. This understanding of iterative progression helps refine optimisation strategies, guiding decision-making in ship design and contributing to enhanced cost-efficiency and performance in maritime operations.

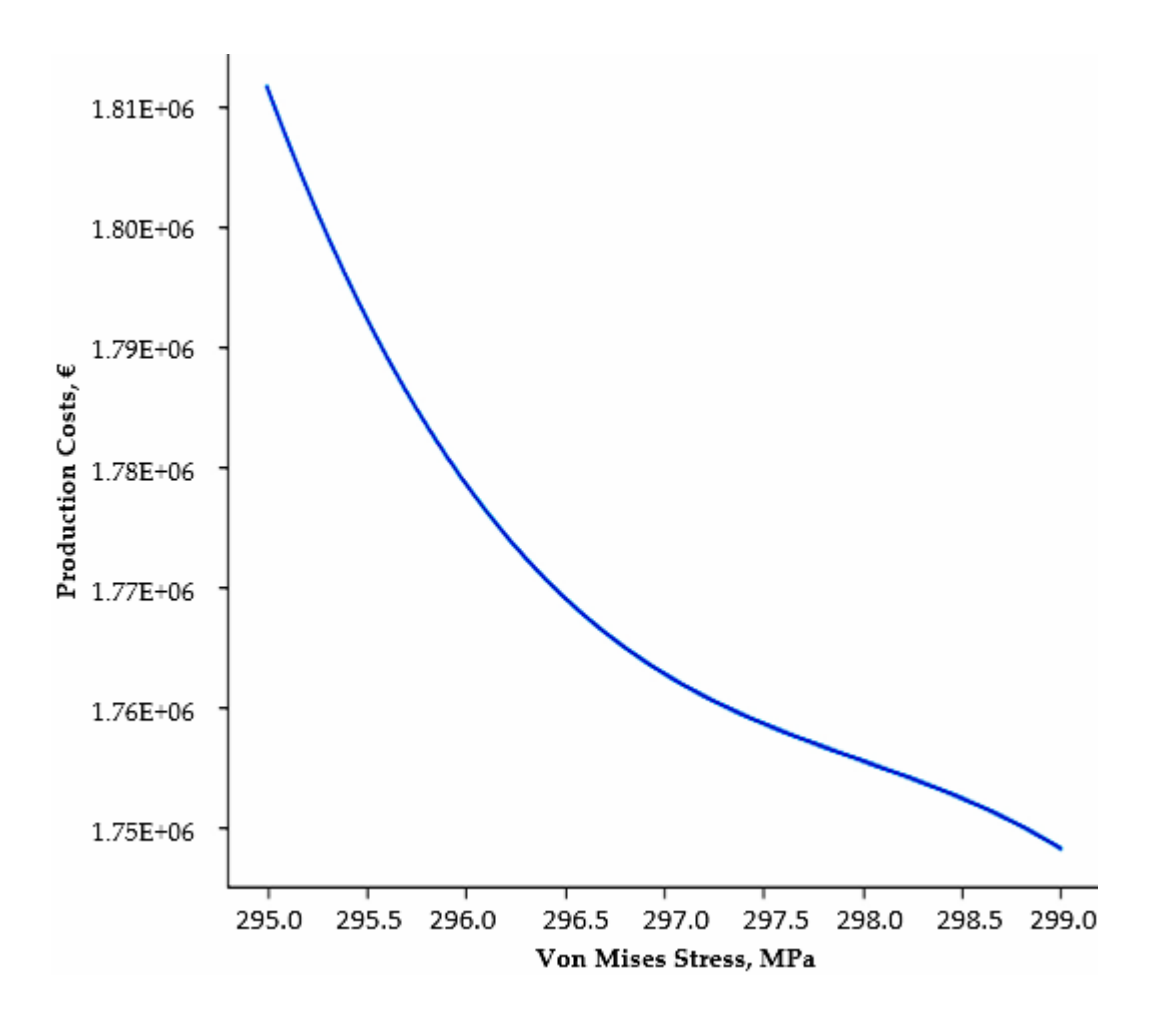


Figure 6-8: Pareto Optimal curve: Costs vs. Stress.

Figure 6–8 shows the Pareto optimal curve, illustrating the relationship between production cost values and hull girder stress values for the optimised analysed ship. This graph is a crucial tool for designers and decision-makers, providing an intuitive way to navigate the complex trade-offs between structural integrity and cost-effectiveness. In this context, the Pareto optimal curve outlines the Pareto front, a set of non-dominated solutions in the multi-objective optimisation setting. In this research, the Pareto optimal frontier occurs at a hull girder stress value of 296.2 MPa, corresponding to a production cost of approximately €1,770,000. The convergence point emphasised in Figure 6–8 provides an excellent solution that balances strong structure and cost-effectiveness. Designers can draw worthwhile information from this figure and opt for the optimal configuration that is consistent with their priorities and constraints. Consequently, Figure 6–8 significantly contributes to ship design as it permits stakeholders to make informed decisions that improve safety and economic viability in challenging maritime environments.

Table 6–1 provides a concise comparison of critical factors in cargo hold design. It lists various components and their corresponding original and optimised net thickness, the initial and optimised cargo hold weight, besides production costs. The "Original Net Thickness" and "Optimised Net Thickness" columns reflect changes in material thickness created during the optimisation process. Conversely, the "Original Cargo Hold Weight" and "Optimised Cargo Hold Weight" columns illustrate weight variations before and after design enhancements. Lastly, the "Original Production Costs" and "Optimised Production Costs" columns offer insights into cost reductions achieved via optimisation. This table functions as a beneficial reference for decision-makers, enabling them to evaluate the overall impact of design changes on cargo hold parameters and production costs.

Table 6–1: Comparison of Original and Optimised Parameters for Cargo Hold Design.

Items	Original Net Thickness (mm)	Optimised Net Thickness (mm)	Cargo Hold Actual Weight (Tonnes)	Cargo Hold Optimised Weight (Tonnes)	Initial Production Costs (€)	Optimised Production Costs (€)
Keel Plate	11.5	10.0				
Bottom Plate	9.5	8.5				
Side Shell Plate	8.5	7.5				
Shear Strake Plate	10.5	9.0				
Main Deck Plate	13.5	11.0				
DB Longitudinal Girder, CL	16.0	19.0				
Inner Side Shell Plate-1	12.5	8.5				
Inner Side Shell Plate-2	7.5	8.5	639.50	573.35	1,971,315.00	1,770,000.00
Inner Side Shell Plate-3	10.5	8.5				
Inner Bottom Plate-1	13.5	11.5				
Inner Bottom Plate-2	10.0	11.5				
Hatch Coaming Plate	14.0	12.5				
Hatch Coaming Top Plate	21.0	19.5				
Web Frame Spacing	1430.0	1484.0				
Stiffener Spacing	631.0	648.0				

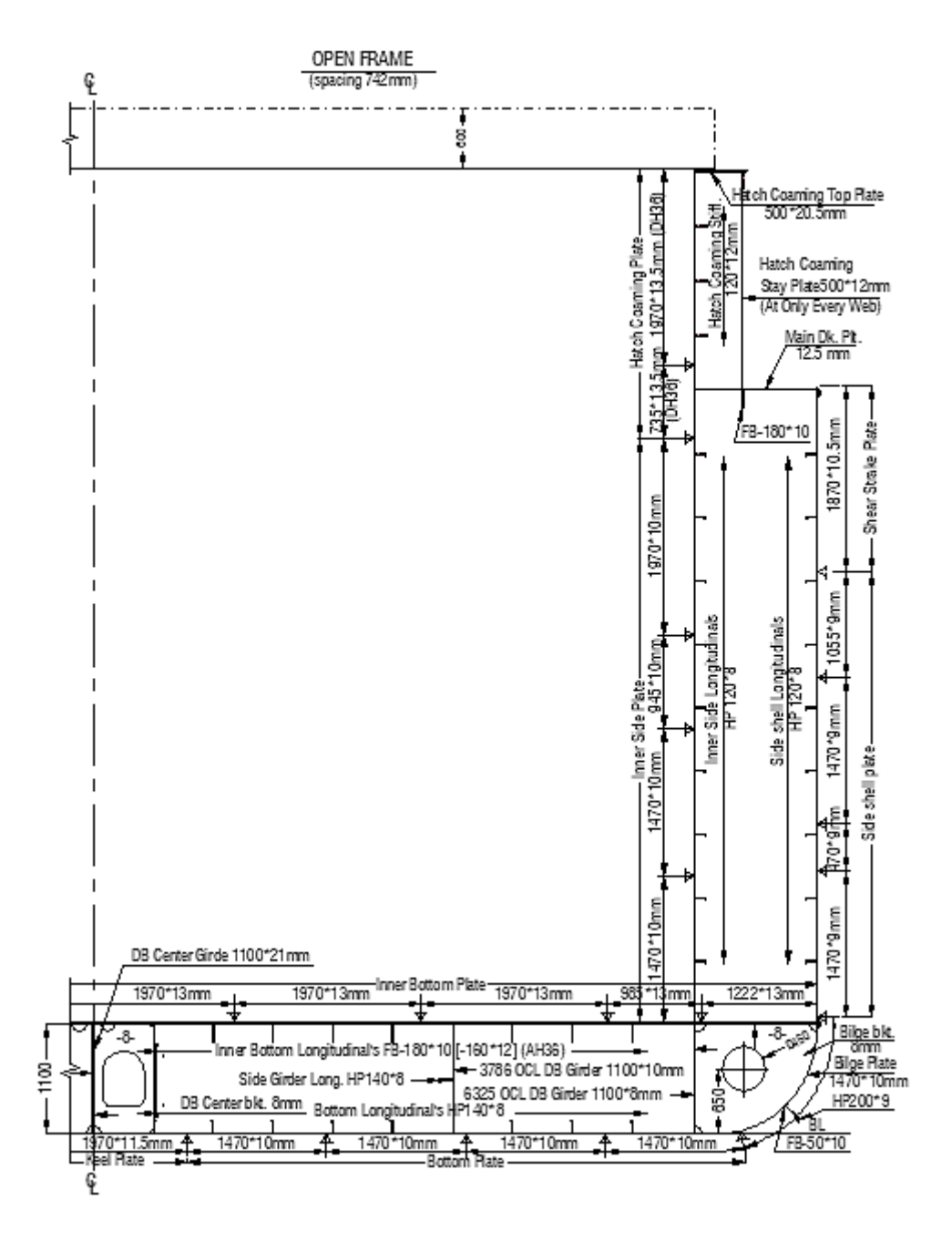


Figure 6-9: Midship section of the investigated ship after optimisation.

Figure 6–9 shows the midship section of a multipurpose cargo ship following an optimisation process. In this revised midship section design, the scantling has been optimised, centring on the gross plate thickness. The gross plate thickness in the figure signifies that it represents the total thickness of structural plates and frames in the midship section of the ship. By optimising the plate thickness, the design aims to enhance structural integrity while minimising weight, thereby improving the overall performance and efficiency of the ship.

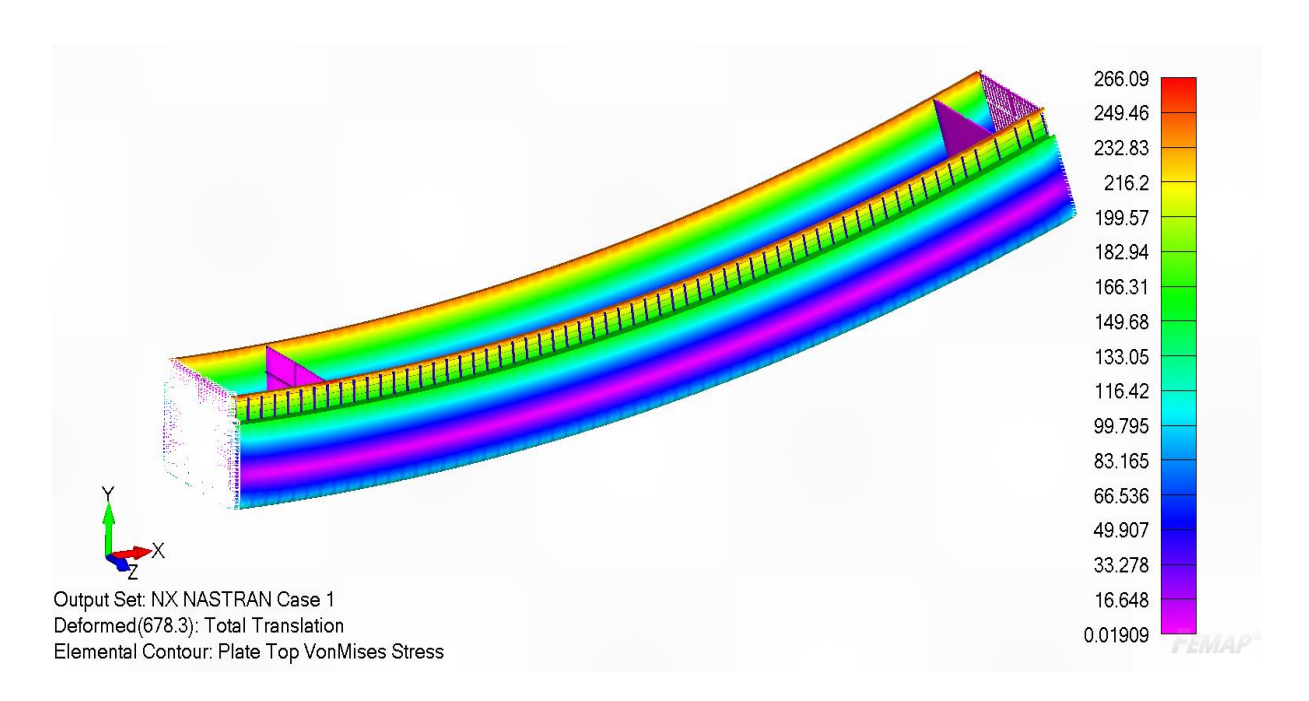


Figure 6-10: Before optimisation, hull girder Von Mises stress at midship (Sagging—upright condition).

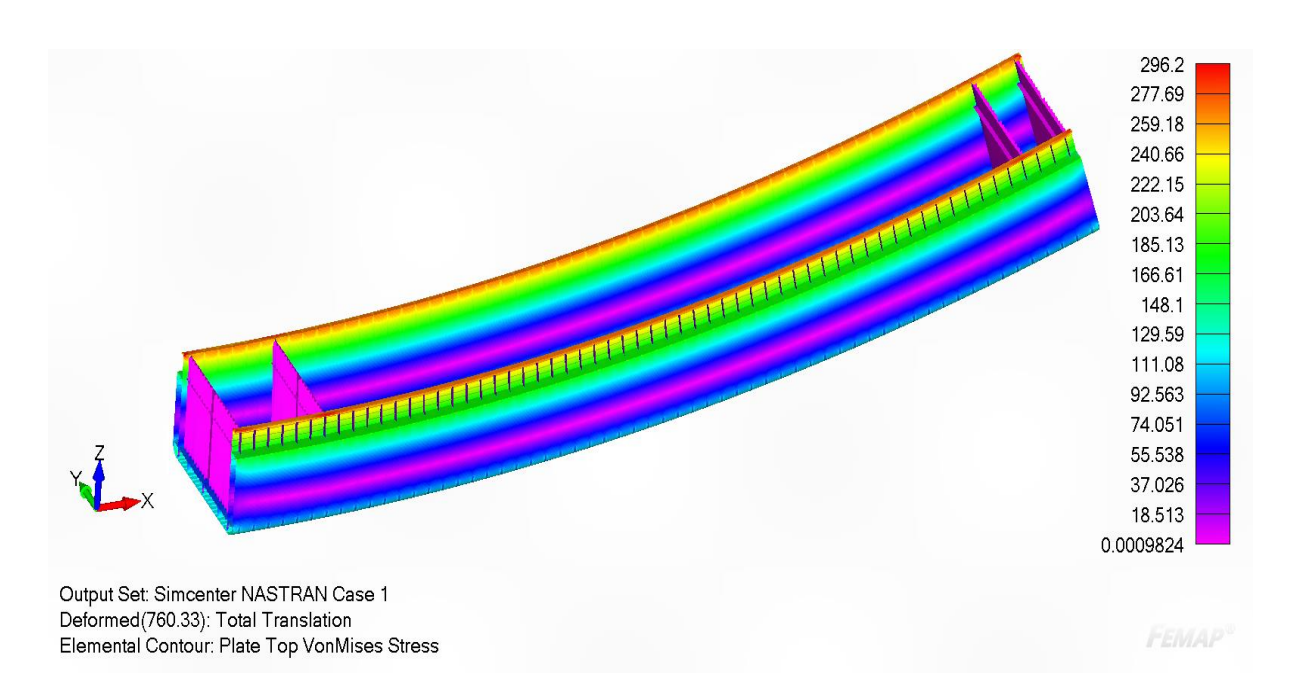


Figure 6-11: After optimisation, hull girder Von Mises stress at midship (Sagging—upright condition).

Figure 6–11 shows the Von Mises stress distribution along the ship's hull girder at the midship section during the sagging (upright) condition following optimisation. A significant increase in Von Mises stress is evident, rising from 266.09 MPa (Figure 6–10) to 296.2 MPa after optimisation. This remarkable variation in stress stems from calculated modifications made

during optimisation, specifically in plate thickness, web frame reconfiguration and stiffener spacing. Von Mises stress measures the stress state at a point and is utilised to predict material yielding under complex loading. The increase in Von Mises stress indicates the potential for yielding or failure in the affected areas of the ship's hull girder, accentuating the importance of carefully considering the structural implications of design modifications aimed at ship performance and safety.

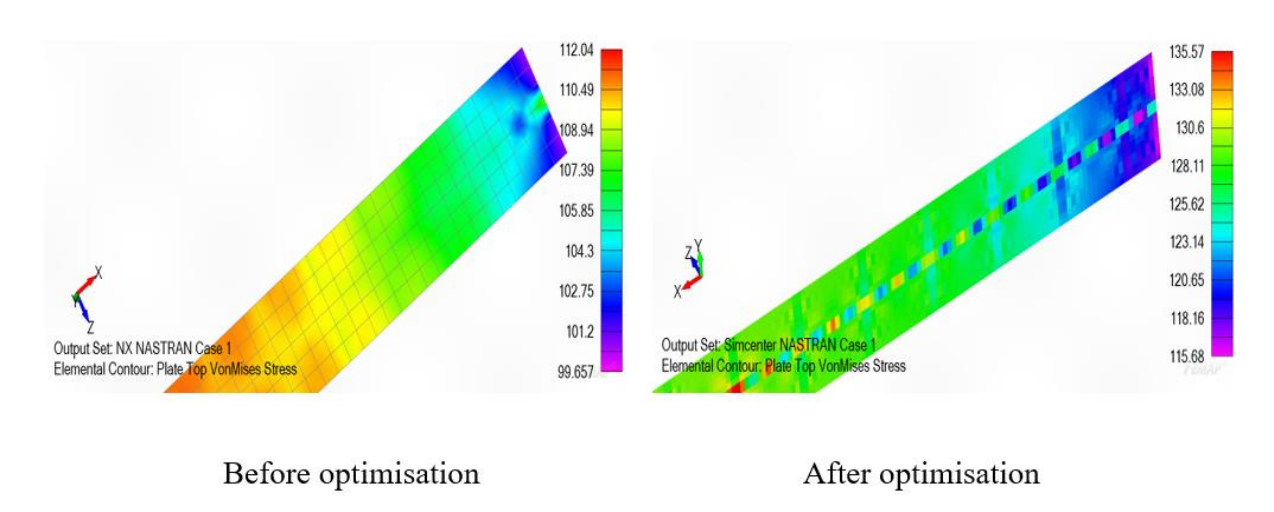


Figure 6-12: Keel plate Von Mises stress.

In Figure 6–12, the Von Mises' stress in the ship's keel plate was registered at 112.04 MPa before optimisation and increased to 135.57 MPa after optimisation. Nevertheless, it is important to state that even after optimisation, these stress levels consistently remained beneath the principal allowable stress limit of 219.42 MPa prescribed for grade-A steel. This demonstrates a safety factor of approximately 1.62, indicating that the keel plate's structural integrity has been maintained within safe operational parameters.

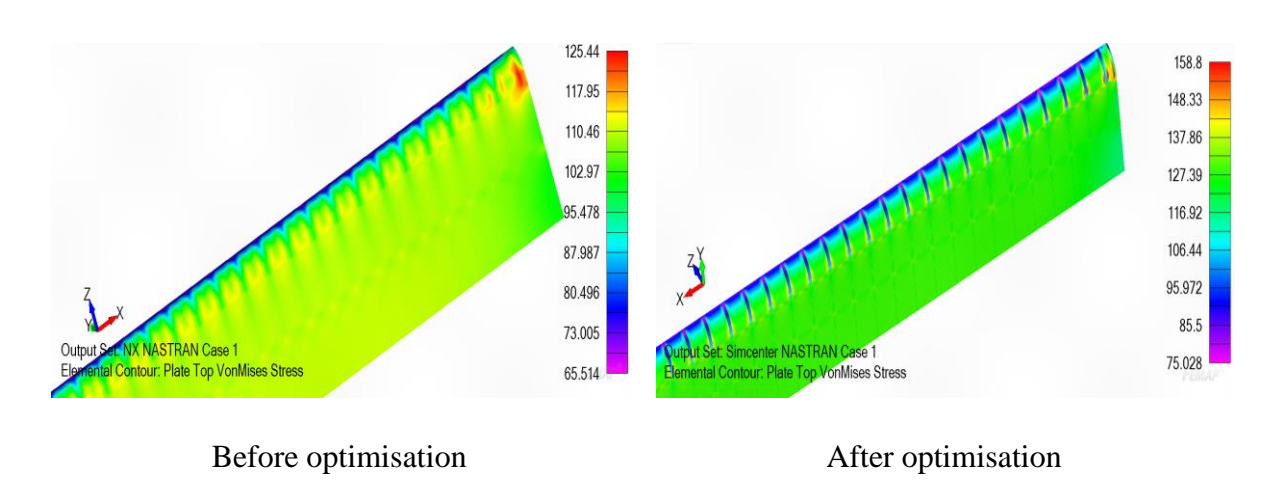


Figure 6-13: Bottom plate Von Mises stress.

Figure 6–13 shows the Von Mises stress distribution in the ship's bottom plate, measuring 125.44 MPa before and 158.8 MPa after optimisation. It is crucial to mention that these stress levels consistently remain within a safe operational range notwithstanding the enhanced stress levels post-optimisation. The master allowable stress limit, set at 219.42 MPa for grade-A steel, remains unbreached, bringing about a safety factor of approximately 1.38.

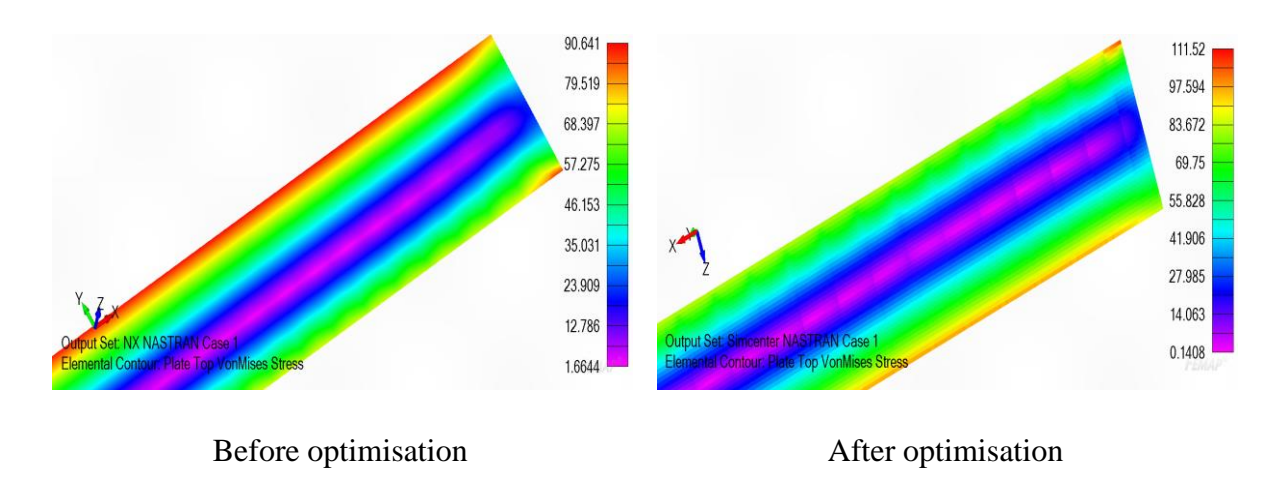


Figure 6-14: Side shell plate Von Mises stress.

Figure 6–14 shows the Von Mises stress distribution in the ship's side shell plate, exhibiting values of 90.64 MPa before optimisation and 111.52 MPa after optimisation. It is evident that post-optimisation stress levels constantly remain significantly below the stringent master allowable stress limit of 219.42 MPa, designed for grade-A steel, producing a safety factor of 1.97. This reaffirms the structural reliability of the ship's side shell plate, demonstrating its continued compliance with stringent safety standards even after the optimisation process.

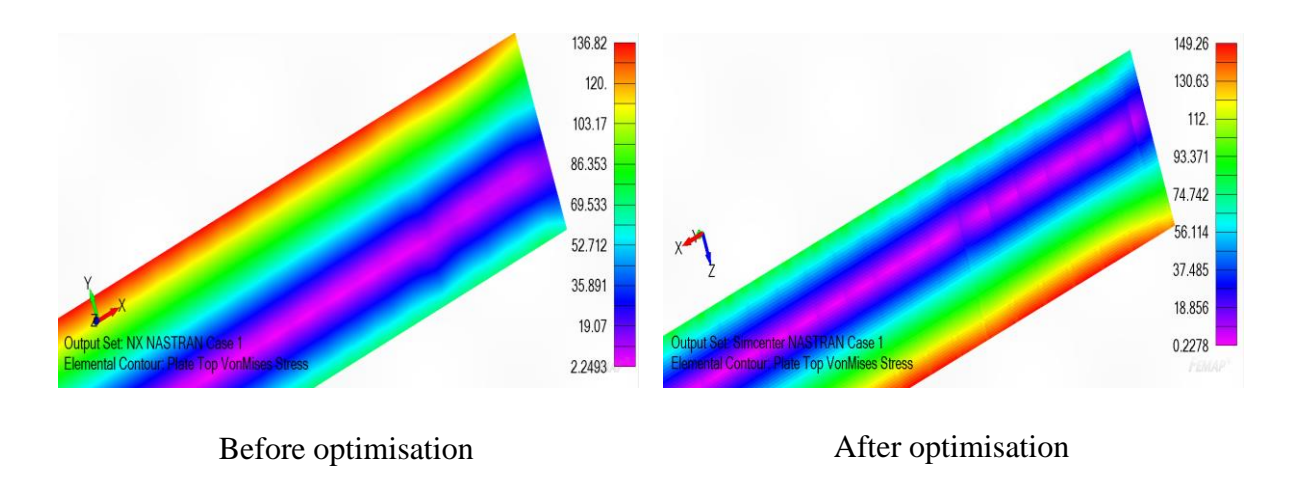


Figure 6-15: Inner side shell plate Von Mises stress.

Figure 6–15 shows the Von Mises stress distribution of the analysed ship's inner side shell plate. The pre-optimisation stress value was 136.82 MPa, which increased to 149.26 MPa post-optimisation. Notwithstanding the reduction in plate thickness and the subsequent increase in stress concentration following optimisation, the Von Mises stress in the optimised inner side shell plate remains comfortably below the defined allowable stress limit of 219.42 MPa for grade-A steel, generating a safety factor of approximately 1.47.

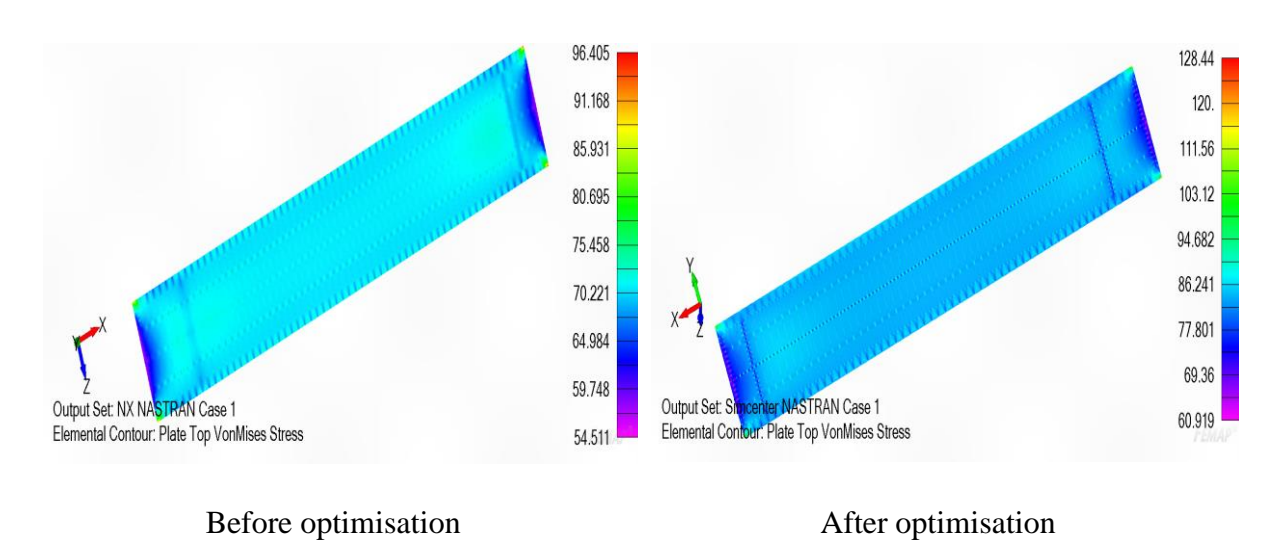


Figure 6-16: Inner bottom plate Von Mises stress.

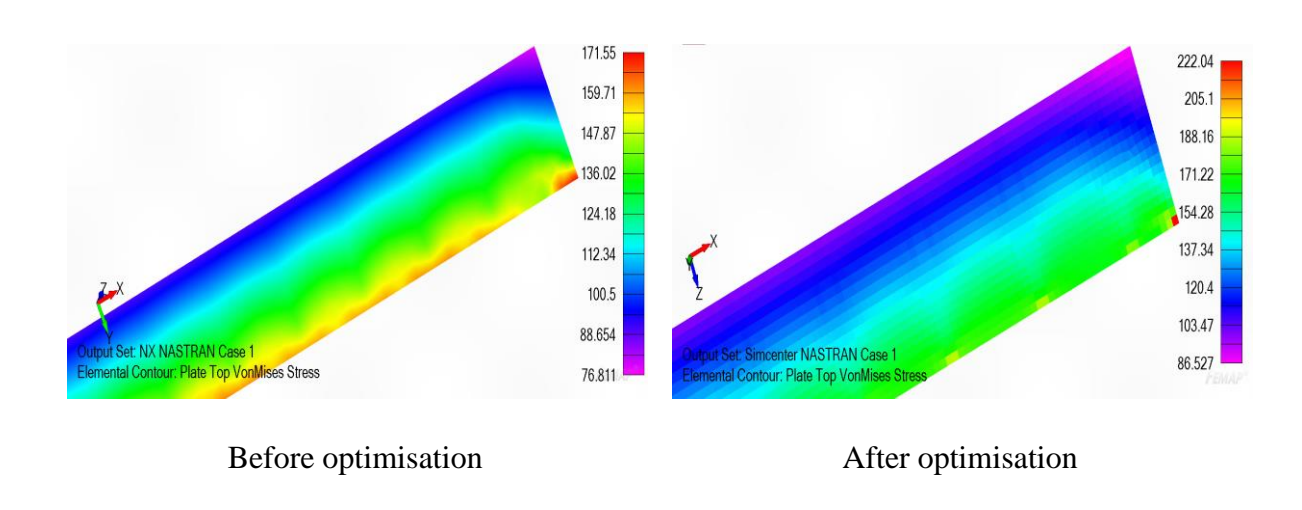


Figure 6-17: Shear strake plate Von Mises stress.

Figure 6–1 shows the Von Mises stress distribution in the analysed ship's shear strake plate. Following a reduction in plate thickness, the stress level increased to 222.04 MPa after optimisation, compared to the pre-optimisation value of 171.55 MPa. It is worth mentioning that even after optimisation, the Von Mises stress remains below the allowable stress threshold

of 331.77 MPa, as identified for high-tensile steel (Grade AH36), prompting a safety factor of approximately 1.49. This observation endorses the preserved structural integrity of the ship's design without compromise.

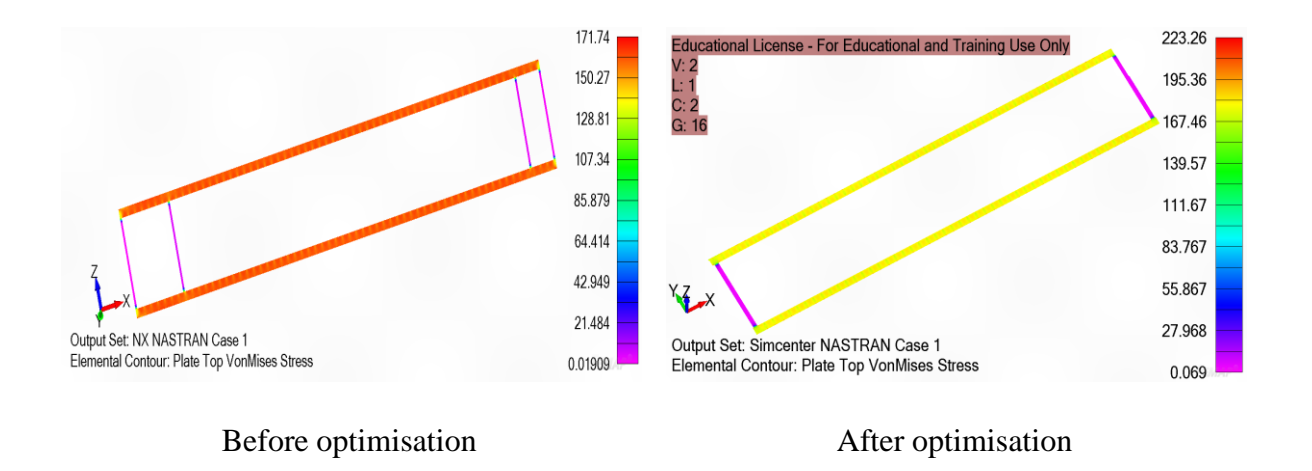


Figure 6-18: Main Deck plate Von Mises stress.

Figure 6–18 shows the Von Mises stress distribution on the analysed ship's main deck. Of note is that the Von Mises stress in the optimised state reached 223.26 MPa, as opposed to the preoptimisation value of 171.74 MPa. Notwithstanding this increase in stress attributable to the thickness reduction of the main deck, the Von Mises stress consistently remains below the allowable stress threshold of 331.77 MPa for high-tensile steel (Grade AH36), generating a safety factor of approximately 1.49. This observation accentuates the structural integrity of the optimised main deck plate, reiterating its continuous adherence to rigorous safety standards.

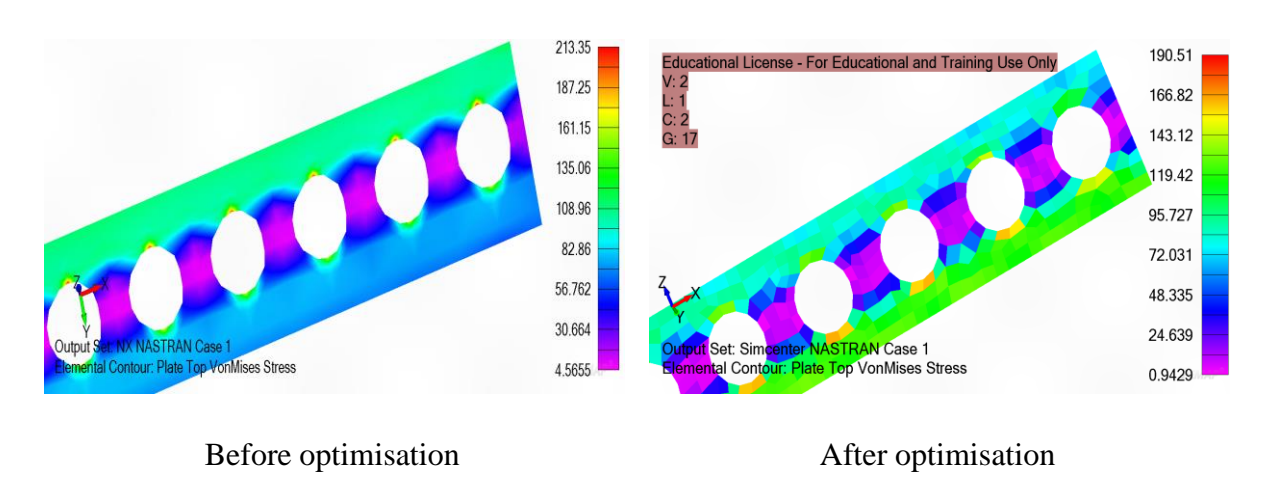


Figure 6-19: DB longitudinal girder, CL (Centre Line) Von Mises stress.

Figure 6–19 shows the Von Mises stress distribution within the analysed ship's DB longitudinal girder, specifically the CL (centre line) section. The Von Mises stress was calculated at 213.35 MPa before optimisation, but an increase in plate thickness decreased to 190.51 MPa post-optimisation. This easily remains well below the allowable stress threshold of 219.42 MPa, as stipulated for mild steel (Grade A), producing a safety factor of approximately 1.15. These results signify the robust structural integrity of the optimised DB longitudinal girder CL, confirming compliance with safety standards and providing evidence of material appropriateness and process effectiveness.

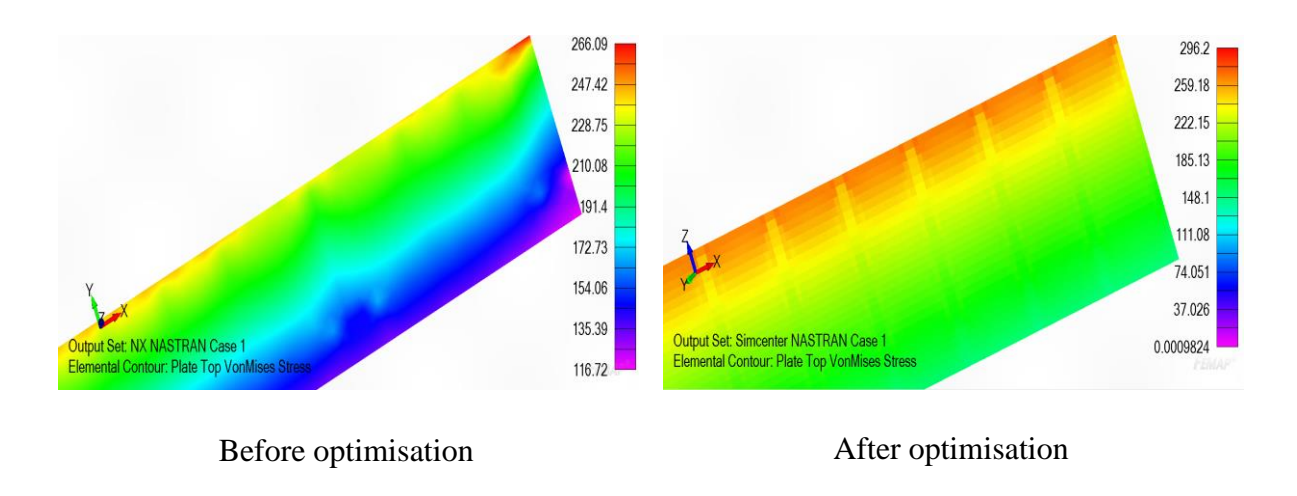


Figure 6-20: Hatch coaming plate Von Mises stress.

Figure 6–20 shows the distribution of Von Mises stress within the hatch coaming plate of the analysed vessel. The Von Mises stress rose from 266.09 MPa to 296.20 MPa in the optimised state compared to its initial condition. While this increase in Von Mises stress is prominent post-optimisation, it remains below the allowable stress threshold of 331.77 MPa, as specified for high-tensile steel (Grade AH-36). This result yields a safety factor of approximately 1.12, asserting the considerable structural integrity of the optimised hatch coaming plate.

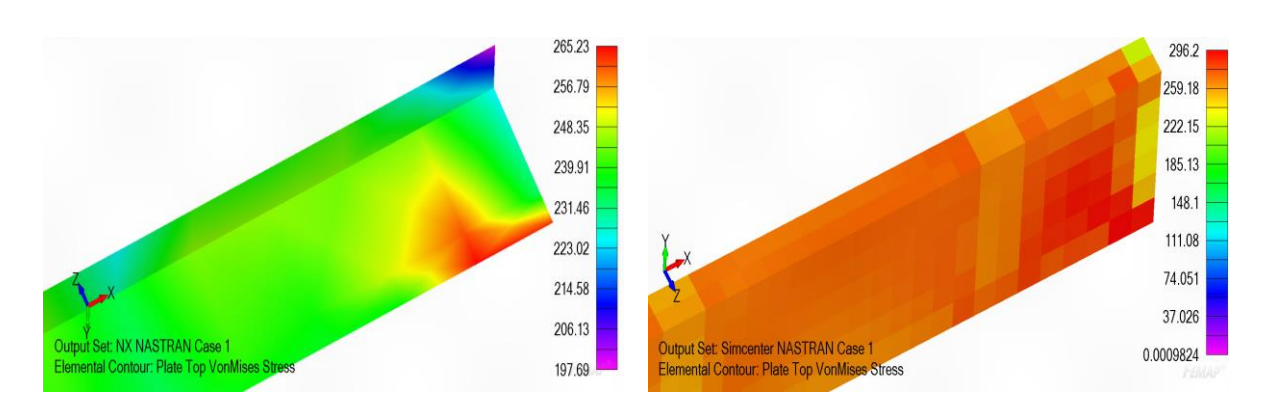


Figure 6-21: Hatch coaming top plate Von Mises stress.

Figure 6–21 shows the Von Mises stress distribution within the hatch-coaming top plate of the analysed vessel. Post-optimisation, the Von Mises stress intensified to 296.20 MPa from its pre-optimisation level of 266.23 MPa. While this notable increase in Von Mises stress accompanies the reduction in plate thickness during optimisation, it consistently remains below the allowable stress threshold of 331.77 MPa, as denoted for high-tensile steel (Grade AH-36). This result generates a safety factor of approximately 1.12, affirming the robust structural integrity of the optimised hatch coaming top plate.

Table 6–2 briefly compares Von Mises stress factors before and after optimisation, alongside allowable stress thresholds. It provides a comprehensive overview of critical ship components, presenting initial stress levels as a baseline, post-optimisation stress values, and acceptable stress limits by industry standards.

Table 6–2: Von Mises stress before and after optimisation.

Sr. No.	Description	Von Mises Stress before Optimisation (MPa)	Von Mises Stress after Optimisation (MPa)	Allowable Stress (MPa)
1	Keel Plate	112.04	135.57	219.42
2	Bottom Plate	125.44	158.8	219.42
3	Side Shell Plate	90.64	111.52	219.42
4	Shear Strake Plate	171.55	222.04	331.77
5	Main Deck Plate	171.74	223.26	331.77
6	DB Longitudinal Girder	213.35	190.51	219.42
7	Inner Side Shell Plate	136.82	149.26	219.42
8	Inner Bottom Plate	96.41	128.44	219.42
9	Hatch Coaming Plate	266.09	296.20	331.77
10	Hatch Coaming Top Plate	265.23	296.20	331.77

6.10 Validation

Optimising ship structures is essential in the maritime sector to improve performance and efficiency [6]. By validating the optimised design, potential issues can be detected and resolved early on, leading to a more economically efficient and reliable final product [210]. Validating optimised ship structures is paramount for several compelling reasons:

- It is critical to ensure safety and reliability by reducing the risk of structural failure during operation [189].
- Validation is fundamental to comply with regulations and standards regarding stability,
 strength and environmental performance [211].
- It is essential to ensure that the improved design functions optimally, studying factors such as hydrodynamics, stability and fuel efficiency [212].
- The validation process can quickly identify potential issues in the design phase, promoting cost-effectiveness by preventing expensive revisions later [189].
- Validation provides stakeholders, including ship owners, operators and regulatory authorities, with confidence that the optimised structure has undergone rigorous testing and is fit for its intended purpose [189].

Validating optimised ship structures is indispensable for safety, regulatory compliance, performance optimisation, cost-efficiency and building trust among customers and stakeholders.

6.10.1 The Imperative for Validating Optimised Midship

Validation checks are essential in ship design and naval architecture to ensure the optimised midship section. These checks serve various purposes, such as guaranteeing safety, verifying improvements in performance, adhering to regulatory standards, promoting cost-efficiency, minimising uncertainty and risks, along with instilling client trust. These assessments are decisive in connecting theoretical design ideas with practical implementation, instilling stakeholder confidence, and mitigating potential risks [210].

- Safety: Confirming that the optimised midship section complies with the necessary structural and stability criteria is paramount. Any imperfections or shortcomings in the midship section's design could give rise to structural breakdowns or problems related to instability while the ship is in operation, potentially leading to accidents, damage or in the worst-case scenario, loss of life [213].
- Performance: An optimised midship section is conventionally tailored to enhance multiple facets of a ship's performance, encompassing fuel efficiency, speed and manoeuvrability. The execution of rigorous validation assessments is crucial in

substantiating the attainment of expected improvements in performance, acknowledging the ship's capability to operate using its intended specifications within real-world operational scenarios [214].

- **Regulatory Compliance:** Ships are subject to many international and domestic regulations and guidelines that dictate their design, construction and operational parameters. The rigorous validation checks are instrumental in verifying the adherence of the optimised midship section to these stipulations, thereby mitigating the risk of encountering legal and operational issues [215].
- Efficiency and Cost-effectiveness: The optimisation of the midship section can lead to cost reductions via decreased fuel consumption and improved cargo capacity. Validation tests verify the actualisation of these advancements in efficiency, consequently enhancing the ship's overall cost-efficiency [214].
- Reducing Risk and Uncertainty: The ship design process entails intricate computations and simulations. Validation assessments act as a way to mitigate the inherent risks and uncertainties associated with an exclusive reliance on theoretical models. These assessments deliver empirical data that corroborate the precision of the design assumptions and forecasts [216].
- Client Confidence: Ship proprietors, operators and prospective customers frequently demand validation assessments to assure the operational proficiency and safety of the vessel they are considering or in regards to operation. Supplying validation data can be a convincing way for ship constructors and architects to sell a vessel [213].

The requisite validation examinations for the optimised midship section are imperative, ensuring the safety, performance, adherence to regulatory standards and the ultimate success of a ship's design. Their essential role in promoting stakeholder confidence and managing potential risks in advance cannot be overstated.

6.10.2 Progressive Collapse Analysis of Ship Hull Girder

Smith's approach has gained extensive recognition for conducting progressive collapse assessments of a ship's hull girder when subjected to longitudinal bending. This technique involves the division of a hull girder's cross-section into plate and stiffened-panel elements,

allowing for the predetermined establishment of an average stress-strain relationship under uniaxial tension/compression, considering factors such as buckling and yielding [217].

A study on the progressive collapse analysis of a hull girder using Smith's method.

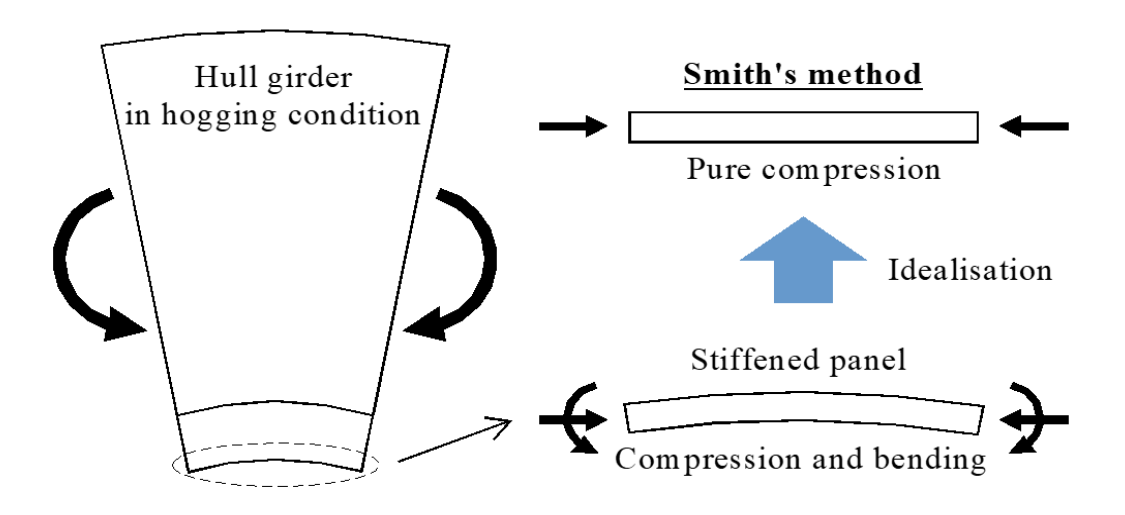


Figure 6-22: Curvature due to hull girder bending [217].

Figure 6–22 offers a comprehensive visual representation of the curvature observed in a ship's hull when it undergoes hogging conditions. It emphasises the hull's upward bending deformation when subjected to the applied load according to Smith's method pertaining to pure compression. This illustration clarifies the complex behaviour of the stiffened panels incorporated within the ship's structural configuration when exposed to the simultaneous influences of compression and bending forces.

The simplified progressive collapse method is dependent on several key assumptions [218]:

- 1. **Simple beam assumption:** This assumption suggests that the cross-section remains plain throughout the progressive collapse process, with deviations occurring only when substantial deflection and local deformation are induced.
- Independency assumption: According to this assumption, there is no interaction or
 influence between adjacent elements during the collapse. It is well supported when the
 cross-section primarily encounters vertical bending.
- 3. **Interframe collapse assumption:** This assumption supposes that transverse frames possess sufficient strength, resulting in the failure of all elements in an inter-frame mode. However, this assumption is limited to traditional ship structural design and has

been addressed by extending the original Smith method. This extension accounts for the likelihood of overall grillage instability in lightweight ship structures.

6.10.3 Validation of the Optimised Midship Section

The validation of the structural integrity for the optimised midship section was meticulously conducted utilising the BV Mars 2000 software in strict adherence to the rigorous BV class rules and regulations. It is recognised that the regulations set forth by classification societies tend to lean toward conservatism. Consequently, when a validation process concurs with these rule-based regulations, it can be reasonably inferred that it will also meet the criteria set by finite element analysis. The design of the midship section of the multi-purpose vessel adheres meticulously to the standards and guidelines identified by the Classification Society. This adherence prudently considers ship structural design principles and factors, for instance loads, motions, accelerations, internal and external pressures, and the forces essential for the ship's hull structural scantling process, safeguarding compliance with yielding, buckling and ultimate strength requirements.

The vertical bending moments on the ship hull are assessed by [219], utilising load cases "a" and "b" for upright conditions (e.g., at rest or with surge, heave and pitch motions) and load cases "c" and "d" for inclined conditions (e.g., sway, roll and yaw motions) [220].

The scantling of the midship section is defined as the net thickness of the plate panel subject to in-plane hull girder stresses on the shorter side, meeting or exceeding the criteria presented in to satisfy yield criteria [220].

$$t = 14.9 \times C_a C_r s \, l \sqrt{\gamma_R \gamma_m \frac{\gamma_{S2} \, p_S + \gamma_{W2} \, p_W}{\lambda_L R_y}} \ge t_{min}, \tag{6-22}$$

where p_s is the still water pressure, p_w is the wave-induced pressure, s is the shorter side of plating, l is the longer side of plating, C_a is the aspect ratio of the plate panel, C_r is the coefficient of curvature, R_y is the minimum yield stress, whilst γ_R , γ_m , γ_{S2} , γ_{W2} are utilisation factors.

The minimum net shear sectional area A_{Sh} and the net section modulus W, for ordinary longitudinal stiffener subjected to lateral pressure, must not be less as stated in [220]:

$$A_{Sh} = 10 \times \gamma_R \gamma_m \beta_S \frac{\gamma_{S2} \, p_S + \gamma_{W2} \, p_W}{R_{\gamma}} \left(1 - \frac{s}{2l} \right) sl \tag{6-23}$$

$$W = \gamma_R \gamma_m \beta_b \frac{\gamma_{S2} p_S + \gamma_{W2} p_W}{m (R_V - \gamma_R \gamma_m \sigma_{X1})} \left(1 - \frac{s}{2l}\right) s l^2 \times 10^3$$
 (6-24)

where β_S and β_b are coefficients of structural members.

The combined critical stress, denoted as σ_{comb} , is determined for plate panels that experience compressive axial, bending and shear stress as described in [67]:

$$F \le 1 \text{ for } \frac{\sigma_{comb}}{F} \le \frac{R_{eH}}{2\gamma_R \gamma_m}$$
 (6–25)

$$F \leq \frac{4\sigma_{comb}}{\frac{R_{eH}}{\gamma_R \gamma_m}} \left(1 - \frac{\sigma_{comb}}{\frac{R_{eH}}{\gamma_R \gamma_m}} \right) \text{ for } \frac{\sigma_{comb}}{F} > \frac{R_{eH}}{2\gamma_R \gamma_m}$$
 (6-26)

where F and R_{eH} are compressive force and upper yield strength, respectively.

The critical buckling stress, σ_c for compressive axial and bending loads is explained as [67]:

$$\sigma_C = \sigma_E \text{ for } \sigma_E \le \frac{R_{eH}}{2}$$
 (6–27)

$$\sigma_C = R_{eH} \left(1 - \frac{R_{eH}}{4\sigma_E} \right) \text{ for } \sigma_E > \frac{R_{eH}}{2}$$
 (6-28)

where σ_E is the Euler buckling stress.

The critical buckling stress of the ordinary stiffeners is estimated as [67]:

$$\frac{\sigma_C}{\gamma_R \gamma_m} \ge |\sigma_b| \tag{6-29}$$

where σ_b is axial stress.

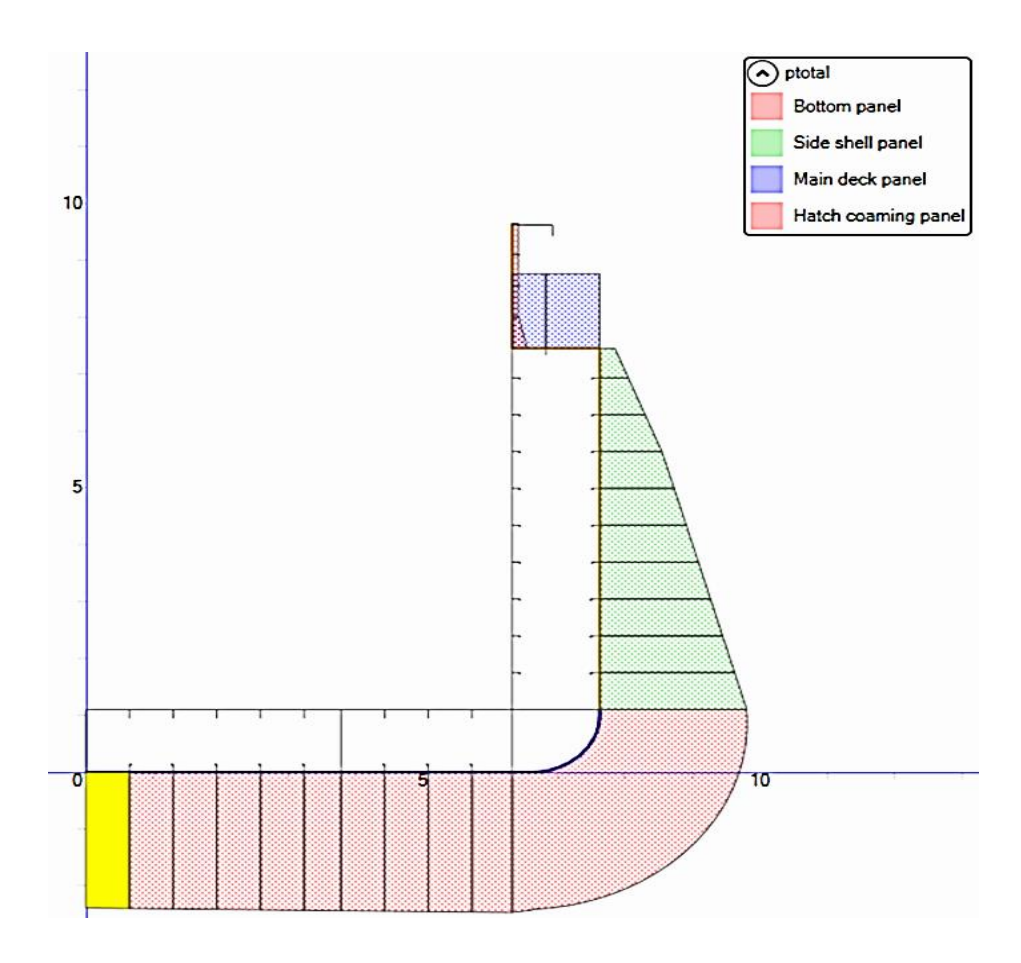


Figure 6-23: Local Sea loads acting on the hull (Head Sea).

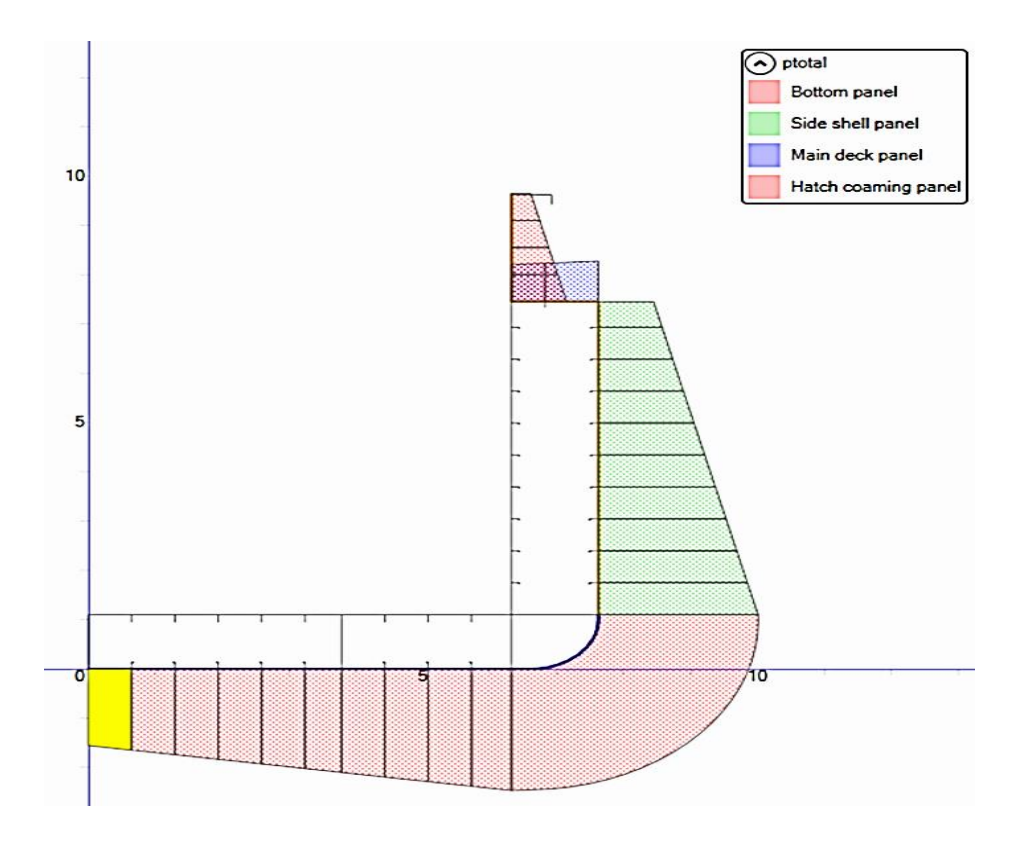


Figure 6-24: Local Sea loads acting on the hull (Beam Sea).

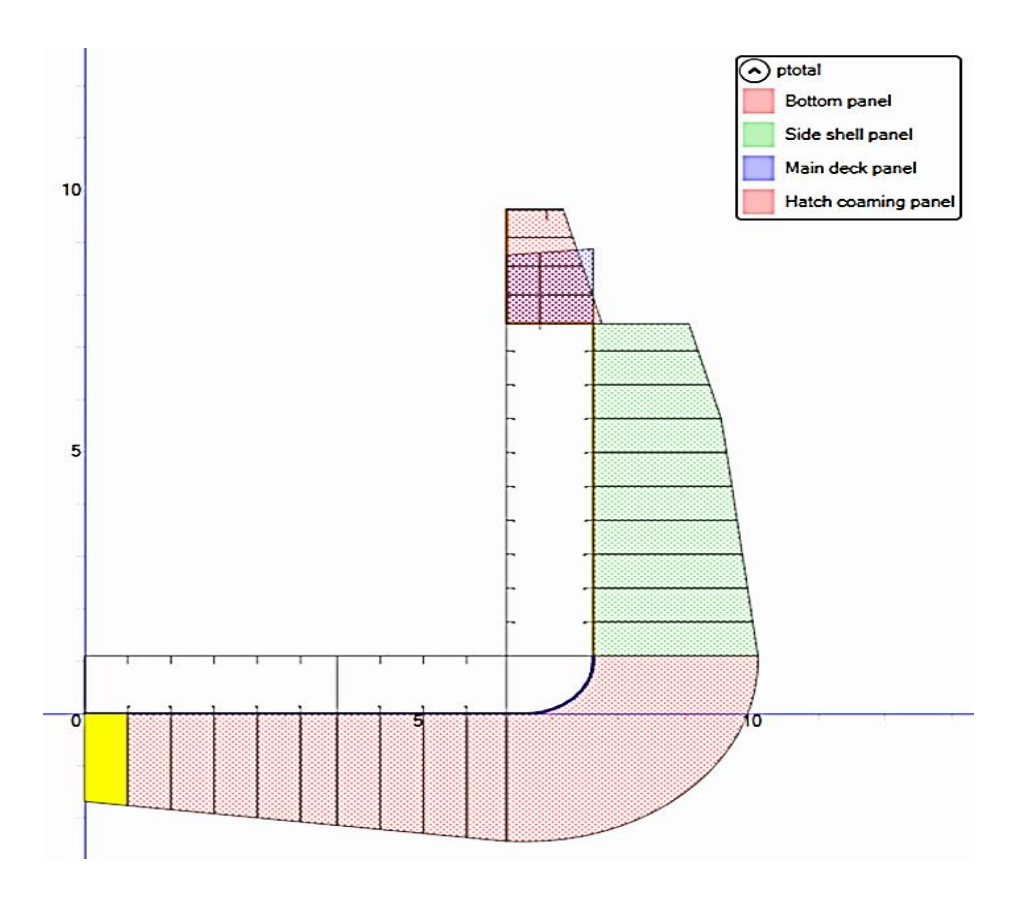


Figure 6-25: Local Sea loads acting on the hull (Oblique Sea).

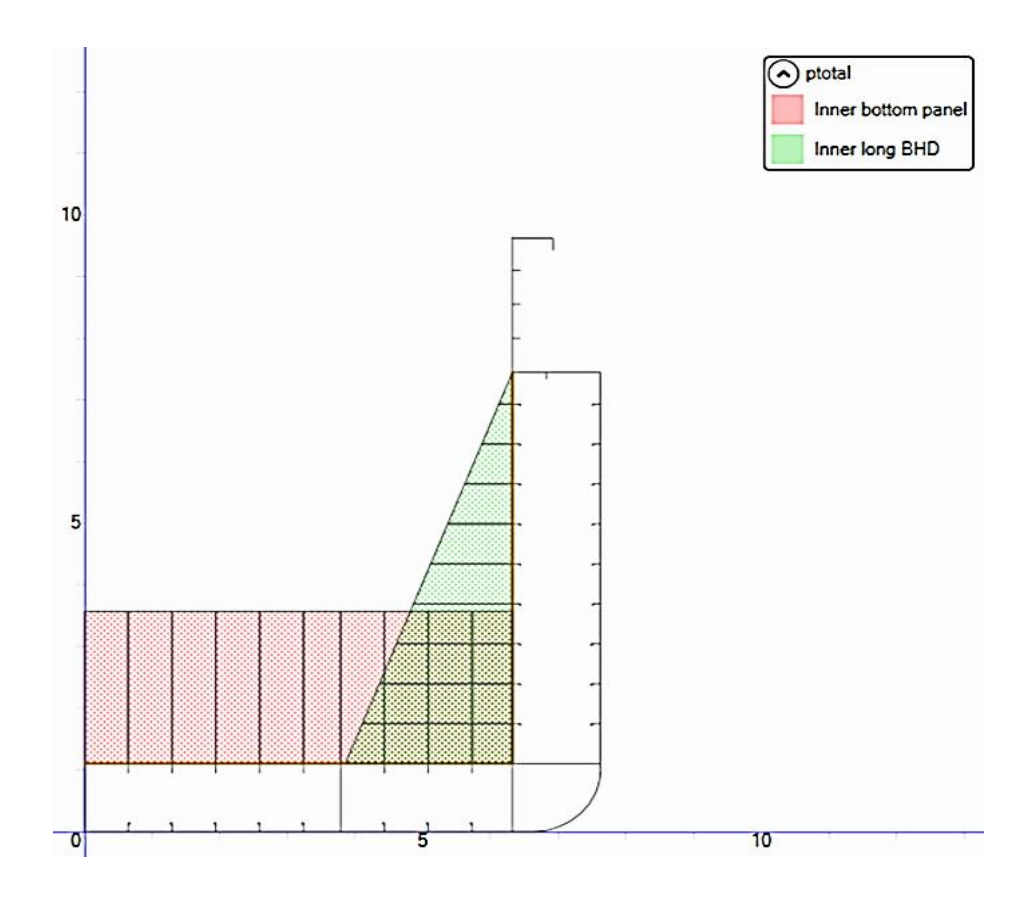


Figure 6-26: Cargo loads acting on the inner bottom and inner side shell.

Figures 6–23, 6–24 and 6–25 represent the local sea loads exerted on the hull, assisting to validate the optimised model. Figure 6–26 shows the cargo load acting on the vessel's inner bottom and inner side shell. The scantlings of the optimised model are determined by integrating these local sea loads and cargo loads with global hull girder loads. Local sea loads comprise hydrostatic pressure, hydrodynamic pressure, exposed deck pressure and weather pressure. Figures 6–23, 6–24 and 6–25 reveal that local sea loads are higher in the Oblique Sea than in the Head and Beam Sea.

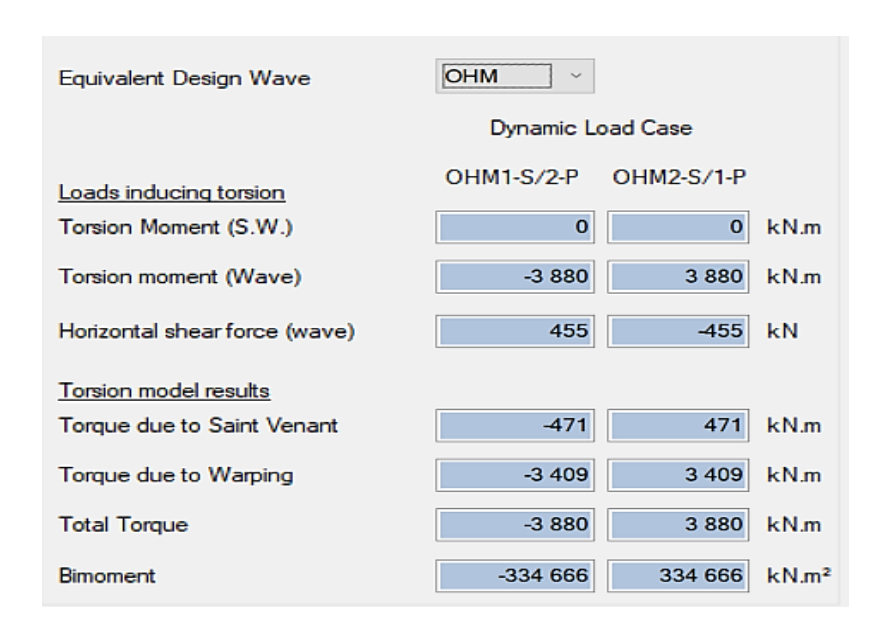


Figure 6-27: Torsional load acting on hull girder.

Figure 6–27 shows the torsional load exerted on the hull girder. It is assumed that there will be no cargo movement during sailing; hence, no still water torsional moment is considered. This assumption simplifies the analysis, focusing solely on the dynamic torsional loads experienced during operation. The torsional moments depicted are crucial for validating the scantlings of the optimised model, ensuring the hull can withstand stresses encountered under various operational conditions. Analysing these loads confirms that the design meets safety and performance standards, contributing to the vessel's structural integrity and longevity.

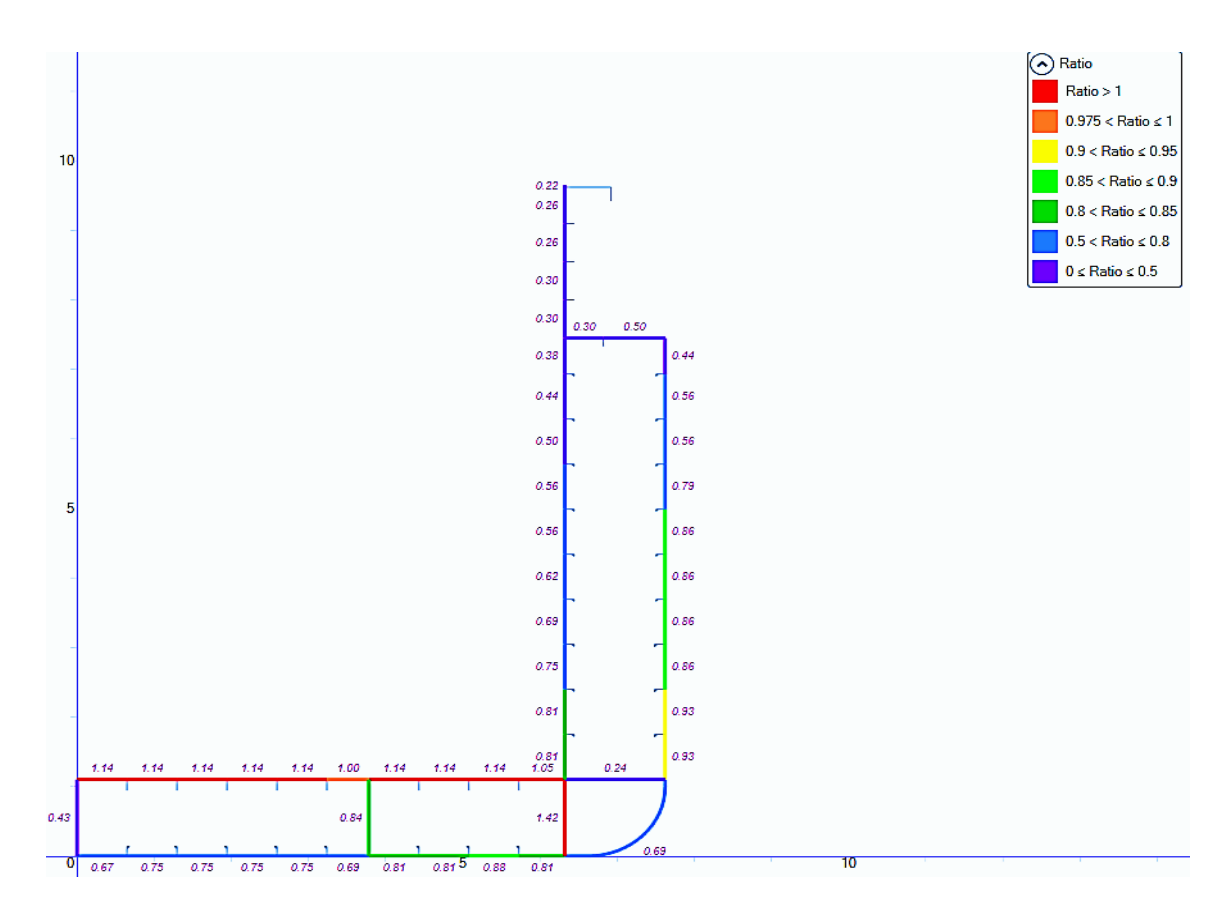


Figure 6-28: Yielding criteria of the optimised midship.

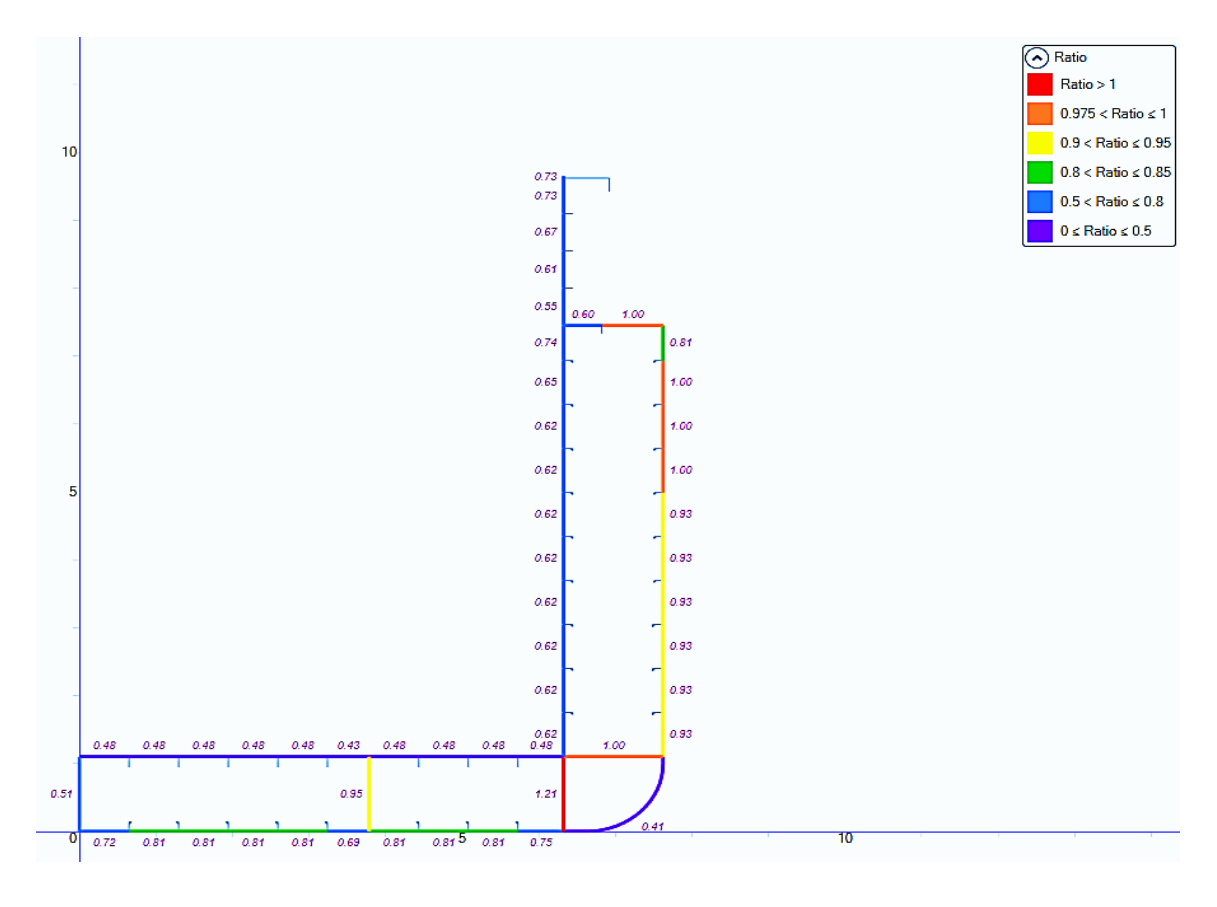


Figure 6-29: Buckling criteria of the optimised midship.

Figures 6–28 and 6–29 present an optimised midship's yielding and buckling criteria, disclosing that the inner bottom plate-1 and the double bottom side girder plate do not meet the class rule yielding criteria. Simultaneously, the double bottom side girder plate also fails to satisfy the class rule buckling criteria. To address these limitations, the inner bottom plate material grade has been upgraded from mild steel (Grade A) to higher tensile steel (Grade AH36), and an additional stiffener has been incorporated into the double bottom side girder. Subsequently, sensitivity analysis was undertaken using BV Mars 2000 software to further assess and validate the optimised midship's compliance with yielding, buckling and ultimate hull girder strength criteria, guaranteeing alignment with industry standards and classification society regulations.

6.10.3.1 *Yielding Assessment*

The validation process for the optimised midship section is crucial for marine vessels, encompassing evaluations so as to ensure structural integrity and functionality. It involves the application of principles and methods to measure the midship section's ability to withstand yielding and abide by permissible stress conditions, including its response to hull girder bending, shear forces, besides the risk of yielding-induced failure. Understanding the midship section's limits and ability to manage various loads is essential concerning designing safe and reliable vessels. The outcomes of this assessment inform critical decisions regarding the midship section's design, material selection and reinforcement strategies. Engineers and naval architects trust this data to optimise the midship section to withstand the rigorous conditions encountered during maritime operations. This comprehensive assessment ensures ships' safe and efficient operation by evaluating their ability to yield, resist bending and shear forces, and adhere to permissible stress conditions. These are all crucial factors in naval architecture and marine engineering [221]. The study made use of Bureau Veritas software MARS 2000 to analyse the ship's structural hull girder's yielding, emphasising the importance of using numerical tools for these particular assessments.

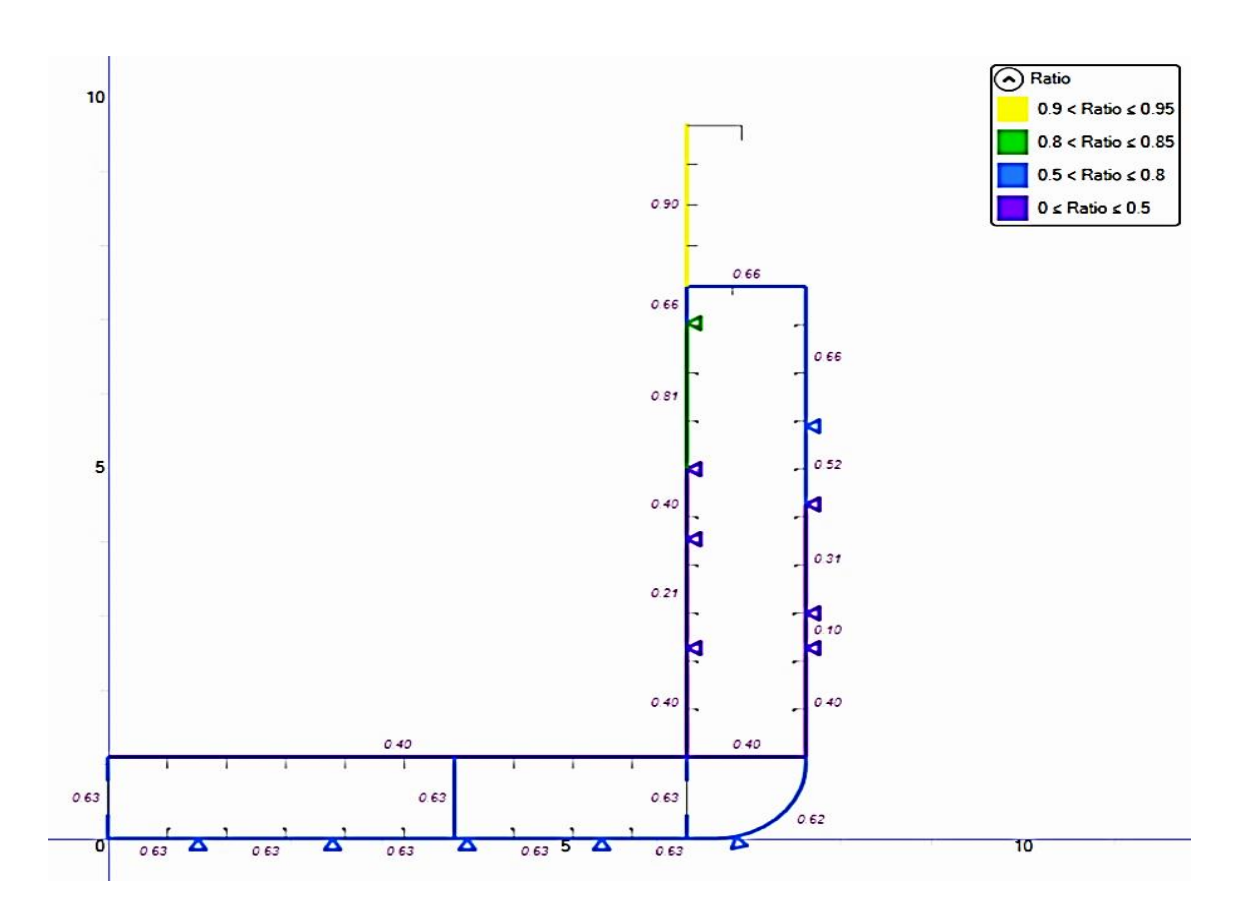


Figure 6-30: Validation of hull girder bending strength for plating (Head Sea).

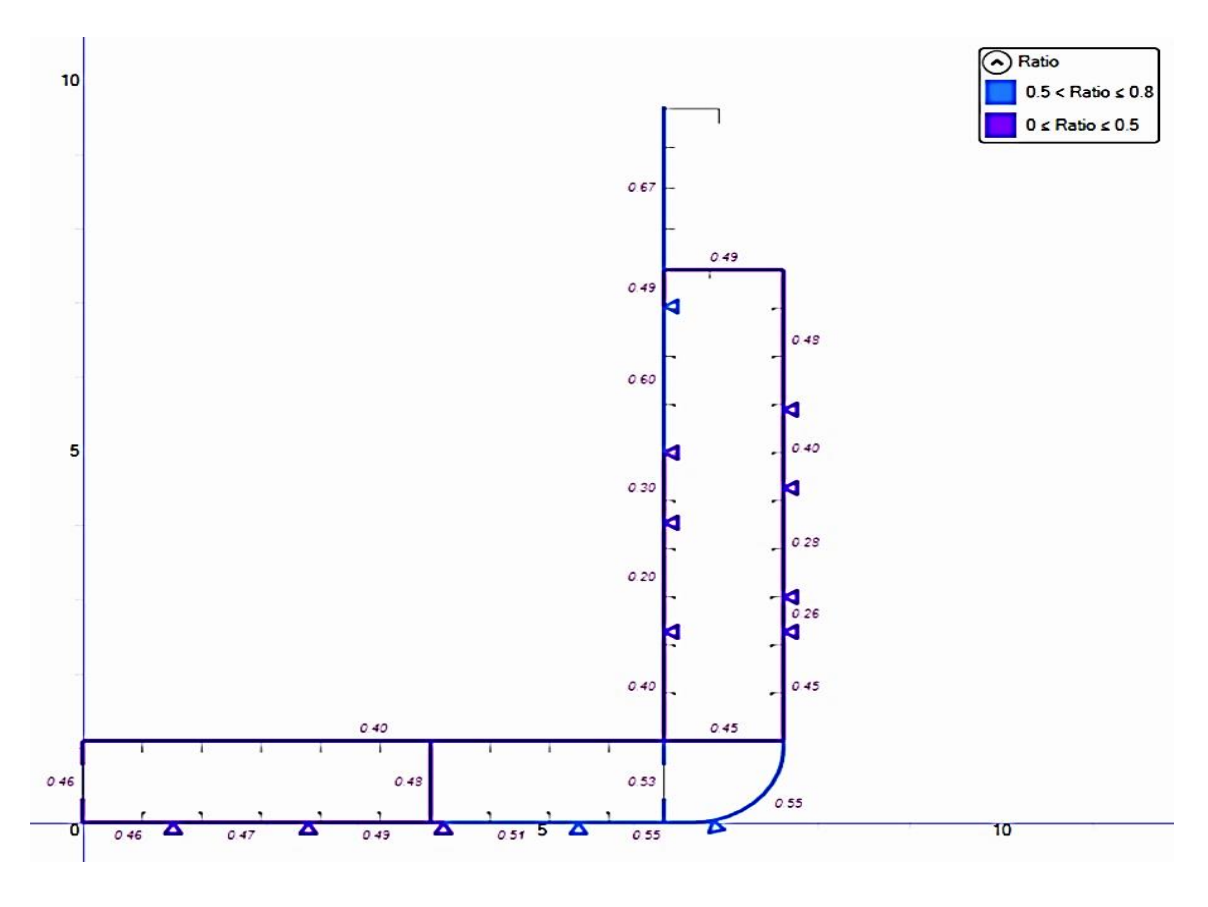


Figure 6-31: Validation of hull girder bending strength for plating (Oblique Sea).

Figures 6–30 and 6–31 demonstrate that the utilisation factor in relation to the hull girder bending strength of the plating remains consistently below one for both head sea and oblique sea conditions, thus effectively meeting the stipulated rule criteria. This analysis determined that head sea conditions are the most challenging, with the highest hull girder bending stress occurring near the hatch coaming area. These results demonstrate that the ship's structural integrity is maintained within acceptable limits by industry regulations. It is important to note that the findings highlight the critical nature of head sea conditions in terms of stress on the hull girder.

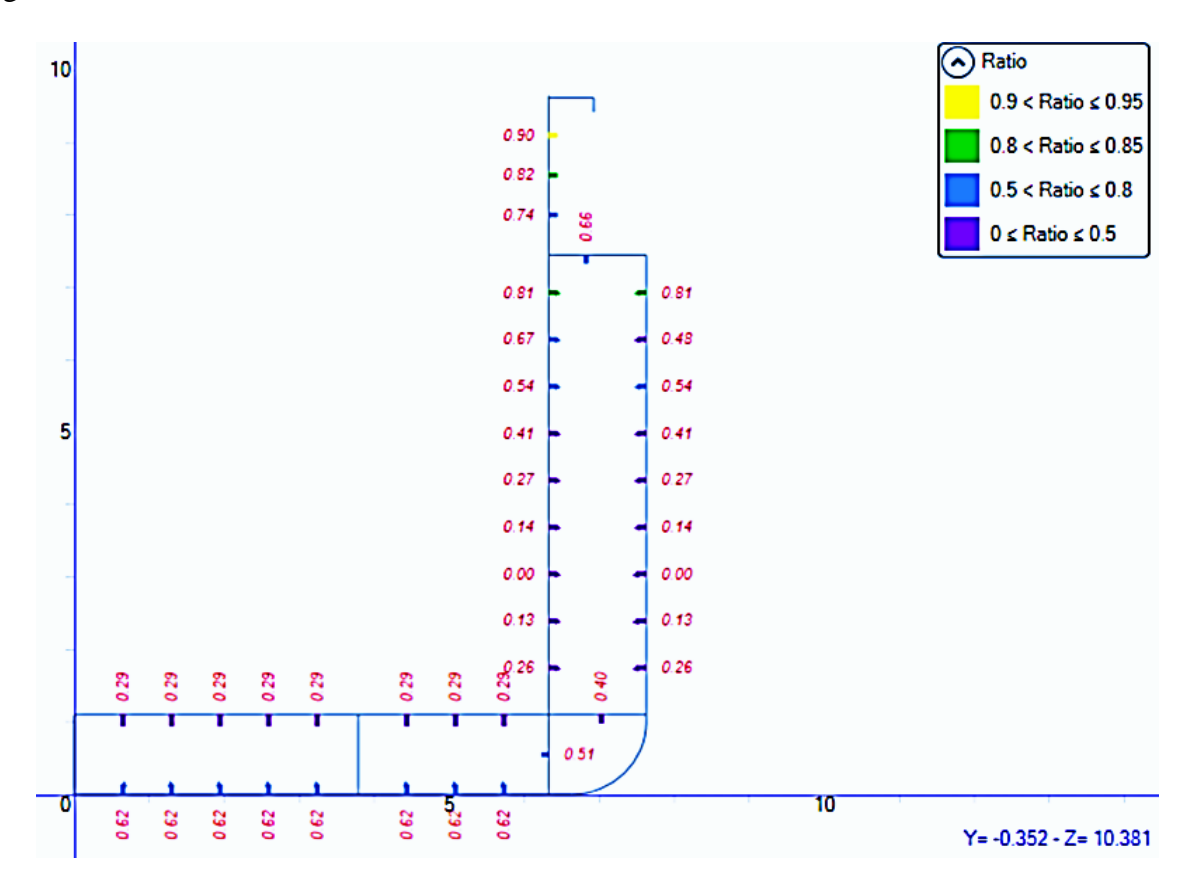


Figure 6-32: Validation of hull girder strength for ordinary stiffener (Head Sea).

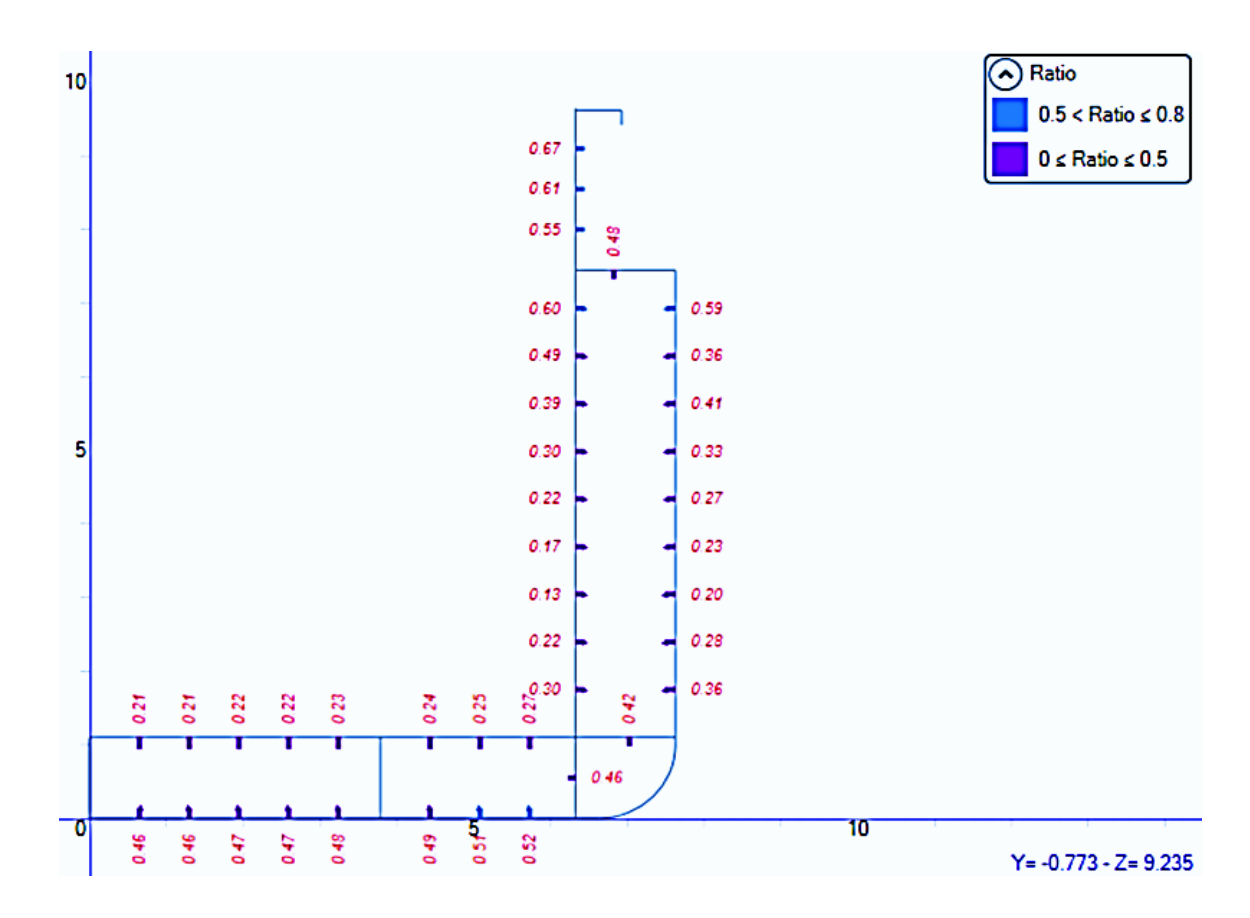


Figure 6-33: Validation of hull girder strength for ordinary stiffener (Oblique Sea).

Figures 6–32 and 6–33 indicate that the utilisation factor of an ordinary stiffener's hull girder strength consistently remains below 1, complying with established rule criteria for both head sea and oblique sea scenarios. The head sea condition is the most challenging, with the highest hull girder stress concentration at the hatch coaming area. These findings have sizable implications with respect to assessing and safeguarding ship structural integrity under various sea conditions.

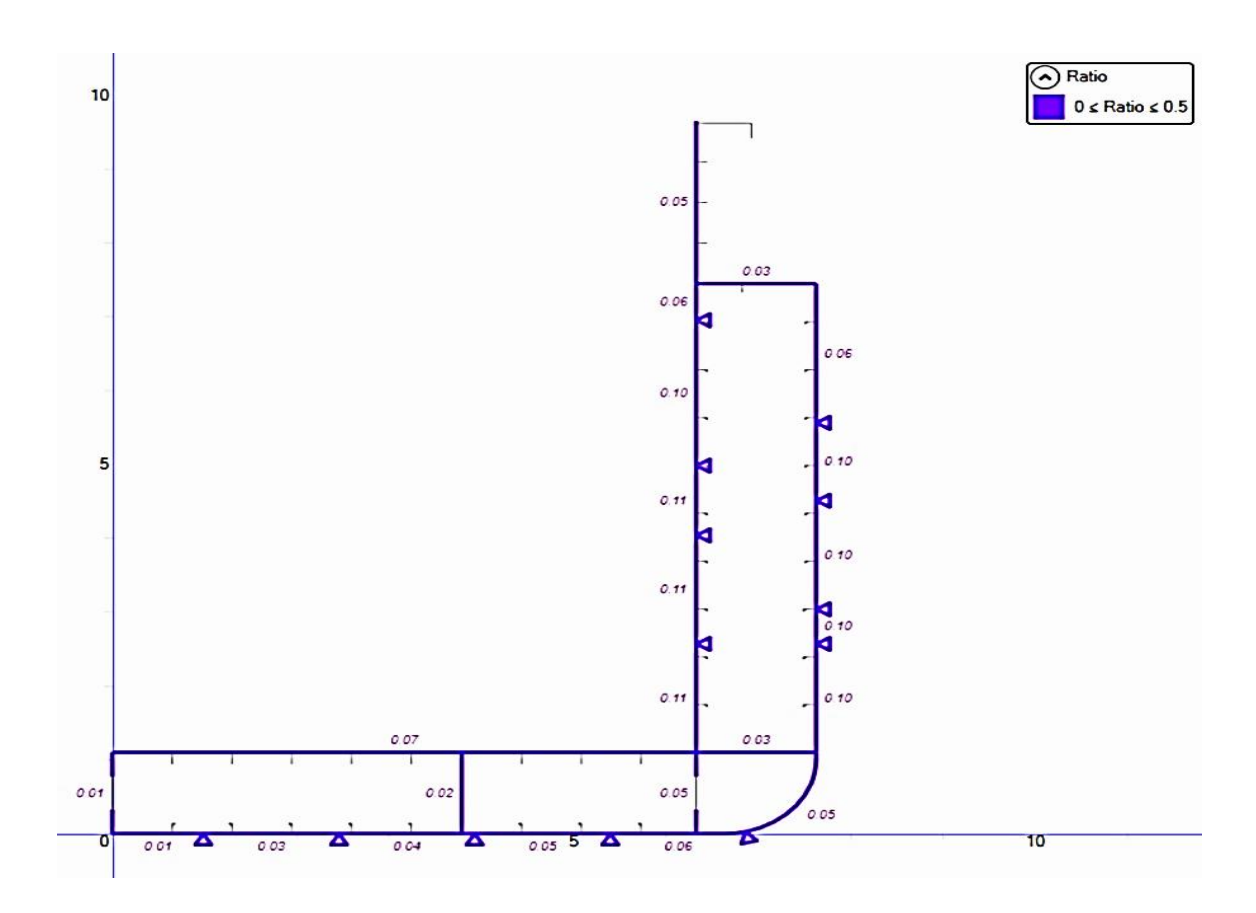


Figure 6-34: Validation of hull girder shear strength for plating (Head Sea).

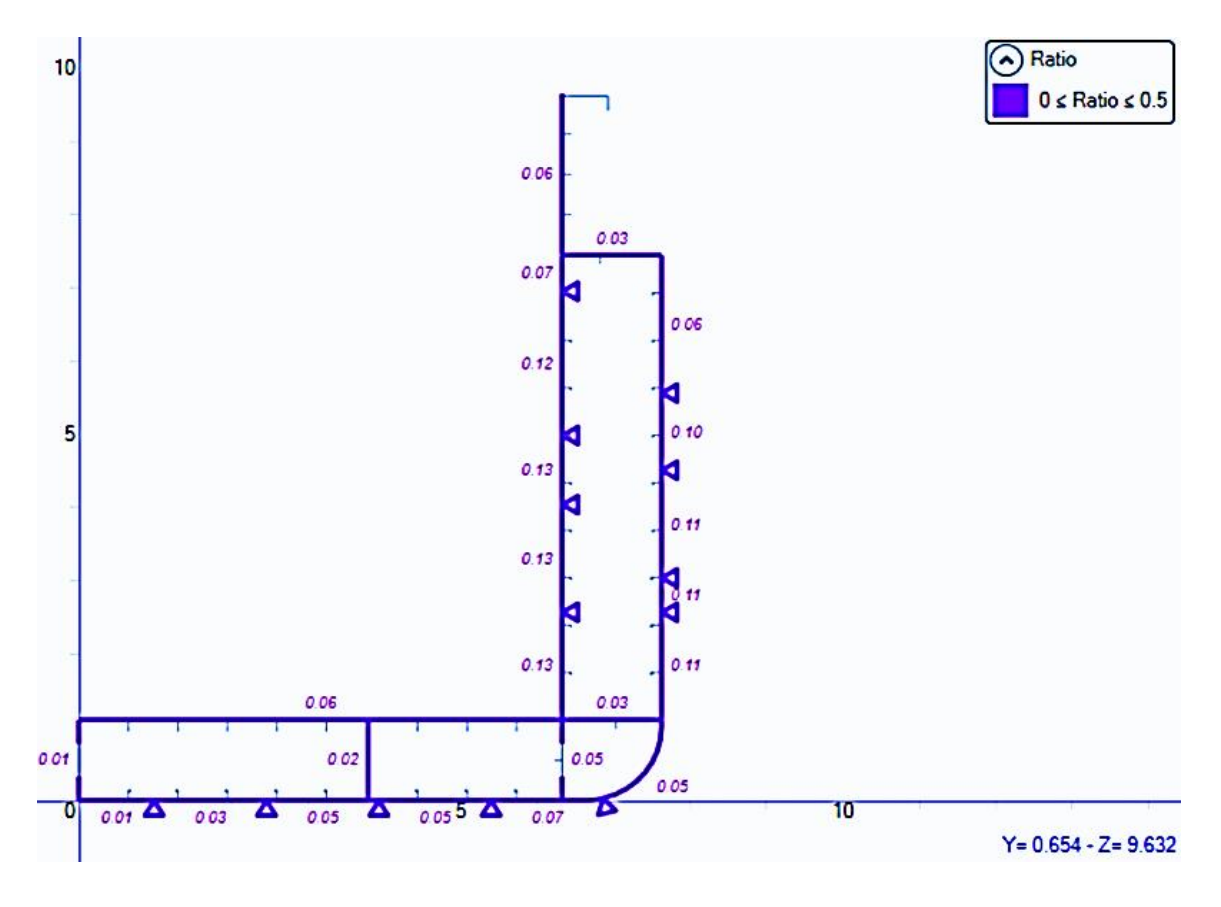


Figure 6-35: Validation of hull girder shear strength for plating (Oblique Sea).

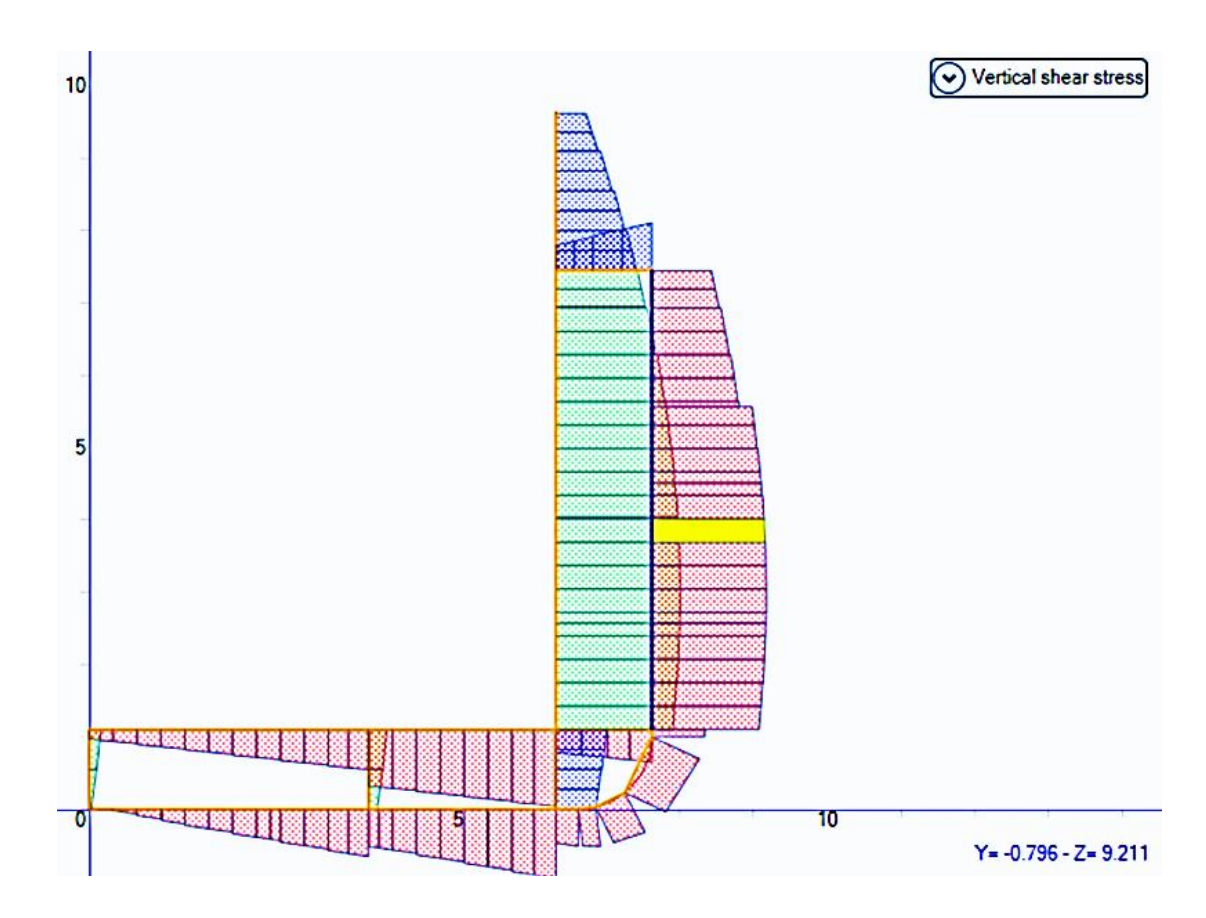


Figure 6-36: Primary vertical hull girder shear stress distribution.

Figures 6–34 and 6–35 show that the utilisation factor regarding the shear strength of plating in the hull girder consistently remains below 1. This indicates that the vessel complies with the established rule criteria, irrespective of whether it encounters head or oblique sea conditions. It is worth mentioning that the area with the highest hull girder shear stress is located near the neutral axis, confirming the findings of previous studies regarding the ultimate strength of ship hull girders. This emphasises the significant role of shear strength in maintaining structural resilience in maritime vessels. Equally, Figure 6–36 provides a graphical representation of the primary vertical distribution of hull girder shear stress, offering valuable knowledge into the subtle stress patterns within the hull girder structure. This distribution pattern aids naval architects and marine engineers pinpoint critical areas that might need extra reinforcement or design adjustments. The graphical representation simplifies the interpretation of complex stress data, enabling more informed decisions during the design process. By examining these stress patterns alongside the utilisation factors shown in Figures 6-34 and 6-35, designers can optimise the hull structure to enhance both safety and efficiency. This approach ensures compliance with regulatory standards while minimising excessive material use and weight.

6.10.3.2 Buckling Assessment

The validation of an optimised midship section necessitates a fundamental buckling assessment, a cornerstone of ship design. This assessment systematically appraises the midship section's structural stability when subjected to compressive loads, preserving its resilience against buckling phenomena. Its pivotal role is safeguarding the ship's structural integrity and safety. The analysis primarily involves scrutinising the midship section's buckling strength to ascertain compliance with pertinent classification society regulations and industry standards. This meticulous buckling assessment, integral to ship design, demands a comprehensive scrutiny of structural stability and strength to guarantee the vessel's safety and dependability. Notably, the study employed Bureau Veritas software, MARS 2000, to achieve a detailed analysis of the hull girder's buckling behaviour, emphasising the critical importance of leveraging numerical tools in these assessments [222].

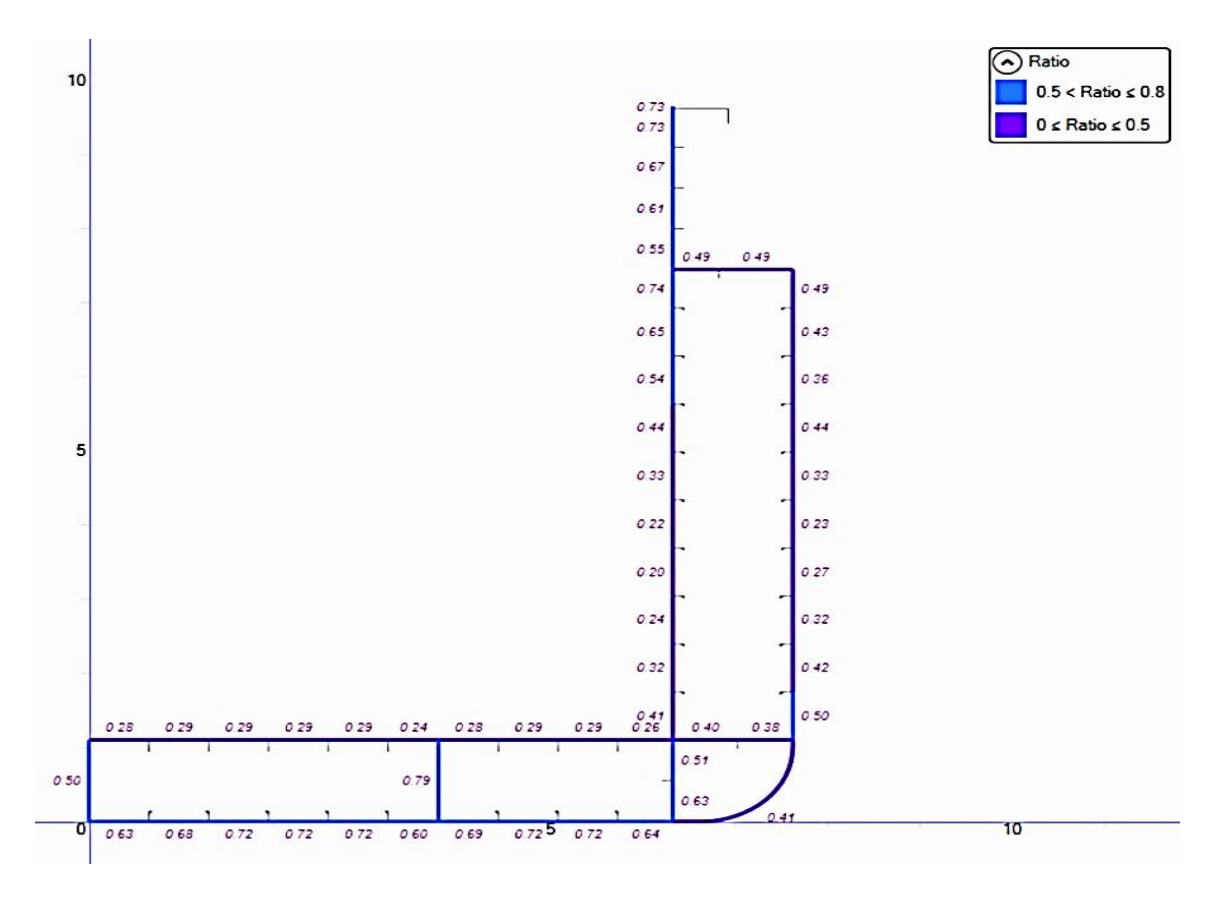


Figure 6-37: Validation of buckling of plate panel.

Figure 6–37 shows the buckling capacity of plate panels within the optimised midship section, abiding by BV (Bureau Veritas) rules. A critical factor is that a buckling factor exceeding 1 indicates a failure to meet the buckling criteria. All plate panels exhibit utilisation factors below

1, demonstrating full compliance with the stipulated rule criteria. The investigation into weight and cost optimisation of the midship section, in accordance with common structural regulations, reiterates the observed increase in plate buckling within the optimal solution. These findings emphasise the importance of buckling capacity and utilisation in guaranteeing the structural integrity of plate panels, particularly in the context of ship construction and design.

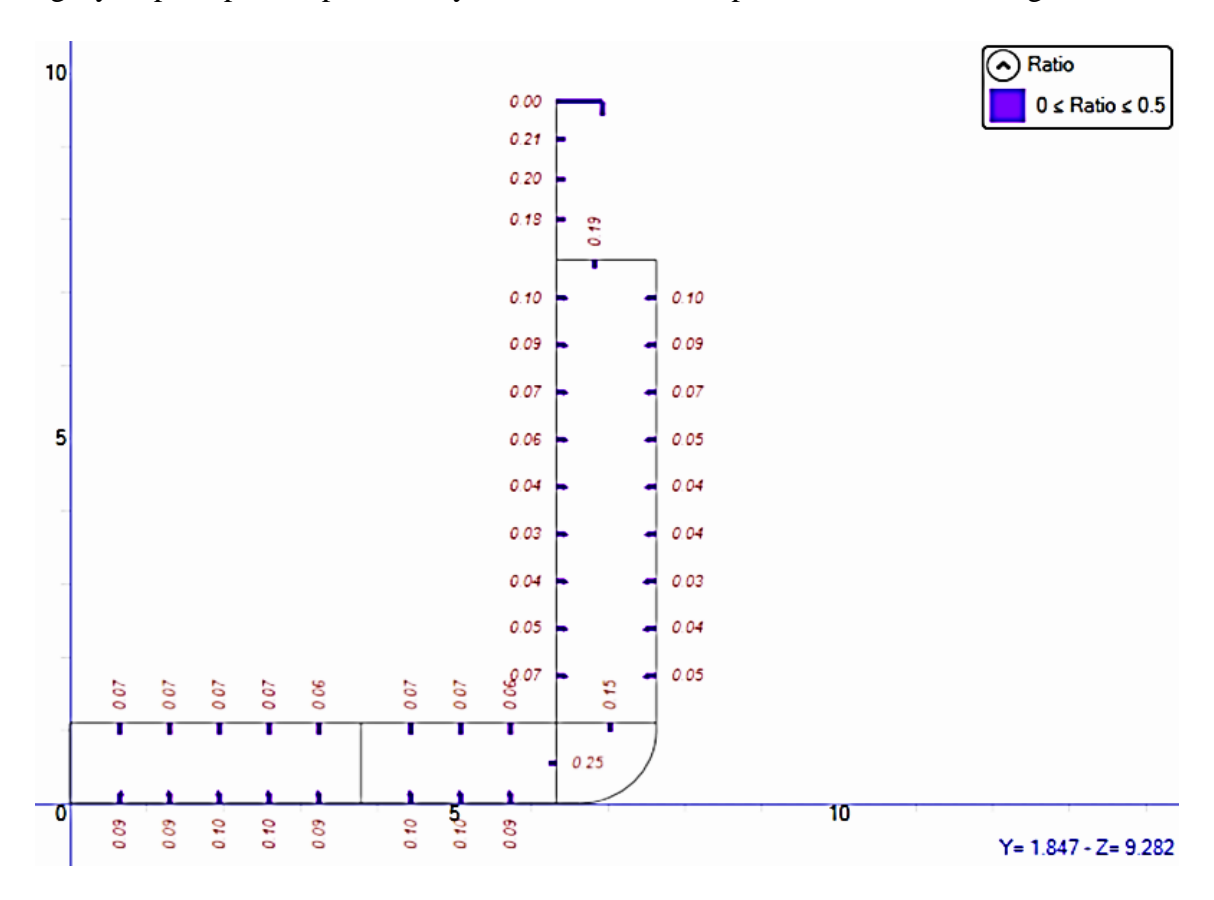


Figure 6-38: Validation of buckling of ordinary stiffener.

In Figure 6–38, the buckling utilisation factor for ordinary stiffeners is consistently less than one, agreeing with the universal methods for determining the buckling capacities of plate panels, stiffeners, primary supporting members and columns as detailed in the applicable rules. This utilisation factor is a crucial parameter in calculating the structural integrity of stiffened panels, with the requirement that it remains below 1 to meet the rule criteria.

6.10.3.3 Ultimate Strength Assessment

The assessment of a ship's hull girder's ultimate strength (HGUS) is paramount in ensuring the structural integrity of a vessel, specifically when validating an optimised midship section. The hull girder's ultimate strength signifies the maximum bending capacity the hull girder can

endure when exposed to longitudinal pressure, a crucial factor in securing the vessel's safety [223]. To conduct this assessment, Bureau Veritas software, MARS 2000, was employed, utilising the progressive collapse method to examine the ultimate strength of the hull girder within the space delineated by two adjacent frames. This analytical approach separates the midship section into structural elements, including the stiffener-attaching plating and hard corner elements, independently evaluating each concerning failure modes. Through an incremental-iterative process, the moment-curvature relationship is determined.

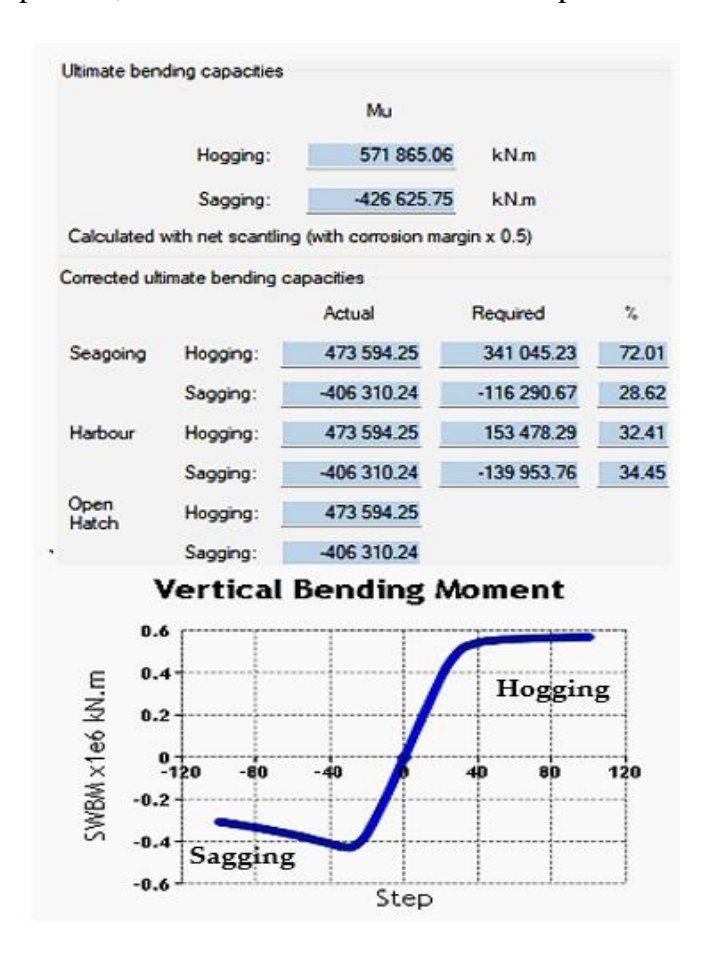


Figure 6-39: Hull girder's ultimate strength.

During the course of the iterations, the bending moment acting on the hull girder's transverse section increases as the curvature is imposed. Structural elements above the neutral axis experience contraction in sagging conditions, while those below lengthen. The precise location of the neutral axis and the ship's cross-section are determined based on the failure mode exhibited by each structural element as external moments are applied. Tensile structural components are characterised by elastic-plastic failure in a single mode, whereas in compression, they exhibit either buckling or yielding modes. As shown in Figure 6–39, the ultimate strength is notably highest under hogging loading conditions and lowest under sagging

loading conditions. The most critical structural failure scenario arises in sagging loading conditions, representing the most challenging condition as regards safeguarding structural integrity.

Figure 6–39 indicates that a modification in ultimate strength can be most efficiently accomplished by adjusting the thickness of structural components [224]. This modification incorporates maintaining the thickness of the structure nearest to the neutral axis constant (including the inner side and side shell) while varying the thickness of the structure located furthest from the neutral axis (such as the bottom, double bottom, and deck structure), where global failure is most likely to arise. The ultimate strength of a material is the maximum stress it can tolerate prior to breaking.

6.11 Robustness of the Optimisation Results

The sensitivity analysis meticulously examined the impact of modifying twelve (12) crucial elements in the search for an ideal thickness and spacing of web frames and longitudinal stiffeners in the cargo hold region of a ship. The two main objectives of this extensive study were to reduce the ship's weight and production costs. It is important to state that this research focused solely on the original material grade, unlike various other design optimisation studies that may consider alterations in material grades. This strategic choice was crucial as it emphasised the importance of reducing weight and production costs without compromising steel quality.

During the optimisation procedure, the thickness of most of the structural components was decreased. For example, the bottom and bilge plates were reduced from 9.5 mm to 8.5 mm, the side shell plate was reduced from 8.5 mm to 7.5 mm, whereas the shear strake plate was reduced from 10.5 mm to 9 mm, among other plates. In contrast, the thickness of the inner bottom plate-2 increased from 10 mm to 11.5 mm, the thickness of the inner side shell plate-2 rose from 7.5 to 8.5 mm, while the DB longitudinal girder and CL plate thickness increased from 16.0 mm to 19.0 mm. To simplify the optimisation problem, it was presumed that the inner shell plate and inner bottom plate would maintain a constant thickness. After painstakingly analysing each component, these adjustments were made to identify areas for weight loss and cost savings while maintaining structural integrity. Of note is that crucial structural components like stiffener spacing and web frame spacing were repositioned during optimisation. This calculated choice

pinpoints the delicate balance between weight reduction and preserving the ship's safety and structural robustness, which is the primary goal of this study.

Strict compliance with time-honoured industry practices and classification society standards is imperative in shipbuilding. Key among these principles is the hierarchy of structural plate thickness, with stipulations that the Keel plate should possess a thickness greater than or equal to the Bottom plate, the Bottom plate thickness should exceed or be equal to that of the Side shell plate, whilst the Shear strake plate thickness should be greater than or equal to the Side shell plate thickness. In this extensive study, meticulous validation and maintenance of these established relationships are apparent, as reflected in Table 6–1. This compliance reaffirms the enduring relevance of these traditional practices and emphasises their essential role in contemporary ship design. Upholding these thickness hierarchies enhances the overall safety, reliability and performance of ships, ensuring their suitability for challenging maritime conditions and reinforcing the pivotal role of industry conventions in modern shipbuilding.

The primary objective of this research is to ensure the ship's structural integrity while lowering its weight and production costs. It is crucial to emphasise the importance of this issue since any compromise in regards to the structural integrity can adversely affect the ship's performance and safety at sea. After optimisation, the stress levels for mild steel (Grade A) and high-tensile steel (Grade AH36 and Grade DH36) are substantially below their allowed limits. The maximum permitted stress for high-tensile steel (Grade AH36 and Grade DH36) is 331.77 N/mm², while it is 219.42 N/mm² for mild steel (Grade A) (refer to Sec. 3.7.1.2). This finding implies that the ship's structural integrity is not compromised, even after reducing the thickness of several components.

The maritime industry can benefit significantly from optimisation initiatives. When the ship's weight and production costs are reduced by approximately 10%, weight reduction and structural robustness exhibit a remarkable interaction. These findings also highlight the effectiveness of the optimisation strategy exploited in this study. Additionally, avoiding structural failure during these reductions recognises the validity of the design decisions made during optimisation.

This sensitivity analysis demonstrates the complexity and interconnectedness of ship structural optimisation. It emphasises the value of efficient optimisation, which reduces weight and production costs while assuring the structural soundness and safety of the ship. These conclusions significantly impact the marine sector and provide beneficial data that could improve ship engineering and design in the future. They demonstrate the importance of

systematic optimisation approaches that bear in mind structural resilience in marine transportation and economic factors.

6.12 Discussion

The study employed the Design of Experiment (DOE) method with a fractional factorial design technique to create regression equations for Von Mises stress and production costs in multipurpose cargo ship design. This comprehensive approach involved scrutinising twelve significant structural components of the ship using Minitab software, examining 128 diverse models. The derived regression equations were subsequently incorporated into a Python-based, Non-dominated Sorting Genetic Algorithm II (NSGA-II) to optimise the multipurpose cargo ship's weight and production costs. Fractional factorial designs are a worthwhile alternative to full factorial designs as they require fewer experimental runs and prove incredibly beneficial when resources are constrained. These designs present various advantages, including economic efficiency achieved by reducing the number of experimental runs. Additionally, they provide a more focused and pertinent approach, supporting the prioritisation of the most impactful factors and effects. This prioritisation is crucial to ensure the structural integrity and cost-effectiveness of the ships.

Preserving a ship's structural integrity is vital to ensure both its crew's and the ship's safety, principally in demanding marine environments marked by saltwater exposure and strong waves. This study focuses on maintaining Von Mises stress levels within critical locations well below permitted stress thresholds. For mild steel (Grade A) and high-tensile steel (Grade AH36 and Grade DH36), the maximum permissible stress thresholds are 219.42 MPa and 331.77 MPa, respectively. Figures 6–9 and 6–11 show the midship section of the optimised ship and its analysed cargo hold model in a sagging condition, demonstrating compliance with these permitted stress thresholds. Figures 6–17, 6–18, 6–20 and 6–21 provide further evidence, revealing that the Von Mises stress levels of the Shear strake plate (Grade AH36), Main Deck plate (Grade AH36), Hatch Coaming plate (Grade DH36) and Hatch Coaming top plate (Grade DH36) remain comfortably below permitted stress thresholds after optimisation, with values of 222.04 MPa, 223.26 MPa, 296.20 MPa and 296.20 MPa, respectively.

Additionally, Figures 6–12, 6–13, 6–14, 6–15, 6–16 and 6–19 present Von Mises stress distributions across various critical ship components, including the Keel plate (Grade A), Bottom plate (Grade A), Side Shell plate (Grade A), Inner Side Shell plate (Grade A), Inner

Bottom plate (Grade A), double Bottom longitudinal girder as well as CL (Grade A), contributing a better understanding of the structural integrity and performance of these components under different loading conditions and providing essential data for assessing their reliability and safety during operational scenarios. In all cases, stress levels consistently remain significantly lower than permitted stress thresholds, with values of 135.57 MPa, 158.80 MPa, 111.52 MPa, 149.26 MPa, 128.44 MPa and 190.51 MPa, respectively. The Von Mises stress of the double Bottom longitudinal girder, CL (Grade A), noticeably decreased from 213.35 MPa before optimisation to 190.51 MPa after optimisation, guaranteeing ample safety factors. These findings emphasise the vital role of structural optimisation in enhancing ship safety and performance in challenging maritime conditions. Modifications were made to the main frame spacing, web frame spacing and the repositioning of longitudinal stiffeners, all accomplished without modifying the ship's fundamental dimensions to optimise the cargo hold region.

After optimisation, a novel midship section featuring modified scantlings was carefully designed for the analysed ship. This midship section underwent a comprehensive validation process. Figures 6–28 and 6–29 visually represent the optimised midship's yielding and buckling criteria, clearly portraying the local strength criteria of plates and ordinary stiffeners, such as yielding and buckling, revealing that the inner bottom plates (bottom plate one and bottom plate two) and the double bottom side girder plate do not adhere to the class rule yielding criteria. The double bottom side girder plate also fails to meet the class rule buckling criteria. To rectify these deficiencies, the material grade of the inner bottom plate was upgraded from mild steel (Grade A) to high tensile steel (Grade AH36), and an additional stiffener was integrated into the double bottom side girder. Subsequently, a sensitivity analysis was carried out using BV Mars 2000 software to further evaluate and validate the optimised midship's compliance with yielding (See Figures 6–30, 6–31, 6–32, 6–33, 6–34 and 6–35), buckling (See Figures 6–37 and 6–38), and ultimate hull girder strength (See Figure 6–38) criteria, enabling alignment with industry standards and classification society regulations. It is important to note that the ship has successfully met these rigorous requirements.

The original cargo hold model weighed 639.50 tonnes before optimisation but was reduced to 573.35 tonnes after optimisation. This significant 66-tonne reduction significantly impacts ship performance, enhancing fuel efficiency, speed, manoeuvrability and stability. Additionally, it contributes to approximately a 10% substantial cost reduction in building, operational and maintenance costs. Conspicuously, it positively impacts the environment by reducing greenhouse gas emissions and other pollutants. Concurrently, the production costs related to

the ship's structure decreased from 1,971,315.00 euros to 1,770,000.00 euros after optimisation. This simultaneous 10% reduction in weight and production costs underlines the economic benefits of the optimisation process, highlighting its cost-effectiveness.

This study provides a comprehensive review of relevant literature to position its findings within the broader ship structural optimisation research landscape. For example, Elhewy et al. [70] optimised an offshore supply vessel (OSV) applying the blind search technique, resulting in a 42% reduction in the vessel's steel weight and production cost without compromising structural integrity. Similarly, Motta et al. [23] utilised the LBR-5 programme to optimise the multistructures of a Mega Yacht, leading to a commendable 20% reduction in cost and an 8% reduction in weight compared to the original scantlings. These studies accentuate the advantages of structural optimisation for smaller vessels. Moreover, Rigo and Caprace [6] explored the symbiotic relationship between "Design" and "Optimisation" in ship structures, demonstrating that optimisation efforts can yield cost savings, decreased steel use and enhanced performance by means of multi-objective optimisation techniques. These findings are consistent with the current study's findings, where structural optimisation caused a 10% reduction in steel weight and production costs while preserving the ship's principal dimensions. Similarly, the achievement of the Pareto optimal front, as demonstrated in the work of Alhammadi and Romagnoli [198], accentuates the significance of these findings in the context of previous research. By placing these results within the broader body of work, this study highlights its relevance and substantial contribution to ship structural optimisation, highlighting its critical role in ensuring both the structural integrity and cost-effectiveness of ships in maritime engineering.

In brief, combining the fractional factorial design technique and the Python-based Non-dominated Sorting Genetic Algorithm II (NSGA-II) has proven essential in identifying and optimising the key parameters significantly influencing multipurpose cargo ship performance. The utilisation of this method has resulted in significant reductions in both weight and production costs while concurrently improving the overall structural robustness. This study clears the way for increased fuel efficiency, cost-effectiveness, as well as a more favourable environmental impact in the maritime industry by emphasising the transformative influence of ship design.

6.13 Conclusion

This study addresses a critical research gap in maritime engineering by focusing on the structural optimisation of a three-cargo-hold model for a multipurpose cargo ship. Significant developments have been made in enhancing the structural robustness and cost-effectiveness of ship designs by integrating Design of Experiments (DOE) principles with the Non-dominated Sorting Genetic Algorithm II (NSGA-II). The following conclusions can be drawn:

- Efficient Optimisation Process: Integrating the NSGA-II algorithm allowed efficient optimisation of the multipurpose cargo ship's design objectives, reducing weight and production costs. Through prudent adjustments in plate thickness, web frame positioning and stiffener arrangement, a significant 10% reduction in both ship weight and production costs was achieved, illustrating the effectiveness of the optimisation process.
- Rigorous Validation and Compliance: The optimally designed midship section underwent thorough validation to assure conformity with industry standards and classification society regulations. Essential alterations were made to inner bottom plates and double bottom side girders to meet stringent requirements, emphasising the commitment to structural integrity and safety.
- 3. Economic and Environmental Implications: The results of the optimisation, principally the substantial reductions in steel weight and production costs, have significant financial implications, including enhanced economic efficiency, reduced fuel consumption and lower initial costs. Moreover, these improvements contribute to environmental benefits by curbing greenhouse gas emissions and pollutants and are consistent with the sustainability goals applied in the maritime industry.

Chapter 7

Conclusion and Recommendations

7.1 Introduction

Ship design is a complex real-world process subject to engineering, regulatory and financial constraints and can be framed, therefore, as a multi-objective optimisation problem. The physical complexity of the engineering models places additional constraints on the optimisation process itself, both through the time required to develop the models and the time required to perform the optimisation. Modern heuristic optimisation algorithms often rely on the potential to study tens of thousands of potential design solutions, while traditional optimisation methodologies, by necessity, assume the solution space has an underlying smoothness that can be determined by studying a small selection of design solutions. For a complex problem such as ship design, where evaluating each individual design is itself a cost to be factored in, there is a potential benefit in combining the traditional and the heuristic into a hybrid optimisation approach.

This thesis has studied and developed optimisation techniques that can be applied practically to ship structural design, with the aim of the optimisation being to minimise production costs while reducing weight and ensuring the safety and structural integrity of the ship.

The real-world nature of the problem and its constraints was an important factor. The design and optimisation methodology included a detailed analysis of a ship model with three cargo holds for a comprehensive structural assessment that required evaluating longitudinal strength under the combined influence of bending and torsional loads. This included a detailed analysis of buckling and deflection under various sea conditions, in addition to exploring the torsional effects of different deck configurations (open and closed decks).

The research identified significant ship factors based on ship hull girder stress, torsional stress and production costs. The resulting optimised structural design underwent rigorous validation, consisting of yielding analysis, buckling analysis and assessments of the hull girder's ultimate strength. It is expected that this research will significantly contribute to the shipping industry while acknowledging its limitations and practical implications.

7.2 Research Objectives and Achievements

The following objectives have been successfully achieved:

7.2.1 Assessment of Longitudinal Strength, Deflection and Buckling Analysis

The study began with an assessment of the longitudinal strength, deflection and buckling analysis of a ship's hull girder. To measure the linear longitudinal strength and deflection properties and conduct a buckling analysis of the ship, a 3D finite element model of the cargo hold was used. This research thoroughly assessed the ship's longitudinal strength, deflection and buckling behaviour, highlighting the importance of longitudinal deflection over transverse deflection, specifically concerning open-deck ships.

7.2.2 Torsional Stress Analysis

This study underlines the significance of torsional stress in open-deck ships relative to closed-deck ships. Notable differences in structural behaviour result in substantial torsional moments and stresses in open-deck ships, comprising approximately 20% of the total stress. In contrast, hull girder warping normal stress in closed-deck ships is considerably less significant than in open-deck ships. These differences arise from the reduced torsional rigidity due to large hatch openings in open-deck ships.

Results also show that the horizontal shear force, bi-moment, and torque attain peak values near the aft and forward bulkhead edges in the cargo hold region and are uniformly distributed throughout the length of the cargo hold.

7.2.3 Identification of Significant Factors Affecting Ship Design

This study identified crucial factors impacting ships based on hull girder Von Mises stress, torsional stress and production costs. Understanding these factors is fundamental in ship design as they directly influence structural integrity, safety, performance, sea durability and cost-effectiveness in connection with shipbuilding.

The analysis ascertained the top five factors significantly impacting ship Von Mises stress, namely:

- Hatch Coaming Plate
- Hatch Coaming Top Plate
- Main Deck Plate
- Shear Strake Plate
- Bottom Plate

The impact of ship plate thickness on the Von Mises stress is influenced by load distribution, bending behaviour, material properties, stress concentrations and fatigue. Thicker plates generally lower Von Mises stress due to better load distribution and bending resistance. Studies show that deformation, strain, and Von Mises stress tend to decrease as ship structure thickness increases, emphasising the importance of selecting suitable plate thickness to prevent structural failure.

Additionally, five principal factors were identified as significantly impacting warping stress:

- Bottom Plate
- Side Shell Plate
- Hatch Coaming Plate
- Inner Side Shell Plate
- Hatch Coaming Top Plate

The thickness of a ship's plates influences the warping stress it experiences, as thicker plates enhance warping rigidity, thereby decreasing warping stresses. The theoretical stress within a plate depends on its thickness, with thicker plates offering increased resilience against warping stresses.

This thesis explored the impact of the interaction between web frame and stiffener spacing on warping stress in ships. Wider spacing between these components can increase warping stress due to reduced rigidity and resistance to torsional loads. Optimal spacing is essential to maintain structural integrity and minimise warping stresses, underscoring the significance of thoughtful design considerations.

Regarding ship production costs, the analysis identified the following five factors with the most significant impact:

- Inner Bottom Plate
- Inner Side Plate
- Bottom Plate
- Web Frame Spacing
- Side Shell Plate

Increasing the plate thickness increases the ship's weight, material expenses, and overall production costs. On the other hand, reducing the plate thickness decreases these parameters. Similarly, widening the spacing between web frames minimises the ship's weight and lowers production costs, while narrowing this spacing has the opposite effect. These design considerations are crucial in balancing structural integrity with cost efficiency in ship construction.

7.2.4 Optimisation Strategy

A novel two-stage optimisation method in relation to ship hull structures which builds on the combination of a fractional factorial design technique within the Design of Experiments (DOE) framework and the Non-dominated Sorting Genetic Algorithm II (NSGA-II) is developed. First, using the fractional factorial design approach, this strategy identified the critical parameters affecting hull girder Von Mises stress, warping stress and production costs.

Subsequently, ship design optimisation is performed by integrating regression equations (for Von Mises stress and production costs) (refer to Appendix B) into the NSGA-II Algorithm.

The optimally designed midship section undergoes rigorous validation to guarantee conformity with industry standards and classification society regulations.

7.3 Validation and Results

7.3.1 Yielding Evaluation

The optimised midship section underwent a yielding assessment, as shown in Figure 6–28. The analysis determined that the inner bottom plate (bottom plate one and bottom plate 2) and the double bottom side girder plate did not meet the BV class rule yielding criteria, similar to the

initial design (refer to Tables 3–16 and 3–17). To adhere to the class rule yielding criteria, the inner bottom plate's material grade was upgraded from mild steel (Grade A) to higher tensile steel (Grade AH36), and an extra vertical stiffener (Flat Bar 120 mm x 12 mm) was added to the double bottom side girder at 6325 mm OCL in between two web frames, ensuring compliance.

7.3.2 Buckling Assessment

Following the validation process, a detailed buckling analysis was conducted, as shown in Figure 6–29. The findings revealed that the plate of the double bottom side girder did not meet the class rule's buckling criteria similar to the initial design (refer to Figure 3–53). To comply with the class rule's buckling criteria, an extra vertical stiffener (Flat Bar 120 mm x 12 mm) was added to the double bottom side girder at 6325 mm OCL in between two web frames, ensuring compliance.

7.3.3 Local Sea and Cargo Loads Applied

The scantlings of the optimised model are verified by integrating local sea loads and cargo loads with global hull girder loads, confirming compliance with industry standards and classification society regulations. Figures 6–23, 6–24 and 6–25 demonstrate that local sea loads are higher in the oblique sea compared to head and beam sea conditions.

7.3.4 Analysis of Torsional Moments

Torsional moments validate the structural integrity of the optimised model, confirming compliance with stringent classification regulations by assessing its ability to tolerate challenging maritime loads.

7.3.5 Assessment of Hull Girder Ultimate Strength

Assessments confirmed that the optimised design met the ultimate strength requirements of the ship hull girder, enabling safety and integrity.

7.4 Optimised Midship Section for Structural Compliance and Cost Efficiency

After the optimisation and validation process, a new midship section was achieved. Adjustments to plate thickness, spacing of web frames, and stiffener placement were made to permit adherence to the stringent structural standards mandated by classification society regulations. These modifications were implemented with the dual objective of improving the material's efficiency while simultaneously reducing production costs.

7.5 Summary of Findings

This section provides a summary of the significant findings unearthed by the investigation:

- The investigation emphasises the significance of hull girder normal stresses at midship, demonstrating that stresses resulting from still water and the vertical wave bending moment contribute nearly 70% of the total stress, with stresses from the horizontal wave bending moment contributing approximately 10%, while warping stresses account for around 20% in open-deck ships.
- Torsion has minimal impact on closed-deck ship configurations.
- The thesis also includes an analysis of hull girder deflection, systematically examined using numerical techniques and Euler-Bernoulli beam theory, specifically focusing on the significance of longitudinal deflection over transverse deflection.
- Structural optimisation using the hybrid methodology developed here showed that the ship's weight and production costs could be significantly reduced by 10% compared to its initial design. Several adjustments were made to achieve this outcome, including changes in plate thickness, web frame positioning and stiffener arrangement.

7.6 Implications

The optimisation methodology developed in this thesis has been designed with real-life applications in mind. In structural optimisation, it is necessary to consider not only the structural properties but also the manufacturing costs and additional constraints from standards and

regulations. This thesis has focused on a specific ship design but the methodology can be applied to the ship design generally and has parallels in the wider construction sector.

7.6.1 Practical Applications

Maritime experts can enhance ship design by adopting a holistic approach that considers safety, the environmental impact, cargo capacity and cost-effectiveness. This approach is essential in contemporary ship design because it is in keeping with industry expectations pertaining to efficiency and sustainability, ensures that vessels are environmentally friendly and enhances competitiveness.

7.6.2 Milestone for the Maritime Industry

This optimisation methodology is a tool to support an experienced design engineer. Its goal is to suggest one or more optimised designs, but the selected design will still need careful validation and, if necessary, some final adjustments.

It could potentially revolutionise ship performance by aiding efficient and cost-effective ship design, creating a significant milestone for the maritime sector.

7.7 Conclusion

In conclusion, this study presents key findings in ship hull structural optimisation to identify and optimise the factors affecting the weight and production costs of multipurpose cargo ships using a fractional factorial design technique and the NSGA-II algorithm. For the case study used here, structural optimisation resulted in a 10% reduction in steel weight and a 10% reduction in production costs; such a saving has far-reaching ramifications for economic efficiency, fuel consumption, initial costs and environmental sustainability. Via analytical and numerical methods, a comprehensive understanding of the behaviour of ship hull girders was achieved, paving the way for more effective ship designs to be developed that are less harmful to the environment.

7.8 Comparative Analysis of Current and Al-Based Optimisation Methods

1. Automation:

- **Current Method:** This relies heavily on manual parameter adjustments and predefined workflows, making it time-intensive and laborious.
- **AI-Based Methods:** Automates tasks such as parameter tuning, mesh generation and iterative optimisation by reducing human intervention to an absolute minimum. However, the extent of automation and its benefits require further study [225].

2. Efficiency:

- **Current Method:** Parallel processing is rarely exploited. Each stage requires extensive resources, suggesting that it is exceedingly expensive for large-scale models.
- **AI-Based Methods:** These methods may offer reductions in computation time by inserting predictive modelling and optimisation, but the time-cost of designing and training custom AI model needs to be considered [226].

3. Investigation of Complex Relationships:

- **Current Method:** Deterministic analysis is performed based on finite element modelling with a set number of variables.
- **AI-Based Methods:** These methods could possibly help detect multi-variable complex and non-linear relationships, generating creative design solutions. Human expertise would still be crucial in interpreting and validating these relationships [225].

4. Scalability:

- **Current Method:** Operations are performed manually using specific software tools that result in poor scalability.
- **AI-Based Methods:** It may enable effective scalability in the handling of large datasets or wide design space and permit the investigation of more configurations, but the practical implementation and benefits need further investigation [225].

5. Multi-Objective Optimisation:

- Current Method: NSGA-II is an authoritative genetic algorithm for multi-objective optimisation. However, in most cases, it requires countless iterations to obtain a balance for multi-objective optimisation.
- AI-Based Methods: It might dynamically achieve a real-time balance in terms of conflicting objectives, but human involvement would still be needed in the optimisation and design verification process [227].

6. Data Dependency:

- **Current Method:** Current design methods are principle-based and do not require massive datasets to operate.
- **AI-Based Methods:** These are bound by massive and high-quality datasets for training, which may be limited in domains where data are scarce or incomplete. This could be a significant limitation in ship design application [225].

The implementation of these AI-based techniques into the prevailing frameworks may improve current methods by combining their established reliability with the speed, scalability, and predictive abilities of AI. This could result in a more dynamic and useful approach to ship structural optimisation. However, AI may have the capability to assist with some aspects of the modelling process, but whether the time-cost of designing and training a custom ship-design AI model could be beneficial needs further study. Human involvement would, however, still be needed in the optimisation and design verification process.

7.9 Limitations of the Research

- Manual Parameter Adjustment: This thesis presents a research method comprising
 manual parameter changes and FEMAP analysis for 128 models. This process is timeconsuming and labour-intensive, limiting its scalability for complicated systems or fullship designs.
- Software Limitations: Compared to more advanced simulation platforms such as Ansys APDL, FEMAP requires more comprehensive automation and parametric modelling capabilities. The absence of these capabilities has substantially reduced the

effectiveness of large-scale studies and inhibited the automation of repetitive tasks, for example sensitivity analyses or iterative optimisation methods.

- Simplifications in Finite Element Modelling (FEM): FEM essentially incorporates various calculations to simplify complex problems and assure that they are computationally manageable. Although essential to make the calculations realistic, these simplifications may generate incomplete representations of the complex realities associated with genuine structural behaviour.
- Challenges in Real-World Applications: Implementing these simulations on an actual
 ship hull structure presents significant challenges. Accurately simulating real-world sea
 conditions, incorporating unpredictable factors such as wave height, direction and
 frequency, is tremendously complicated.
- Assumptions in Scaling: Converting the results from scaled models to full-sized ships
 entails assumptions that require validation. Disparities might occur between the
 simulated results and actual performance, owing to variations in material behaviour,
 fabrication tolerances and operational scenarios.
- Limitations of Multi-Objective Optimisation: Most current optimisations focus on weight reduction and cost minimisation by overlooking other significant variables, e.g., moment of inertia, the centre of gravity and the overall operational efficiency in a multiobjective framework.
- Lack of Experimental Validation: Insofar as the physical tests of scaled models or even full-size structures are concerned, these results have not been validated by means of experimental validation. This would help to bolster the results by allowing comparisons to determine any differences from the results of the simulation.
- Material and Fabrication Variability: The simulations did not explain the variability
 in the material and fabrication, which can notably impact the performance of actual ship
 hull structures compared to the predicted results.

7.10 Direction of Future Research

Further research should aim to develop full-ship models by expanding the current simplified cargo hold model, with the intention of widening the application of optimisation techniques.

Full-ship models will afford a better understanding of the complex interaction between structural components in real-world operation and deliver more realistic and reliable results in support of different ship designs.

The addition of fatigue constraints in the optimisation process is another significant objective. This approach will expand the accuracy of the durability assessments because it will detect failure points in advance, reducing the risk of structural issues and decreasing their relevant maintenance costs during the ship's operational lifetime.

This presents an excellent opportunity to upgrade ship structural optimisation by combining hybrid genetic algorithms with state-of-the-art tools, for example machine learning and constraint-based reasoning. Hybrid genetic algorithms are effective in investigating complex design spaces. Machine learning is capable of predicting the outcome and accelerating the optimisation process, whereas constraint-based reasoning guarantees adherence with important safety and regulatory requirements. By combining these perceptions, this would allow further research to radically improve the efficacy of ship design, establishing new standards pertaining to safety, performance and environmental sustainability.

References

- [1] Wang X-Z, Xu E-H. Encyclopedia of Ocean Engineering. Springer; 2022. p. 1669-79.
- [2] Hughes O. Ship structural analysis and design. *The Society of Naval Architects and Marine Engineers*, New Jersey; 2010.
- [3] Okumoto Y, Takeda Y, Mano M, Okada T. Design of ship hull structures: A practical guide for engineers. *Springer Science & Business Media*; 2009.
- [4] Bayatfar A, Amrane A, Rigo P. Towards a ship structural optimisation methodology at the early design stage. *International Journal of Engineering Research and Development*. 2013;9(2):76-90.
- [5] Bay M, Crama Y, Richir T, Rigo P. A mixed-integer heuristic for the structural optimisation of a Cruise Ship. Proceedings of the 6th International Conference on Computer Applications and Information Technology in the Maritime Industries. COMPIT '07;2007.
- [6] Rigo P, Caprace J-D. Optimisation of ship structures. *Marine Technology and Engineering*. 2011;1:925-44.
- [7] Tadros M, Ventura M, Guedes Soares C. Review of the decision support methods used in optimising ship hulls towards improving energy efficiency. *Journal of Marine Science and Engineering*. 2023;11(2):835.
- [8] Hirakawa S, Maki M, Kitamura M, Nonami R. Classification of Design Variables Based on Constraint Conditions and Structural Optimal Design: Application to Structural Optimal Design of Midship Section. *Ship Technology Research*. 2014;61(2):34-47.
- [9] Kondratenko AA, Kujala P, Hirdaris SE. Holistic and sustainable design optimisation of Arctic ships. *Ocean Engineering*. 2023;275:114095.
- [10] Sekulski Z. Structural weight minimisation of high-speed vehicle-passenger catamaran by genetic algorithm. *Polish Maritime Research*. 2009;16(3):11-23.
- [11] Wium D, Lataire E, Belis J. Considerations for the integration of glass in superyacht structures. *Challenging Glass Conference Proceedings*.2022.
- [12] Eyres DJ, Bruce GJ. Ship construction. Butterworth-Heinemann; 2012.
- [13] Papanikolaou A. Ship design: methodologies of preliminary design. Springer; 2014.
- [14] Tupper EC. Introduction to naval architecture. Butterworth-Heinemann; 2013.
- [15] Souppez J-B. Structural Challenges of Low-Emission Vessels: A Review. *International Journal of Maritime Engineering*. 2023;165:165-78.
- [16] Keane RG, McNatt T, Beach JE. Reducing Total Ownership Cost: Designing Robust Ship Structures. *Naval Engineers Journal*. 2017;129:41-57.
- [17] Abedin J, Franklin F, Mahmud SI. A Two-Stage Optimisation of Ship Hull Structure Combining Fractional Factorial Design Technique and NSGA-II Algorithm. *Journal of Marine Science and Engineering*. 2024;12:411.
- [18] Papanikolaou A. Holistic ship design optimisation. Computer-Aided Design. 2010;42(10):1028-44.
- [19] Parsons MG. Applications of optimisation in early-stage ship design. *Ship Science and Technology*. 2009;3(1):9-32.
- [20] Rigo P, Žanić V, Ehlers S, Andrić J. Design of innovative ship concepts using an integrated decision support system for ship production and operation. *Brodogradnja: Teorija i praksa brodogradnje i pomorske tehnike*. 2010;61(4):367-81.
- [21] Frangopoulos CA. Developments, trends, and challenges in optimisation of ship energy systems. *Applied Sciences*. 2020;10(13):4639.
- [22] Pedersen PT, Nielsen NR. Structural optimisation of ship structures.In: *Computer Aided Optimal Design: Structural and Mechanical Systems*. Springer; 1987. p. 921-41.
- [23] Motta D, Caprace J-D, Rigo P, Boote D. Optimisation of Hull Structures for a 60 meters Mega Yacht. *Proceedings of the 11th International Conference on Fast Sea Transportation (Fast 2011)*; 2011.
- [24] Caprace J-D, Bair F, Rigo P. Early Structural Assessment and Optimisation of Passenger Ships. *Proceedings of the International Conference on Design and Operation of Passenger Ships*. 2011.
- [25] de Winter R. Efficient Constraint Multi-Objective Optimisation with Applications in Ship Design. *Doctoral Thesis*. Leiden University; 2024.

- [26] Fagerberg L. Wrinkling of sandwich panels for marine applications. Farkost och flyg; 2003.
- [27] Im N, Lee S. Effects of Forward Speed and Wave Height on the Seakeeping Performance of a Small Fishing Vessel. Journal of Marine Science and Engineering. 2022;10:1936.
- [28] Lee S-H, Kim C, Paik K-J, Kim H, Chun J. A numerical study of added resistance performance and hydrodynamics of KCS hull in oblique regular waves and estimation of resistance in short-crested irregular waves through the spectral method. International Journal of Naval Architecture and Ocean Engineering. 2024;16:100563.
- [29] Yudo H, Yulianti S, Pratiwi OR, Tuswan T. The conversion strategy from landing craft tank into livestock carrier: An overview of technical evaluation and economical benefit. Brodogradnja: An International Journal of Naval Architecture and Ocean Engineering for Research and Development. 2021;72:29-44.
- [30] Dolz M, Martinez X, Sá D, Silva J, Jurado A. Composite materials, technologies and manufacturing: Current scenario of European Union shipyards. *Ships and Offshore Structures*. 2024;19(2):1157-72.
- [31] Chernyshov E, Romanov A, Romanova E. High-strength shipbuilding steels and alloys. *Metallurgist*.2016;60(3-4):186-90.
- [32] Wahid MA, Siddiquee AN, Khan ZA. Aluminium alloys in marine construction: characteristics, application, and problems from a fabrication viewpoint. *Marine Systems & Ocean Technology*. 2020;15(1):70-80.
- [33] Oryshchenko A, Gorynin I, Leonov V, Kudryavtsev A, Mikhailov V, Chudakov E. Marine titanium alloys: Present and future. *Inorganic Materials: Applied Research.* 2015;6(5):571-79.
- [34] Alexander D. Ferrocement and its use in vessels and offshore structures. *New Zealand Engineering*. 1979;34(2):50-4.
- [35] Rubino F, Nisticò A, Tucci F, Carlone P. Marine application of fibre reinforced composites: A review. *Journal of Marine Science and Engineering*. 2020;8(1):26.
- [36] Veritas B. NR 467: Rules for the Classification of Steel Ships. Paris, France; 2018.
- [37] Shubham, Ray BC. Introduction to Composite Materials. In: Fibre-Reinforced Polymer (FRP) Composites in Ballistic Protection: Microstructural and Micromechanical Perspectives. Springer; 2024. p. 1-20.
- [38] De Mora S, Fileman T, Vance T. Environmental Impact of Ships. Cambridge: *Cambridge University Press*; 2020.
- [39] Abhijith A, Manoj A, Prasad AA, Prasad AA, Joseph A. Topology Optimisation of Deep Beam Using Ansys. *International Journal of Scientific Research and Reviews*. Available online: www.ijsrr.org. ISSN: 2279–0543. Federal Institute of Science and Technology, Angamaly, Ernakulam, Kerala, India.
- [40] Andric J, Prebeg P, Zanic V. Multi-level Pareto supported design methodology: Application to RO-PAX structural design. *Marine Structures*. 2019;67:102638.
- [41] McNatt T, Ma M, Hunter S. Historical perspective on the structural design of special ships and the evolution of structural design methods. *Ships and Offshore Structures*. 2013;8(4):404-14.
- [42] Tang J. Developing evolutionary structural optimisation techniques for civil engineering applications. PhD Thesis. *RMIT University*; 2011.
- [43] Song HC, Kim T-J, Jang CD. Structural design optimisation of racing motor boat based on nonlinear finite element analysis. *International Journal of Naval Architecture and Ocean Engineering*. 2010;2(3):217-22.
- [44] Kim DH, Paik JK. Ultimate limit state-based multi-objective optimum design technology for hull structural scantlings of merchant cargo ships. *Ocean Engineering*. 2017;129:318-34.
- [45] Algarra GAM, Tovar A. Integrating topology and shape optimisation: A way to reduce weight in structural ship design. *Ship Science and Technology*. 2009;3(2):83-92.
- [46] Qiu W, Liu K, Liu H, Zong S, Wang J, Gao Z. Crashworthiness Optimisation Method of Ship Structure under Multi-Working Conditions. *Journal of Marine Science and Engineering*. 2023;11(3):1335.
- [47] Palaversa M, Prebeg P, Andrić J. Current state of development of ship structural design and optimisation methods. *Pomorski zbornik*. 2020;59:171-87.

- [48] Rahman M. Optimisation of panel forms for improvement in ship structures. *Structural optimisation*. 1996;11(3):195-212.
- [49] Rigo P, Liege Uo. An integrated software for scantling optimisation and least production cost. *Ship Technology Research*. 2003;50(2):125-40.
- [50] Klanac A, Jelovica J. A concept of omni-optimisation for ship structural design. *Advancements in Marine Structures: Proceedings of MARSTRUCT*. 2007:473-81.
- [51] Yu Y-Y, Jin C-G, Lin Y, Ji Z-S. A practical method for ship structural optimisation. *The Twentieth International Offshore and Polar Engineering Conference*. International Society of Offshore and Polar Engineers; 2010.
- [52] Caprace J-D, Bair F, Rigo P. Scantling multi-objective optimisation of a LNG carrier. *Marine Structures*. 2010;23(2):288-302.
- [53] Ma M, Hughes O, Paik JK. Ultimate strength-based stiffened panel design using multi-objective optimisation methods and its application to ship structures. *Proceedings of the PRADS2013 CECO*. 2013.
- [54] Ma M, Freimuth J, Hays B, Danese N. Hull Girder Cross Section Structural Design using Ultimate Limit States (ULS) Based Multi-Objective Optimisation. *13th International Conference on Computer Applications and Information Technology in the Maritime Industries*;2014.
- [55] Sekulski Z. Ship hull structural multiobjective optimisation by an evolutionary algorithm. *Journal of Ship Research*. 2014;58(1):45-69.
- [56] Yu Y-Y, Lin Y, Chen M, Li K. A new method for ship inner shell optimisation based on parametric technique. *International Journal of Naval Architecture and Ocean Engineering*. 2015;7(2):142-56.
- [57] Akpan UO, Koko T, Ayyub BM, Dunbar T. Reliability-based optimal design of steel box structures. II: Ship structure applications. *ASCE-ASME Journal of Risk and Uncertainty in Engineering Systems, Part A: Civil Engineering.* 2015;1(2):04015010.
- [58] Bayatfar A, Mishael J, Warnotte R, Rigo P. An integrated framework for ship structural optimisation in the contract design phase. *Annals of "Dunarea de Jos" University of Galati Fascicle XI Shipbuilding*. 2019;42:109-16.
- [59] Nwaoha TC, Adumene S. Ship structural safety optimisation: an integrated artificial intelligence and multi-criteria decision-making method. *Journal of Structural Integrity and Maintenance*. 2019;4(3):239-47.
- [60] Louvros P, Boulougouris E, Coraddu A, Vassalos D, Theotokatos G. Multi-objective optimisation as an early design tool for smart ship internal arrangement. *Ships and Offshore Structures*. 2022;17(3):1392-402.
- [61] Cui J-j, Wang D-y. Application of knowledge-based engineering in ship structural design and optimisation. *Ocean Engineering*. 2013;72:124-39.
- [62] Guan G, Yang Q. Ship Structural Members Design and Optimisation Based on Knowledge-Based Engineering. *Proceeding of the 2016 International Conference on Industrial Informatics-Computing Technology, Intelligent Technology, Industrial Information Integration (ICIICII)*. IEEE; 2016. p. 268-73.
- [63] Guan G, Yang Q. Design and Optimisation for Ship Structure Based on Knowledge-Based Engineering. *Journal of Ship Production and Design*. 2018;34(2):191-201.
- [64] Huang H-y, Wang D-y. Static and dynamic collaborative optimisation of ship hull structure. *Journal of marine science and application*. 2009;8(2):77-82.
- [65] Papanikolaou A, Zaraphonitis G, Boulougouris E, Langbecker U, Matho S, Sames P. Multi-objective optimisation of oil tanker design. *Journal of marine science and technology*. 2010;15(3):359-73.
- [66] Saravanan M, Kumar DB. A review on navy ship parts by advanced composite material. *Materials Today: Proceedings*. 2021;45(1):6072-7.
- [67] Pereira T, Garbatov Y. Multi-attribute decision-making ship structural design. *Journal of Marine Science and Engineering*. 2022;10(4):1046.
- [68] Hamada K, Takezawa A, Kitamura M, Kanaikari K, University H. A multi-step design optimisation method for mid-ship sections. *Ship Technology Research*. 2009;56(2):110-20.
- [69] Zanic V, Andric J, Prebeg P. Design synthesis of complex ship structures. *Ships and offshore Structures*. 2013;8(3):383-403.

- [70] Elhewy AM, Hassan AM, Ibrahim MA. Weight optimisation of offshore supply vessel based on structural analysis using finite element method. *Alexandria Engineering Journal*. 2016;55(2):1005-15.
- [71] Brown A, Freimuth J, Ma M, McNatt T. Naval ship hull structural scantling optimisation by reducing weight, increasing safety and lowering vertical centre of gravity. *SNAME Maritime Convention: OnePetro*; 2016.
- [72] Li K, Yu Y, Wang Y, Hu Z. Research on structural optimisation method of FRP fishing vessel based on artificial bee colony algorithm. *Advances in Engineering Software*. 2018;121:250-61.
- [73] Raikunen J, Avi E, Remes H, Romanoff J, Lillemäe-Avi I, Niemelä A. Optimisation of passenger ship structures in the concept design stage. *Ships and Offshore Structures*. 2019;14(4):320-34.
- [74] Putra GL, Kitamura M, Takezawa A. Structural optimisation of stiffener layout for stiffened plate using hybrid GA. *International Journal of Naval Architecture and Ocean Engineering*. 2019;11(3):809-18.
- [75] Sun L, Wang D. A new rational-based optimal design strategy of ship structure based on multi-level analysis and super-element modelling method. *Journal of Marine Science and Application*. 2011;10(3):272-80.
- [76] Putra GL, Kitamura M. Material Cost Minimization Method of the Ship Structure Considering Material Selection. *Journal of Marine Science and Engineering*. 2023;11(2):640.
- [77] Oñate E. Introduction to the finite element method for structural analysis. In: *Structural analysis with the finite element method: linear statics.* 2009. p.1-42.
- [78] Aliabadi FM. Boundary element methods. In: *Encyclopedia of continuum mechanics*. Springer; 2020. p. 182-93.
- [79] Weaver W, Gere JM, Weaver W, Gere JM. Fundamentals of the Stiffness Method. In: *Matrix Analysis of Framed Structures*.McGraw-Hill;1990. p.117-80.
- [80] Nielsen R, Chang P, Deschamps L. Structural analysis of longitudinally framed ships. Technical report, Ship Structure Committee; 1972.
- [81] DeMaria S, Squassafichi N. Grillage beams calculations in ship structures. Technical report; 1967.
- [82] Sigmund O, Maute K. Topology optimisation approaches: A comparative review. *Structural and multidisciplinary optimisation*. 2013;48(5):1031-55.
- [83] Zhan T. Progress on different topology optimisation approaches and optimisation for additive manufacturing: a review. *Journal of Physics: Conference Series*. IOP Publishing; 2021. p. 012101.
- [84] Li H, Sanner S, Luo K, Wu G. A ranking optimisation approach to latent linear critiquing for conversational recommender systems. *Proceedings of the 14th ACM Conference on Recommender Systems*;2020. p. 13-22.
- [85] Venter G. Review of optimisation techniques. Technical report; 2010.
- [86] Rao SS. Engineering optimisation: theory and practice. John Wiley & Sons; 2019.
- [87] Sekulski Z. Structural weight minimisation of high-speed vehicle-passenger catamaran by genetic algorithm. *Polish Maritime Research*. 2009;16(3):11-23.
- [88] Young Y, Baker J, Motley M. Reliability-based design and optimisation of adaptive marine structures. *Composite structures*. 2010;92(2):244-53.
- [89] Li K, Yu Y, He J, Zhao D, Lin Y. Structural optimisation of Hatch cover based on bi-directional evolutionary structure optimisation and surrogate model method. *Journal of Shanghai Jiaotong University (Science)*. 2018;23(3):538-49.
- [90] Sha O, Ray T, Gokarn R. An artificial neural network model for preliminary ship design. Technical report;1994.
- [91] Calle MA, Salmi M, Mazzariol LM, Alves M, Kujala P. Additive manufacturing of miniature marine structures for crashworthiness verification: Scaling technique and experimental tests. *Marine Structures*. 2020;72:102764.
- [92] Braidotti L, Prpić-Oršić J. Bulkheads' Position Optimisation in the Concept Design of Ships under Deterministic Rules. *Journal of Marine Science and Engineering*, 2023;11(3):546.
- [93] Pedersen PT. Marine structures: future trends and the role of universities. *Engineering*. 2015;1(2):131-8.
- [94] Wang H, Mao W, Zhang D. Voyage optimisation for mitigating ship structural failure due to crack propagation. *Proceedings of the Institution of Mechanical Engineers, Part O: Journal of Risk and Reliability*. 2019;233(1):5-17.

- [95] Tezzele M, Fabris L, Sidari M, Sicchiero M, Rozza G. A multifidelity approach coupling parameter space reduction and nonintrusive POD with application to structural optimisation of passenger ship hulls. *International Journal for Numerical Methods in Engineering*. 2023;124:1193-210.
- [96] MacCutcheon E, Oakley O, Stout R. Ship Structure Committee Long-range Research Plan: Guidelines for Program Development. US Coast Guard. Office of Merchant Marine Safety; 1983.
- [97] Yao T. Hull girder strength. Marine Structures. 2003;16:1-13.
- [98] Novikov VV, Antonenko SV, German AP, Kitaev MV. Effect of Ship Torsion with Wide Hatches on the Hull's Stress State. *The Twenty-fifth International Ocean and Polar Engineering Conference*. OnePetro; 2015.
- [99] Shama M. Torsion and shear stresses in ships. Springer Science & Business Media; 2010.
- [100] Elbatouti A, Liu D, Jan H. Structural analysis of sl-7 containership under combined loading of vertical, lateral and torsional moments using finite element techniques (SL-7-3). Technical report;1974.
- [101] Ostapenko A, Chu P-C. Torsional Strength of Longitudinals in Marine Structures. *Lehigh University, Department of Civil Engineering*; 1986.
- [102] Vernon TA, Nadeau Y. Thin-Walled Beam Theories and Their Applications in the Torsional Strength Analysis of Ship Hulls. *Defence Research Establishment Atlantic Dartmouth (Nova Scotia)*; 1987.
- [103] Valsgard S, Svensen TE, Thorkildsen H. A computational method for analysis of container vessels. Technical report; 1995.
- [104] Paik JK, Thayamballi AK, Pedersen PT, Park YI. The ultimate strength of ship hulls under torsion. *Ocean Engineering*. 2001;28:1097-133.
- [105] Iijima K, Shigemi T, Miyake R, Kumano A. A practical method for torsional strength assessment of container ship structures. *Marine structures*. 2004;17:355-84.
- [106] Senjanović I, Tomašević S, Rudan S, Senjanović T. Role of transverse bulkheads in hull stiffness of large container ships. *Engineering Structures*. 2008;30:2492-509.
- [107] Chirică R, MUŞAT SD, Boazu D, Beznea E-F. Torsional Analysis of Ship Hull Model. Technical report; 2009.
- [108] Parunov J, Uroda T, Senjanović I. Structural analysis of a general cargo ship. *Brodogradnja: Teorija i praksa brodogradnje i pomorske tehnike*. 2010;61:28-33.
- [109] Senjanović I, Vladimir N, Tomić M. Investigation of torsion, warping and distortion of large container ships. *Ocean Systems Engineering*. 2011;1:73-93.
- [110] Rörup J, Maciolowski B, Darie I. FE-based strength analysis of ship structures for a more advanced class approval. *Proceedings of PRADS2016*. 2016;4:8th.
- [111] Tang H, Ren H, Zhong Q. Design and model test of structural monitoring and assessment system for trimaran. *Brodogradnja: Teorija i praksa brodogradnje i pomorske tehnike*. 2019;70:111-34.
- [112] Jurišić P, Parunov J. Structural aspects during conversion from general cargo ships to cement carriers. *Brodogradnja: Teorija i praksa brodogradnje i pomorske tehnike*. 2021;72:37-55.
- [113] Bauchau OA, Craig JI. Euler-Bernoulli beam theory. In: Structural analysis. 2009:173-221.
- [114] Ogeman V. Analysis of the effect of bending and torsion for fatigue in container ships. Technical report; 2013.
- [115] Fengfeng M. Longitudinal ultimate bending strength analysis of ship structure for emergency response. Technical report; 2015.
- [116] Mbachu VC. Analysis of continuous thin-walled box beam in pure and warping torsion. *Department Of Civil Engineering, University Of Nigeria, Nsukka*; 2010.
- [117] Librescu L, Song O. Thin-walled composite beams: theory and application. *Springer Science & Business Media*; 2005.
- [118] Senjanović I, Senjanović T, Tomašević S, Rudan S. Contribution of transverse bulkheads to hull stiffness of large container ships. *Brodogradnja: Teorija i praksa brodogradnje i pomorske tehnike*. 2008;59:228-38.
- [119] Torralba Ben Amar DE. Analytical and numerical determination of the hull girder deflection of inland navigation vessels. Technical report; 2015.
- [120] Dedetaş B. 9100 Dwt Lik Çok Amaclı Geminin Yapısal Analizi. Fen Bilimleri Enstitüsü; 2010.
- [121] Rigo P, Rizzuto E. Analysis and design of ship structure. *Ship design and construction*. Taylor & Francis; 2003.p.18-1.

- [122] **Efford, A.** (n.d.). Structural Image of a Multi-purpose Cargo Ship. Retrieved from https://www.marinetraffic.com/he/photos/by/copyright:Anthony%20Efford.
- [123] Shama M. Buckling of ship structures. Springer Science & Business Media; 2012.
- [124] Wang X, Moan T. Stochastic and deterministic combinations of still water and wave bending moments in ships. *Marine Structures*. 1996;9:787-810.
- [125] Chen Z, Gui H, Dong P, Yu C. Numerical and experimental analysis of hydroelastic responses of a high-speed trimaran in oblique irregular waves. *International Journal of Naval Architecture and Ocean Engineering*. 2019;11:409-21.
- [126] Rörup J, Darie I, Maciolowski B. Strength analysis of ship structures with open decks. *Ships and Offshore Structures*. 2017;12:S189-S99.
- [127] Huang L, Li B, Wang Y. FEM and EFG Quasi-Static Explicit Buckling Analysis for Thin-Walled Members. *Open Journal of Civil Engineering*. 2017;7:432-52.
- [128] Ahmed F. Development of guidelines allowing to predict the contribution of the superstructure to the hull girder strength. Technical report; 2017.
- [129] Samal AK, Rao TE. Analysis of stress and deflection of cantilever beam and its validation using ANSYS. *Journal of Engineering Research and Applications*. 2016;6:119-26.
- [130] Baker N, Kelly G, O'Sullivan PD. A grid convergence index study of mesh style effect on the accuracy of the numerical results for an indoor airflow profile. *International Journal of Ventilation*. 2020;19:300-14.
- [131] Lockard DP. Reprint of: In search of grid converged solutions. *Procedia IUTAM*. 2010;1:224-33.
- [132] Brassey CA, Margetts L, Kitchener AC, Withers PJ, Manning PL, Sellers WI. Finite element modelling versus classic beam theory: comparing methods for stress estimation in a morphologically diverse sample of vertebrate long bones. *Journal of the Royal Society Interface*. 2013;10:20120823.
- [133] Jurišić P, Parunov J, Garbatov Y. Aging effects on ship structural integrity. *Brodogradnja: Teorija i praksa brodogradnje i pomorske tehnike.* 2017;68:15-28.
- [134] Sun H, Wang X. Buckling and ultimate strength assessment of FPSO structures. *SNAME Maritime Convention*. SNAME; 2005. p. D021S03R04.
- [135] Crudu L, Neculet O, Marcu O. Hull deflection in still water and in waves of a pipe layer barge. *IOP Conference Series: Materials Science and Engineering*. IOP Publishing; 2018. p. 062002.
- [136] Bai Y, Bendiksen E, Pedersen PT. Collapse analysis of ship hulls. *Marine Structures*. 1993;6:485-507.
- [137] Ziha K. Displacement of a deflected ship hull. *Marine technology and SNAME news*. 2002;39:54-61.
- [138] Mennitt SH. The effects of ship load variations and seastate on hull girder deflection and combat system alignment [manuscript];1990.
- [139] Lee Y-J, Kim U-K, Kim J-S. Hull Deflections Affecting on the Ship's Propulsion Shafting Alignment in 46K Oil/Chemical Carrier. *Journal of Advanced Marine Engineering and Technology*. 2006;30:800-7.
- [140] Niebylski J. Methods of evaluation of global and local ship hull deflections based on periodic geodesic measurements assuming linear model of deflections. WIT Transactions on The Built Environment. 1970;12.
- [141] Antoniou A. On the maximum deflection of plating in newly built ships. *Journal of ship research*. 1980;24:31-9.
- [142] Lee Y-J, Kim U-K. A Study on hull deflection and shaft alignment interaction in VLCC. *Journal of Advanced Marine Engineering and Technology*. 2005;29:785-94.
- [143] Šverko D. Investigation on hull deflection and its influence on propulsion shaft alignment. *SNAME Maritime Convention: OnePetro*; 2005.
- [144] Naar H. Ultimate strength of hull girder for passenger ships: *Helsinki University of Technology*; 2006.
- [145] Dardamanis A. Development of a Model for the Calculation of Ship Hull Deflection, with Application to the Optimal Alignment of the Propulsion Shafting System. *Doctoral Thesis*. National Technical University of Athens; 2022.
- [146] Farias MdR, Vaz LA, Troyman AC, Baptista LAR. Optimisation of Shafting Alignment in Medium-Sized Vessels Considering Hull Deflection. Available at SSRN 4566663.

- [147] Zhou W, Zhao Y, Yuan H, Wang X. Study of the hull structural deformation calculation using the matrix displacement method and its influence on the shaft alignment. *Journal of Marine Science and Engineering*. 2023;11:1495.
- [148] Freire Duenas WT, Winklemann de la Cruz G. The effect of initial deflection on the stress distribution in a panel of plating of a ship under tensile load. *Massachusetts Institute of Technology*; 1954.
- [149] Okumoto Y, Takeda Y, Mano M, Okada T. Deflection of Hull Structures. In: *Design of Ship Hull Structures: A Practical Guide for Engineers*. Springer; 2009. p. 285-96.
- [150] Molland AF. The maritime engineering reference book: A guide to ship design, construction and operation. *Elsevier*; 2011.
- [151] Korbetis G, Vlachos O, Charitopoulos AG, Papadopoulos CI. Effects of hull deformation on the static shaft alignment characteristics of VLCCs: A case study. *Proceedings of the 13th International Conference on Computer Applications and Information Technology in the Maritime Industries*; 2014. p. 12-4.
- [152] ABS. Guidance Notes on 'Propulsion Shafting Alignment. American Bureau of Shipping Houston, TX, USA; 2019.
- [153] Quimby TB. A beginner's guide to the steel construction manual. *University of Alaska Anchorage*; 2008.
- [154] Altenburg CJ, Scott RJ. Design Considerations for Aluminium Hull Structures: Study of Aluminium Bulk Carrier. *US Coast Guard Headquarters*; 1971.
- [155] Rawson K, Tupper E. Basic Ship Theory. Volume 2. Longman Group Limited, London, England; 1976.
- [156] Martic I, Degiuli N, Farkas A, Basic J. Mesh Sensitivity Analysis for the Numerical Simulation of a Damaged Ship Model. *ISOPE International Ocean and Polar Engineering Conference*.ISOPE; 2017. p. ISOPE-I-17-624.
- [157] Gallo HLM, Salman RLL, Montaña DIF. Design and Structural Analysis of a SWATH type vessel using the Finite Element Method and its response to Slamming events. *Ciencia y tecnología de buques*. 2020;14:55-66.
- [158] Perez-Martinez J, Perez Fernandez R. Material and Production Optimisation of the Ship Design Process by Introducing CADs from Early Design Stages. *Journal of Marine Science and Engineering*. 2023;11:233.
- [159] Tadahiko K. The application of finite element methods to ship structures. *Computers & Structures*. 1973;3:1175-94.
- [160] Rahman MM, Kamol RS, Islam R. Structural analysis of a ship on global aspect using ANSYS. *AIP Conference Proceedings*. AIP Publishing; 2017.
- [161] Antony J. Design of experiments for engineers and scientists. *Elsevier*; 2023.
- [162] Nair V, Strecher V, Fagerlin A, Ubel P, Resnicow K, Murphy S, et al. Screening experiments and the use of fractional factorial designs in behavioural intervention research. *American journal of public health*. 2008;98:1354-9.
- [163] Vizzari D, Chailleux E, Lavaud S, Gennesseaux E, Bouron S. Fraction factorial design of a novel semi-transparent layer for applications on solar roads. *Infrastructures*. 2020;5:5.
- [164] Natoli C. Classical Designs: Fractional Factorial Designs. STAT Center of Excellence: Hobson Way, Wright-Patterson AFB, OH, USA; 2018.
- [165] Hester MW, Usher J. Factor screening experiments using fractional factorial split plot designs and regression analysis in developing a top-down nanomanufacturing system for recycling of welding rod residuals. *Production & Manufacturing Research*. 2017;5:118-39.
- [166] Pamnani R, Vasudevan M, Vasantharaja P, Jayakumar T. Optimisation of A-GTAW welding parameters for naval steel (DMR 249 A) by design of experiments approach. *Proceedings of the Institution of Mechanical Engineers, Part L: Journal of Materials: Design and Applications.* 2017;231:320-31.
- [167] Kuo H-C, Wu J-L. A new approach with an orthogonal array for global optimisation in the design of experiments. *Journal of Global Optimisation*. 2009;44:563-78.
- [168] Gorshy H, Chu X, Gao L, Li P. An approach combined response surface method and particle swarm optimisation to ship multidisciplinary design and optimisation. 2009 IEEE International Conference on Industrial Engineering and Engineering Management. IEEE; 2009. p. 1810-4.

- [169] Allen TT, Chantarat N, Taslim C. Fractional factorial designs that maximise the probability of identifying the important factors. *International Journal of Industrial and Systems Engineering*. 2009;4:133-50.
- [170] Hawkins D, Lye LM. Use of DOE methodology for investigating conditions that influence the tension in marine risers for FPSO ships. *First International Structural Specialty Conference*; 2006.
- [171] Lamb T. Ship design and construction. Editor Thomas Lam. *The SNAME*; 2003.ISBN: 0-939773-40-6.
- [172] Bai Y. Marine structural design. *Elsevier*; 2003.
- [173] Li Z, Ringsberg JW, Storhaug G. Time-domain fatigue assessment of ship side-shell structures. *International journal of fatigue*. 2013;55:276-90.
- [174] Campanile A. Analysis of warping and shear stresses for ship structures. *Theoretical developments and numerical applications*. 2009.
- [175] Leal M, Gordo JM. Hull's manufacturing cost structure. *Brodogradnja: Teorija i praksa brodogradnje i pomorske tehnike*. 2017;68:1-24.
- [176] Montgomery DC. Design and analysis of experiments. John Wiley & Sons. 2017.
- [177] Shina S. Industrial Design of Experiments: A Case Study Approach for Design and Process Optimisation. *Springer Nature*. 2022.
- [178] Krishnan P. When and how to use factorial design in nursing research. Nurse researcher, 29.2021.
- [179] Zhao T, Yang G, Xi J, Shen Y, Song K-i. Factorial Experiment Study on the Mechanical Properties of Sandstone–Concrete Specimens Under Different Freeze-Thaw Conditions. *Frontiers in Physics*. 2020;8:322.
- [180] Diewald BG, Ehlers S. On the influence of primary and secondary structural members on the global strength of ship structures. *Maritime Technology and Engineering*. 2016;3:435-41.
- [181] Priyadharshini SD, Bakthavatsalam A. Optimisation of phenol degradation by the microalga Chlorella pyrenoidosa using Plackett–Burman design and response surface methodology. *Bioresource Technology*. 2016;207:150-6.
- [182] Tyssedal J, Samset O. Analysis of the 12-run Plackett-Burman design. Preprint, Statistics. 1997.
- [183] Abdel-Fattah YR, El-Helow ER, Ghanem K, Lotfy W. Application of factorial designs for optimisation of avicelase production by a thermophilic Geobacillus isolate. *Research Journal of Microbiology*, 2,13-23. 2007.
- [184] Karlapudi AP, Krupanidhi S, Reddy R, Indira M, Md NB, Venkateswarulu T. Plackett-Burman design for screening of process components and their effects on the production of lactase by newly isolated Bacillus sp. VUVD101 strain from Dairy effluent. *Beni-Suef University journal of basic and applied sciences*. 2018;7:543-6.
- [185] Gunst RF, Mason RL. Fractional factorial design. *Wiley Interdisciplinary Reviews: Computational Statistics*. 2009;1:234-44.
- [186] Montgomery DC, Runger GC. Applied statistics and probability for engineers. *John Wiley & Sons*; 2020.
- [187] Fahrmeir L, Kneib T, Lang S, Marx BD. Regression models. In: *Regression: Models, methods and applications*. Springer; 2022. p. 23-84.
- [188] Caprace J-D, Bair F, Rigo P. Multi-criteria scantling optimisation of cruise ships. *Ship Technology Research*. 2010;57:210-20.
- [189] Andric J, Prebeg P, Palaversa M, Zanic V. Influence of different topological variants on optimised structural scantlings of passenger ship. *Marine Structures*. 2021;78:102981.
- [190] Qiu L-m, Sun L-f, Liu X-j, Zhang S-y. Material selection combined with optimal structural design for mechanical parts. *Journal of Zhejiang University SCIENCE A*. 2013;14:383-92.
- [191] Lu Y, Chang X, Hu A-k. A hydrodynamic optimisation design methodology for a ship bulbous bow under multiple operating conditions. *Engineering Applications of Computational Fluid Mechanics*. 2016;10:330-45.
- [192] Nebro AJ, Galeano-Brajones J, Luna F, Coello Coello CA. Is NSGA-II Ready for Large-Scale Multi-Objective Optimisation? *Mathematical and Computational Applications*. 2022;27:103.
- [193] Jelovica J, Klanac A. Multi-objective optimisation of ship structures: using guided search vs. conventional concurrent optimisation. *Proceedings of the 2nd International Conference on Marine Structures (MARSTRUCT 2009)*, Taylor & Francis Group, London, UK.; 2009.

- [194] Ghanta S, Rayguru MM, Pathmakumar T, Kalimuthu M, Elara MR, Sheu BJ. Uniform hydro blasting for ship hull maintenance: A multi-objective optimisation framework. *Ocean Engineering*. 2021;242:109977.
- [195] Deb K, Pratap A, Agarwal S, Meyarivan T. A fast and elitist multiobjective genetic algorithm: NSGA-II. *IEEE transactions on evolutionary computation*. 2002;6:182-97.
- [196] Christensen PW, Klarbring A. An introduction to structural optimisation. *Springer Science & Business Media*; 2008.
- [197] Caprace J-D, Bair F, Rigo P. Multi-criterion Scantling Optimisation of Passenger Ships. *COMPIT'10-9th International Conference on Computer Applications and Information Technology in the Maritime Industries*;2010.
- [198] Alhammadi HY, Romagnoli JA. Incorporating environmental, profitability, heat integration and controllability considerations. *The integration of process design and control*. 2004;17:264.
- [199] Selvi ST, Baskar S, Rajasekar S. Application of evolutionary algorithm for multiobjective transformer design optimisation. Classical and recent aspects of power system optimisation. *Elsevier*; 2018. p. 463-504.
- [200] De Buck V, López CAM, Nimmegeers P, Hashem I, Van Impe J. Multi-objective optimisation of chemical processes via improved genetic algorithms: A novel trade-off and termination criterion. *Computer Aided Chemical Engineering: Elsevier*; 2019. p. 613-8.
- [201] Wang L, Ng AH, Deb K. Multi-objective evolutionary optimisation for product design and manufacturing. *Springer*; 2011.
- [202] Burke RS. Rigid Body Dynamics of Ship Hulls via Hydrostatic Forces Calculated from FFT Ocean Height Fields. *Clemson University*; 2021.
- [203] Suzuki S, Muraoka R, Obinata T, Endo S, Horita T, Omata K. Steel products for shipbuilding. JFE technical report. 2004;2:41.
- [204] Green AE, Zerna W. Theoretical elasticity. Courier Corporation; 1992.
- [205] Giaccone D, Fanelli P, Santamaria U. Influence of the geometric model on the structural analysis of architectural heritage. *Journal of Cultural Heritage*. 2020;43:144-52.
- [206] Ergin A. DYNAMIC RESPONSE. Proceedings of the 15th International Ship and Offshore Structures Congress: 3-volume set: Elsevier. 2003. p. 193.
- [207] Committee UMPR, Council NR. Unit manufacturing processes: issues and opportunities in research. *National Academies Press*. 1995.
- [208] Yu J, Tang G, Song X, Yu X, Qi Y, Li D, et al. Ship arrival prediction and its value on daily container terminal operation. *Ocean Engineering*. 2018;157:73-86.
- [209] Sørensen SN, Sørensen R, Lund E. DMTO-A method for discrete material and thickness optimisation of laminated composite structures. *Structural and Multidisciplinary Optimisation*. 2014;50:25-47.
- [210] Esmailian E, Steen S. A new method for optimal ship design in real sea states using the ship power profile. *Ocean Engineering*. 2022;259:111893.
- [211] Yu Y-Y, Jin C-G, Lin Y, Ji Z-S. A practical method for ship structural optimisation. *ISOPE International Ocean and Polar Engineering Conference: ISOPE*; 2010. p. ISOPE-I-10-511.
- [212] Zakerdoost H, Ghassemi H. Application of a variable-fidelity hydrodynamic optimisation strategy in fuel-efficient ship design. *Proceedings of the Institution of Mechanical Engineers, Part C: Journal of Mechanical Engineering Science*. 2019;233:6293-306.
- [213] Caprace J-D. Cost Effectiveness and Complexity Assessment in Ship Design within a Concurrent Engineering and" Design for X" Framework. 2010.
- [214] Yuan J, Nian V, He J, Yan W. Cost-effectiveness analysis of energy efficiency measures for maritime shipping using a metamodel-based approach with different data sources. *Energy*. 2019;189:116205.
- [215] Eliopoulou E, Papanikolaou A, Diamantis P, Hamann R. Analysis of tanker casualties after the Oil Pollution Act (USA, 1990). *Proceedings of the Institution of Mechanical Engineers, Part M: Journal of Engineering for the Maritime Environment*. 2012;226:301-12.
- [216] Sendi P. Dealing with bad risk in cost-effectiveness analysis: the cost-effectiveness risk-aversion curve. *Pharmacoeconomics*. 2021;39:161-9.
- [217] Tatsumi A, Iijima K, Fujikubo M. A Study on Progressive Collapse Analysis of a Hull Girder Using Smith's Method–Uncertainty in the Ultimate Strength Prediction. *Practical Design of Ships and*

- Other Floating Structures: Proceedings of the 14th International Symposium, PRADS; 2019. Yokohama, Japan-Volume II 14: Springer; 2021. p. 128-44.
- [218] Li S, Hu Z, Benson S. A cyclic progressive collapse method to predict the bending response of a ship hull girder. *Trends in the Analysis and Design of Marine Structures*. 2019:149-57.
- [219] Mardani A, Jusoh A, Nor K, Khalifah Z, Zakwan N, Valipour A. Multiple criteria decision-making techniques and their applications—A review of the literature from 2000 to 2014. *Economic research-Ekonomska istraživanja*. 2015;28:516-71.
- [220] Veritas B. Rules for the classification of steel ships. *The Bureau*; 2000.
- [221] Chowdhury M. On the probability of failure by yielding of hull girder midship section. *Ships and Offshore Structures*. 2007;2:241-60.
- [222] Soleimani E, Tabeshpour MR, Seif MS. Parametric study of buckling and post-buckling behaviour for an aluminium hull structure of a high-aspect-ratio twin hull vessel. *Proceedings of the Institution of Mechanical Engineers, Part M: Journal of Engineering for the Maritime Environment*. 2020;234:15-25
- [223] Faqih I, Adiputra R, Prabowo AR, Muhayat N, Ehlers S, Braun M. Hull girder ultimate strength of bulk carrier (HGUS-BC) evaluation: Structural performances subjected to true inclination conditions of stiffened panel members. *Results in Engineering*. 2023;18:101076.
- [224] Hørte T, Wang G, White N. Calibration of the hull girder ultimate capacity criterion for double hull tankers. *Proc PRADS 2007 Conference: Citeseer*; 2007.
- [225] Thakur S, Saxena NV, Roy PS. Generative AI in Ship Design. arXiv preprint, arXiv:240816798. 2024.
- [226] Mao W, Larsson S. Increase shipping efficiency using ship data analytics and AI to assist ship operations. *Lighthouse Reports[PDF]*. 2022.
- [227] Mazari JA, Reverberi A, Yser P, Sigmund S. Multi-Objective Hull Form Optimisation with CAD Engine-based Deep Learning Physics for 3D Flow Prediction. *arXiv* preprint, arXiv:230612915. 2023.

Appendix A

Cross Section Characteristics Gross scantling

Geometric Properties (For the whole cross-section)

Geometric Area of Cross-Section

	Steel (235)	Steel (355)	Total Area
Strakes	0.680468	0.162842	0.843310
Longitudinals	0.059520	0.073352	0.132872
Total (m ²)	0.739988	0.236194	0.976182

Geometric area of cross-section
$Effective area. \\ 0.976183 \text{ m}^2$
Single moment above neutral axis
Single moment of half section
$Moment of inertia / G_y \ axis. \\ \hspace*{2cm} (IG_y) \ \ 9.101366 \ m^4$
$Moment \ of \ inertia \ / \ G_z \ axis. \ \hspace{1.5cm} (IG_z) \ \ 31.638720 \ m^4$
Position of neutral axis(above base line) (N) 3.00834 m
$Modulus \ at \ deck. \\ (7.450 \ m) \dots (Z_{AD}) \ 2.049091 \ m^3$
$Modulus \ at \ bottom. \qquad \qquad (0.000 \ m) \ \dots (Z_{AB}) \ 3.025378 \ m^3$
Modulus at top $(Z_{vt} = 9.578 \text{ m})$ (Z_{AT})
$(Z_{vt} = 9.578 \text{ m}; V_t = 6.570 \text{ m}; Y_t = 6.803 \text{ m}; Z_t = 9.650 \text{ m})$
Transverse sectional area of deck flange
Transverse sectional area of bottom flange

These characteristics (except geometric area) are effective values assuming a homogeneous material of $206000 \, (\text{N/mm}^2)$ as Young modulus.

Profiles

Type	Scantling		Number
flat	180 x 10.0		18
flat	120 x 12.0		6
bulb	140 x 8.0		16
bulb	120 x 8.0		36
angle	500 x 22.0	150 x 22.0	2

Strakes

Thickness (mm)	Length* (m)
18.000	1.100
15.000	20.640
14.000	2.940
13.000	1.970
12.000	12.323
11.000	14.809
10.000	8.930
9.000	7.030

^{*} The length indicated is the total length for the strakes having the same thickness.

Cross Section Characteristics Net scantling

Geometric Properties (For the whole cross-section)

Geometric Area of Cross-Section

	Steel (235)	Steel (355)	Total Area
Strakes	0.581708	0.145530	0.727237
Longitudinals	0.046094	0.062068	0.108162
Total (m ²)	0.627801	0.207598	0.835399

Geometric area of cross-section. 0.835398 m ²
$Effective area. \\ 0.835398 \text{ m}^2$
Single moment above neutral axis(/ neutral axis) 1.141195 m ³
Single moment of half section(/centre line) 2.184669 m ³
$Moment of inertia / G_y axis. \qquad \qquad \qquad \\ (IG_y) 8.023850 m^4$
$Moment \ of \ inertia \ / \ G_z \ axis. \qquad \qquad (IG_z) \ \ 27.120220 \ m^4$
Position of neutral axis(above base line) (N) 3.00834 m
$Modulus \ at \ deck. \\ \hspace*{1.5cm} (7.450 \ m) (Z_{AD}) \ 1.837189 \ \ m^3$
$\label{eq:modulus} \mbox{Modulus at bottom.} \qquad \qquad (0.000 \ m) \ \dots (Z_{AB}) \dots \ 2.603001 \ m^3$
Modulus at top($Z_{vt} = 9.578 \text{ m}$)(Z_{AT}) 1.235224 m ³
Transverse sectional area of deck flange
Transverse sectional area of bottom flange
These characteristic (except geometric area) are effective values assuming a homogeneous material of 206000 (N/mm²) as Young modulus.

Hull Girder Loads

Vertical Bending Moment

	Hogging (kNm)	Sagging (kNm)
S.W.B.M. Builder's proposal in Basic Ship Data	0.	0.
S.W.B.M. Builder's proposal at $X = 49.27 \text{ m}$	-	-
S.W.B.M. preliminary value at midship	125 651.	- 113 909.
S.W.B.M. preliminary value at $X = 49.27 \text{ m}$	125651.	- 113 909.
Rule Vertical Wave Bending Moment at $X = 49.27 \text{ m}$.	177 581.	- 192 769.

Design Hull Girder Loads at X = 49.27 m

	Hogging (kNm)	Sagging (kNm)
S.W.B.M	125 651.	- 113 909.
Wave bending moment (Rule)	177 581.	- 192 769.
Horizontal wave bending moment	93 037.	
	Positive (KN)	Negative (KN)
Vertical still water shear force	2 000.	
Vertical wave shear force	3 735.	- 3 735.
dmissible Vertical Shear Forces		
dmissible Vertical Shear Forces otal Admissible Vert. Shear Force ositive Admissible Vert. Still Water Shear Force	(KN) (KN)	25 430. 21 695.
otal Admissible Vert. Shear Force	` ,	
otal Admissible Vert. Shear Force ositive Admissible Vert. Still Water Shear Force	(KN)	21 695.
otal Admissible Vert. Shear Force ositive Admissible Vert. Still Water Shear Force egative Admissible Vert. Still Water Shear Force	(KN) (KN)	21 695. 21 695.
otal Admissible Vert. Shear Force ositive Admissible Vert. Still Water Shear Force egative Admissible Vert. Still Water Shear Force ection moduli and Inertia	(KN) (KN)	21 695. 21 695. 49.270
otal Admissible Vert. Shear Force ositive Admissible Vert. Still Water Shear Force egative Admissible Vert. Still Water Shear Force ection moduli and Inertia section.	(KN) (KN)	21 695. 21 695. 49.270 49.268

Rule section moduli

	Deck	Bottom	Тор
	(m^3)	(m^3)	(m ³)
Minimum section modulus	1.2618	1.7524	1.2618
Modulus based on design BM, Hog. (306 677.1 kNm)	1.2618	3 1.7524	1.2618
Modulus based on design BM, Sag. (- 306 677.1 kNm)	1.2618	1.7524	1.2618
Rule Modulus	1.2618	1.7524	1.2618

Check of section moduli and inertia

		Rule	Actual
Deck	(7.450 mk =0.72)	1.2618	2.0491
Bottom	(0.000 mk = 1.00)	1.7524	3.0254
Top	(9.578 mk =0.72)	1.2618	1.3853
Inertia		5.1803	9.1014

Check of Net/Gross Moduli

		Actual Gross	Actual Net	%
Deck	(7.450 m)	2.0491	1.8372	89.7
Bottom	(0.000 m)	3.0254	2.6030	86.0
Тор	(9.578 m)	1.3853	1.2352	89.2

Appendix B

Regression Equations for Von Mises Stress, Warping Stress and Production Costs

Plackett-Burman Screening Plan

Regression Equation (Von Mises Stress) = 376.2 + 0.184A - 1.459B - 0.447C - 1.973D + 0.572E - 1.407F - 1.525G - 5.381H - 2.214J + 0.027K + 0.00409L + 0.1037M

where *A, B, C, D, E, F, G, H, J, K, L* and *M* denote Keel plate, Bottom plate, Side Shell plate, Shear Strake plate, Inner Bottom Plate, Inner Side Shell plate, Main Deck Plate, Hatch Coaming Plate, Hatch Coaming Top Plate, DB Longitudinal Girder (CL), Web Frame Spacing and Stiffener Spacing, respectively.

Fractional Factorial Design

Regression Equation (Von Mises Stress) = 935.3 - 2.58A - 11.21B - 3.21C - 5.60D - 4.69E - 2.10F - 4.37G -6.09H - 5.68J - 1.78K - 0.1504L -0.3567M + 0.0007AB -0.0281AC + 0.0235AD - 0.0042AE - 0.0355AF - 0.0170AG + 0.0281AH + 0.0256AJ - 0.0218AK + 0.000266AL + 0.00270AM - 0.0366BC + 0.1120BD + 0.0406BE - 0.0224BF + 0.1475BG + 0.1402BH + 0.1798BJ - 0.0097BK + 0.00059BL + 0.00086BM + 0.0608CD - 0.0433CE - 0.0106CF - 0.0004CG + 0.0719CH + 0.0440CJ - 0.0364CK + 0.000228CL + 0.00236CM + 0.0151DE + 0.0602DF + 0.0540DG + 0.0682DH + 0.0086DJ + 0.0240DK - 0.000152DL - 0.00191DM - 0.0464EF - 0.0267EG + 0.0322EH + 0.0169EJ + 0.0013EK + 0.000531EL + 0.00470EM + 0.0100FG + 0.1580FH + 0.0736FJ - 0.0323FK - 0.000284FL - 0.00255FM - 0.0184GK + 000087GL + 0.00076GM + 0.0160HK - 0.000652HL -0.00651HM - 0.0009JK + 0.000013JL - 0.00150JM + 0.000268KL + 0.00291KM + 0.000219LM

Regression Equation (Warping Stress) = 758.3 + 0.38A - 22.74B - 4.57C - 0.62D - 12.77E + 3.09F + 1.31G + 5.52H + 3.58J + 1.394K - 0.24838L - 0.7734M - 0.0068AB - 0.0053AC - 0.0012AD - 0.0075AE + 0.0085AF + 0.0171AG - 0.0037AH + 0.0065AJ - 0.0522AK + 0.000028AL + 0.00027AM + 0.0466BC + 0.01426BD + 0.0393BE + 0.0089BF + 0.0463BG + 0.0359BH + 0.0237BJ + 0.0046BK + 0.00188BL + 0.02008BM - 0.0189CD + 0.0175CE + 0.0033CF - 0.0038CG + 0.0361CH + 0.0100CJ - 0.0024CK + 0.000201CL + 0.00232CM - 0.000201CL + 0.000232CM - 0.000201CL + 0.000232CM - 0.000201CL + 0.000232CM - 0.000201CL + 0.000201CL + 0.000232CM - 0.000201CL + 0.000201CL + 0.000232CM - 0.000201CL + 0.00020

0.0047DE - 0.0086DF + 0.0504DG - 0.2033DH + 0.0358DJ + 0.0020DK - 0.000019DL + 0.00027DM + 0.0008EF + 0.0022EG + 0.0006EH - 0.0058EJ + 0.0188EK + 0.001293EL + 0.01352EM + 0.0031FG + 0.0509FH + 0.0158FJ - 0.0016FK - 0.000637FL - 0.00634FM + 0.0108GK - 0.000389GL - 0.00380GM - 0.0012HK - 0.000825HL - 0.00653HM - 0.0315JK - 0.000522JL - 0.00565JM - 0.000061KL - 0.00062KM + 0.000367LM

Regression Equation (Production Costs) = 892606 + 4557A + 25778B +15108C + 8445D +29447E +22487F +6468G +7193H + 3720J - 1100K - 122.71L -111.1M + 19.1AB +19.1AC -16.4AD - 17.5AE + 16.1AF - 16.1AG + 13.7AH - 13.5AJ + 13.8 AK - 0.115AL - 1.18AM - 23.3BC + 19.9BD + 21.2BE - 19.4BF + 19.5BG - 16.2BH + 16.5BJ - 16.4BK + 0.134BL + 1.38BM + 19.7CD + 21.0CE - 19.4CF + 19.2CG - 16.3CH + 16.5CJ - 16.5CK + 0.138CL +1.41CM - 18.0DE + 16.5DF - 16.3DG + 20.2DH - 19.5DJ + 14.0DK - 0.163DL - 1.68DM + 17.6EF - 17.4EG + 14.8EH - 15.1EJ + 15.1EK - 0.125EL - 1.29EM + 16.0FG - 13.6FH + 13.6FJ -13.8FK + 0.114FL + 1.18FM + 13.8GK - 0.116GL - 1.19GM - 11.7HK + 0.136HL + 1.40HM + 11.8JK - 0.134JL - 1.38JM + 0.099KL + 1.01KM - 0.0240LM

Appendix C

Python Code

The Python code presented in this thesis acts as the computational foundation, implementing the NSGA-II algorithm for multi-objective optimisation. It also includes regression equations for modelling Von Mises stress and production costs, thus enabling a comprehensive analysis of engineering designs.

Set up to suppress warnings to ensure clean output

warnings.filterwarnings('ignore')

```
import numpy as np
import matplotlib.pyplot as plt
from deap import base
from deap import creator
from deap import tools
import random
import warnings

warnings.filterwarnings('ignore')

stress = []
costs = []
kp = 0.0
bp = 0.0
sp = 0.0
sstp = 0.0
```

def plot_pareto_frontier(Xs, Ys, maxX=True, maxY=False):

```
sorted_list = sorted([[Xs[i], Ys[i]] for i in range(len(Xs))], reverse=maxY)
pareto_front = [sorted_list[0]]
for pair in sorted_list[1:]:
    if maxY:
        if pair[1] >= pareto_front[-1][1]:
            pareto_front.append(pair)
    else:
        if pair[1] <= pareto_front[-1][1]:
            pareto_front.append(pair)

pf_X = [pair[0] for pair in pareto_front]

pf_Y = [pair[1] for pair in pareto_front]

x = np.array(pf_X)
y = np.array(pf_Y)
p = np.polyfit(x, y, 3)
x_range = np.linspace(min(x), max(x), num=500)
y_range = np.polyval(p, x_range)</pre>
```

plt.scatter(Xs, Ys)

```
plt.plot(x_range, y_range)
plt.xlabel("Stress")
plt.ylabel("Costs")
plt.show()
```

def semiround(f):

```
if f == int(f):
    return f
elif f <= int(f) + 0.5:
    return int(f) + 0.5
else:
    return int(f) + 1.0</pre>
```

def run_nsga(KeelPlate, BottomPlate, SideShellPlate, ShearStrakePlate,
InnerBottomPlate, InnerSideShellPlate, MainDeckPlate, HatchCoamingPlate,
HatchCoamingTopPlate, dblgcl, WebFrameSpacing, StiffenerSpacing,
thresholdval, crossover prob=0.7, mutation prob=0.3,gen=500, pop=128):

```
ef get_KeelPlate():
   kp = random.uniform(min(KeelPlate), max(KeelPlate))
    return semiround(kp)
def get BottomPlate():
   bp = random.uniform(min(BottomPlate), kp)
   return semiround(bp)
def get SideShellPlate():
   sp = random.uniform(min(SideShellPlate), bp)
def get ShearStrakePlate():
   return semiround(sstp)
def get_InnerBottomPlate():
def get_InnerSideShellPlate():
    return semiround (random.uniform (min (InnerSideShellPlate),
def get_MainDeckPlate():
max(MainDeckPlate)))
def get_HatchCoamingPlate():
   return semiround(random.uniform(min(HatchCoamingPlate),
max(HatchCoamingPlate)))
```

```
def get HatchCoamingTopPlate():
    return semiround (random.uniform (min (HatchCoamingTopPlate),
max(HatchCoamingTopPlate)))
def get dblgcl():
    return semiround(random.uniform(min(dblgcl), max(dblgcl)))
def get WebFrameSpacing():
    return semiround (random.uniform (min (WebFrameSpacing),
max(WebFrameSpacing)))
def get StiffenerSpacing():
    return semiround(random.uniform(min(StiffenerSpacing),
max(StiffenerSpacing)))
def evaluation(individual):
    BottomPlate = individual[1]
    SideShellPlate = individual[2]
    ShearStrakePlate = individual[3]
    InnerBottomPlate = individual[4]
    InnerSideShellPlate = individual[5]
    MainDeckPlate = individual[6]
    HatchCoamingPlate = individual[7]
    dblgcl = individual[9]
    WebFrameSpacing = individual[10]
    StiffenerSpacing = individual[11]
```

```
def myMutate(individual, indpb=0.10):
   if random.random() < indpb:</pre>
        individual[0] = toolbox.attr KeelPlate()
   if random.random() < indpb:</pre>
        individual[1] = toolbox.attr BottomPlate()
   if random.random() < indpb:</pre>
        individual[2] = toolbox.attr SideShellPlate()
   if random.random() < indpb:</pre>
        individual[3] = toolbox.attr ShearStrakePlate()
        individual[4] = toolbox.attr InnerBottomPlate()
   if random.random() < indpb:</pre>
        individual[5] = toolbox.attr InnerSideShellPlate()
   if random.random() < indpb:</pre>
        individual[6] = toolbox.attr MainDeckPlate()
   if random.random() < indpb:</pre>
        individual[7] = toolbox.attr HatchCoamingPlate()
   if random.random() < indpb:</pre>
        individual[8] = toolbox.attr HatchCoamingTopPlate()
   if random.random() < indpb:</pre>
        individual[9] = toolbox.attr dblqcl()
   if random.random() < indpb:</pre>
        individual[10] = toolbox.attr WebFrameSpacing()
   if random.random() < indpb:</pre>
       individual[11] = toolbox.attr StiffenerSpacing()
```

```
return [semiround(935.3 - 2.58 * KeelPlate - 11.21 * BottomPlate - 3.21 * SideShellPlate - 5.60 *
                 ShearStrakePlate - 4.69 * InnerBottomPlate - 2.10 * InnerSideShellPlate - 4.37 *
                 MainDeckPlate - 6.09 * HatchCoamingPlate - 5.68 * HatchCoamingTopPlate - 1.78 * dblgcl
                 - 0.1504 * WebFrameSpacing - 0.3567 * StiffenerSpacing + 0.0007 * KeelPlate * BottomPlate
                 - 0.0281 * KeelPlate * SideShellPlate + 0.0235 * KeelPlate * ShearStrakePlate - 0.0042 *
                 KeelPlate * InnerBottomPlate - 0.0355 * KeelPlate * InnerSideShellPlate - 0.0170 *
                 KeelPlate * MainDeckPlate + 0.0281 * KeelPlate * HatchCoamingPlate + 0.0265 * KeelPlate *
                 HatchCoamingTopPlate - 0.0218 * KeelPlate * dblgcl + 0.000266 * KeelPlate * WebFrameSpacing +
                 0.00270 * KeelPlate * StiffenerSpacing - 0.0366 * BottomPlate * SideShellPlate + 0.1120 *
                 BottomPlate * ShearStrakePlate + 0.0406 * BottomPlate * InnerBottomPlate - 0.0224 *
                 BottomPlate * InnerSideShellPlate + 0.1475 * BottomPlate * MainDeckPlate + 0.1402 *
                 BottomPlate * HatchCoamingPlate + 0.1798 * BottomPlate * HatchCoamingTopPlate - 0.0097 *
                 BottomPlate * dblqcl + 0.000059 * BottomPlate * WebFrameSpacing + 0.00086 * BottomPlate *
                 StiffenerSpacing + 0.0608 * SideShellPlate * ShearStrakePlate - 0.0433 * SideShellPlate *
                 InnerBottomPlate - 0.0106 * SideShellPlate * InnerSideShellPlate - 0.0004 * SideShellPlate *
                 MainDeckPlate + 0.0719 * SideShellPlate * HatchCoamingPlate + 0.0440 * SideShellPlate *
                 HatchCoamingTopPlate - 0.0364 * SideShellPlate * dblgcl + 0.000228 * SideShellPlate *
                 WebFrameSpacing + 0.00236 * SideShellPlate * StiffenerSpacing + 0.0151 * ShearStrakePlate *
                 InnerBottomPlate + 0.0602 * ShearStrakePlate * InnerSideShellPlate + 0.0540 *
                 ShearStrakePlate * MainDeckPlate + 0.0682 * ShearStrakePlate * HatchCoamingPlate + 0.0086 *
                 ShearStrakePlate * HatchCoamingTopPlate + 0.0240 * ShearStrakePlate * dblgcl - 0.000152 *
                 ShearStrakePlate * WebFrameSpacing - 0.00191 * ShearStrakePlate * StiffenerSpacing
                 - 0.0464 * InnerBottomPlate * InnerSideShellPlate - 0.0267 * InnerBottomPlate * MainDeckPlate
                 + 0.0322 * InnerBottomPlate * HatchCoamingPlate + 0.0169 * InnerBottomPlate *
                 HatchCoamingTopPlate + 0.0013 * InnerBottomPlate * dblgcl + 0.000531 * InnerBottomPlate *
                 WebFrameSpacing + 0.00470 * InnerBottomPlate * StiffenerSpacing + 0.0100 * InnerSideShellPlate
                 * MainDeckPlate + 0.1580 * InnerSideShellPlate * HatchCoamingPlate + 0.0736 *
                 InnerSideShellPlate * HatchCoamingTopPlate - 0.0323 * InnerSideShellPlate * dblgcl
                 - 0.000284 * InnerSideShellPlate * WebFrameSpacing - 0.00255 * InnerSideShellPlate *
                 StiffenerSpacing - 0.0184 * MainDeckPlate * dblgcl + 0.000087 * MainDeckPlate *
                 WebFrameSpacing + 0.00076 * MainDeckPlate * StiffenerSpacing + 0.0160 * HatchCoamingPlate *
                 dblgcl - 0.000652 * HatchCoamingPlate * WebFrameSpacing - 0.00651 * HatchCoamingPlate *
                 StiffenerSpacing - 0.0009 * HatchCoamingTopPlate * dblgcl + 0.000013 * HatchCoamingTopPlate *
                 WebFrameSpacing - 0.00150 * HatchCoamingTopPlate * StiffenerSpacing + 0.000268 * dblgcl *
                 WebFrameSpacing + 0.00291 * dblgcl * StiffenerSpacing + 0.000219 * WebFrameSpacing *
                 StiffenerSpacing),
```

```
892606 + 4557 * KeelPlate + 25778 * BottomPlate + 15108 * SideShellPlate + 8445 * ShearStrakePlate +
29447 * InnerBottomPlate + 22487 * InnerSideShellPlate + 6468 * MainDeckPlate + 7193 * HatchCoamingPlate
+ 3720 * HatchCoamingTopPlate - 1100 * dblgcl - 122.71 * WebFrameSpacing - 111.1 * StiffenerSpacing
+ 19.1 * KeelPlate * BottomPlate + 19.1 * KeelPlate * SideShellPlate - 16.4 * KeelPlate *
ShearStrakePlate - 17.5 * KeelPlate * InnerBottomPlate + 16.1 * KeelPlate * InnerSideShellPlate - 16.1
* KeelPlate * MainDeckPlate + 13.7 * KeelPlate * HatchCoamingPlate - 13.5 * KeelPlate *
HatchCoamingTopPlate + 13.8 * KeelPlate * dblgcl - 0.115 * KeelPlate * WebFrameSpacing - 1.18 *
KeelPlate * StiffenerSpacing - 23.3 * BottomPlate * SideShellPlate + 19.9 * BottomPlate *
ShearStrakePlate + 21.2 * BottomPlate * InnerBottomPlate - 19.4 * BottomPlate * InnerSideShellPlate
+ 19.5 * BottomPlate * MainDeckPlate - 16.2 * BottomPlate * HatchCoamingPlate + 16.5 * BottomPlate *
HatchCoamingTopPlate - 16.4 * BottomPlate * dblgcl + 0.134 * BottomPlate * WebFrameSpacing + 1.38 *
BottomPlate * StiffenerSpacing + 19.7 * SideShellPlate * ShearStrakePlate + 21.0 * SideShellPlate *
InnerBottomPlate - 19.4 * SideShellPlate * InnerSideShellPlate + 19.2 * SideShellPlate * MainDeckPlate
- 16.3 * SideShellPlate * HatchCoamingPlate + 16.5 * SideShellPlate * HatchCoamingTopPlate - 16.5 *
SideShellPlate * dblgcl + 0.138 * SideShellPlate * WebFrameSpacing + 1.41 * SideShellPlate *
StiffenerSpacing - 18.0 * ShearStrakePlate * InnerBottomPlate + 16.5 * ShearStrakePlate *
InnerSideShellPlate - 16.3 * ShearStrakePlate * MainDeckPlate + 20.2 * ShearStrakePlate *
HatchCoamingPlate - 19.5 * ShearStrakePlate * HatchCoamingTopPlate + 14.0 * ShearStrakePlate * dblgcl
- 0.163 * ShearStrakePlate * WebFrameSpacing - 1.68 * ShearStrakePlate * StiffenerSpacing
+ 17.6 * InnerBottomPlate * InnerSideShellPlate - 17.4 * InnerBottomPlate * MainDeckPlate
+ 14.8 * InnerBottomPlate * HatchCoamingPlate - 15.1 * InnerBottomPlate * HatchCoamingTopPlate
+ 15.1 * InnerBottomPlate * dblgcl - 0.125 * InnerBottomPlate * WebFrameSpacing- 1.29 * InnerBottomPlate
* StiffenerSpacing + 16.0 * InnerSideShellPlate * MainDeckPlate - 13.6 * InnerSideShellPlate *
HatchCoamingPlate + 13.6 * InnerSideShellPlate * HatchCoamingTopPlate - 13.8 * InnerSideShellPlate *
dblgcl + 0.114 * InnerSideShellPlate * WebFrameSpacing + 1.18 * InnerSideShellPlate * StiffenerSpacing
+ 13.8 * MainDeckPlate * dblgcl - 0.116 * MainDeckPlate * WebFrameSpacing - 1.19 * MainDeckPlate *
StiffenerSpacing - 11.7 * HatchCoamingPlate * dblgcl + 0.136 * HatchCoamingPlate * WebFrameSpacing
+ 1.40 * HatchCoamingPlate * StiffenerSpacing + 11.8 * HatchCoamingTopPlate * dblgcl - 0.134 *
HatchCoamingTopPlate * WebFrameSpacing - 1.38 * HatchCoamingTopPlate * StiffenerSpacing + 0.099 *
dblgcl * WebFrameSpacing + 1.01 * dblgcl * StiffenerSpacing - 0.0240 * WebFrameSpacing *
StiffenerSpacing]
```

```
feasible(individual)
    if (evaluation(individual)[0] < thresholdval[0]) and (evaluation(individual)[1] < thresholdval[1]):
def distance(individual):
    return abs(evaluation(individual)[0] - thresholdval[0])
def myMutate(individual, indpb=0.10):
       individual[0] = toolbox.attr_KeelPlate()
       individual[1] = toolbox.attr_BottomPlate()
       individual[2] = toolbox.attr_SideShellPlate()
       individual[3] = toolbox.attr_ShearStrakePlate()
    if random.random() < indpb:</pre>
       individual[4] = toolbox.attr_InnerBottomPlate()
       individual[5] = toolbox.attr_InnerSideShellPlate()
       individual[6] = toolbox.attr_MainDeckPlate()
       individual[7] = toolbox.attr_HatchCoamingPlate()
       individual[8] = toolbox.attr_HatchCoamingTopPlate()
       individual[9] = toolbox.attr_dblgcl()
       individual[10] = toolbox.attr_WebFrameSpacing()
    if random.random() < indpb:
       individual[11] = toolbox.attr_StiffenerSpacing()
```

```
toolbox.register("evaluate", evaluation)
toolbox.decorate("evaluate", tools.DeltaPenality(feasible, 5.0, distance))
toolbox.register("mate", tools.cxTwoPoint)
toolbox.register("mutate", myMutate, indpb=0.25)
toolbox.register("select", tools.selNSGA2)
pop = toolbox.population(n=POPSIZE)
invalid_ind = [ind for ind in pop if not ind.fitness.valid]
fitnesses = toolbox.map(toolbox.evaluate, invalid_ind)
for ind, fit in zip(invalid_ind, fitnesses):
    ind.fitness.values = fit
for q in range(NGEN):
    offspring = toolbox.select(pop, len(pop))
    offspring = list(map(toolbox.clone, offspring))
    for child1, child2 in zip(offspring[::2], offspring[1::2]):
        if random.random() < CXPB:
           c1 = toolbox.clone(child1)
           c2 = toolbox.clone(child2)
            toolbox.mate(child1, child2)
            if c1 != child1; del child1.fitness.values
            if c2 != child2; del child2.fitness.values
    for mutant in offspring:
        if random.random() < MUTPB:
            m1 = toolbox.clone(mutant)
            toolbox.mutate(mutant)
            if m1 != mutant: del mutant.fitness.values
    invalid_ind = [ind for ind in offspring if not ind.fitness.valid]
    fitnesses = list(map(toolbox.evaluate, invalid_ind))
```

```
for ind, fit in zip(invalid_ind, fitnesses):
    ind.fitness.values = fit

pop[:] = offspring
    best_ind = tools.selBest(pop, POPSIZE)[0]

stress.append(best_ind.fitness.values[0])
    costs.append(best_ind.fitness.values[1])

return best_ind, best_ind.fitness.values
```

```
if __name__ == '__main__':
   KeelPlate = [14.5, 8.5]
   BottomPlate = [12.5, 7.5]
   SideShellPlate = [6.5, 11.5]
   ShearStrakePlate = [13.5, 8.5]
   InnerBottomPlate = [14.5, 9]
   InnerSideShellPlate = [13.5, 7.5]
   MainDeckPlate = [16, 10]
   HatchCoamingPlate = [16, 10]
   HatchCoamingTopPlate = [23, 17]
   dblqcl = [13, 20]
   WebFrameSpacing = [1430, 2145]
   StiffenerSpacing = [631, 700]
   thresholdval = [300, 20000000]
   print('Please wait while processing data...')
   (calc_KeelPlate, calc_BottomPlate, calc_SideShellPlate, calc_ShearStrakePlate, calc_InnerBottomPlate,
    calc_InnerSideShellPlate, calc_MainDeckPlate, calc_HatchCoamingPlate, calc_HatchCoamingTopPlate, calc_dblgcl,
    calc_WebFrameSpacing, calc_StiffenerSpacing), \
   <u>fitness</u> = run_nsga(KeelPlate, BottomPlate, SideShellPlate, ShearStrakePlate, InnerBottomPlate,
                      InnerSideShellPlate, MainDeckPlate, HatchCoamingPlate, HatchCoamingTopPlate, dblgcl,
                      WebFrameSpacing, StiffenerSpacing, thresholdval=thresholdval)
```

```
print('Keel plate :', calc_KeelPlate)
print('Bottom plate :', calc_BottomPlate)
print('Side Shell Plate :', calc_SideShellPlate)
print('Side Shell Plate :', calc_ShearStrakePlate)
print('Inner Strake Plate :', calc_ShearStrakePlate)
print('Inner bottom plate :', calc_InnerBottomPlate)
print('Inner Side Shell Plate :', calc_InnerSideShellPlate)
print('Main Deck Plate :', calc_MainDeckPlate)
print('Hatch Coaming Top Plate:', calc_HatchCoamingTopPlate)
print('Hatch Coaming Top Plate:', calc_HatchCoamingTopPlate)
print('Gelgel:', calc_dblgcl)
print('Web Frame Spacing:', calc_WebFrameSpacing)
print('Stiffener Spacing:', calc_StiffenerSpacing)
print('Stiffener Spacing:', fitness)
print('threshold values: ', fitness)
print('threshold values: ', thresholdval)

plt.title("Num Iterations vs Best Individual Stress Value")
plt.plot(stress)
plt.show()

plt.title("Num Iterations vs Best Individual Cost Value")
plt.plot(costs)
plt.show()

xy = list(zip(stress, costs))
xy = list(set(xy))
xy.sort(key=lambda item: item[0])
stress, costs = zip(*xy)
plot_pareto_frontier(stress, costs)
```